2008-9

Investigation of UV-LED Initiated Photopolymerisation of Bio-compatible HEMA

Sharon McDermott
Technological University Dublin

Investigation of UV-LED Initiated Photopolymerisation of Bio-compatible HEMA

Sharon McDermott

A thesis submitted to the Dublin Institute of Technology,
for the degree of Doctor of Philosophy

School of Physics
Dublin Institute of Technology
Kevin Street, Dublin 8.
SEPTEMBER 2008

Abstract

Ultraviolet (UV) fluorescent lamps are widely used in photopolymerisation processes. However, there a number of disadvantages to these lamps, namely, their intensity varies over time and has to be constantly monitored. This thesis is concerned with the possibility of replacing these lamps with UV Light Emitting Diodes (UV-LEDs).

A number of emission characteristics of both the fluorescent lamp and the UV-LEDs were measured and compared to ensure that the optical properties of the UV-LEDs were equivalent to those of the lamps. From this study it was shown that the UV-LEDs have a quicker warm up time and exhibit a more stable output than the fluorescent lamps, while also emitting in the required region for photopolymerisation.

The ability of each source to initiate photopolymerisation in a HEMA sample was then monitored using FTIR (Fourier Transform Infrared) and Raman spectroscopy and the percentage cure calculated. These studies proved that UV-LEDs could produce a degree of cure that was comparable to that produced by the fluorescent lamp.

The last section of the study was concerned with investigating how pulsed UV radiation affected the curing process and thus the mechanical properties of the final polymer. This work was performed using FTIR spectroscopy and Dynamic mechanical analysis (DMA). The study showed that the curing profiles and the mechanical properties of the polymer were not only affected by the irradiation wavelength but also by the duration of the pulsing.

The findings of this thesis show that due to the inherent advantages that LEDs have over fluorescent lamps and the fact that they produce a comparable photopolymerisation as that achieved with the fluorescent lamps, LED photopolymerisation is a viable possibility in replacing fluorescent lamps in the manufacturing of biomaterials.

Declaration

I certify that this thesis which I now submit for examination for the award of PhD, is entirely my own work and has not been taken from the work of others save and to the extent that such work has been cited and acknowledged within the text of my work.

This thesis was prepared according to the regulations for postgraduate studies by research of the Dublin Institute of Technology and has not been submitted in whole or in part for an award in any other Institute or University. The work reported on in this thesis conforms to the principles and requirements of the Institute's guidelines for ethics in research.

The Institute has permission to keep, or lend or to copy this thesis in whole or in part, on condition that any such use of the material or the thesis be duly acknowledged, subject to access being granted.

Signature Sharon McDermott Date 09/09/08

Acknowledgements

Firstly, I would like to thank Dr Robert Howard and Dr James Walsh for giving me the opportunity to do this thesis. Their advice, guidance, encouragement and above all else patience throughout the years was invaluable.

A huge thank you to all the technical staff at the Focas Institute, Garrett Farrell, Anne Shanahan and Andrew Hartnett. I've lost count of how often you got me out of trouble. Special thanks to Joe Keogh of the Physics Department for his electrical know-how and to Trevor Woods of the Polymer Research Group, Materials Ireland, TCD, for his help and assistance with the DMA.

Special thanks to Dr Hugh Byrne and Dr Mary McNamara for their selfless help and advice both to myself and all students at the Focas Institute over the years.

To Dave, Luke and Ray thanks for making the journey so much fun and keeping me sane over the years. Your willingness to always to be there to go for a pint and a chat was much appreciated many times!! To all my colleagues at the Focas Institute and in DIT thanks for all the laughs over the years.

To Mam & Dad thanks for the love, encouragement and support (financial and otherwise!!) over the years. Without you this thesis would not have been possible.

And finally, a huge thanks to Stephen for helping me through the difficult times. Thanks for listening to my throughout the years and for encouraging me to never give up.

Abbreviations

A	Absorbance
AC	Alternating current
a.u.	Absorbance units
c	Sample concentration
CQ	Camphorquinone
dc	Direct current
DC	Degree of conversion
DH	Hydrogen donor
DMA	Dynamic mechanical analysis
EM	Electromagnetic
DSC	Differential Scanning Calorimetry
FTIR	Fourier Transform Infrared Spectroscopy
HEMA	2-hydroxyethyl methacrylate
IR	Infrared
KrF	Krypton/Fluorine
l	path length
LED	Light Emitting Diode
LCUs	Light curing units
MW	Molecular weight
NMR	Nuclear Magnetic Resonance
pHEMA	poly 2-hydroxyethyl methacrylate
PMMA	poly(methyl methacrylate)

R·	Free radical
SSL	Solid state lighting
T_g	Glass transition temperature
T_r	Room temperature
Tan δ	Mechanical damping factor
UV	Ultraviolet
UV-LED	Ultraviolet Light Emitting Diode
UV/vis	Ultraviolet/visible
UV/vis/NIR	Ultraviolet/visible/near infrared
XeCl	Xenon/Chlorine
XeF	Xenon/Fluorine
E*	Complex modulus
E'	Storage modulus
E''	Loss modulus
ε_λ	Molar Absorptivity
ε	Strain
σ	Stress
λ_{max}	Maximum output wavelength
δ	Phase difference

List of Figures

List of Tables

Table of Contents

Chapter 1 Theory

1.1 Introduction

Light-induced polymerisation (photopolymerisation) of monomers has become a well-accepted technology which has found a use in a wide variety of industrial applications due to its distinct advantages i.e. a high rate of polymerisation can be achieved in a fast time at ambient temperatures [1]. Another reason for the wide spread use of this technique is its ease of operation and cost efficiency [2]. This technology is used in a number of areas ranging from the coating industry, to paints, to the manufacturing of biomaterials such as contact lenses [3-5]. It is the use of this technique in the manufacturing of the latter that is of concern to this research. This chapter gives an introduction to the theory behind photopolymerisation and discusses how it is used in the manufacturing of contact lenses.

1.2 Manufacturing of contact lenses

The earliest known reference to contact lenses was made by Leonardo da Vinci over 500 years ago in which he described a clear shell that could be placed against the eye to correct vision [6, 7]. However it was not until the latter half of the 1900's that the contact lens manufacturing industry began to expand [7]. The first contact lens was created in 1888 by A.E. Fick who suggested their potential use in aphakia (absence of the lens of an eye) and as cosmetic/prosthetic lenses; these lenses were cast in blown glass [7, 8]. In 1889 A. Müller corrected his own myopia by wearing a glass-blown scleral contact lens. These lenses sat across all the visible ocular surface [8]. It was not until after the Second World War that the

first corneal contact lens was manufactured, these lens were smaller than the previous scleral lenses and sat only on the cornea [9, 10]. This type of lens became known as hard or rigid contact lenses and was manufactured from poly(methyl methacrylate) (PMMA) [11, 12]. One of the main disadvantages to these PMMA lenses is their low gas permeability which means oxygen cannot penetrate through the lens to the cornea and conjunctiva, which can lead to eye damage [13, 14]. With the discovery of 2-hydroxyethyl methacrylate (HEMA) by Otto Wichterle [15] during the 1950's and the subsequent development of the 'spin-casting' production [16] method, the first large-scale production of HEMA lenses by Bausch & Lomb took place in 1971 [6]. HEMA belongs to a class of polymers known as hydrogels. These polymers can retain a large fraction of water without dissolving [17]. These soft lenses offer immediate comfort to the wearer where hard lenses require a period of adjustment before full comfort is reached. Since the 1970s there has been a large increase in the type of contact lenses available including numerous different soft contact lenses with different water content, oxygen permeability and wear time [10]. The most recent development has been the manufacturing of silicone hydrogel lenses [7, 18]. As oxygen is far more soluble in silicone than in PMMA and water these lenses allow for further comfort to the wearer due to their high oxygen permeability while still allowing for water absorption [16, 19]. Recently relatively cheap disposable soft contact lenses [7] became available these have became very popular and allow the wearer to dispose of them after certain periods of time. They can be disposed after either each day of wear or can be worn for up to 30 consecutive nights [20].

The two main methods of contact lens manufacturing are moulding and lathe-cutting also known as generating [7]. There are three types of moulding; casting, injection and compression. Spin casting combined with photopolymerisation is the method favoured by companies such as Bausch & Lomb and Johnston & Johnston [7], due to the ease at which large amounts of contact lenses can be manufactured in a relatively short time. This procedure begins by injecting a hydrogel monomer mix into a concave mould which is rotated at a suitable speed, for example 350 rpm [21]. The back surface of the lens is governed by the speed of spin. Therefore different rates of spin are used depending on the required lens specification. The centripetal force then causes the monomer mix to spread to the edges of the mould, forming the required shape. Photopolymerisation is then initiated by exposing the mixture to UV radiation. Photopolymerisation is completed while the moulds are spinning, after which the moulds are removed and immersed in a large volume of distilled water, which is maintained at 87 °C to remove any un-reacted monomer that may irritate the wearers' eyes. The lenses are then checked, hydrated in saline and finally sealed in pharmaceutical vials [7, 12, 16].

The main disadvantage to the spin casting technique is the expense in setting up the laboratory therefore it is usually limited to large scale production. Small to medium size manufacturers favour the lathe-cutting technique. This technique is labour intensive and is generally reserved for individual prescription work. Lathe-cutting does not involve the use of UV light to produce the lenses. It involves mounting a blank lens on a heated stepped steel button. The button is then cooled and placed in a high precision lathe, where the lens is cut to the

required shape and thickness. The blank is then placed on a clean steel button and polished. The lens is then cut to the required dimensions and polished [7, 12].

Due to the rising interest in disposable lenses, manufacturers need to produce a large mass of lenses using a less labour intensive technique while considering production costs. This has resulted in the widespread use of spin casting photopolymerisation and it is this process that is the main area of interest to this thesis.

1.3 Polymers

People have been using polymers for centuries in the form of oil, tars, silk and gums. However it was not until the development of vinyl, polystyrene and nylon that polymer science took off. Polymers are a large class of materials consisting of many small molecules (called monomers) that can be linked together to form long chains that are known as polymers (or macromolecules). The reactions by which polymers are synthesised from monomers are termed polymerisation [22]. It was not until 1909 that the first truly synthetic polymer, Bakelite was engineered. Since then engineering polymers has grown with the development of a number of synthetic polymers and rubbers including polystyrene, nylon, polyethylene and polyvinylchloride [23]. The main interest in engineering polymers is due to their unique properties, which allows a wide range of different polymers to be produced for use in a large number of fields and at lower costs compared to many alloys and ceramics. The macromolecule structure of synthetic polymers can provide good biocompatibility and allows them to be used in many biological tasks that cannot be preformed by other synthetic

materials. These include contact lenses, dental restorative materials, bone cement, artificial tendons, ligaments and joints including intervertebral discs [23-25].

1.3.1 Classification of Polymers

There are a number of methods used to classify polymers. One method divides them into thermosets and thermoplastics depending on their reaction to thermal treatment [26]. Thermoset polymers are highly crosslinked and cannot melt when heated due to restrictions on the ability of the network polymers to flow, therefore they cannot be moulded. Thermoplastics on the other hand are linear or branched polymers that melt when heated and can be moulded and remoulded into virtually any shape. This type of classification has the benefit of giving a physical distinction between the two groups. A thermoplastic polymer is a linear chain one-dimensional polymer which is formed by joining one or more monomers by no more than two chemical bonds. On the other hand thermoset polymers consist of a three-dimensional highly crosslinked network, which makes them better suited to higher temperature applications than thermoplastics [26, 27].

Another method used to classify polymers divides polymers into condensation and addition polymers. This classification is based on whether there is a difference between the repeating unit of the polymer and the monomer used to synthesise it [28]. A condensation polymer is one in which a small molecule such as water is eliminated during the condensation of any two units. Addition polymers are formed from many monomers bonding together without the loss of a small molecule and the repeating units in the polymer have the same composition

as the monomer units. The corresponding polymerisation processes would then respectively be called condensation and addition polymerisation [28].

With the development of polymer science it was found that this classification could lead to ambiguity. Therefore another classification was introduced which is based on the mechanism of the polymerisation reactions [26, 28]. This defines polymers in terms of step and chain polymerisation reactions. Step polymerisation proceeds in a stepwise reaction with the monomer transforming into a dimer, trimer, tetramer and so on until eventually a large polymer molecule is formed. The size of the polymer molecules increases at a relatively slow rate in step polymerisation. Chain polymerisation on the other hand requires an initiator species with a reactive centre. Chain polymerisation occurs by the propagation of the reactive centre by the successive linking of the monomer molecules to the end of a growing chain. This process occurs in a much shorter time (matter of seconds) than step polymerisation and involves three distinct steps, initiation, propagation and termination [22, 28]. The most important of the chain polymerisation methods is called free radical polymerisation [23] and is almost solely used in the manufacturing of polymers from monomers containing C=C [29]. It is this type of polymerisation that is utilised in the manufacturing of contact lenses and is therefore the main mechanism that is of interest to this research and will be discussed in detail in the next section.

1.4 Photopolymerisation

Photopolymerisation is the initiation of a chain polymerisation process by light. It is achieved by adding a light-sensitive compound (photoinitiator) to an

appropriate polymerisable substance; the photoinitiator is then activated by light of an appropriate wavelength (λ) and converts the absorbed light energy into ions or free radicals. The type of radiation used is most commonly UV (200-400 nm) or visible (400-800 nm), however in rare cases infrared (800-2500 nm) radiation may be utilised [30].

Photoinitiated polymerisation (photopolymerisation) is one of the most efficient methods of transforming a liquid monomer to a solid polymer while having a number of advantages such as being solvent free, which makes this type of process environmentally friendly [3]. Another major advantage of this type of polymerisation is that it is essentially independent of temperature therefore the process can occur at room temperature with minimal heat production [31, 32]. Furthermore, the reaction can be controlled by varying a number of factors such as the photoinitiator and the light intensity [22, 33]. This type of polymerisation has found use in a number of applications. These applications include but are not limited to the coating industry [3] for the surface protection of various materials such as plastics, wood and metals, curing of dental material [34] and the manufacturing of holograms [35]. The main disadvantage to photopolymerisation is oxygen inhibition. Oxygen acts as a quencher that can terminate initiating and propagating radicals. However this inhibition can easily be overcome by purging the sample with an inert gas or by simply covering the sample, for example with a glass slide, to minimise oxygen diffusion into the sample during photopolymerisation [36].

In most polymerisable monomers a carbon-carbon double bond (C=C) is present. These monomers are known as vinyl monomers. These vinyl monomers

form polymers by breaking the C=C during polymerisation and replacing it with a single bond [22]. With chain polymerisation the reaction starts by the generation of a reactive centre. These reactive centres can be anions or cations but are typically free radicals [26]. Radical chain polymerisation is the most widely used method of chain polymerisation and is almost solely used in the manufacturing of polymers from monomers containing C=C [29]. In radical chain polymerisation the free radical generated attacks the double bond in the monomer by linking itself to the monomer molecule and then regenerates another radical which has the same identity as the one previous [22]. This chain reaction results in the growth of the polymer. As the free radicals involved are so reactive chain polymerisation does not continue indefinitely until all of the monomer is used up [26], instead it terminates when the free radicals react with each other rendering the chain end inactive [23]. An explanation of the three steps involved in radical chain photopolymerisation is given below.

Initiation:

This involves the formation of the free-radical centre and usually occurs in two steps. The first is the formation of free radicals, which occurs when the initiator dissociates as the light is absorbed. The second step involves the addition of one of the radicals to a monomer molecule, which in turn breaks the double bond [22, 23].

Propagation:

This involves the growth of the polymer chain by the subsequent addition of the radical to other monomer molecules. This process will continue until all the monomer molecules are consumed or until a termination reaction renders the chain end inactive [22, 28].

Termination:

In this step the growth of the polymer chain is terminated. There are two methods to termination in radical polymerisations these are combination or disproportionation [22, 23].

Combination: This occurs when two free radicals react together sharing their single odd electron to form a single polymer molecule.

Disproportionation: A hydrogen atom is transferred from one chain to another leading to the formation of two polymer molecules.

The radical chain photopolymerisation of a HEMA monomer is shown in figure 1.1. HEMA belongs to a class of materials known as hydrogels. Hydrogels are capable of absorbing large amounts of water and are quickly gaining importance as biomaterials [37]. Due to their significant water content they posses a degree of flexibility very similar to natural tissue making them an ideal material to be used in biomedical applications, including the areas of orthopaedics, medical devices and ophthalmology [16, 38]. Their hydrophilicity arises from the presence of certain chemical groups whose primary function is to

attract and bind water within the structure, in HEMA –OH is such a group [7, 12, 23].

In general a hydrogel lens consists of a hydrophilic monomer, a photopolymerisation initiator and cross-linkers. Although HEMA is the primary hydrophilic monomer used in the manufacturing of soft contact lenses [39] other components may be added to change or improve the lenses properties. N-vinyl-2 pyrrolidone (NVP) may be added as a second hydrophilic monomer to obtain an increase in water content [7, 12], while the addition of a crosslinker such as ethylene glycol dimethacrylate (EGDMA) achieves some key mechanical properties such as modulus and tear strength while providing dimensional stability [18, 40]. In addition to these other components can be added to aid in the manufacturing process or to achieve certain desirable properties in the lens. A hydrophobic monomer may be added to modify the physical and mechanical properties of the lens but this will also affect the final water content of the contact lens [39]. Tints may also be added for two reasons (1) visibility, a slight tint makes the lens more visible out of the eye and therefore easier to locate [7] and/or (2) cosmetic reasons to change or enhance the wearer's eye colour [41]. The central objective of this study was to verify that UV-LEDs could polymerise a HEMA monomer. As such only HEMA samples containing a photoinitiator were used in this research.

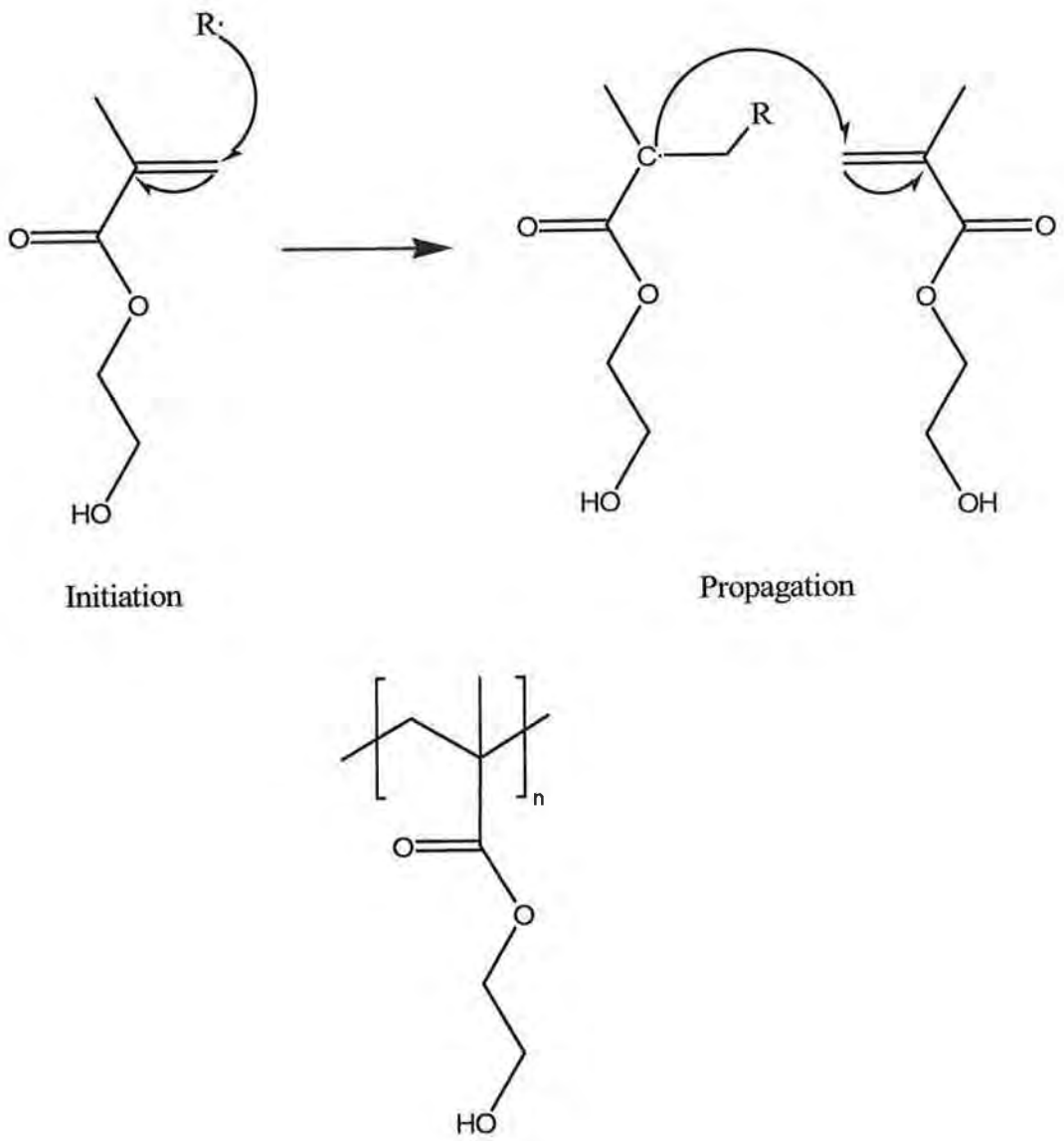

Figure 1.1: Radical chain photopolymerisation of HEMA, R· represent free radical.

1.4.1 Photoinitiators

For a photochemical reaction (i.e. photopolymerisation) to occur the medium must absorb light. However as most monomers are transparent to the radiations required to produce an initiation species it is necessary to introduce into the curable monomer a photoinitiator that will effectively absorb the incident

radiation [33, 42]. A photoinitiator is a compound, which upon absorption of radiation (ultraviolet or visible) undergoes a photoreaction that produces reactive species. These species are capable of initiating a chemical reaction, which results in changes to the physical properties of the monomer [32]. There are a variety of initiators available which can be formulated to respond to a range of wavelengths (most commonly used photoinitiators react between 300 nm-400 nm but visible and IR active ones are available [43]) to produce reactions. In order for an initiator system to function as a good source of radicals it should be stable under ambient or refrigerated temperature, produce a practical rate of radicals at non-excessive temperatures (approximately <150°C) and exhibit a large absorption in the emission range of the light source [4, 22].

In industries where photochemical reactions are used the photoinitiators traditionally respond to ultraviolet wavelengths [1, 33]. The reason for this is if the initiators responded to temperature producing infrared and visible light the system would have to be completely isolated from normal lighting and temperature surroundings. For this reason fluorescent lamps that emit in the near-ultraviolet region are usually used to initiate photopolymerisation reactions.

For photopolymerisation processes it is important to select photoinitiators that have absorption spectra that overlap with the emission spectra of the irradiation sources, as a high absorption process is vital to increase the reaction efficiency [44]. Therefore in this research a number of different UV sensitive photoinitiators were investigated. Figure 1.2 gives the chemical structure and trade names (in bold) of the photoinitiators used in this study. Throughout this thesis the photoinitiators will be identified by their trade names. All six

photoinitiators were generously supplied by Ciba Speciality Chemicals Inc. (Basel, Switzerland) [45] and used as received without further purification.

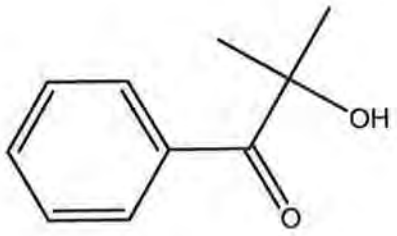

Darocur 1173 2-hydroxy-2-methyl-1-phenyl-propan-1-one MW = 164.2 $gmol^{-1}$

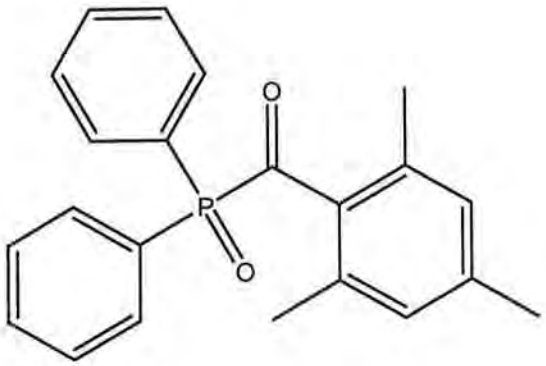

Darocur TPO 2,4,6-Trimethylbenzoyl-diphenyl-phosphineoxide MW = 348.4 $gmol^{-1}$

Figure 1.2: Chemical structure of the photoinitiators used in this study.

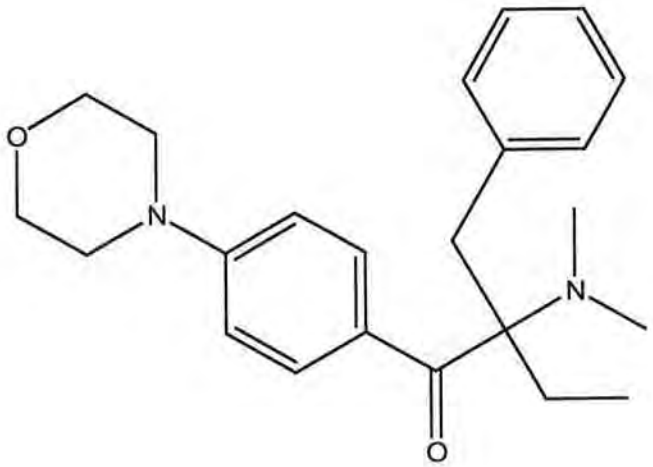

Irgacure 369 2-benzyl-2-dimethylamino-1-(4-morpholinophenyl)-butanone-1
MW = 366.5 $gmol^{-1}$

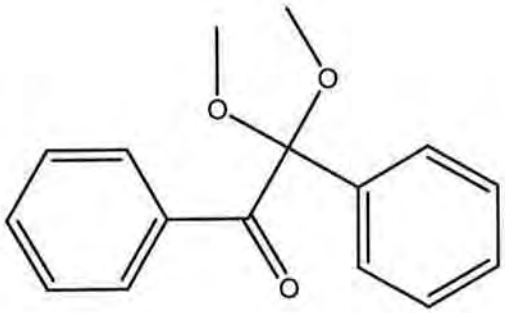

Irgacure 651 2,2-dimethoxy-1,2-diphenylethan-1-one MW = 256.3$gmol^{-1}$

Figure 1.2 contd.: Chemical structure of the photoinitiators used in this study.

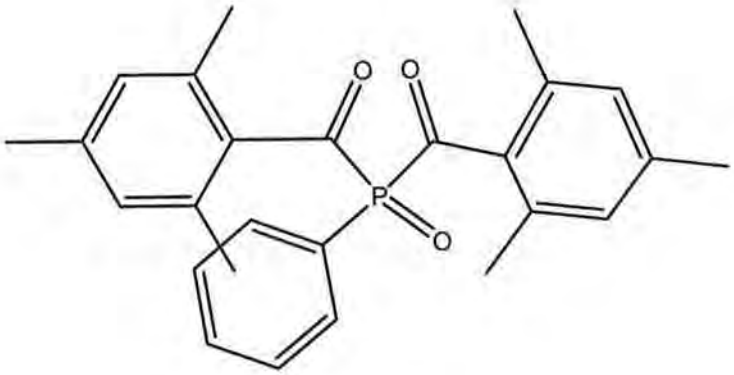

Irgacure 819 Bis(2,4,6-trimethylbenzoyl)-phenylphosphineoxide MW = 418.5 gmol-1

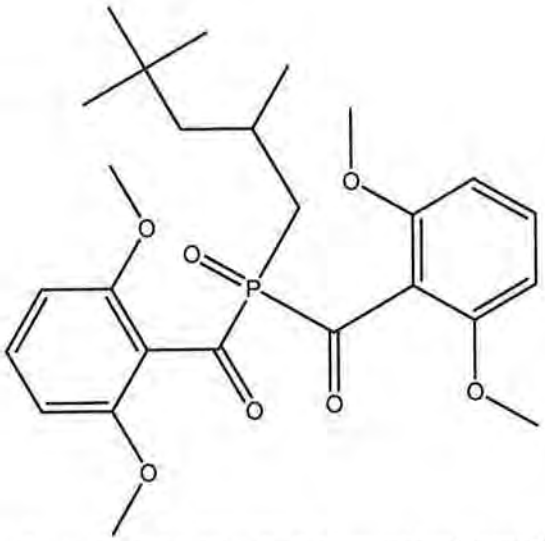

25% bis(2,6-dimethoxybenzoyl)-2,4,4-trimethyl-pentylphosphineoxide MW = 490.5 $gmol^{-1}$

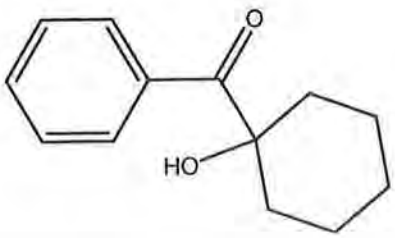

75% 1-Hydroxy-cyclohexyl-phenyl-ketone MW = 204.3 $gmol^{-1}$

Irgacure 1800

Figure 1.2 contd: Chemical structure of the photoinitiators used in this study.

1.4.2 Photoinitiator types

The photoinitiator plays a crucial role in the UV curing process, as it is this species that absorbs the incident radiation which in turn induces a chemical reaction resulting in the formation of a polymer. These photoinitiator species can be either free radical or cationic but as mentioned previously the vast majority are based on the formation of free radicals [22, 32]. Free radical photoinitiators can be subdivided into either 'alpha cleavage type' or 'hydrogen abstraction type' with both producing free radicals in a slightly different way. Alpha cleavage photoinitiators are the most widely used and generally have a higher efficiency due to fact that they need only absorb light in order to generate radicals [46]. However, as will be seen in chapter 6, some photoinitiators are based on hydrogen abstraction. Hydrogen abstraction photoinitiators require the excited state photoinitiator to find a hydrogen-donating source, such as an amine [47, 48], in order to generate free radicals [46].

The rate of initiation (r_i) (radical production) is dependant on the intensity of the incident light (I_o), the sample thickness or path length (l), the molar absorptivity (ε_λ), photoinitiator concentration ([PI]) and the quantum yield for initiation (Φ) which is the number of initiating species produced per photon absorbed (Eq 1.1) [22, 32, 33]. The maximum value of Φ is 1 [22], different photoinitiators will have different quantum yields and therefore will produce different rates of initiation. Hydrogen peroxide has a measured Φ value of 0.87 [49], while other photoinitiators can have Φ values as low as 0.13 [50].

$$r_i = \Phi I_o (1 - \exp(-\varepsilon_\lambda l[PI]) \qquad \text{Eq. 1.1}$$

1.5 Sample Description

As mentioned in section 1.4 in general a hydrogel lens consists of a hydrophilic monomer, a polymerisation initiator and cross-linkers. The properties of the resulting polymer depend on the chemical components used. The final water content, which influences the oxygen permeability of a hydrogel lens, depends on the hydrophilic monomer used. The monomer used in this research is HEMA (figure 1.3) which upon photopolymerisation forms the polymer poly 2-hydroxyethyl methacrylate (pHEMA). pHEMA is a widely used polymer for manufacturing soft contact lenses and other biomaterials such as bone prostheses due to its biocompatibility [5, 17, 24, 25]. The properties of this polymer changes drastically depending on its surroundings, in dry environments it is rigid and brittle but when hydrated it is soft and flexible [5]. Contact lenses manufacturers make use of the hydrated state as the high oxygen permeability and water absorption allows for more comfort to the wearer. However for biomedical applications the hydrated material does not have sufficient mechanical strength. Therefore a hydrophobic component is often incorporated to improve the mechanical properties [16, 38, 51].

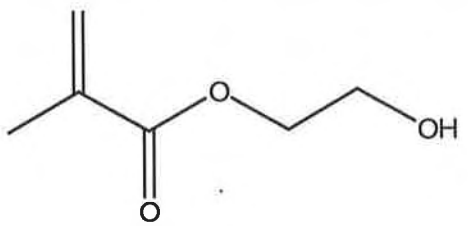

Figure 1.3: Chemical structure of HEMA MW = 130.1 $gmol^{-1}$

1.6 Previous curing studies of HEMA

As stated in section 1.4, HEMA belongs to the hydrogel class of polymers and is an important component in many applications especially in the area of biomaterials. As such a number of studies have investigated the curing process of HEMA [52].

As already stated (section 1.2) contact lenses are presently manufactured by exposing the monomer to UV radiation from a fluorescent lamp. Due to the number of disadvantages associated with fluorescent lamps several studies have been undertaken to replace these lamps in the manufacturing of contact lenses. McBrierty et al. [53] have investigated the potential to polymerise the contact lens material with UV lasers having a wavelength range of between 200 nm and 400 nm. This study utilised a number of excimer lasers KrF, XeCl and XeF (operating at 248 nm, 308 nm and 351 nm respectively), and a N_2 laser operating at 337 nm, it found that the most useful lasers for complete photopolymerisation were likely to be the XeCl and XeF excimer lasers and the N_2 laser.

A further in-depth study into the use of the N_2 lasers in the photopolymerisation of contact lenses was conducted by Martin [54]. This study used Nuclear Magnetic Resonance (NMR) and Fourier Transform Infrared (FTIR) spectroscopy to monitor in real time the UV photoinitiated and thermal curing dynamics of contact lens material. Typical cure times using the N_2 laser were between 1500 and 2000 seconds. However depending on the monomer mixture a cure time could exceed this.

The advantages of using a laser as the source to initiate photopolymerisation include shorter polymerisation times, improved control and

less maintenance than that required with conventional lamps. A further study by Lai [55] has attempted to improve the curing time of HEMA by achieving a "peak time" of about 180 seconds. In relation to this study it should be noted that the "peak time" is a reference to the early point in polymerisation when the polymerisation reaction is at its most intense point and not the point when the reaction is deemed to be complete ("stall time"). This study was concerned with varying the photoinitiator concentration and type and used a Sylvania F4T5/350BL lamp, which is a fluorescent bulb emitting between 300-400 nm having a peak at 350 nm. Using this lamp and photoinitiator concentrations varying from 0.1 to about 1.0 weight percent, peak times of between approximately 140 and 600 seconds were recorded. When the ideal formulation of photoinitiator type and concentration was found the HEMA mixture was then cured using a Philips UV lamp in approximately 90 seconds.

As previously mentioned the basis to this research is to investigate the potential of UV-LEDs in replacing the traditional used fluorescent lamps in the manufacturing of biomaterials, namely contact lenses. UV-LEDs are the latest development in a constantly developing lighting industry, where scientists and engineers have strived towards creating the 'ideal' light source. The next section gives an account of how light sources have evolved from early incandescent lamps to gas emission source, such as fluorescent lamps, and then into the recently developed solid-state sources that are light emitting diodes (LEDs).

1.7 History of lighting technology

Lighting technology is constantly striving to develop ideal light sources with improved specifications such as output spectrum, ruggedness, longer

lifetime, better efficiency and stability for use in a range of domestic and industrial applications [56, 57]. The first commercially available electrical light source was the incandescent light bulb. This type of lamp contains a filament which heats up and produces light when an electric current passes through it. The filament is kept in a vacuum which is enclosed by a glass bulb. Although it is the filament that produces the light it is the filament that is their weak point and principal cause of failure, as without the filament no current can flow and no light is generated. These lamps are very inefficient at converting electricity to light with about 90 % of the energy input being released as heat. Some applications make use of the heat generated such as incubators and heat lights for reptile tanks. Although these lamps are inefficient they are still widely used in household applications due to their low cost (less than 50 pence each [58]) and the fact they require no external regulating equipment. They have a lamp lifetime of approximately 1000 hours [59]. Another advantage to these types of lamps is that they emit over a broad range of wavelengths (figure 1.4).

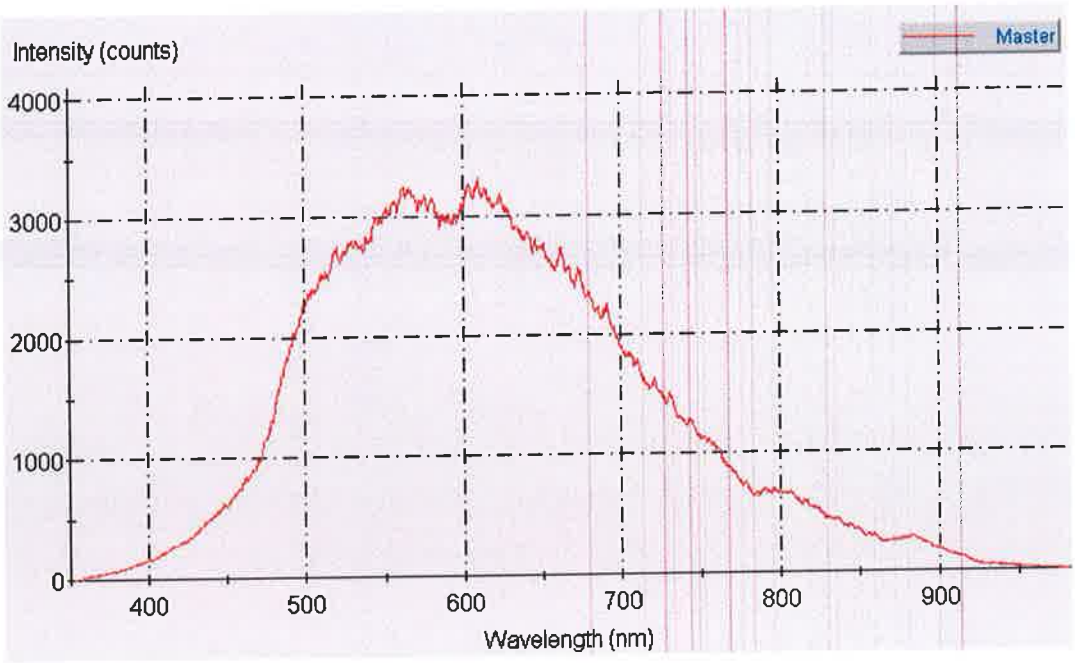

Figure 1.4: Spectral output of a typical incandescent bulb [60].

Halogen lamps, also known as tungsten-halogen lamps were introduced as an improvement to incandescent lamps. These lamps also contain a filament however unlike their predecessor the filament is not sealed in a glass bulb but in a transparent envelope usually made of quartz and filled with a halogen gas. This allows the lamp to run at higher temperatures allowing for greater brightness, whiter colour temperature and at a slightly higher efficiency than ordinary incandescent lamps. However this higher operating temperature can be a disadvantage as it means excess heat is discarded into the atmosphere. The quartz encasing allows these lamps to become a source of UV-B radiation as it is transparent to this spectral range. This may be one of their most significant side effects though conversely some instruments such as those used in medical and scientific applications make use of this UV radiation. These types of light sources are commonly used in dentistry to photopolymerise dental resin composites.

However as these lamps produce a very broad spectrum (similar to that of incandescent bulbs) a filter is needed to restrict the emitted light to the blue region of the spectrum, were the absorption spectra of the photoinitiator used occurs [61-63]. A typical tungsten halogen lamp has an operational lifetime of approximately 2000 hours, which is twice a long as a typical incandescent lamp.

The next development in electric lighting technology seen the introduction of gas discharge lamps. Unlike incandescent lamps, gas discharge lamps have no filament and do not produce light as a result of something solid getting hot (although heat is a by-product). Rather these types of lamps generate light (either visible or UV) by sending an electrical discharge through an ionised gas. The colour produced depends on both the mixture of gasses inside the tube as well as the pressure. Gas discharge lamps offer longer lifetime, up to 10,000 hours and are more efficient than incandescent lamps, a typical gas discharge lamp consumes only about 15 % of the electricity that an ordinary incandescent lamp needs [59, 64]. However they are more complicated to manufacture and unlike incandescent bulbs they require electronics to provide the correct current flow through the gas. They also suffer from environmental issues and have to be specially disposed off as they contain hazardous materials such as mercury.

Gas discharge lamps can be sub-divided into low and high pressure discharge lamps. When the gas is at low pressure a line spectrum is emitted, as the pressure is increased the spectral lines broaden until at super high pressure a continuous spectrum occurs [65]. Low pressure discharge lamps comprise of fluorescent and low pressure sodium lamps. While high pressure discharge lamps include high pressure sodium lamps, high pressure mercury-vapour lamps and

metal halide lamps. The fluorescent lamp is probably the best known gas discharge lamp. This type of lamp has been further developed into the compact fluorescent lamp (CFL) which may have a conventional ballast located in the fixture or the ballast integrated in the bulb, allowing them to fit into existing incandescent lamps fixtures. It is the use of these CFLs in photopolymerisation applications that is of interest to this research. The purchase price of a gas discharge lamp is higher than that of an incandescent lamp, but this cost is recovered in energy savings and replacement costs over the bulb's lifetime. A typical emission spectrum of a CFL is shown in figure 1.5.

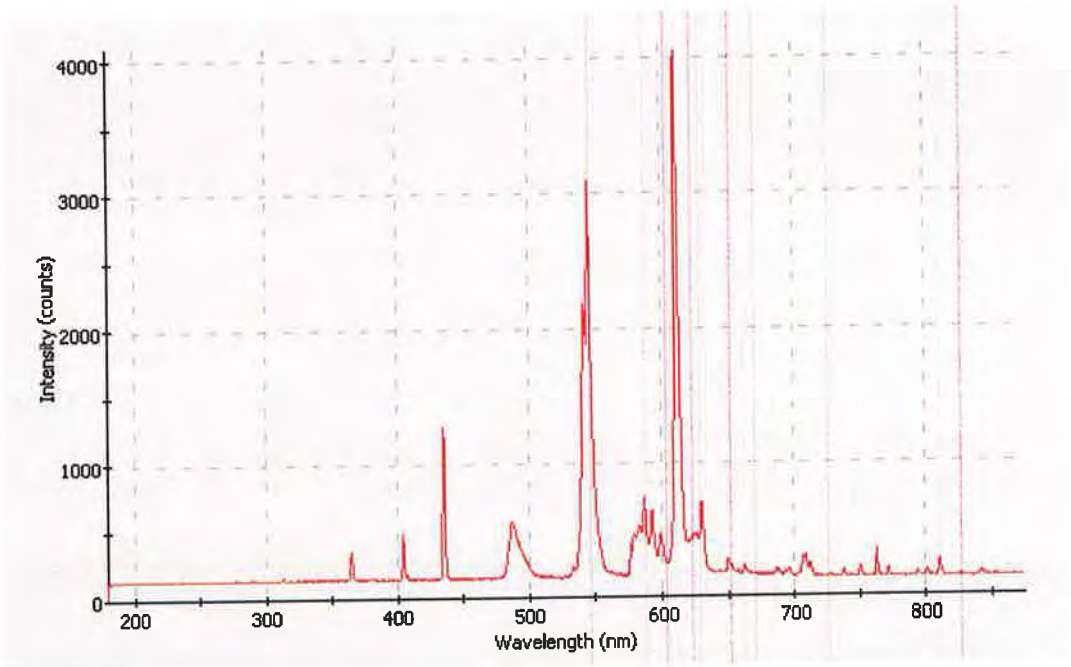

Figure 1.5: Spectral output of a typical compact fluorescent light bulb [66].

The most recent progress has seen the production of light emitting diodes (LEDs) which has lead to the development of Solid State Lighting (SSL). Unlike incandescent and gas discharge lamps were a heated filament or gas is required the light from an LED is emitted solely from the movement of electrons in a

semiconductor material. An LED contains a diode which comprises of a p-n junction, when the diode is subjected to an electric current, electrons and holes recombine at the LEDs p-n junction and release energy in the form of photons. The wavelength and thus the colour of the light emitted depends on the bandgap energy of the materials forming the p-n junction. Advances in material science have made it possible for LEDs to be produced that emit light at variety of different wavelengths. This alleviates the need for filters that were required with previous light sources. The purchase price of LEDs varies from a few cent up to hundreds of euros depending on the type of irradiation required [67, 68]. However overall like every new technology the price of this technology has decreased as LEDs become more widely available. The higher initial cost of SSL compared to incandescent and gas discharge lamps can be recovered due to their extremely long lifetime which can be as much as 100,000 hours for single colour LEDs and 35,000 for white LEDs. SSL also reduces maintenance costs and energy consumption, SSL can be as much as 20 times more efficient than incandescent lights and 5 times more efficient than fluorescent lighting [61, 69]. Due to their semiconductor nature they generate no or little heat and are more environmentally friendly than gas discharge lamps as they contain no harmful mercury. In addition their solid-state nature provides greater resistance to shock and vibration. It is the application of these LED-based systems and how they can be used to replace the previous sources in photopolymerisation processes, while eliminating many of the physical and commercial drawbacks that is of interest to this research.

When choosing an ideal light source for industrial applications such as contact lens photopolymerisation a number of factors need to be considered. Table 1.1 outlines the specifications for an ideal light source to be used in photopolymerisation applications. From the discussion previously it can be seen that LED based systems exhibit most of these ideal conditions. Throughout this research the specifications of a gas discharge lamp as well as numerous LEDs will be measured and compared to the ideal specifications that are outlined in table 1.1. Some of the ideal specifications listed in table 1.1 will be mutually exclusive in actual lamps available so compromises are required when choosing the final design. For example, high optical specifications may mean the light source is more expensive to produce or a high dose of UV radiation may increase the dangers to employees so extra safety guidelines would need to be put in place.

Table 1.1: 'Ideal' light source specifications for photopolymerisation processes.

1	Wavelength range	UV
2	Filters required	No
3	% of light in required λ range	100 %
4	Irradiance	Maximised at key UV λ
5	Electrical power in for photons out	All electrical power converted to photons
6	Output over time	Continuous or "DC" Pulsed or "AC" may effect photopolymerisation rate
7	Switch on time to stable output	Instantaneous
8	Long term stability	Constant
9	Lifetime	Infinite
10	Beam uniformity	0% variation in output field
11	Heat produced	No heat as heat effects polymerisation rate
12	Cost	Minimal
13	Ruggedness	Shock & vibration resistant
14	Environmentally friendly	No hazardous materials
15	Ease of replacement	Quick replacement to reduce downtime

1.8 Light Emitting Diodes replacing traditional light sources

Since the production of the first light bulb light sources have continued to evolve from gas emission sources such as fluorescent lamps through to recently developed solid-state sources such as light emitting diodes (LEDs). These latter LED-based systems have begun to replace incandescent lamps in many applications due to their inherent advantages; this research is concerned with replacing the currently used fluorescent lamps in photopolymerisation processes with this new technology.

UV fluorescent lamps have been used as the main source of UV radiation in the manufacturing of biomaterials such as contact lenses. Despite their popularity these light sources suffer from an array of problems such as, their output intensity varying and their short lifetime span. The intensity and the stability of the UV radiation being emitted is a crucial factor in photopolymerisation. If the lamp is not emitting at the required intensity the monomer may not fully polymerise, which could leave a toxic substance present and thus effect the lifetime, reliability and quality of the biomaterial. The output of these lamps decrease over time so they have to be constantly monitored and replaced regularly. These lamps must also be activated for a period of time before they can be used in photopolymerisation processes this is to ensure that the lamps have sufficiently warmed up. Another disadvantage is that switching them on and off wears out the electrodes, reducing the lifetime. This is because the mercury ions collide with the electrodes and erode the tungsten. Therefore more frequent starts (shorter burning cycles) reduce the lamp life. All of these problems lead to increased costs and down time for the manufacturer.

Since the development of solid state lighting (SSL), LED technology has been replacing traditional lamps in a number of areas due to their inherent advantages. LEDs offer lower energy consumption, stable optical properties and are more efficient at converting electricity into visible light than their counterparts. Also unlike traditional light sources LEDs produce visible light with virtually no heat. In addition due to their semiconductor nature they have longer lifetimes, their lifespan is further increased due to their ruggedness, which allows for greater resistance to shock and vibration. It is the lifetime of a light source that is of great interest to contact lens manufacturers. The lifetime of a lamp or LED is defined as how long the source provides light until half of the unit fails, that is until the emission of the device has decreased to 50% of the initial intensity [70]. With traditional light sources, such as incandescent lamps, the weak point and principal cause of failure is filament breach, without the filament no current can flow and no light generated. In contrast LEDs produce light using doped semi-conductors therefore they require no filament to emit light [61]. It has been reported that fluorescent lamps have a lifetime of between 2,000 and 10,000 hours [64]. In 1996 LEDs had an operational lifetime of only a few hours [70] however it has now been reported that LEDs have a lifetime of between 50,000 to 100,000 hours [71, 72] although this is not infinite it is a considerate increase on the lifetime of the lamps now being used.

One area that has seen this type of replacement technology is dentistry were tungsten-halogen light sources has been replaced by blue spectrum LEDs in the photopolymerisation of dental composites [34, 73, 74]. The main drawback with halogen sources is that their light output decreases with time. Since the

clinical performance of light induced dental composites is greatly influenced by the quality of light used the decrease in light intensity may produce a dental composite with poor physical properties which could lead to the premature failure of the restoration [61]. Also light curing units (LCUs) utilising halogen lamps require special filters to filter out unnecessary portions of the spectrum so that the wavelength is limited to 370-550 nm to fit the absorption spectra of the photoinitiator used [61, 63]. As LEDs can be manufactured to emit at narrow wavelength bands they allow for better control of the photopolymerisation process by emitting at the exact wavelength required to initiate the photoinitiator.

A number of studies have been undertaken to investigate and compare the effectiveness of polymerisation achieved with new LED LCUs and conventional halogen LCUs. These studies have investigated different properties for dental resin cured with the halogen lamp and the LEDs. These properties included degree of conversion, compressive strength, barcol hardness as well as depth of cure and flexural properties. These studies along with previous ones have shown that these blue LEDs produced a depth of cure and a degree of conversion that was significantly greater than those obtained using the halogen lamp even if the level of irradiance for the two sources was the same. Tests to investigate the compressive strength and the barcol hardness have found that dental composites cured with the LEDs will not be weaker than those cured with the lamps and the flexural properties of these composites do not change significantly when they are cured with the lamps and the LEDs.

In the past few years LED SSL technology has become commercially viable for general lighting applications. The brightness levels of LEDs are now

feasible for many applications and their continued improvements are allowing them to compete with the performance and cost of traditional light sources for general use [69]. Therefore it is expected that over the coming years the use of LED SSL in homes will increase. Already LED technology is used in a number of industrial and domestic areas. For example they can now be used as information indicators, e.g. as on/off lights in various audio and visual equipment. Due to their long lifetime and high efficiency LED clusters are now used in traffic lights. Their initial higher cost can be recovered in a short time due to their energy savings (traffic lights using LEDs instead of incandescent lamps consume one-tenth the power) and longevity, which reduces the manpower required for maintenance. Their long lifetime is also increasing their usage in car break lights and indicators as it allows for less frequent replacement. Their use in public displays has steadily increased over the years due to their capability to display instant real time measurements at low power consumption and low maintenance. Another advantage to using LEDs in public displays is that they are scalable and a batch of LEDs can be made as big as needed, from 1 cm up to metres. Indeed the overall display size is only limited by cost and the space available.

1.9 Conclusion

The use of LED technology as a viable alternative to halogen lamps in the photopolymerisation of dental composites has been proven. However the use of UV-LEDs in such processes has not been investigated. Any non-traditional curing method must be fully evaluated to ensure that complete through-cure is achieved and that the properties of the developed polymer is equivalent or better to those developed in the traditional manner. This thesis is concerned with developing a

novel curing method utilising UV-LEDs for use in the photopolymerisation of contact lenses which will be more efficient and have the potential to reduce manufacturers' costs. A thorough investigation of the optical and electrical properties of UV-LEDs was conducted with the findings being compared to those of the traditionally used fluorescent lamps. Each light source was used to photopolymerise a test contact lens monomer with the degree of cure being compared. Another novel aspect to this thesis and one which to the author's knowledge has not been published before was the use of pulsed LEDs to alter the mechanical properties of a contact lens.

This thesis describes an alternative method for curing a HEMA monomer and demonstrates the effect photoinitiator, wavelength and pulse rate has on the rate of cure and mechanical properties of the final polymer. The methodology applied in this research is just one example of the potential applications for UV-LEDs in photopolymerisation techniques and is not limited to this use. The findings in this research have potential use in a number of areas of polymer production and can be utilised in the coating industry for the formation of coatings or paints and in dentistry for the formation of dental composites.

1.10 References

[1] C. Decker. "Light-induced crosslinking polymerization". Polym. Int. 2002; vol 51: pp.1141-1150.

[2] L-T. Ng, S. Swami, C. Gordon-Thomson. "Hydrogels synthesised through photoinitiator-free photopolymerisation technique for delivering drugs including a tumour-tracing porphyrin". Radiat. Phys. Chem. 2006; vol 75: pp.604-612.

[3] C. Decker. "Kinetic study and new applications of UV radiation curing". Macromolecular Rapid Communications 2002; vol 23: pp.1067-1093.

[4] C. Decker. "Photoinitiated crosslinking polymerisation". Progress in Polymer Science 1996; vol 21: pp.593-650.

[5] R. Di Maggio, F. Rossi, L. Fambri, A. Fontana. "Raman and Brillouin scattering measurements on hybrid inorganic-organic materials obtained from tetraethoxysilane and methacrylic monomers". J. Non-Cryst. Solids 2004; vol. 345&346: pp.591-595.

[6] E. Goodlaw. "A personal perspective on the history of contact lenses". International Contact Lens Clinic 2002; vol. 27: pp.139-145.

[7] A.J. Phillips, L. Speedwell. "Contact Lenses 4th Ed." Oxford: Butterworth-Heinemann, 1997.

[8] R.M. Pearson. "Karl Otto Himmler, manufacturer of the first contact lens". Contact lens and anterior eye 2007; vol.30: pp.11-16.

[9] K.M. Tuohy. "Contact Lens", US Patent No. 2510438. 1950.

[10] G.E. Lowther, C. Snyder. "Contact lenses: procedures and techniques. 2nd Ed." Oxford: Butterworth-Heinemann, 1992.

[11] M. Ruben. "A colour atlas of contact lenses". London: Wolfe Medical Publications LTD., 1982.

[12] N. Efron. "Contact Lenses A-Z". Oxford: Butterworth-Heinemann, 2002.

[13] S. Loshaek, C.M. Shen. "Gas-permeable lens", United States Patent No. 4111535. 1978.

[14] S.W. Cohen. "A history of oxygen permeability". Contact lens and anterior eye 1998; vol.21: pp.35-40.

[15] Y. Kiritoshi, K. Ishihara. "Synthesis of hydrophilic cross-linker having phosphorylcholine-like linkage for improvement of hydrogel properties". Polymer 2004; vol. 45: pp.7499-7504.

[16] R.B Mandell. "Contact lens practice. 3rd Ed." Illinois: Charles C. Thomas, 1981.

[17] K. Mohomed, T.G. Gerasimov, F. Moussy, J.P. Harmon. "A broad spectrum analysis of the dielectric properties of poly(2-hydroxyethyl methacrylate)". Polymer 2005; vol 46: pp.3847-3855.

[18] Y.C. Lai. "A novel crosslinker for UV copolymerization of N-vinyl pyrrolidone and methacrylates to give hydrogels". J. Polym. Sci., Part A: Polym. Chem. 1997; vol. 35: pp.1039-1046.

[19] D. Sweeney. "Silicone hydrogels: the rebirth of continuous wear contact lenses". Oxford: Butterworth-Heinemann, 2000.

[20] U.S. Food and Drug Administration. "FDA Talk Paper: FDA approves 30-night continuous wear contact lenses". 2001.

[21] V. McBrierty, J. Magan, W. Blau. "Laser curing of contact lens". In: 0447169 EPON, 1991.

[22] G. Odian. "Principles of Polymerization. 3rd Ed." New York: John Wiley & Sons Inc, 1991.

[23] L.H. Sperling. "Introduction to physical polymer science. 4th Ed." New Jersey: John Wiley & Sons, 2006.

[24] J.M. Yang, H.M. Li, M.C. Yang, C.H. Shih. "Characterization of acrylic bone cement using dynamic mechanical analysis". J. Biomed. Mater. Res. 1999; vol. 48: pp.52-60.

[25] A.Gloria, F.Causa, R. De Santis, P.A. Netti, L. Ambrosio. "Dynamic-mechanical properties of a novel composite intervertebral disc prosthesis". Journal of Materials Science: Materials in Medicine 2007; vol. 18: pp. 2159-2165.

[26] J.W. Nicholson. "The chemistry of polymers." Cambridge: The Royal Society of Chemistry, 1991.

[27] D. Campbell, R.A. Pethrick, White. "Polymer characterization. Physical techniques. 2nd Ed." Gloucestershire: Stanley Thornes Ltd, 2000.

[28] M.P. Stevens. "Polymer chemistry: an introduction. 3rd Ed." New York: Oxford University Press, 1999.

[29] R.J. Young, P.A. Lovell. "Introduction to polymers. 2nd Ed." Chapman & Hall, 1991.

[30] J.P. Fisher, D. Dean, P.S. Engel, A.G. Mikos. "Photoinitiated polymerization of biomaterials". Annual Review of Materials Research 2001; vol 31: pp.171-181.

[31] K.T. Nguyen, J.L. West. "Photopolymerizable hydrogels for tissue engineering applications". Biomaterials 2002; vol 23: pp.4307-4314.

[32] G. Oster, N.L. Yang. "Photopolymerization of vinyl monomers". Chem. Rev. 1968; vol 68: pp.125-151.

[33] C. Decker. "The use of UV irradiation in polymerization". Polym. Int. 1998; vol 45: pp.133-141.

[34] A. Uhl, R.W. Mills, K.D Jandt. "Polymerization and light-induced heat of dental composites cured with LED and halogen technology". Biomaterials 2003; vol 24: pp.1809-1820.

[35] R. Jallapuram, I. Naydenova, S. Martin, R. Howard, V.Toal, S. Frohmann, S. Orlic, H.J. Eichler. "Acrylamide-based photopolymer for microholographic data storage". Optical Materials 2006; vol.28: pp.1329-1333.

[36] P.X. Ma, J.H. Elisseeff. "Scaffolding in tissue engineering". Florida: CRC Press, 2005.

[37] J.V. Cauich-Rodriguez, S. Deb, Smith. "Effect of cross-linking agents on the dynamic mechanical properties of hydrogel blends of poly(acrylic acid)-poly(vinyl alcohol-vinyl acetate)". Biomaterials 1996; vol. 17: pp.2259-2264.

[38] L Ambrosio, R De Santis, L Nicolais. "Composite hydrogels for implants". Proc. Inst. Mech. Eng. [H]. 1998; vol. 212: pp.93-99.

[39] P.C. Nicolson, J. Vogt. "Soft contact lens polymers: an evolution". Biomaterials 2001; vol.22: pp.3273-3283.

[40] Y.C. Lai. "Effect of crosslinkers on photocopolymerization of N-vinylpyrrolidone and methacrylates to give hydrogels". J. Appl. Polym. Sci. 1997; vol.66: pp.1475-1484.

[41] K. Fisher, T. Comstock. "Clinical comparison of opaque tint soft contact lenses". International Contact Lens Clinic 1996; vol.23: pp.128-137.

[42] C. Decker. "Light-induced polymerisation of photoinitiator-free vinyl ether/maleimide systems". Macromolecular Chemistry and Physics 1999; vol 200: pp.1005-1013.

[43] http://www.ciba.com/photoinitiator.htm accessed 01 February 2008.

[44] M.G. Neumann, W.G. Miranda Jr., C.C. Schmitt, F.A. Ruggeberg, I.C. Corrêa. "Molar extinction coefficients and the photon absorption efficiency of dental photoinitiators and light curing units". J. Dent. 2005; vol 33: pp.525-532.

[45] Ciba Inc. Coating Effects, Klybeckstrasse 141, Basel 4002, Switzerland.

[46] http://www.ciba.com/ind-paints_and_coatings_technologies_curing-uvcuring-2.htm accessed 1st February 2008.

[47] J. Jakubiak, X. Allonas, J.P. Fouassier, A. Sionkowska, E. Andrezejewska, L.Å. Linden, J.F. Rabek. "Camphorquinone-amines photoinitiating systems for the initiation of free radical polymerization". Polymer 2003; vol 44: pp.5219-5226.

[48] J. Jakubiak, A. Wrzyszczyński, L.Å. Linden, .F. Rabek. "The role of amines in the camphorquinone photoinitiated polymerization of multifunctional monomer". J. Macromol. Sci., Chem. 2007; vol 44: pp.239-242.

[49] J.C. Salamone. Polymeric Materials Encyclopedia. Florida: CRC Press, 1996.

[50] J.J. Florio, D.J. Miller. Handbook of Coatings Additives. Florida: CRC Press, 2004.

[51] P.A. Davis, L. Nicolais, L. Ambrosio, S.J. Huang. "Poly(2-hydroxyethyl methacrylate)/Poly(caprolactone) semi-Interpenetrating polymer networks". J. Bioac. Comp. Pol. 1988; vol. 3: pp.205-218.

[52] M. Fernández-García, M.F. Torrado, G. Martínez, M. Sánchez-Chaves, E.L. Madruga. "Free radical copolymerization of 2-hydroxyethyl methacrylate with butyl methacrylate: determination of monomer reactivity ratios and glass transition temperatures". Polymer 2000;vol. 41: pp.8001-8008.

[53] V. McBrierty, J. Magan, W. Blau. "Laser curing of contact lens". In: 5154861 USPN, 1992.

[54] S.J. Martin. "Curing of complex monomer systems: A spectroscopic and thermal analysis", Doctural thesis. Department of Physics. Dublin: Trinity College, 2000.

[55] Y.C. Lai. "Method of curing methacrylate-based compositions", US Patent No. 5610204. 1997.

[56] C Gardner. "The use and misuse of coloures light in the urban environment". Optics and Laser Technology 2006; vol 38: pp. 366-376.

[57] S.L. McDermott, J.E. Walsh, R.G. Howard. "A comparison of the emission characteristics of UV-LEDs and fluorescent lamps for polymerisation applications". Optics and Laser Technology 2008; vol. 40: pp.487-493.

[58] http://www.shopelectrical.net accessed 10 November 2007.

[59] http://catalog.myosram.com/ accessed 27th November 2007.

[60] http://home.att.net/~ledmuseum/specx41.htm accessed 10 November 2007.

[61] W. Teshima, Y. Nomura, N. Tanaka, H. Urabe, M. Okazaki, Y. Nahara. "ESR study of camphorquinone/amine photoinitiator systems using blue light-emitting diodes". Biomaterials 2003; vol 24: pp. 2097-2103.

[62] T.H. Yoon, Y.K. Lee, B.S. Lim, C.W. Kim. "Degree of polymerization of resin composites by different light sources". J. Oral Rehabil. 2002; vol 29: pp.1165-1173.

[63] J.C. Ontiveros, R.D. Paravina. "Light-emitting diode polymerization: A review of performance, part 1". Acta Stomatologica Naissi 2006; vol 22: pp.601-610.

[64] F.G. Rosillo. "Lifetime evaluation of DC-supplied electronic ballasts with fluorescent lamps for photovoltaic applications". Renewable Energy 2004; vol 29: pp.961-974.

[65] L.O Björn. "Photobiology: The science of light and life": Springer, 2002.

[66] http://home.att.net/~ledmuseum/spectra7.htm accessed 10 November 2007.

[67] http://radionics.rs-online.com/ accessed 10 November 2007.

[68] http://www.uvprocess.com/product.asp?code=UV+LED+++C. accessed 15 November 2006.

[69] Radionics. "Solid State Lighting, your application and product guide".

[70] A. Berntsen, Y. Croonen, C. Liedenbaum, H. Schoo, R.J. Visser, J. Vleggaar, P. van de Weijer. "Stability of polymer LEDs". Optical Materials 1998; vol 9: pp.125-133.

[71] N. Narendran, Y. Gu, J.P. Freyssinier, H. Yu, L. Deng. "Solid-state lighting: failure analysis of white LEDs". J. Cryst. Growth 2004; vol 268: pp.449-456.

[72] A. Dodabalapur. "Organic light emitting diodes". Solid State Commun. 1997; vol 102: pp.259-267.

[73] R.W. Mills, A. Uhl, G.B. Blackwell, K.D. Jandt. "High power light emitting diode (LED) arrays versus halogen light polymerization of oral biomaterials: Barcol hardness, compressive strength and radiometric properties". Biomaterials 2002; vol 23: pp.2955-2963.

[74] F. Stahl, S.H. Ashworth, K.D. Jandt, R.W. Mills. "Light-emitting diode (LED) polymerisation of dental composites: flexural properties and polymerisation potential". Biomaterials 2000; vol 21: pp.1379-1385.

Chapter 2: Methods for light source characterisation and intercomparison

2.1 Introduction

When choosing ideal light source specifications for industrial processes, such as contact lens photopolymerisation, a number of factors need to be considered. These include output intensity, wavelength range and the related electrical output efficiency (i.e. conversion from electric energy to radiation energy), whether the light output is continuous or modulated (i.e. dc or AC), lifetime and start-up characteristics. For photopolymerisation processes it is important that the light source emits the majority of the output intensity at the key photopolymerisation wavelength with high efficiency, rapid start-up and stabilisation as well as having a constant output. The ability to accurately measure these characteristics is an important part of this research. This chapter details the different experimental techniques used to measure and compare the specifications of the lamp and the LEDs in order to evaluate the potential for LEDs to replace fluorescent lamps as the source of UV radiation in photopolymerisation process.

2.2 Light sources used

A number of different light sources were characterised and their behavioural properties inter-compared. At present the main source of UV radiation for use in the photopolymerisation processes is from fluorescent lamps. An example of the type of fluorescent lamps used by contact lens manufacturers is the Philips PL-S 9W/10 low pressure Hg lamp (Eindhoven, The Netherlands)[1], figure 2.1. These fluorescent lamps, representative of those used in

manufacturers' photopolymerisation processes, consist of two single-ended fluorescent tubes fused together and operate on the same universal ballast as other compact fluorescent PL-S lamps. Overall the majority of photopolymerisation processes utilise UV radiation as if infrared or visible light was used the system would have to be completely isolated from normal lighting and temperature surroundings, as such the fluorescent lamps used in photopolymerisation emit UVA [2] radiation in the 350-400 nm region. The properties of these lamps were measured and then compared to a number of different UV-LEDs.

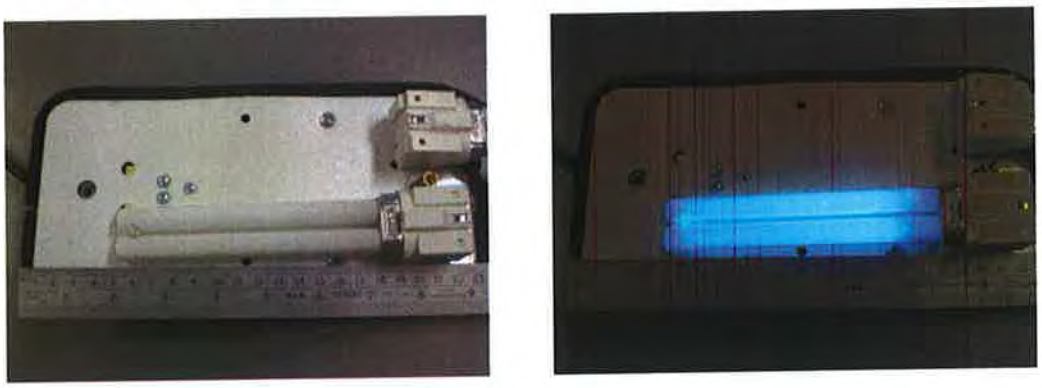

Figure 2.1: Photo of Philips PL-S 9W/10 low pressure Hg lamp.

Over the course of this research UV-LED production progressed and as a result a number of different UV-LEDs became available on the market. The LEDs used in this study were ones available that had a peak wavelength closest to that of the fluorescent lamp. At the start of the study the closest UV-LED available that matched the required specification was the Roithner Lasertechnik (Vienna, Austria) [3] UV-LED370-10 ball lens (figure 2.2). These LEDs also emit in the

UVA region of the electromagnetic (EM) spectrum and have a peak wavelength of 370 nm [4] which is approximately the same as the fluorescent lamp determined by the Hg emission. This LED circuit was set up as shown in figure 2.3 and throughout this thesis will be known as the single LED.

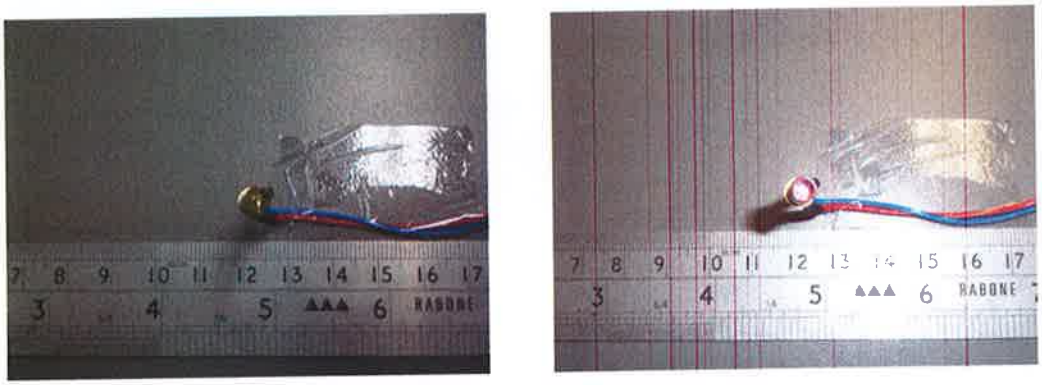

Figure 2.2: Photo of the single LED (UV-LED370-10 ball lens).

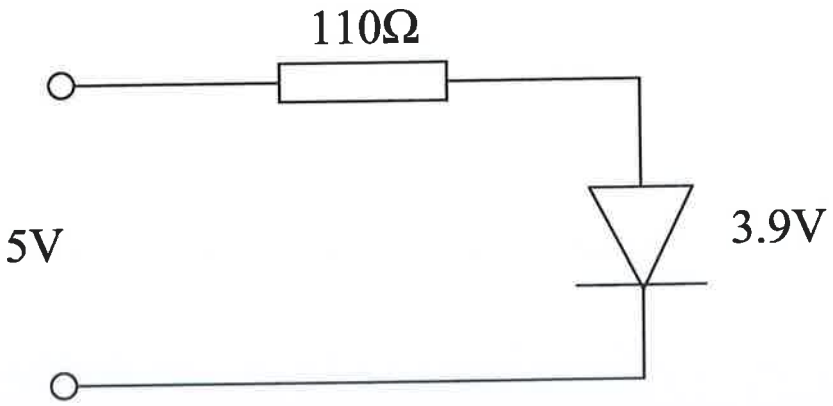

Figure 2.3: Circuit diagram of the single LED, showing a dc supply, regulating series resistor and forward biased diode.

Although this single LED was fully characterised and tested in a photopolymerisation set up, the next LED that became available became the main LED of interest due to its higher UV output. The manufacturers' specifications give a total output power of 750 μW for the single LED compared to 20 mW for the LED array at their respective wavelengths. Due to the completely different nature of the fluorescent lamp, for example the surface area, a comparative figure is not available. However its electrical power is given as 9 W which would be related to its total light output power by its efficiency, which is not readily available and as the output is a function of all the output wavelengths the UV efficiency is not easily obtained. In addition, lamp output efficiencies are generally given in lumens/Watt that would not include any UV output power. This LED array was the Roithner Lasertechnik (Vienna, Austria) [3] LED375-66-60-110 array model. As this LED was an array consisting of a total of 60 UV diode chips it had a higher output intensity than the single LED, like the previous two sources this LED array also emitted in the UVA region but had a higher peak output wavelength of 375 nm [5]. Throughout this thesis this LED will be known as the LED array. Figure 2.4 shows a photo of this LED array while its circuit diagram is shown in figure 2.5.

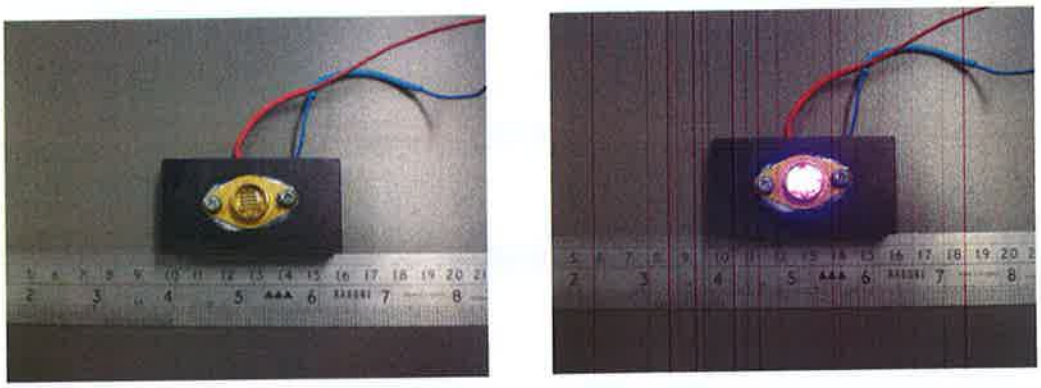

Figure 2.4: Photo of the LED array (LED375-66-60-110 array model).

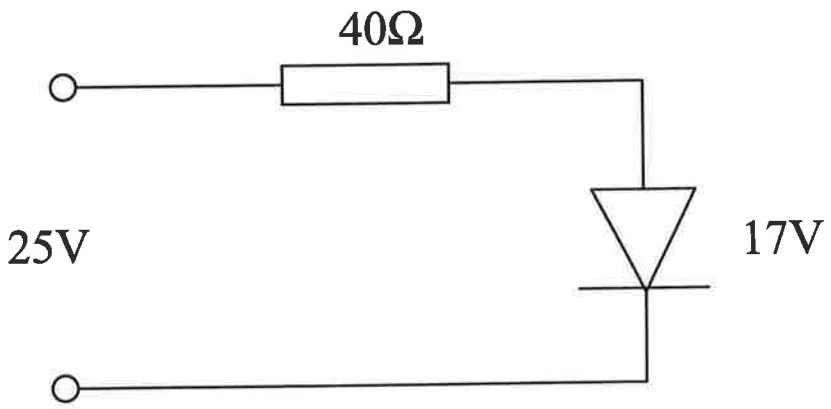

Figure 2.5: Circuit diagram of the LED array showing a dc supply, regulating series resistor and forward biased diode.

The third type of LED used in this research was the LED cure-all™ linear 100 array supplied by UV process (Illinois, USA) [6]. Two of these LEDs were purchased one that emits at 375 nm and the other at 450 nm. These devices are larger than those previously used and will be known as large LED arrays during this thesis. The relevant circuit for the LED arrays is contained within their

modular dc power supply unit, supplied by the manufacturers. These LEDs did not become available until late in the study and were used to investigate the affect of pulsing on the photopolymerisation process, after the initial proof of concept was achieved with the first two LEDs. Figure 2.6 shows a photograph of one of the large LED array used in this study. Their characteristic study is discussed later in chapter 6, section 6.2. The results of the characterisation study of the fluorescent lamp, the single LED and the LED array are discussed in chapter 3.

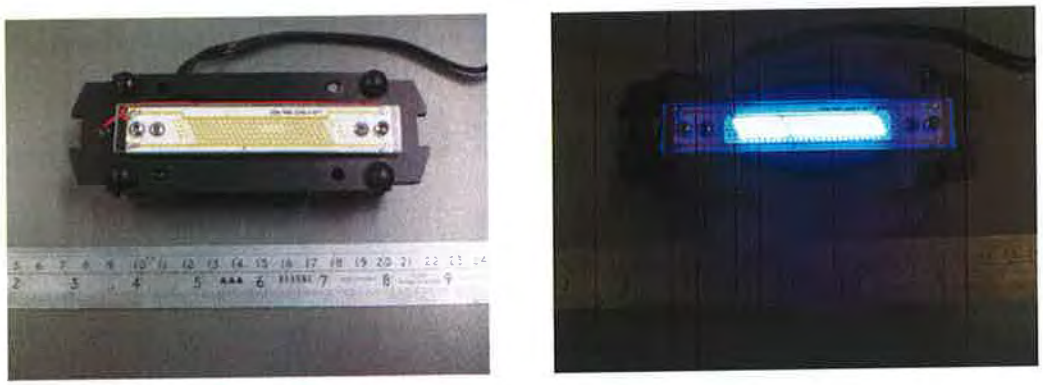

Figure 2.6: Photo of the large LED array.

2.3 Properties measured

From a photopolymerisation perspective there are a number of key specifications that need to be considered when choosing what light source to use. Table 2.1 gives a list of such specifications and the ideal behaviour of each for a photopolymerisation process. Each of the light sources was fully characterised, using these guidelines as a template, by using a number of different techniques. At the end of chapter 3 these ideal specifications are compared to the actual specifications achieved for each of the first three light sources used in this study. The order of specifications in the table is also the order in which they were

measured; the reason for this is that specific behavioural outputs needed to be prioritised so that other characteristics could be measured.

Table 2.1: Ideal light source specifications

Specifications	Ideal
AC/dc	Continuous output
Warm-up Time	Instantaneous switch on
Stability	Continuous stable output
Lifetime	Limitless
Current -v- Intensity	Maximum light output for minimum electrical power in
Wavelength range/ Peak wavelength	Emits only over wavelength range needed for photopolymerisation
Intensity -v- Distance	Maximised intensity at light source sample distance in manufacturing set up
UV output intensity	Maximum for minimum number of lights
Efficiency	100 %

2.3.1 Continuous (dc) or modulated (AC) light output

Fluorescent lamps 'flicker' due to the nature of their electrical supply which is AC (i.e. 50 Hz in Europe) This causes repeated changes in their output light intensity that cannot be seen by the human eye, as human flicker fusion is typically greater than 20 Hz, but may effect fast photopolymerisation reactions.

LEDs on the other hand can be powered by a dc supply meaning their output intensity is not affected by 'flickering'. Note: in this chapter and chapter 3 the acronym dc refers to direct current while later on DC refers to degree of conversion. To investigate how much the intensity of the fluorescent lamp varies due to the AC nature its output intensity was observed and measured using a fast photodiode attached to an oscilloscope. This was then compared to the dc nature of the LEDs, which is ideal for use in the manufacturing process.

2.3.2 Warm up time, long term stability and lifetime

Warm up is an important factor to be considered when using UV light sources in manufacturing processes (i.e. the time after switch on for the device to achieve sufficient electrical and thermal stability). It has been well documented that fluorescent lamps need to be activated for a period of time prior to use to allow them to sufficiently warm up while due to the semiconductor nature of LEDs it is expected that they will emit at a constant output as soon as they are switched on.

Frequent sampling of temperature and intensity over time was recorded for each light source to investigate their warm up time after which their stability was measured. The intensity of the LEDs was recorded using a Solar Light PMA2100 radiometer with the PMA2107 UVA/B detector attached. This detector has a broad response from 260 nm to 400 nm which is relatively flat in the region from 300 nm to 370 nm (see figure 2.7). It incorporates a diffuser whose Lambertian response makes it suitable for measuring diffuse and/or direct radiation from extended sources. The Solar Light PMA2100 radiometer is primarily used to measure the intensity of dc powered light sources and is not ideal for making

direct intensity readings from AC sources such as the fluorescent lamp, as it has a 1 s sampling rate. However this section of the study is only concerned with how the relative output intensity behaves over time and not the actual output intensity. Therefore this radiometer can be used to obtain the relative intensity profile of the light source characteristics while also measuring absolute intensity values when required.

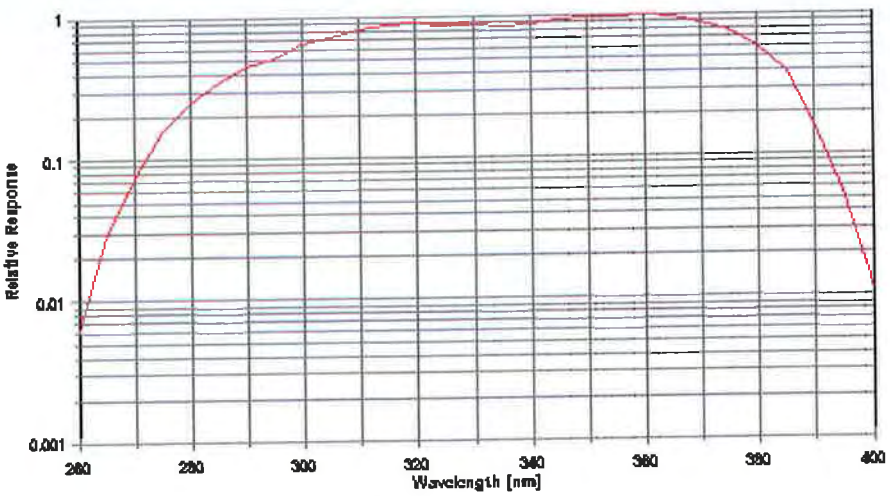

Figure 2.7: Spectral response of PMA 2107 detector [7].

To measure the warm up time the intensity readings from each light source were recorded every minute for the first 30 minutes after which their stability was measured by recording the intensity output every hour over an eight-hour period. It had been hoped to measure the stability over a few days. However preliminary results showed that the lamp became very hot after a short period of time so for safety reasons the lamp was only left on during the day, under supervision. Ideally, to measure lifetime this study would have involved continuous measurement of the output intensity over a prolonged period of time. However

since LEDs have been quoted as having a lifetime of up to 100,000 hours this would have involved a considerable amount of time that this study did not allow for.

2.3.3 Current -v- Intensity measurements

As the output intensity for the single LED and the LED array can be varied by varying current it was important to examine this relationship to ensure that the LEDs were at their maximum output intensity for minimum power consumption. For each LED tested the output irradiance was measured using the Solar Light radiometer at a fixed distance over a range of currents from 0 mA to the maximum specified current. As the output of the fluorescent lamp is determined by the manufacturers ballast circuit the current-intensity relationship was not easily determined and is largely pre-set by the fluorescent lamp's design.

2.3.4 Spectral output and peak wavelength

To experimentally compare the specifications of the fluorescent lamp and the UV-LEDs a number of important factors relating to their respective configurations and operating principles need to be considered. The most important of these is how to relate the light output from a fluorescent tube to that of an LED so that a reasonable logical intercomparison can be made. Due to their smaller size the output of the LEDs is relatively straight forward to measure. A more complex problem arises with the fluorescent lamp, as the lamp consists of two 128 mm long, 13 mm diameter tubes they do not compare well to the LED in their output light field. To overcome this problem the lamp was completely masked off except for an area equal to the diameter of the LED array. The output nature of these two

light sources was then reasonably similar assuming no front lens is present, so that certain specification comparisons could be made. To decide what area to leave exposed the intensity along the tube length was recorded, after which the point along the tube at which the greatest intensity was emitted was left unexposed. It was this point that would then be used in all future measurements.

As already stated the Solar Light radiometer is not ideal to make direct intensity readings from AC sources like the lamp. To use this radiometer to measure the intensity output of the AC fluorescent lamp it was connected to an oscilloscope and the equivalent detector voltage readings were recorded. These voltage readings were then converted to intensity values using a prior calibration from the dc LED source (i.e. by measuring the intensity value and the maximum voltage reading of the LED, the voltage reading of the lamp could be converted to an intensity value).

As photopolymerisation is wavelength dependent one of the most important properties of the light sources to be investigated was the peak wavelength and spectral output. The spectrometer system used to investigate the peak wavelength and spectral output of the light sources was the Ocean Optics IRRAD2000 spectrometer (Dunedin, Florida) [8]. This system operates over a broad range in the UV, visible and near-infrared regions from 350 nm to 950 nm [9] and was wavelength calibrated using a Ocean Optics Cal 2000 Mercury Argon calibration light source lamp and intensity calibrated using the Ocean Optics LS 1 cal [10]. The test light sources were coupled to the spectrometer using a 200 μm diameter UV/Vis fibre with a cosine-corrector irradiance probe attached to the fibre. The cosine-corrector attaches onto the end of the optical fibre and when

coupled to the Ocean Optics spectrometer can be used to measure UVA and UVB radiation collected from a 180° field of view [11].

The spectral output of each of the test light sources was then recorded using the Ocean Optics software, OOIBase32. From these spectra the wavelength range and the peak wavelength emitted by each source was found and compared to the manufacturer's data. The output spectra of each light source at fixed distances (0 mm, 5 mm, 10 mm, 20 mm, 30 mm, 40 mm, 50 mm and 60 mm) away from the fibre optic were recorded. This gave a visible profile of how the intensity of each source behaved with distance and discover the size of the near field and far field with the current set up.

The overall peak intensity output could also be measured by examining these spectra; this was carried out by integrating the peak wavelength for the full-width at half-maximum (FWHM i.e. 50% bandwidth) [12]. To verify the measurement method the intensity was also measured using the Solar Light PMA2100 radiometer. This technique is presented in section 2.3.5.

2.3.5 UV light intensity using Solar Light radiometer

In order to allow for optimum conditions for photopolymerisation it is important to know the light intensity emitted by each source, the nature of the output beam and how the intensity behaves over distance. There are many inherent difficulties that arise when inter-comparing light sources that have different shapes, sizes, output spectra and colour temperature. These differences can be minimised by reducing as many of the variables as possible and checking the results against a calibrated broad band calibrated radiometer [12].

Once again the intensity of the LEDs were recorded using a Solar Light PMA2100 radiometer with the PMA 2107 UVA/B detector attached, while the intensity of the fluorescent lamp was measured using the oscilloscope set up detailed earlier and in published literature [12]. These voltage readings were then converted to intensity values allowing for a direct comparison of the output intensity for each source.

2.3.6 Intensity at Different Distances

Another factor to be considered when designing the photopolymerisation set up was at what distance to place the light sources from the monomer sample. Intensity against distance studies for each light source were previously recorded using the Ocean Optics spectrometer (section 2.3.3). However as a comparison the intensity-distance relationship was also recorded using the Solar Light radiometer. To observe how intensity varied with distance each light source was moved away from the detector in steps of 5 mm to a maximum distance of 50 mm, recording the intensity at each step.

2.3.7 Beam Uniformity

As the fluorescent lamps produce irradiation over a wide area it can be presumed that this irradiation is uniform. However it is not certain what effect the presence of the lens on the single LED would have on uniformity. To see what, if any, effect the front lens optics would have the beam uniformity of this LED its spatial output was measured using a CCD camera and analysed using MatLab software. The spatial output of the other light sources was not investigated as it was confident that they would behave well as no optics were present.

2.4 Conclusion

When choosing ideal light source specifications for industrial processes, such as contact lens photopolymerisation, a number of factors need to be considered. These include warm up time, stability, wavelength range and peak wavelength output. In this study each of these specifications among others were investigated for each light source used. A number of different experimental techniques were used to measure these properties, reducing variables for best possible intercomparison. The results of these experimental techniques are discussed in chapter 3.

2.5 References

[1] http://www.prismaecat.lighting.philips.com PL-S 9W/10/2P UNP datasheet accessed 4 February 2007.

[2] CIE International Lighting Vocabulary. Bureau Central de la Commission Internationale de l'Eclairage Paris, 1970.

[3] Roithner Lasertechnik Vienna Austria Europe.

[4] www.roithner-laser.com UV-LED370-10 datasheet accessed 12 March 2006.

[5] www.roithner-laser.com LED375-66-60-110 datasheet accessed 14 August 2007.

[6] UV Process Supply Inc. Chicago Illinois.

[7] http://www.solar.com/pma2107.htm accessed 08 March 2007.

[8] Ocean Optics. Dunedin Florida.

[9] Ocean Optics. Operating manual and user's guide. IRRAD2000 miniature fiber optic spectroradiometers. 1999.

[10] http://www.micropack.de/d/specto/pdf_downoads/light_sources.pdf pg. 118 accessed 5 November 2006.

[11] Ocean Optics. Operating manual and user's guide. S2000 miniature fiber optic spectrometers and accessories. 2005. p.87.

[12] S.L. McDermott, J.E. Walsh, R.G. Howard. "A comparison of the emission characteristics of UV-LEDs and fluorescent lamps for polymerisation applications". Optics and Laser Technology 2008; vol. 40: pp.487-493.

Chapter 3 Result for light source characterisation

3.1 Introduction

In this chapter detailed accounts of the light source specifications required for photopolymerisation, and those achieved with the fluorescent lamp, the single LED and the LED array used in this research are given. The emission characteristics of the newer UV-LEDs that became available later in research are discussed in chapter 6. A number of different techniques, discussed in chapter 2, were utilised to characterise the properties of the light sources. For photopolymerisation processes it is important that the light source emits the majority of the output intensity at the key photopolymerisation wavelength with high efficiency and constant output while displaying a rapid start-up. As each source was fully characterised the results allowed for an intercomparison of how each source behaved and comparisons made for the given specifications outlined in table 2.1. No one light source satisfies all the conditions of an 'ideal' source as listed in table 2.1 as with all optical designs a compromise must be made. However it is proposed that the novel UV-LED sources used in this study exhibit more of the 'ideal' specifications listed than the traditionally used fluorescent lamps [1].

3.2 Continuous or modulated light output

Figure 3.1 compares the AC output nature of the lamp to the stable DC nature of the LED array as measured using the Solar Light PMA2100 radiometer coupled directly to an oscilloscope, therefore avoiding the slow 1 s sampling rate of the Solar Light radiometer electronic read out module. In this figure the output

intensity of the fluorescent lamp is repeated approximately every 20 ms, corresponding to a frequency of 50 Hz, which is the frequency of mains electricity in Ireland. Although it has not been investigated what effect a delivered AC UV dose has on the photopolymerisation process it is expected to be insignificant as the switching time of the AC source is so short (order of milliseconds) compared to typical photopolymerisation times which are of the order of 100 s [1].

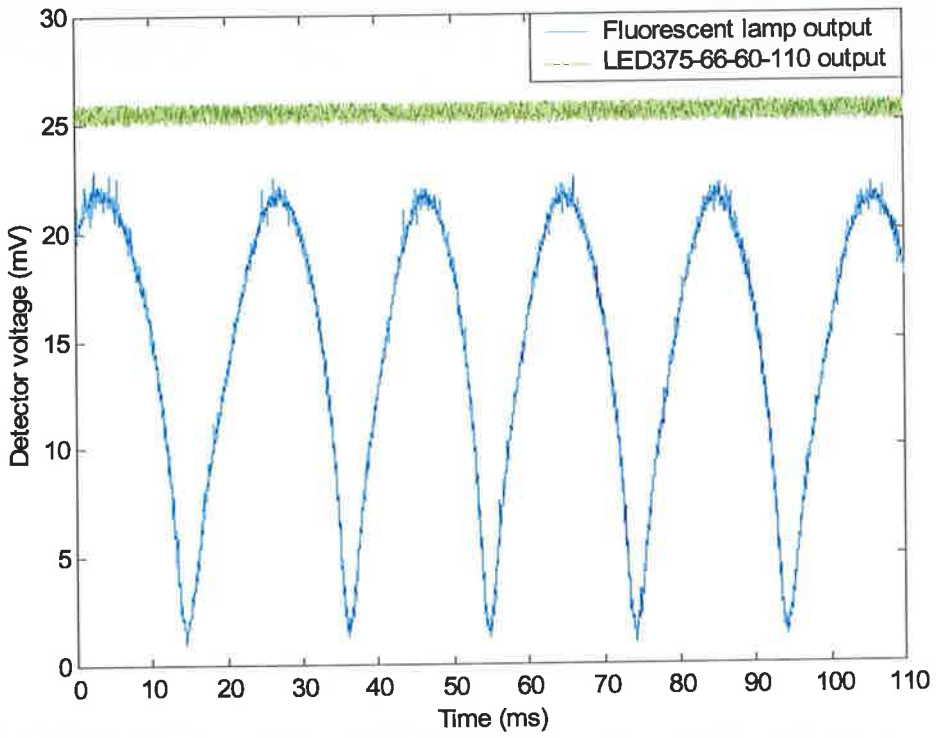

Figure 3.1: Temporal nature of output light intensity, showing the oscillating AC output nature of fluorescent lamp and the stable DC nature of LED.

3.3 Warm up time, long term stability and lifetime

Ideally for photopolymerisation processes a light source would exhibit a very rapid on/off characteristic; this would allow for a minimum warm up time and permit the light source to be used immediately after switch on reducing the

activation time required prior to curing. Typically a 30 minute activation time is required before fluorescent lamps can be used in a photopolymerisation process. Minimising this activation time would lead to savings in time, energy and money for the manufacturer. Figure 3.2 shows the output stability for the three light sources over an 8-hour period, with the first hour of warm up time inset. From these results it can be seen that the lamp has a warm up time of approximately 120 minutes while the LED array took approximately 30 minutes for its intensity to stabilise. Although this is not ideal it is four times faster than the lamp. However from the single LED it can be seen that it is possible for a UV emitting LED to stabilise almost instantaneously after switch on. This LED reaches its maximum intensity output almost instantly and emits at constant output over time. To understand why the LED array did not instantly emit at a constant output its temperature was recorded using a thermocouple, during this warm up time (figure 3.3). It was found that the LED array intensity output stabilised when the temperature stabilised. The reason for this unexpected behaviour is due to the thermal-electric characteristics of this LED array [1]. It has been reported that the thermal-stability of LEDs varies depending on the type of material used to manufacturer them [2]. This problem may have been overcome by applying a larger heat-sink to the LED array, as this would allow the temperature of the LED array to stabilise more quickly.

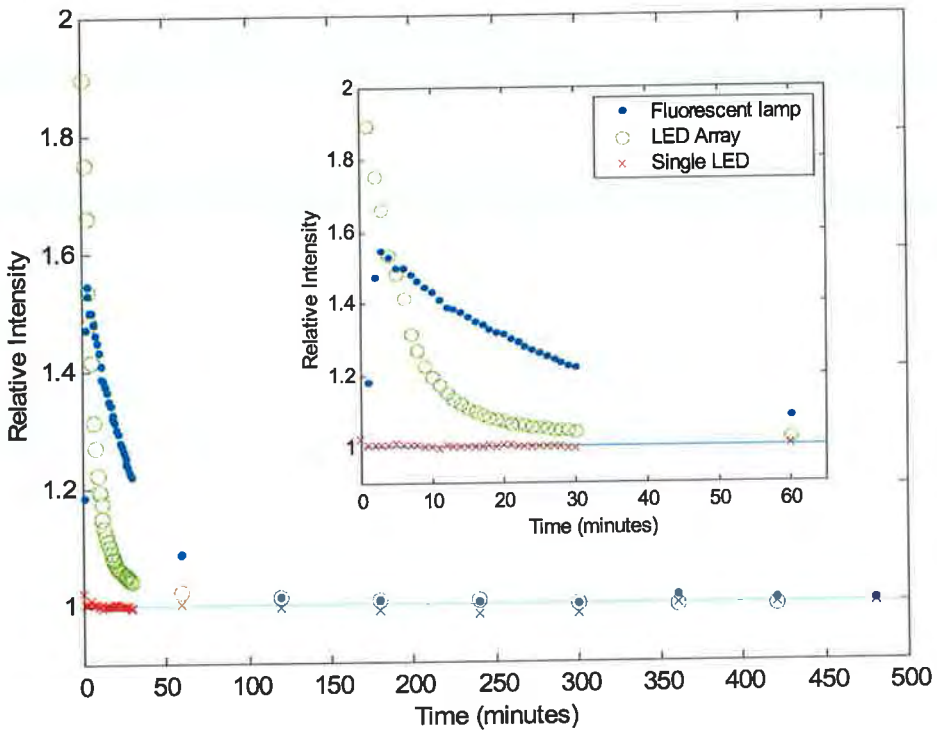

Figure 3.2: Intensity stability and warm-up time of lamp, the single LED and the LED array.

Another area that is of interest to manufacturers is the lifetime of the light source. The problem with lifetime measurements is the long duration of the tests, for example 100,000 hours is over 11 years 24/7 continuous operation making it impossible to undertake lifetime measurements for this study. However, it has been reported that fluorescent lamps have a lifetime of between 2,000 and 10,000 hours [3, 4]. In 1996 LEDs had an operational lifetime of only a few hours [5]. However it has now been reported that LEDs have a lifetime of between 50,000 to 100,000 hours [6, 7]. Although this is not infinite it is a considerable increase on the lifetime of the lamps currently being used.

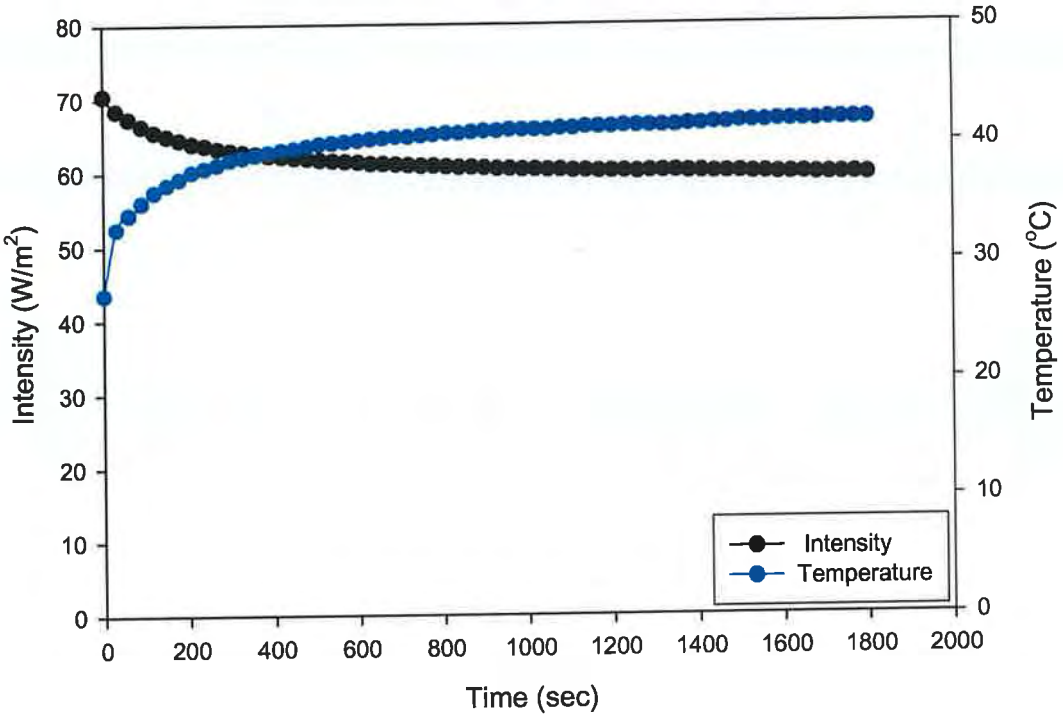

Figure 3.3: Thermal stability of LED array.

3.4 Intensity -v- Current

Due to their set up the output intensity of the LEDs could be varied by varying current. It was not possible to vary the intensity output of the fluorescent lamp as due to its nature the lamp is either 'on' or 'off'. To obtain intensity-current graphs for each LED the output irradiance was measured using the Solar Light radiometer at a fixed distance (10 mm) over a range of currents from 0 mA to the maximum specification current. It was expected that for each LED the maximum output irradiance would occur when the LEDs were run at maximum current specified by the manufacturers.

3.4.1 Single LED

To examine the relationship between current and the amount of UV radiation being emitted by the single LED the current was altered from 0 mA to 12 mA. The current was measured using an ammeter while the intensity was recorded using the Solar Light detector. From figure 3.4 it can be seen that the intensity increased linearly at low current and at currents above 10 mA the output of the LED behaves well.

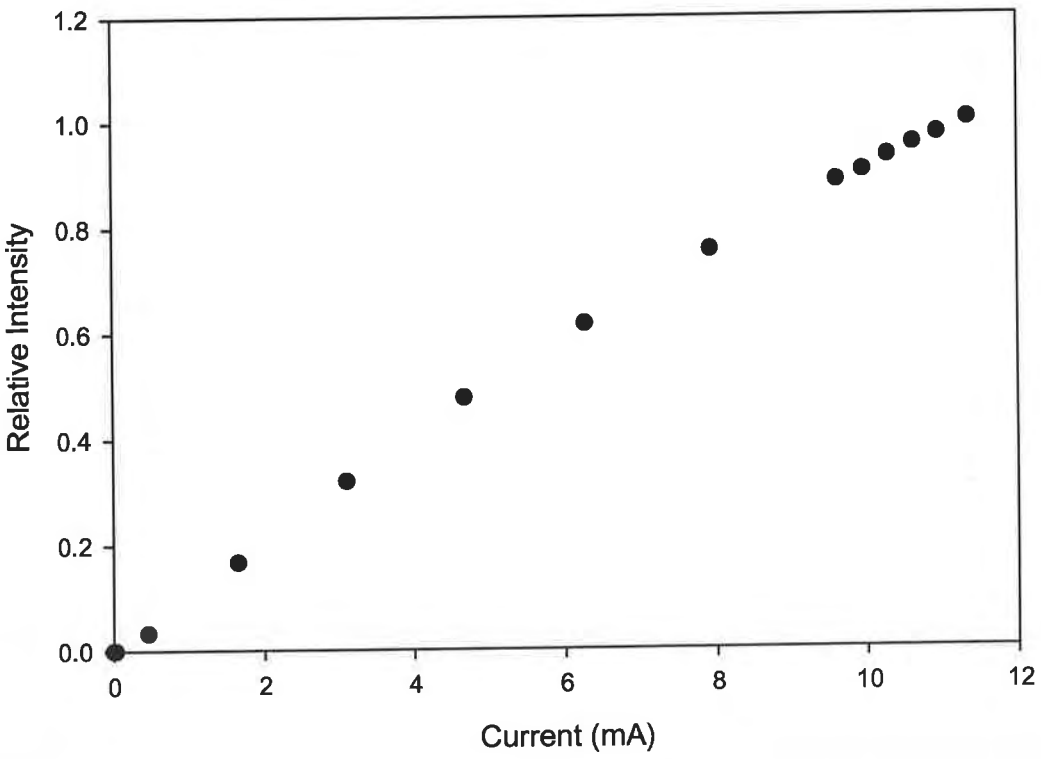

Figure 3.4: Current -v- Intensity profile for single LED.

3.4.2 LED Array

For the LED array the current was altered from 0 mA to about 200 mA. The corresponding voltage across the LED was measured, as was the intensity

emitted. Figure 3.5 shows how the output of this LED increases with increasing current. This LED did not increase linearly like the previous LED.

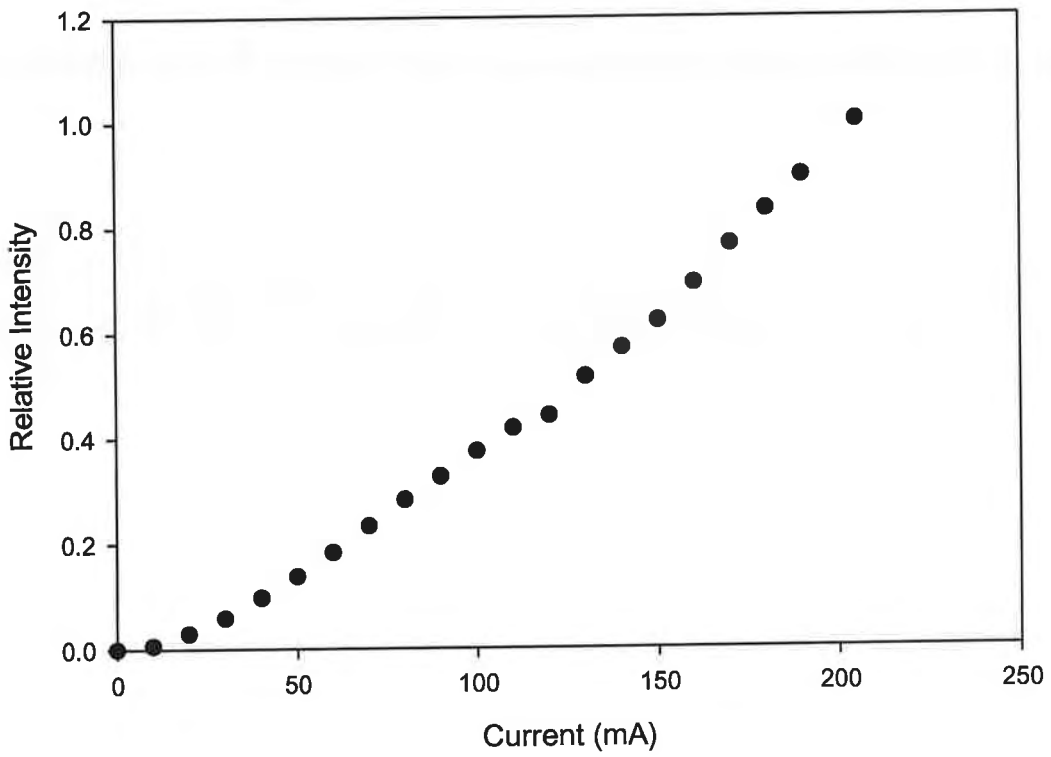

Figure 3.5: Current -v- Intensity profile for LED array.

3.5 Spectral characterisation of light sources

Photopolymerisation is achieved by adding a light sensitive compound (photoinitiator) that is activated by light of an appropriate wavelength. As the light energy (usually UV) is emitted it is absorbed by the photoinitiator causing it to fragment into its reactive species inducing photopolymerisation. As photoinitiators are wavelength dependent it is important to know the spectral output and peak wavelength of the light source so that the emission spectrum of

the light source can overlap with the absorption spectrum of the photoinitiator. This section is concerned with measuring and comparing these properties.

3.5.1 Variation in intensity along the length of the fluorescent lamp

As explained in section 2.3.3, an area of the fluorescent lamp the same diameter of the LED array was masked off, to make their output fields reasonably similar. To find what section of the lamp had the highest intensity for repeatability and therefore the section to leave exposed, the Solar Light radiometer was used to measure the intensity along the length of the tube. Figure 3.6 shows how the intensity varies along the length of the bulb, with 0 mm corresponding to the insertion part of the lamp (i.e. the piece that insets into the ballast). From this graph it can be seen that the highest output intensity from the lamp was found at a distance of 50 mm from the insertion point. Therefore it was this point along the bulb that was left exposed and where all future measurements were taken.

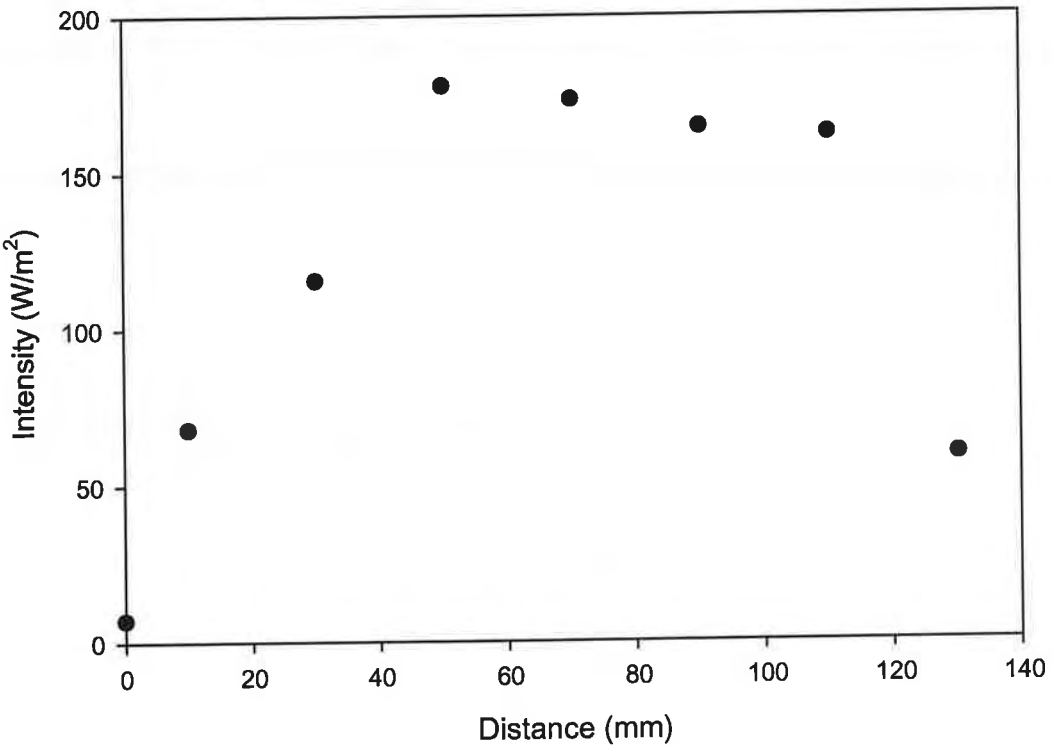

Figure 3.6: Intensity output along length of fluorescent lamp.

3.5.2 Spectral output and peak wavelength

Figure 3.7 shows the output spectra of the fluorescent lamp at different distances as seen by the Ocean Optics spectrometer (discussed in section 2.3.3). From this data it was found that the lamp had a maximum wavelength peak of 372 nm and emitted peaks over a wavelength range of 350 nm to 625 nm. The manufacturers stated this source as having a peak wavelength of about 370 nm. Note that there are also several peaks (405 nm, 436 nm, 547 nm and 579 nm) emitted in the visible region which are not required for the current photopolymerisation industrial processes. The peak at 372 nm is the main peak of interest for this process.

Several UV-LED370-10 ball lens single LEDs, which according to the manufacturers had a peak wavelength of 370 nm, were examined to get a typical peak wavelength and spectral output. These LEDs were found to emit over a wavelength range of 360 nm to 414 nm (figure 3.8) but unlike the lamp had only one peak wavelength, which occurred at 377 nm. The manufacturers stated the LED array as having a peak wavelength of 375 nm emitting over a wavelength range of 365 nm-385 nm. Using the Ocean Optics set up the LED array was found to have one peak wavelength at 382 nm over a range of 360 nm to 420 nm (figure 3.9). While the measured peak wavelength of each LED did not exactly match those stated by the manufacturers a ± 10 nm variance is acceptable according to the manufacturers [8].

From these results it was observed that the lamp also emits radiation in the visible region while the LEDs did not. This is one of the advantages that LEDs have over fluorescent lamps; they emit radiation at the required wavelength without producing any unnecessary radiation in other regions. And since only wavelengths where the photoinitiator absorbs are useful for photopolymerisation (as it is this absorption that promotes the molecule to an excited state leading to the production of free radicals [9]), this makes LEDs very desirable for use in curing process. It can also be seen that the single LED has a lower output intensity compared to the fluorescent lamp and the LED array. The LED array has a higher intensity than the lamp at the required wavelength for photopolymerisation. As the amount of radiation being emitted has an effect on the photopolymerisation process [10, 11] it is important to know the output intensity of the sources. This specification is discussed in section 3.5 and 3.6.

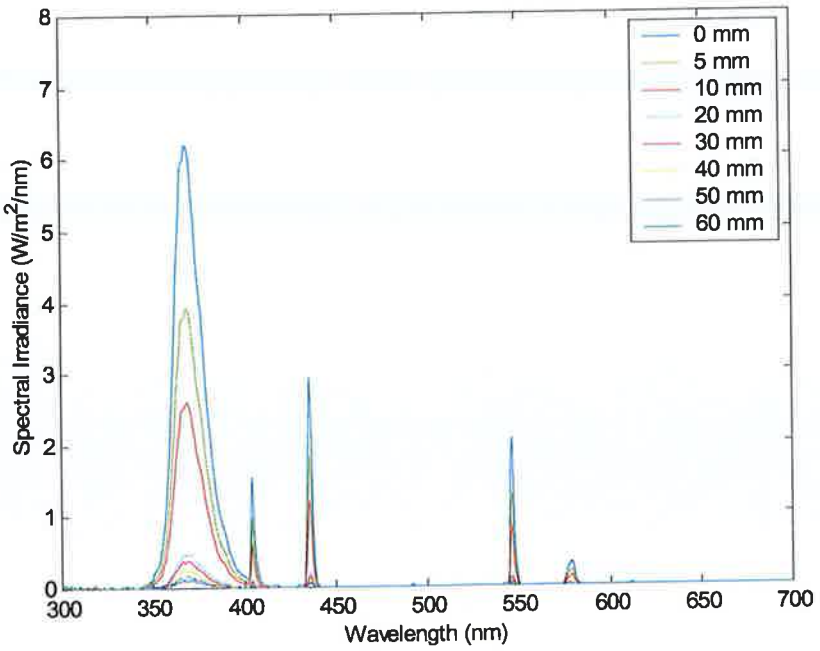

Figure 3.7: Spectral output of fluorescent lamp at different distances as seen by Ocean Optics spectrometer.

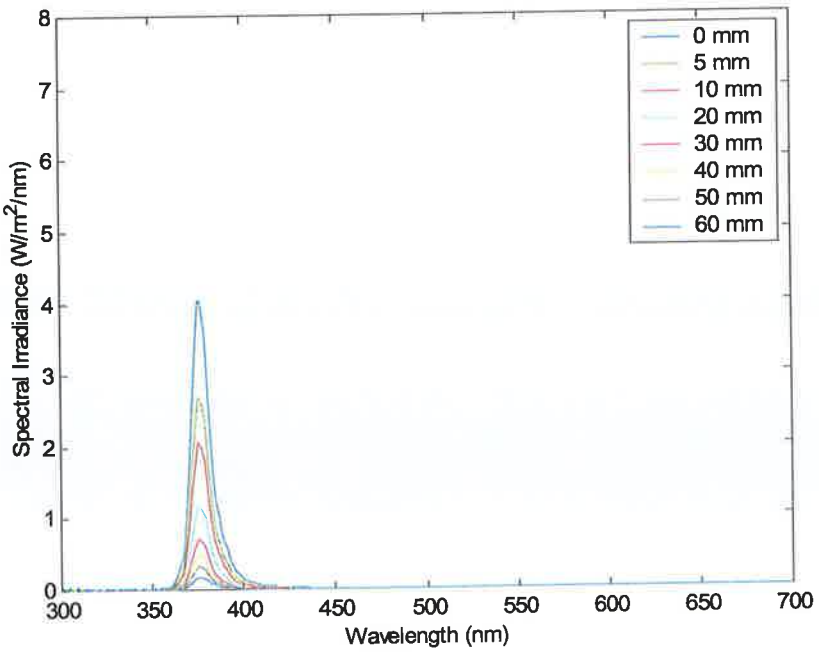

Figure 3.8: Spectral output of single LED at different distances as seen by Ocean Optics spectrometer.

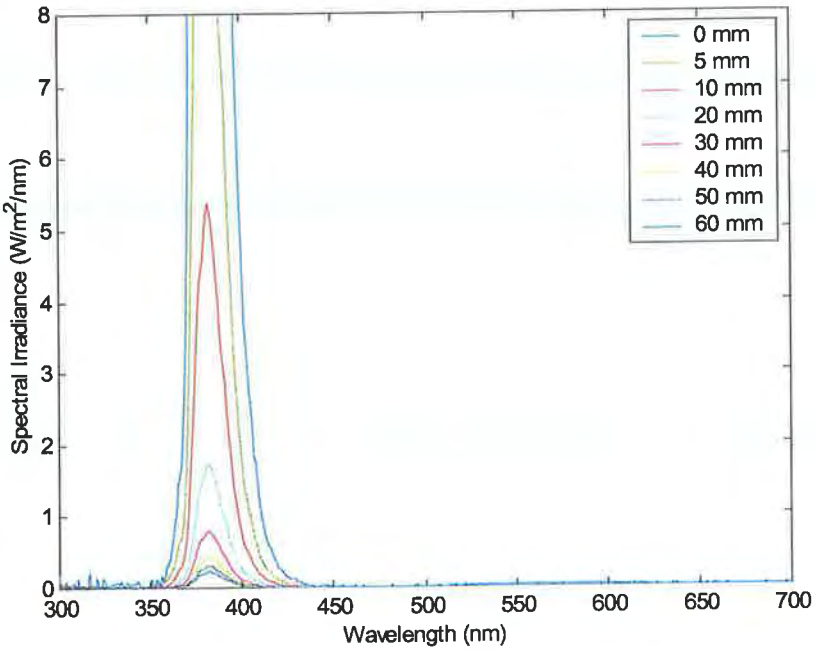

Figure 3.9: Spectral output of the LED array at different distances as seen by Ocean Optics spectrometer.

3.6 UV light intensity

3.6.1 Intensity as measured using Ocean Optics spectrometer

As photopolymerisation is not only dependent on wavelength but also on intensity [10, 12] it is important to know the intensity of each light source irradiating the monomer sample. The previous spectral output spectra (figures 3.5-3.7) were used to measure the intensity at a certain distance. Figure 3.10 shows the relative spectral output of each light source at a distance of 50 mm as obtained using the Ocean Optics spectrometer (section 3.4.2). On examining the fluorescent lamp spectrum, it was found to have a peak intensity output at 372 nm of 0.15 W/m^2, while the single LED has a peak intensity of 0.32 W/m^2 at 377 nm. At first glance the intensity of the single LED at 50 mm appears to be similar to

that of the LED array whose output intensity is approximately 0.30 W/m^2 at 382 nm. However on closer inspection the LED array has a wider bandwidth, with a full-width at half-maximum (FWHM i.e. 50% bandwidth) of 20 nm compared to a FWHM of just 13 nm for the single LED. This meant that the output intensity of the LED array will in fact be higher than the single LED as its output is over a wider spectral range. It should be noted that the spectral resolution of the fibre optic spectrometer used was less than 3 nm which is more than adequate to determine the bandwidth of the lamp and LED peaks examined [13].

The output intensity values for each light source were obtained by integrating under the FWHM area. The peaks emitted by the fluorescent lamp in the visible region are not included in this calculation, as they do not affect the photopolymerisation process; however energy is lost in these sidebands which do not occur in the LED. Using this principle the output intensity of the fluorescent lamp was found to be approximately 1.5 W/m^2 (for 372 nm peak only), while the intensity of the single LED was calculated to be 2.13 W/m^2. The LED array had the highest output intensity of 2.90 W/m^2. It was not expected that the single LED would be more intense than the fluorescent lamp, especially when considering figures 3.7 and 3.8 where the fluorescent lamp clearly has a higher output intensity than the single LED. One reason that explains this difference is that the intensity value of the lamp does not take into account the other wavelengths emitted by the fluorescent lamp, if the other wavelengths were included in this calculation naturally the overall intensity value would increase.

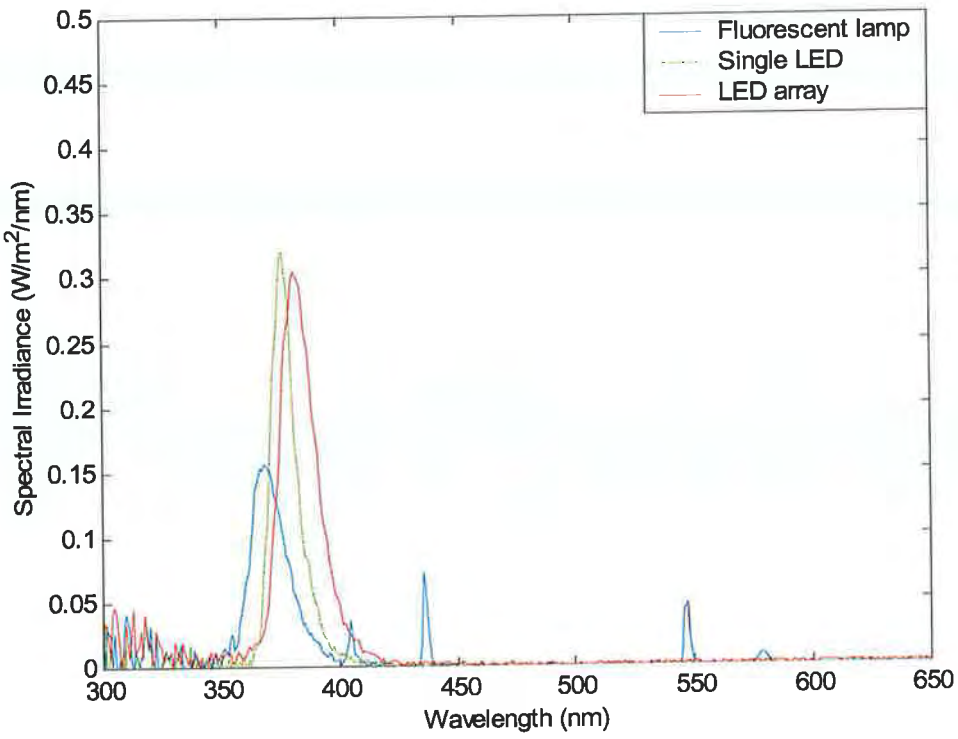

Figure 3.10: Relative spectral output of each light source at a distance of 50 mm.

3.6.2 Intensity as measured using Solar Light radiometer

The previous calibrated spectrometer was used to show the relative spectral output, from which intensity could be calculated, as a comparison to these intensity values the intensity of each light source was also measured using the Solar Light PMA2100 radiometer. The Solar Light radiometer allowed for the total UV radiation output to be directly measured without having to integrate under the graphs. For these readings the light sources where held at the same distance of 50 mm away from the PMA2107 UVA/B detector. Using this technique the fluorescent lamp was found to have an intensity value of 2.46 ±0.5 W/m^2 at the masked off area, while intensity values of 1.51 ±0.5 W/m^2 and 2.76 ±0.5 W/m^2 were found for the single LED and the LED array respectively.

However as the spectral response of the PMA2107 UVA/B s detector drops off above 365 nm (figure 2.7), the intensity values obtained for each light source using this detector had to be corrected for this spectral response. When corrected for the spectral response of this detector the intensity of the lamp was found to be 2.70 ±0.5 W/m^2, the single LED had an intensity output of 2.16 ±0.5 W/m^2, while the LED array had an output intensity of 5.52 ±0.5 W/m^2. These values are of the same order of magnitude as those measured using the Ocean Optics spectrometer.

3.6.3 Beam uniformity of LED with lens

As the presence of the front end lens on the single LED affect its output characteristics it was then decided to see how the lens affected beam uniformity. For this, the spatial output of this LED was recorded using a CCD camera. Figure 3.11 (a) and (b) show an image of the single LED as captured by the camera. In both of these images a dimple can be seen in the middle of the LED image. Although the dimple size is quite small, accounting for about 20 of the 250 digital numbers, it is something that should be taken into account when choosing an LED. This may make LEDs that have lenses unsuitable for photopolymerisation processes as the output field is not uniform and complicates matters. This feature requires further research but as this LED was the only light source that had a front lens it was not necessary to measure the beam uniformity of the other two sources as it was confident that they would behave well.

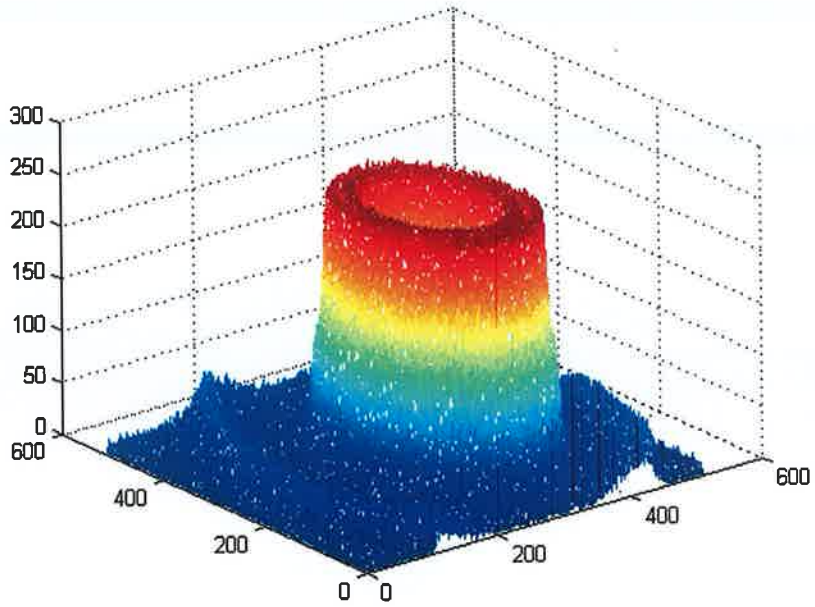

Figure 3.11 (a): Image structure of low output LED (axis in digital units)

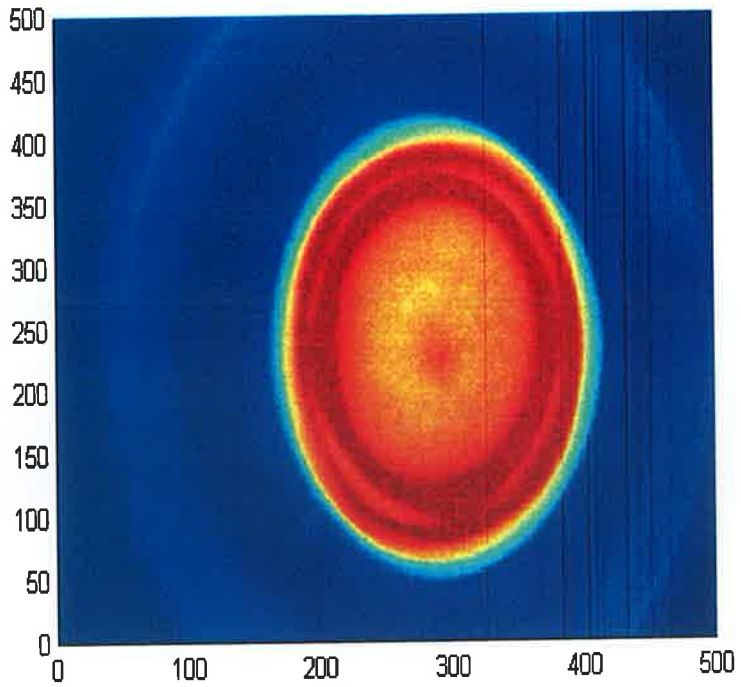

Figure 3.11 (b): Cross-section image of low output LED (axis in digital units)

3.7 Conclusion

This study used two different techniques to characterise and compare the optical properties of the fluorescent lamp, the single LED and the LED array. The Ocean Optics IRRAD2000 calibrated spectrometer was used to show the relative spectra of each light source from which the intensity at each λ_{max} was calculated, using FWHM. The Solar Light PMA2100 radiometer was also used to measure the amount of radiation being emitted from each source but this technique had the advantage of allowing for a direct measurement of the total UV radiation emitted. As these two systems are vastly different it was not known if the intensity values obtained using the two techniques would be comparable. However on analysis it was established that the two gave intensity values that were of the same order of magnitude.

It was found that the three light sources had a similar λ_{max} with all three emitting in the UV region of the EM spectrum, which is the required range for photopolymerisation. The fluorescent lamps also emit radiation in the visible region while the LEDs do not. This is one of the advantages that LEDs have over fluorescent lamps; they emit radiation at the required wavelength without producing any unnecessary radiation in other regions. And since only wavelengths where the photoinitiator absorbs are useful for photopolymerisation this makes UV-LEDs very desirable for use in photopolymerisation processes.

The experiments to measure warm up time and stability found that the fluorescent lamp took a significantly long time to stabilise, while the LED array produced constant output intensity four times quicker than the lamp. It was also shown with the single LED that it is possible to obtain UV-LEDs with

instantaneous warm up times. Minimising this activation time would lead to savings in money, energy and time for the manufacturer and therefore is of importance to them.

Although the intensity values obtained for each source using the Ocean Optics spectrometer and the Solar Light radiometer compare well it should be noted that there is an inherent error involved when comparing the different light output fields of the lamp and the LEDs. Different detection systems (i.e. Ocean Optics IRRAD2000 and the PMA2107 UVA/B detector) see the sources and their corresponding light fields and this should be taken into account when comparing the values obtained [1].

Table 3.2 gives an account of the specifications for an ideal light source compared to the specifications identified for each light source used in this study. No one light source satisfies all the conditions of an 'ideal' source, listed in table 2.1. Therefore a trade off is required and a light source must be chosen on what specifications are more important to fulfil the idea of an 'ideal' light source. However this study did show that the currently available UV-LEDs used in this study exhibited some of the 'ideal' specifications while being comparable to the currently used fluorescent lamps in terms of intensity, maximum peak wavelength and spectral output. The next stage was to investigate if UV-LEDs could initiate a photopolymerisation process and produce a degree of cure similar to that produced with the fluorescent lamps. If that was found to be the case UV-LEDs could be used as a more reliable and more efficient source of UV radiation in photopolymerisation processes.

Table 3.2: Comparison of the ideal light source specifications to the actual specifications.

Specifications	**Ideal**	**Fluorescent Lamp**	**Single LED**	**LED Array**
AC/DC	Continuous output	AC	DC	DC
Warm-up Time	Instantaneous switch on	~120 mins	Almost instantaneous	~30 mins
Stability	Continuous stable output	Stable after warm up time	Stable after switch on	Stable after warm up time
Useful Lifetime	Limitless	2,000 hours	Not measured	Not measured
Current -v- Intensity	Maximum light output for minimum electrical power in	Fixed	Maximum value at minimum input	Maximum value at minimum input
Wavelength range	Emits only over λ range needed for photopolymeri-sation	Emits radiation over a broad range	Emits over narrow bandwidth	Emits over narrow bandwidth
Peak wavelength	Emits only one peak at required λ for photopolymerisat ion	Has many peak λs	one λ_{max}	one λ_{max}

3.8 References

[1] S.L. McDermott, J.E. Walsh, R.G. Howard. "A comparison of the emission characteristics of UV-LEDs and fluorescent lamps for polymerisation applications". Optics and Laser Technology 2008; vol. 40: pp.487-493.

[2] Y-H. Kim, J-H. Ahn, D-C. Shin, H-S. Kim, Kwon. "Novel blue-light-emitting poly(terphenylenevinylene) derivative". Optical Materials 2002; vol 21: pp.175-180.

[3] Philips Lighting. PL-S 9W/10/2P UNP datasheet 2007. vol. 2007.

[4] F.G. Rosillo. "Lifetime evaluation of DC-supplied electronic ballasts with fluorescent lamps for photovoltaic applications". Renewable Energy 2004; vol 29: pp.961-974.

[5] A. Berntsen, Y. Croonen, C. Liedenbaum, H. Schoo, R.J. Visser, J. Vleggaar, P. van de Weijer. "Stability of polymer LEDs". Optical Materials 1998; vol 9: pp.125-133.

[6] A. Dodabalapur. "Organic light emitting diodes". Solid State Commun. 1997; vol 102: pp.259-267.

[7] N. Narendran, Y. Gu, J.P. Freyssinier, H. Yu, L. Deng. "Solid-state lighting: failure analysis of white LEDs". J. Cryst. Growth 2004; vol 268: pp.449-456.

[8] Authors' personal correspondence with Roithner Lasertechnik April 2005.

[9] W.D. Cook. "Spectral distributions of dental photopolymerization sources". J. Dent. Res. 1982; vol 61: pp. 1436-1438.

[10] C. Decker. "The use of UV irradiation in polymerization". Polym. Int. 1998; vol 45: pp.133-141.

[11] J. Kindernay, A. Blažková, J. Rudá, V. Jančovičová, Z. Jakubíková. "Effect of UV light source intensity and spectral distribution on the photopolymerisation reactions of a multifunctional acrylated monomer". J. Photochem. Photobiol., A 2002; vol 151: pp.229-236.

[12] C. Decker. "Kinetic study and new applications of UV radiation curing". Macromolecular Rapid Communications 2002; vol 23: pp.1067-1093.

[13] J.E. Walsh, K.Y. Kavanagh, S. Fennell, J. Murphy, M. Harmey. "Fibre-optic micro-spectrometers for biomedical sensing". Transactions of the Institute and Control 2000; vol 22: pp.355-369.

Chapter 4 Experimental: Investigation of UV sources for photopolymerisation applications

4.1 Introduction

The characterisation of the curing process in this research uses well established spectroscopy techniques. The UV and visible absorption properties of each of the photoinitiators used in this research was measured using UV/vis spectroscopy. This is an important aspect to this research as the absorption spectra give an indication where in the EM spectrum each photoinitiator will absorb. These absorption spectra can also be used to calculate the molar absorptivity (ε_λ) which is also of importance as it gives an indication how much light of a particular wavelength each photoinitiator will absorb.

After the identification of suitable photoinitiators the degree of conversion or percentage cure achieved with each light source was calculated. Two vibrational spectroscopy techniques, infrared (IR) and Raman were employed to analyse the polymerisation process. Both techniques allow the degree of conversion to be recorded by monitoring the disappearance of the characteristic spectral peaks (e.g. C=C at 1636 cm^{-1}) upon exposure to UV radiation. Initially, the concept needed to be proven, i.e. could UV-LEDs be used in the photopolymerisation process? After which the effect on percentage cure using different light sources was investigated fully.

All three spectroscopic techniques presented in this chapter were of great importance as they gave information on the curing profiles of the HEMA samples and allowed for an intercomparison between the expected and determined cure

profiles achieved with the newly developed UV-LEDs and the traditionally used fluorescent lamp. These initial findings then allowed for an investigation into the thermomechanical properties of pHEMA, which is discussed in chapter 6.

4.2 Electronic and Vibrational Spectroscopy

4.2.1 Electronic Absorption Spectroscopy

UV/vis absorption spectroscopy is a measurement of the wavelength against intensity of absorption of ultraviolet and visible radiation by a sample. It works by probing the electronic transitions of molecules as they absorb such radiation. When a molecule absorbs EM radiation of appropriate wavelength it causes a transition in the electronic energy levels of a molecule and results in the promotion of an electron from the ground state into a higher energy state. The absorption will occur if the energy of the photon corresponds exactly to that of the transition. The absorption of a sample at any particular wavelength causes a reduction in the light intensity falling on a photoelectric detector. This causes a reduction in the signal from the photoelectric device, after which an absorption curve relating wavelength and absorption is plotted [1, 2].

For absorption spectroscopy, the intensity of the incident radiation decreases when it interacts with the molecules. The extent to which the radiation reacts with a particular species at a certain wavelength depends on the concentration of the species and on the path length of the sample [2]. The absorption of the radiant energy by a species can be described using the general principle known as the Beer-Lambert law [3]. This law states that there is a linear relationship between absorbance (A) and the concentration of the substance (c).

The intensity of the radiation decreases exponentially with increasing path length (l) and sample concentration (c). The Beer-Lambert law is important in spectroscopy as it allows for the determination of the molar absorptivity (ε_λ), which indicates how much light of a particular wavelength a species will absorb for a given concentration and path length, the greater the probability of a particular absorption the greater the ε_λ value [4, 5]. This law is expressed in equation 4.1, where I_0 and I are the intensities of the incident and transmitted light respectively.

$$\log_{10}\frac{I_o}{I} = A = \varepsilon_\lambda cl \qquad \text{Eq. 4.1 [6]}$$

4.2.2 Vibrational Spectroscopy

The vibrational levels of molecules are primarily separated by energies in the IR region of the electromagnetic spectrum (i.e. from 1 cm^{-1} to 10000 cm^{-1} [7]). Molecules absorb radiation if the frequency of the radiation absorbed is exactly the same as the vibrational frequency of the molecule. Analysis of the frequencies at which absorption occurs gives information about the functional groups in the molecule and therefore yields information about the identity of the substance. The frequencies at which molecules vibrate depend on the mass of the atoms, the strength of the bonds between the atoms and the geometry of the molecule. The stronger the forces between the atoms the higher the vibrational frequency while heavier atoms exhibit lower vibrational frequencies. Two experimental techniques that are used to detect vibrational transitions are IR and Raman spectroscopy; however both methods rely on different selection rules [8, 9].

The absorption of IR radiation does not result in an electronic transition instead it causes the molecules to vibrate, rotate or bend, while the molecule itself remains in its electronic ground state. Absorption of IR radiation can only occur when the electric dipole moment of the molecule changes during the vibration or rotation. Only frequencies that correspond to the vibrational frequencies will be absorbed causing a change in the amplitude of the molecular vibrations. The positions of atoms in molecules are not rigid and therefore subjected to different vibrations. The two main types of bond vibration are stretching (higher energy) and bending (lower energy), and are shown in figure 4.1. Each radiation frequency corresponds to a certain molecular vibration, therefore by measuring the IR absorption spectrum over a range of frequencies it is possible to obtain a series of absorptions corresponding to the characteristic vibrations of particular bonds. Analysis of these absorptions can aid in the identification of the molecule structure and thus the sample under investigation [9].

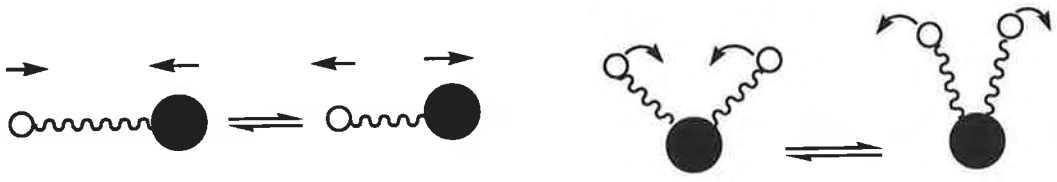

Stretching vibration Bending vibration

Figure 4.1: Stretching and bending molecular vibrations.

Vibrational transitions can also result from the scattering of radiation by the molecules, which is the basis of Raman spectroscopy. When radiation is absorbed by a molecule the predominant mode of scattering is Rayleigh scattering

(elastic scattering), this occurs when the scattered light is of the same frequency as the incident light. Raman scattering (inelastic scattering) is a result of the incident photons interacting with the molecule in such as way that energy is either lost or gained. This results in a higher (anti-Stokes) or lower (Stokes) frequency being emitted (figure 4.2). In Raman scattering the difference in frequency between the incident and the scattered relates to the vibrational energies of the molecule. In anti-Stokes Raman scattering the molecule begins in a higher vibrational energy state and after the scattering process ends up in a lower vibrational state. Thus the vibration in the material is lost as a result of the interaction. This results in the scattered radiation gaining energy and being of a higher energy than the incident radiation. In Stokes Raman scattering the interaction of the incident light with the molecule creates a vibration in the material as the molecule starts out in a lower vibrational state and after the scattering process ends up in a higher vibrational energy state. Here the scattered radiation loses energy and is of a lower energy than the incident radiation. In either case the resulting difference between Raman lines and the exciting lines correspond to specific energy level differences for the material under investigation and give an insight into its molecular structure [9].

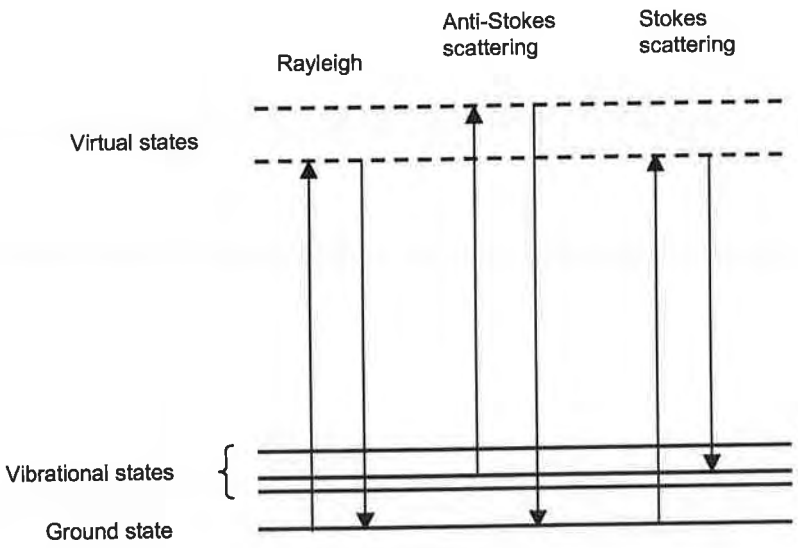

Figure 4.2: Energy diagram showing the different types of scattering processes.

As both IR and Raman spectroscopy can be used to study vibrational transitions the spectra obtained using both techniques will be similar. However they will not be identical, as all transitions are not allowed. For a vibrational motion to be IR active there must be a change in the dipole moment of the molecule. While for a transition to be Raman active there must be a change in the polarisability of the molecule during the vibration. Therefore the type of transitions that can be probed by IR and Raman spectroscopy will depend if the vibrations are IR or Raman active. The two techniques complement each other and both are used to fully characterise the photopolymerisation process described in this work.

4.3 Ultraviolet-Visible Spectroscopy

4.3.1 Introduction

Ultraviolet-visible spectroscopy (UV/vis) was used to measure the UV and visible absorption characteristics of the six different photoinitiators and the neat monomer. This gave an account of the amount of UV radiation that would be absorbed by the monomer at the emission wavelength of the light sources used to photoinitiate the free radical photopolymerisation process. The spectrometer was also used to record the absorption spectrum of blank NaCl plates (which are used for the IR measurements), to ensure that they transmitted the required UV radiation. The UV absorption spectra of NaCl plates with uncured and partially cured monomer were also recorded. The reason for this was to see if there was a difference between the UV absorption of the monomer and the partially cured monomer as this could have an effect on the amount of UV radiation absorbed, which in turn could affect the amount of photopolymerisation achievable.

4.3.2 Instrumentation

UV/vis spectroscopy probes the electronic transitions of molecules by measuring the light they absorb in the UV and visible regions of the electromagnetic spectrum.

The Perkin Elmer Lambda 900 UV/vis/NIR spectrometer (Figure 4.4) was used to obtain the required spectra. This spectrometer [10] is a double-beam, double monochromator ratio recording system. The wavelength range of between 175 nm and 3300 nm is achieved through two separate light sources, a tungsten-halogen lamp and a deuterium lamp. The wavelength range has an accuracy of

0.08 nm in the UV/vis and 0.3 nm in the NIR region. Figure 4.4 shows a diagram of the principle components of the instrument. The UV/vis spectrometer works by splitting a beam of light from the visible and/or UV light source into its component wavelengths. Each monochromatic beam is then split into two equal intensity beams by a half-mirrored device. One of these beams passes through a cuvette containing a reference (i.e. pure solvent), while the other beam passes through an identical cuvette containing the sample dissolved in the solvent. The intensities of these beams are then measured and compared. The intensity of the reference beam is defined as I_o and should absorb little or no light while the intensity of the sample beam is defined as I. If the sample does not absorb light of a given wavelength, then the reference and the sample beam are equal (I_o=I). However if the sample does absorb light then the sample beam is less than the reference beam and it is this difference that is plotted against wavelength.

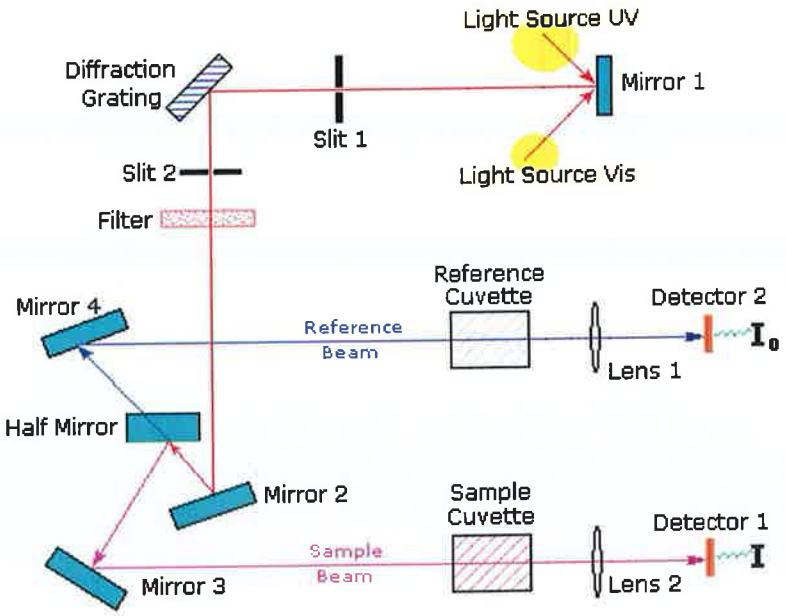

Figure 4.3: Schematic of the UV/vis spectrometer [11].

4.3.3 Sample Preparation

Each photoinitiator was dissolved in acetonitrile as recommended by their supplier Ciba Speciality Chemicals Inc. (Basel, Switzerland), which is transparent down to about 190 nm, and made up to set concentrations [3, 12]. In order to undertake a Beer-Lambert law study three different concentrations were used. For each photoinitiator the concentration was decreased by a factor of ten. The concentrations used for each photoinitiator are given in table 4.1.

Table 4.1: Concentrations used for each photoinitiator for the Beer-Lambert Law investigation.

Photoinitiators	**Concentrations (mol/L)**		
Darocur 1173	4.79×10^{-3}	4.79×10^{-4}	4.79×10^{-5}
Irgacure 651	3.07×10^{-3}	3.07×10^{-4}	3.07×10^{-5}
Irgacure 1800	2.85×10^{-3}	2.85×10^{-4}	2.85×10^{-5}
Irgacure 369	2.15×10^{-3}	2.15×10^{-4}	2.15×10^{-5}
Darocur TPO	2.25×10^{-3}	2.25×10^{-4}	2.25×10^{-5}
Irgacure 819	1.88×10^{-3}	1.88×10^{-4}	1.88×10^{-5}

4.3.4 Method

The UV/vis absorption spectrum of the blank NaCl plates was obtained by placing the two plates in the sample holder and leaving the reference cell holder empty. This determined whether the NaCl plates would transmit the UV radiation from each light source. These NaCl plates were used in the IR spectroscopic investigation of the photopolymerisation process. So it was important to determine if they could transmit appropriate amounts of UV radiation for the photopolymerisation studies. Measurements of the UV/vis absorption properties of the monomer were also performed. A drop of the monomer was then placed between the NaCl plates and the absorption of the solution before and after exposure to UV light was recorded. Once again the reference holder was empty. The reason for this was to see if there was any difference in the amount of UV radiation being transmitted by the monomer as it cured.

Two optically matched quartz cuvettes of 10 mm pathlength were used to obtain the absorption spectra of each of the photoinitiators. One cuvette containing pure acetonitrile was placed in the reference holder while the other, containing the initiator in acetonitrile was placed in the sample cell holder. This allowed for the automatic subtraction of the solvent spectrum from the photoinitiator spectrum. The spectrum was recorded over a range from 200 nm – 800 nm, using an integration time of 0.48 sec and a 1.00 mm slit. Absorption spectra of each photoinitiator were recorded and the molar absorptivity at the emission wavelength $\varepsilon_{\lambda max}$ of the UV sources, were calculated from the absorbance values using the Beer-Lambert law (equation 4.1).

4.4 Fourier Transform Infrared Spectroscopy

4.4.1 Introduction

Fourier Transform Infrared (FTIR) spectroscopy was used to investigate the UV-photoinitiated curing profile of a number of monomer/photoinitiator samples. This was achieved by recording the vibrational spectra during the photopolymerisation process. These samples consisted of HEMA and the different photoinitiators outlined previously. This type of spectroscopy has long been used to characterise and study polymers due to its high acquisition speed, good spectral resolution and high signal-noise ratios. A number of studies have utilised FTIR spectroscopy as a characterisation technique for photopolymerisation processes [13-16].

The majority of commercially available FTIRs are based upon the Michelson interferometer. FTIR measures the frequencies at which infrared

radiation is absorbed by the sample and the magnitude of the absorption. Each individual chemical functional group in a polymer chain absorbs radiation at a specific frequency. By monitoring certain bonds e.g. C=C at 1636 cm^{-1} the curing profile can be determined.

4.4.2 Instrumentation

The FTIR spectrometer used to measuring the curing profiles achieved with the fluorescent lamp, the single LED and the LED array was the Nicolet Nexus FTIR. This FTIR allowed for a quick scan time so that the curing spectra were measured quickly in between exposure to the light sources.

Figure 4.5 shows a schematic of the Michelson interferometer at the heart of a typical FTIR spectrometer and the light path of the infrared radiation. The optical system of an FTIR spectrometer is very simple: the interferometer requires two mirrors, an infrared light source, an infrared detector and a beam-splitter. The infrared light is collected and passed into the Michelson interferometer where the beam splitter reflects 50% of the radiation to a fixed mirror and transmits the remaining 50% to a moving mirror. The beam splitter is the heart of the interferometer and is essentially a half-silver mirror. The two mirrors then reflect both beams back to the beam splitter, where the beams recombine and interfere constructively or destructively depending on the relationship between their path differences. This recombined beam produces an output wave known as an interferogram; from this a spectral plot of intensity against frequency is produced [17].

Since the FTIR spectrometer used was not a double beam instrument a background spectrum was collected before recording the sample spectrum. This

background spectrum was automatically subtracted from each sample spectra. This removed any peaks that were due to the atmosphere as well as the emission spectrum of the radiation source so that a flat baseline was produced in the absence of any sample.

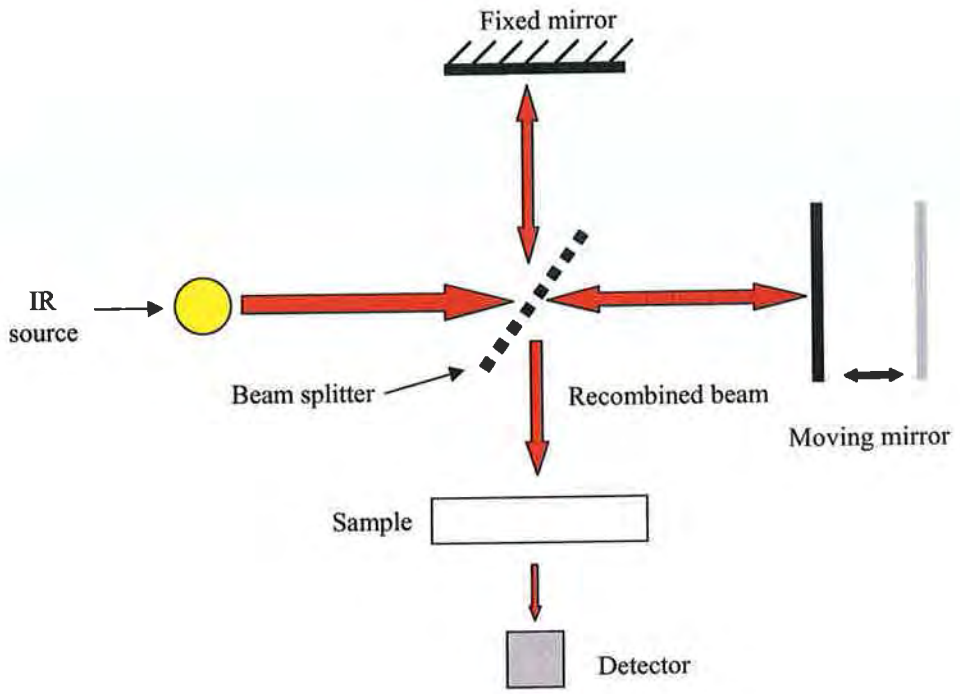

Figure 4.4: Schematic of the Michelson Interferometer in a typical FTIR spectrometer.

4.4.3 Table of molecular vibrations and HEMA spectra

Table 4.2 gives a list of the FTIR spectral band assignment in the monomer used in this work i.e. 2-hydroxyethyl methacrylate (HEMA). Figure 4.6 shows a typical HEMA spectrum recorded before exposure to UV radiation. The vibrations used to monitor the curing process are the symmetric stretch of the C=C bond at 1636 cm^{-1} and the symmetric stretch of the CO-C bond at 1174 cm^{-1}

which was used as an internal reference, are highlighted both in table 4.2 and figure 4.6.

Table 4.2: Molecular vibration assignment of bands detected by FTIR in a HEMA spectrum [18-20].

Bond *Vibration type*	**Wavenumber (cm^{-1})**
O-H *symmetric stretch*	3429
C-H_3 *antisymmetric stretch*	2957
C=O *symmetric stretch*	1718
C=C *symmetric stretch*	1636
C-H_3 *antisymmetric deformation*	1455
O-H	1404
C-H_3 *symmetric deformation*	1379
C-H_2	1321
C-H_2	1298
C-O-C *symmetric stretch*	1174
C-H_3	1078
C-O *symmetric stretch*	1030
C-H_2	945
C-H_2	902
C=C	815
O-H	655

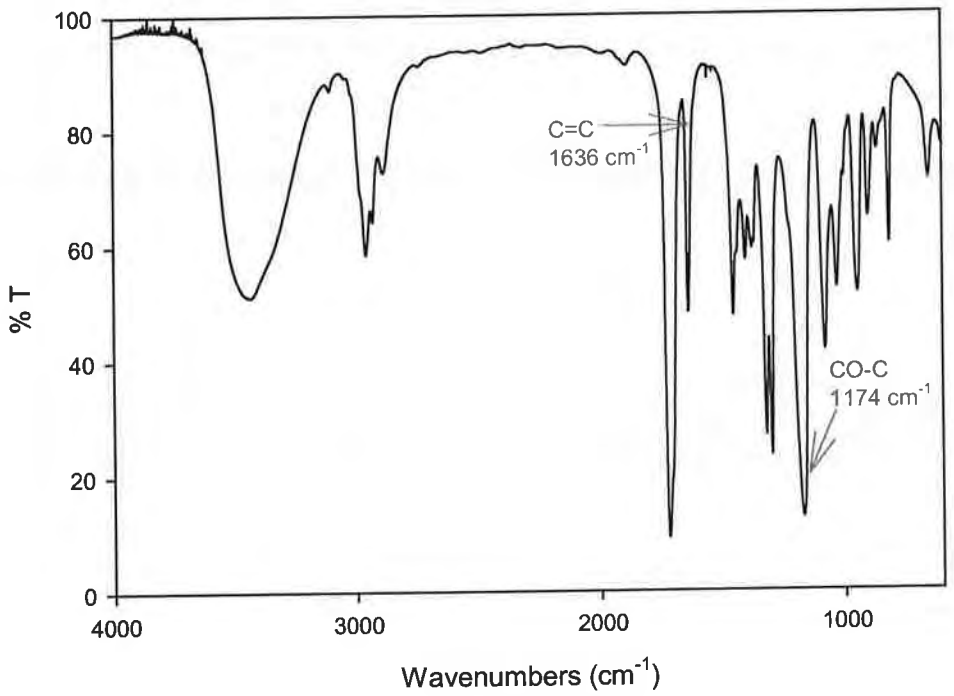

Figure 4.5: Typical FTIR spectrum of HEMA. The C=C and reference peak used to monitor cure are indicated.

4.4.4 Calculating the Degree of Conversion

The degree of conversion (DC, which is the amount of methacrylate C=C bonds converted to C-C) for each sample was determined by comparing the ratio of the transmission of the carbon-carbon double bond (C=C) with that of the reference bond (CO-C), for the cured and uncured state [21]. The C=C bond has a vibrational peak around 1636 cm^{-1}, while the CO-C peak occurs around 1174 cm^{-1}. This internal reference at 1174 cm^{-1} is an unreactive group and is not involved in the polymerisation reaction. The reference peak is used to normalise the change in absorption or transmission and will compensate for changes in transmission which are not due to the polymerisation process [22]. By measuring the ratio change of the absorption or transmission (i.e. peak height) of the C=C to

the peak height of the CO-C before and after polymerisation, the DC can be calculated using the following equation [23, 24]:

$$DC = \left[1 - \left[\left(\frac{C=C}{CO-C}\right)cured \Big/ \left(\frac{C=C}{CO-C}\right)uncured\right]\right] * 100 \quad \textit{Equation 4.2}$$

4.4.5 Sample preparation for photopolymerisation studies

A study of the photopolymerisation process initiated by the three different lights sources (fluorescent lamp, single LED and LED array) was undertaken. For this study each HEMA sample contained a set concentration of 6 x 10^{-3} mol/L of each photoinitiator. Each sample was then exposed to each light source emitting at the maximum intensity achievable after which the percentage cure was calculated.

The infrared spectra of the uncured and cured monomer were obtained with the Nicolet Nexus FTIR using a resolution of 2 cm^{-1} between 4000 cm^{-1} and 500 cm^{-1}. The sample holder consisted of two NaCl plates separated by a Teflon® spacer 0.1 mm thick. After collecting a background spectrum of the NaCl plates, a small drop of monomer was placed between the two plates and a spectrum recorded. As the plates were sealed oxygen diffusion, which would have inhibited the photopolymerisation process, was prevented [25, 26]. The plates were then removed from the bench and exposed to one of the UV light sources for two minutes, after which another spectrum was recorded. This was repeated until the C=C bond at 1636 cm^{-1} had sufficiently disappeared indicating photopolymerisation had occurred. The percentage cure (degree of conversion) was then calculated as explained previously.

Initially studies found that the percentage cure achieved was low. The FTIR spectrometer recorded an area which was bigger than the exposed (cured) area. It was therefore suspected that the FTIR recorded the absorption from the unpolymerised monomer as well as the polymerised polymer. For this reason it was decided to mask part of the NaCl plates with optically black tape so the exposed part was the exact size of the light source. For the single LED the NaCl plate was masked off to give an exposed diameter of 5 mm, the exposed diameter for both the LED array and the lamp was 12.3 mm. This meant that the FTIR was only recording the part of the monomer that was exposed to the lamp/LED (i.e. the polymerised polymer). The background spectrum recorded was of the blank NaCl plates which had a masked off area equal to the sample. The procedure outlined in the previously paragraph was then repeated for each light source.

4.4.6 In-situ spectroscopy study of the photopolymerisation process

It was also decided to monitor the curing process in-situ so that a continuous profile of the curing process could be obtained. At first this was done with the single LED, as it was the only UV-LED commercially available at the time. In this case the LED was placed inside the FTIR spectrometer. It was not possible to illuminate the sample through the face of the NaCl plate as was done with the external photopolymerisation, as it would have blocked the IR beam. Instead the NaCl plates and monomer sample were illuminated from the side by the LED; due to this only a fraction of the total light that was emitted by the LED actually cured the monomer. To try to increase the amount of radiation falling onto the monomer two LEDs were used, one placed at either side of the NaCl plates. However this did not dramatically increase the amount of UV light

irradiating the sample and as the rate of cure is proportional to the square root of the absorbed light intensity it was expected that the amount of cure achieved here would be low [22, 27].

Next the LED array was used in-situ, once again the monomer was illuminated from the side by the LED. As the LED array is more intense than the single LED it was expected that the final percentage cure achieved would be higher.

As this set up is not an accurate reflection on how the LEDs would illuminate the monomer in a manufacturing process it was decided to monitor the cure in-situ using Raman spectroscopy (see section 4.5). This allowed the LED to be placed perpendicular to the monomer, illuminating the sample through the face of a quartz slide.

4.5 Raman spectroscopy

4.5.1 Introduction

One of the problems with the FTIR spectroscopy experimental set up was that it is very difficult to monitor the photopolymerisation process in-situ, as it is difficult to place the light sources into the system. Martin et al. [18, 28] reported curing by this method but that involved using a N_2 laser as a source which has a much higher intensity than these LEDs. With Raman spectroscopy the LED could be placed directly under the monomer, which would allow for real time measurements of the curing process. This set up represents a more realistic arrangement of the manufacturing curing process where the light sources are placed parallel to the monomer.

4.5.2 Instrumentation

Raman spectroscopy was preformed using an Instruments SA Labram confocal imaging microscope system. Both Helium-Neon (632.8 nm) and Argon Ion (514.5 nm) lasers are available as sources, with the Argon Ion laser being used in this study. The light is imaged to a diffraction–limited spot (typically 1 μm) via the objective of an Olympus BX40 microscope. This system has a range from 150 cm^{-1} to 4000 cm^{-1} in a single image or with greater resolution in a combination of images.

Figure 4.8 shows a schematic diagram of a Raman spectrometer. When radiation passes through the sample, the sample scatters some of the light in all different directions. The scattered light is collected by a lens. A small fraction of the scattered radiation has different wavelengths compared to the incident beam. The difference in wavelength corresponds to the energy difference of the vibrational energy levels. The signal is then measured and processed by a computer, which plots the Raman spectrum [19].

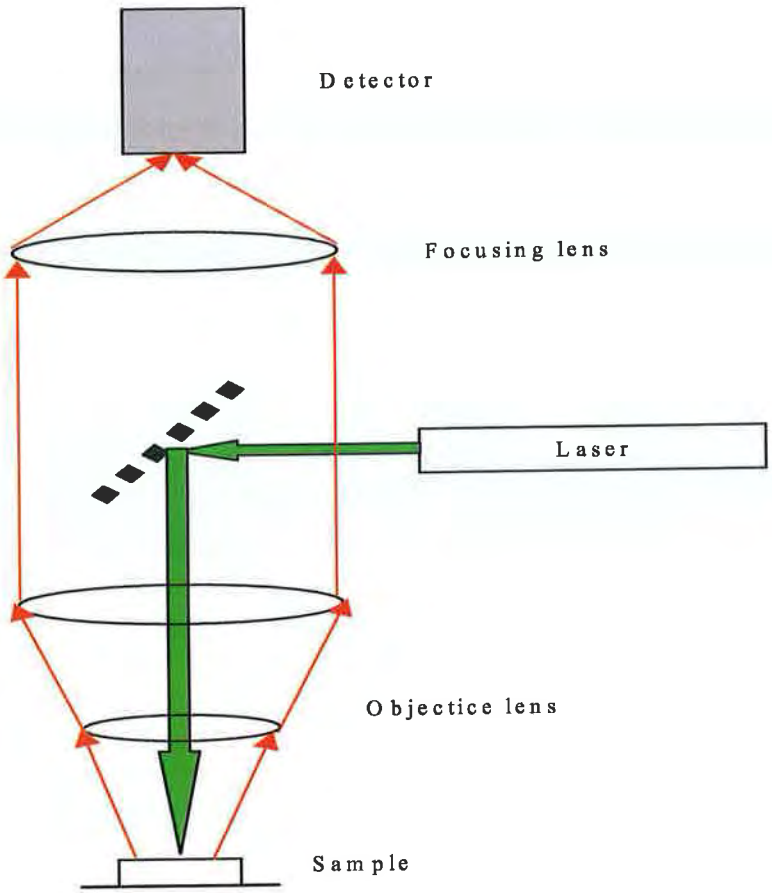

Figure 4.6: Schematic diagram of the Raman spectrometer.

4.5.3 Table of vibrations

Table 4.3 gives a list of the Raman band assignment for HEMA [19, 20]. Figure 4.9 (a) shows a typical HEMA spectrum recorded before exposure to UV radiation, while figure 4.9 (b) shows the same spectrum rescaled to see the peaks of interest. The vibrations used to monitor the curing process are the C=C bond at 1636 cm^{-1} and the CH_3 at 1455 cm^{-1} which is used as an internal reference, are highlighted both in table 4.3 [19, 20] and figure 4.9. The symmetric stretch of the CO-C (1174 cm^{-1}) bond that was used in the IR curing study as the internal reference could not be used here as this bond does not appear to be strongly

Raman active. Likewise although the CH_3 peak (1455 cm^{-1}) did appear in IR spectra it could not be used as the reference peak as it was not fully resolved.

Table 4.3: Molecular vibration assignment of bands detected by Raman spectroscopy for HEMA [19, 20].

Bond	**Wavenumber (cm^{-1})**
C-H_3 *antisymmetric stretch*	2954
C-H_2 *antisymmetric stretch*	2932
C=O	1718
C=C	1636
C-H_3 *antisymmetric stretch*	1455
O-H	1405
C-H_3 *symmetric stretch*	1380
C-H_2	1297
C-O	1033
C-H_2	947
C-H_2	907

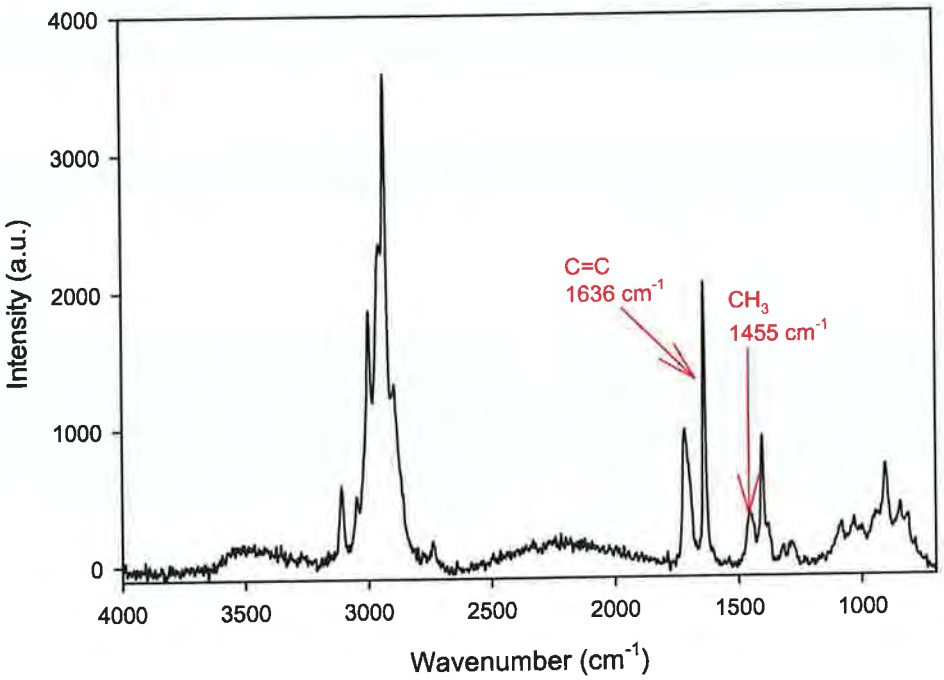

Figure 4.7 (a): Full range (700 cm^{-1} – 4000 cm^{-1}) Raman spectrum of HEMA.

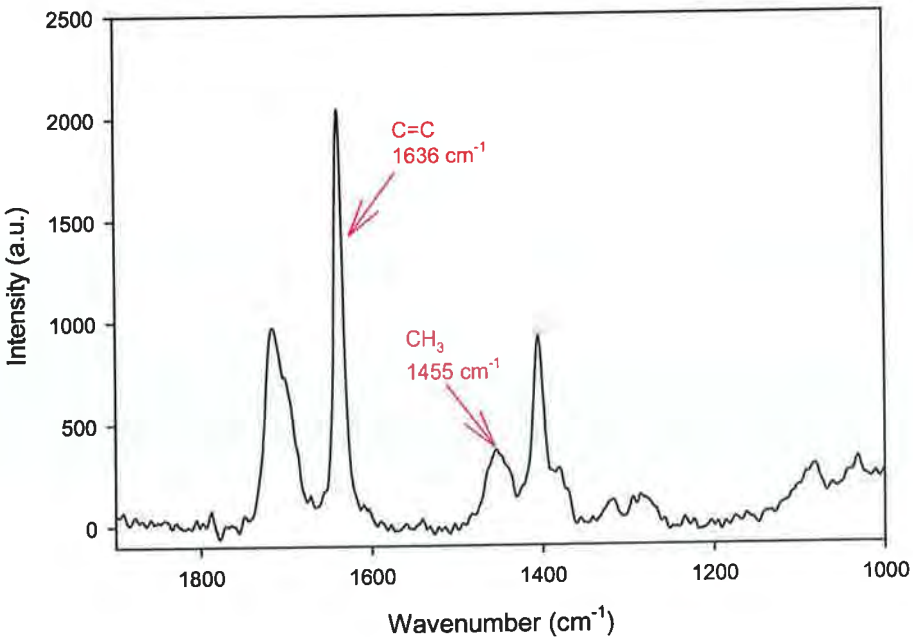

Figure 4.7 (b): Raman spectrum showing area of interest.

4.5.4 Calculating the Degree of Conversion

Once again the degree of conversion (DC) or percentage cure for each sample was determined by comparing the ratio of the absorption of the carbon-carbon double bond (C=C) with that of the reference bond, for the cured and uncured state. The bond used as a reference here was the CH_3 at 1455 cm^{-1}. The C=C has a Raman peak at 1636 cm^{-1}. By measuring the ratio change of the absorption (i.e. peak height) of the C=C to the peak height of the CH_3 before and after polymerisation, the DC can be calculated using the following equation:

$$DC = \left[1 - \left[\left(\frac{C=C}{CH_3}\right)cured \Big/ \left(\frac{C=C}{CH_3}\right)uncured\right]\right] * 100 \qquad \textit{Equation 4.3 [23, 24]}$$

4.5.5 Sample Preparation

A number of curing set ups were designed and tested before one was found that worked. It was not possible to cure with the fluorescent lamp, due to its size and bulkiness it could not be placed under the microscope stage of the spectrometer. Therefore only the LED array was used in this study. As in the FTIR an area the size of the LED was masked off to ensure that the exposure size of the monomer was the same size as the LED. The LED was then placed directly underneath the stage of the Raman, ensuring it was directly below where the sample would be placed. Here quartz slides were used in place of the NaCl plates, so UV light would be transmitted onto the monomer without any loss of radiation. A small drop of one of the monomer mixtures was placed onto a quartz slide and covered with a glass cover slip; an initial uncured spectrum was recorded. The sample was then exposed to UV radiation from the LED for 30 seconds and

another spectrum was recorded. Unfortunately the Raman detector was saturated by the intensity of the LED array making it impossible to obtain a Raman spectrum with the LED present, to overcome this problem a shutter was used to block the UV radiation from entering the spectrometer when the spectrum was being recorded. Once a spectrum was recorded the shutter was opened to allow further curing. This procedure was repeated a number of times until the peak at 1636 cm^{-1} had sufficiently disappeared.

4.6 References

[1] J. Mohan. "Organic spectroscopy. Principles and applications. 1st Ed." New Delhi: Narosa Publishing House, 2000.

[2] S. Duckett, B. Gilbert. "Oxford Chemistry Primers: Foundations of Spectroscopy". New York: Oxford University Press Inc., 2000.

[3] D.H. Williams, I. Fleming. "Spectroscopic methods in organic chemistry. 4th Ed." Berkshire: McGraw-Hill, 1986.

[4] M.G. Neumann, W.G. Miranda Jr., C.C. Schmitt, F.A. Ruggeberg, I.C. Corrêa. "Molar extinction coefficients and the photon absorption efficiency of dental photoinitiators and light curing units". J. Dent. 2005; vol 33: pp.525-532.

[5] R.J. Anderson, D.J. Bendell, P.W. Groundwater. "Organic spectroscopic analysis". Cambridge: The Royal Society of Chemistry, 2004.

[6] D. Kealey, P.J. Haines. "Instant notes, Analytical Chemistry". Oxford: BIOS Scientific Publishers Ltd, 2002.

[7] P.C. Painter, M.M. Coleman, J.L. Koenig. "The theory of vibrational spectroscopy and its application to polymeric materials. 1st Ed." USA: John Wiley & Sons, 1982.

[8] D. Campbell, R.A. Pethrick, White. "Polymer characterization. Physical techniques. 2nd Ed." Gloucestershire: Stanley Thornes Ltd, 2000.

[9] P.W. Atkins. "The Elements of Physical Chemistry. 2nd Ed." Oxford: Oxford University Press, 1996.

[10] http://www.focas.dit.ie/core/core-uvvis.html accessed 29 November 2007.

[11] http://bouman.chem.georgetown.edu/S00/handout/spectrometer.htm accessed on 20th April 2007.

[12] Ciba Speciality Chemicals photoinitiator datasheets.

[13] J.L. Ferracane, E.H. Greener. "Fourier Transform Infrared Analysis of Degree of Polymerization in Unfilled Resins-Methods Comparison". J. Dent. Res. 1984; vol. 63:pp.1093-1095.

[14] F.A. Ruggeberg, R.G. Craig. "Correlation of parameters used to estimate monomer conversion in a light-cured composite". J. Dent. Res. 1988; vol 67:pp. 932-937.

[15] C. Decker. "The use of UV irradiation in polymerization". Polym. Int. 1998; vol 45: pp.133-141.

[16] M. Sangermano, G. Malucelli, R. Bongiovanni, A. Priola. "Photopolymerization of oxetane based systems". Eur. Polym. J. 2004; vol.40: pp.353-358.

[17] S. Wartewig. "IR and Raman spectroscopy. Fundamental processing. 1st Ed." Weinheim: Wiley-VCH, 2003.

[18] S.J. Martin. "Curing of complex monomer systems: A spectroscopic and thermal analysis", Doctural thesis. Department of Physics. Dublin: Trinity College, 2000.

[19] C.N. Banwell, E.M. McCash. "Fundamentals of molecular spectroscopy. 4th Edition". London: McGraw-Hill, 1994.

[20] G. Socrates. "Infrared and Raman characteristic group frequencies. Tables and Charts. 3rd Edition". West Sussex: John Wiley & Sons, LTD, 2001.

[21] W. Teshima, Y. Nomura, A. Ikeda, T. Kawahara, M. Okazaki, Y. Nahara. "Thermal degradation of photo-polymerized BisGMA/TEGDMA-based dental resins". Polym. Degrad. Stab. 2004; vol.84: pp.167-172.

[22] N.S. Allen. "Photoinitiators for UV and visible curing of coatings: mechanisms and properties". J. Photochem. Photobiol., A 1996; vol 100: pp.101-107.

[23] T.H. Yoon, Y.K. Lee, B.S. Lim, C.W. Kim. "Degree of polymerization of resin composites by different light sources". J. Oral Rehabil. 2002; vol 29: pp.1165-1173.

[24] R. H. Halvorson, R. L. Erickson, C. L. Davidson. "The effect of filler and silane content on conversion of resin-based composite". Dent. Mater. 2003; vol 19: pp.327-333.

[25] C. Decker, K. Zahouily, D. Decker, T. Nguyen, T. Viet. "Performance analysis of acylphosphine oxides in photoinitiated polymerization". Polymer 2001; vol 42: pp.7551-7560.

[26] P.X. Ma, J.H. Elisseeff. "Scaffolding in tissue engineering". Florida: CRC Press, 2005.

[27] J.P. Fouassier, J.F. Rabek. "Radiation curing in polymer science and technology". London: Elsevier Science, 1993.

[28] S.J. Martin, V.J. McBrierty, D.C. Douglass. "Comparison of real-time monitoring of copolymer formation and composition by NMR, FTIR, and numerical simulation". Macromolecules 2001; vol.34: pp.8934-8943.

Chapter 5 Results: Spectroscopic investigation of the photopolymerisation process of HEMA

5.1 Introduction

This chapter gives a detailed account of the spectroscopic studies used to characterise the curing process, the aim of which was to prove the concept that UV-LEDs can replace fluorescent lamps in the photopolymerisation of the contact lens monomer HEMA. Six different photoinitiators were used in this study, to ensure that each of these initiators absorbed in the emission region of the three light sources, UV/vis spectroscopy was used to obtain their absorbance characteristics. The molar absorptivity (ε_λ) (equation 4.1) of each photoinitiator was then calculated, this value gives an indication into how much light of a particular wavelength (λ) the species will absorb [1, 2]. This is an important aspect in this research as it will give an indication of which photoinitiator has the most potential to initiate photopolymerisation with each light source.

Fourier Transform Infrared (FTIR) and Raman spectroscopy were then used to measure the percentage cure of the monomer after exposure to each light source. The first part of this study compared the amount of cure achieved by each light source for a certain photoinitiator. After which an intercomparison was made between the different initiators and the one that yielded the highest percentage cure for each light source was identified.

5.2 Ultraviolet-Visible spectroscopy

5.2.1 Introduction

As the monomer would be placed between NaCl plates for the monitoring of photopolymerisation by FTIR it was important to know the absorption characteristics of the NaCl plates to ensure that they would allow the transmission of the UV radiation onto the monomer. UV/Vis spectroscopy was used to measure the absorption characteristics of these plates. The absorption spectra of the uncured and partially cured monomer were recorded to see how the amount of absorption changed during the photopolymerisation process. The UV absorption spectra of the different photoinitiators at different concentrations were also recorded so that the ε_λ values could be calculated.

5.2.2 Ultraviolet/Absorption characteristics of NaCl Plates

Figure 5.1 shows the absorbance spectra of a blank NaCl plate and the NaCl plates containing uncured and partially cured monomer, with the λ_{max} of each source indicated. The blank NaCl plates absorb very little radiation (0.13.) in the wavelength region were the lamp (372 nm) and the LEDs (377 nm and 382 nm) emit. At the maximum wavelength emitted by each light source the uncured monomer absorbs the most UV light with an absorbance value of 0.28. This is due to the presence of the photoinitiator which absorbs UV radiation [3]. The partially cured monomer has an absorption value of 0.15 which is almost identical to that of the blank plates. Upon exposure to UV radiation the absorbing photoinitiator is consumed and this results in the lower absorbance value seen in the partially cured monomer [4, 5].

From this figure it is seen that the NaCl plates will transmit the majority of UV radiation being emitted by the lamp and the LEDs and therefore will not unduly interfere with the photopolymerisation process.

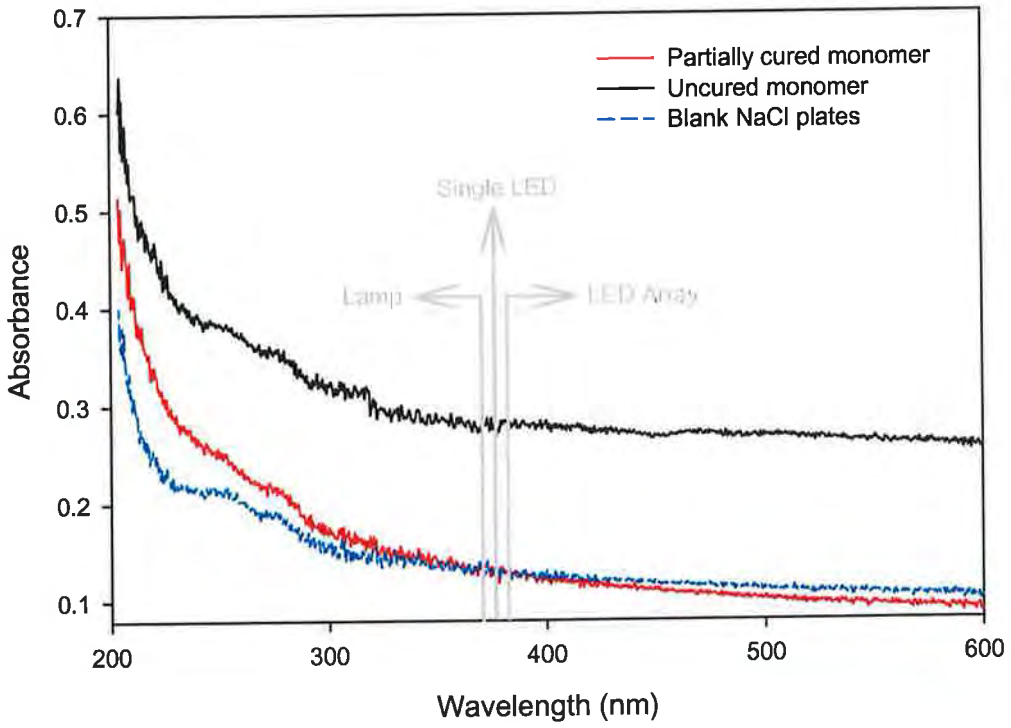

Figure 5.1: Absorption spectra of blank NaCl plates and plates containing uncured and partially cured monomer. The absorbance at the λ_{max} of the three light sources is also indicated.

5.2.3 Molar Absorptivity (ε_λ) of the six photoinitiators

Photopolymerisation has become a well adapted technology which has found usage in a large variety of industrial applications; as such it has become a field of central importance in polymer science and technology [6, 7]. As most neat monomers will not undergo polymerisation (homopolymerisation) when exposed to UV and/or visible radiation it is essential to introduce a photoinitiator

into their formulation [8]. These photoinitiators are capable of absorbing radiation and proceed to initiate the conversion of the monomer into a polymer. A number of issues must be considered when choosing a photoinitiator for the polymerisation of a biomaterial; two major factures are the absorption wavelength and the molar absorptivity (ε_λ). In this section the absorption spectra of the six photoinitiators at different concentrations were measured after which ε_λ, which gives an experimental indication of the probability of absorption at a certain wavelength, was calculated [9].

Figure 5.2 (a) shows the UV/vis absorption spectra of the photoinitiator Darocur 1173 in acetonitrile at three different concentrations. The λ_{max} for each light source is also illustrated. The absorbance is shown from 0 - 3 to allow for comparison between the other photoinitiators with absorbance values greater than one (e.g. figure 5.7 (a)). It can be seen from figure 5.2 (a) that as photoinitiator concentration increases so does the amount of absorption in the UVA region (320 nm-400 nm), which is the area of interest. This is in agreement with the Beer-Lambert law. This occurs with all the other photoinitiator UV/vis absorption spectra which are shown in figures 5.3 (a) through to figure 5.7 (a). The degree to which these materials absorb light over the wavelength range 200 nm-400 nm is important to this study as it not only defines their suitability for use in the photopolymerisation process but also governs the rate of initiation [10, 11]. It can also be observed from these absorption profiles that Irgacure 819, Darocur TPO, Irgacure 1800 and to some extent Irgacure 369 have an absorption tail that extends into the visible region making it possible to use these photoinitiators with LEDs that emit in this region i.e. blue.

The amount of absorbance by Darocur 1173 at the λ_{max} of the three sources for the three concentrations is plotted in figure 5.2 (b). For this photoinitiator the highest absorption occurs at the λ_{max} of the fluorescent lamp (372 nm) with the lowest absorption at the maximum concentration occurring at a λ_{max} of 382 nm (LED array). The amount of absorption by this photoinitiator at 382 nm (0.026 a.u.) is approximately half the maximum absorption that occurs at λ_{max} for the fluorescent lamp (0.051 a.u.). The absorbance values at each λ_{max} are presented in table 5.1. Based solely on the absorbance values for this initiator it would be expected that the highest percentage cure achieved during the curing studies should be observed when the monomer is exposed to the fluorescent lamp.

The absorption at λ_{max} against concentration for each of the other photoinitiators are presented in figures 5.3 (b) to 5.7 (b), and their corresponding absorbance values are presented in tables 5.2 - 5.6. For the six photoinitiators it can be seen that the highest absorption for each photoinitiator occurs at the maximum wavelength emitted by the lamp (372 nm) with the least absorption occurring at the maximum wavelength emitted by the LED array with the one exception being Darocur TPO (figure 5.6). For this initiator the absorption profiles are flipped with the maximum absorption occurring at the λ_{max} of the LED array and the least at 372 nm (lamp).

For Irgacure 819 at the highest concentration there is little difference between the maximum and minimum absorption at λ_{max}, meaning the degree of cure achieved for this initiator with each source should be similar. This is also true for Darocur TPO and to some extent Irgacure 1800. Like Darocur 1173, Irgacure 651 and Irgacure 369 both exhibit large absorption differences at

maximum concentration for each λ_{max}, implying that the amount of cure attained by each source for each individual initiator should vary significantly. There is very little difference exhibited between the actual absorption values at the lower concentrations for each photoinitiator.

As the concentration of each sample is different it is not possible to intercompare their absorption values. To allow for such a comparison the ε_λ of each photoinitiator at the λ_{max} of each source needed to be calculated. This should then give an indication which photoinitiator suits each light source. This is discussed further on page 117.

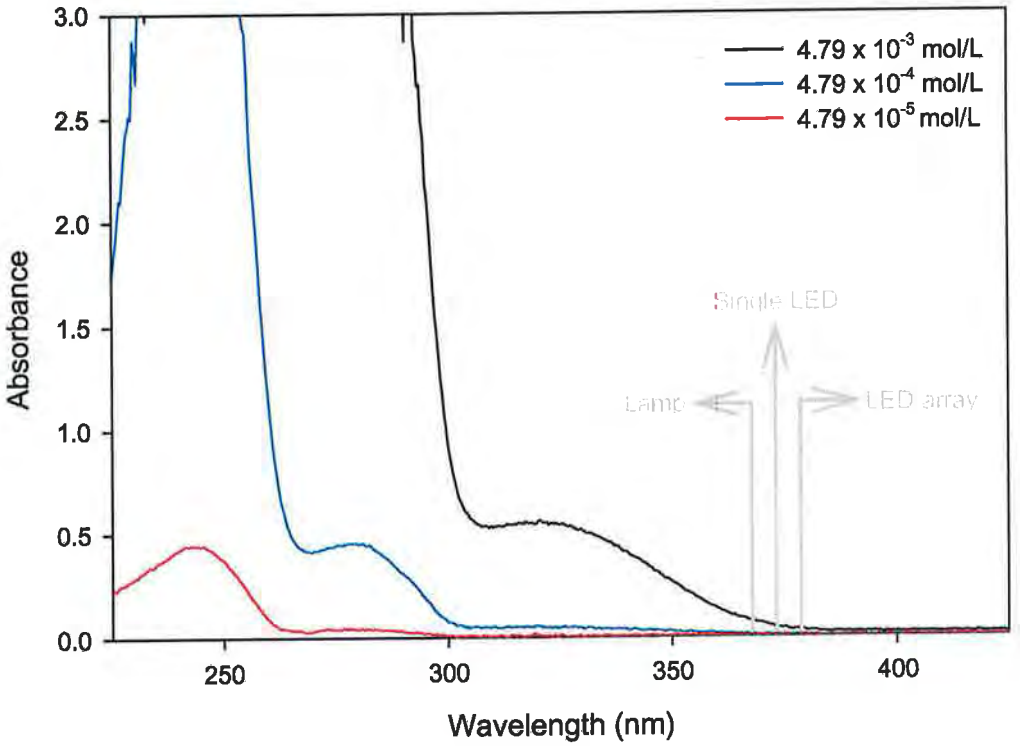

Figure 5.2 (a): UV/Vis absorption spectra of Darocur 1173.

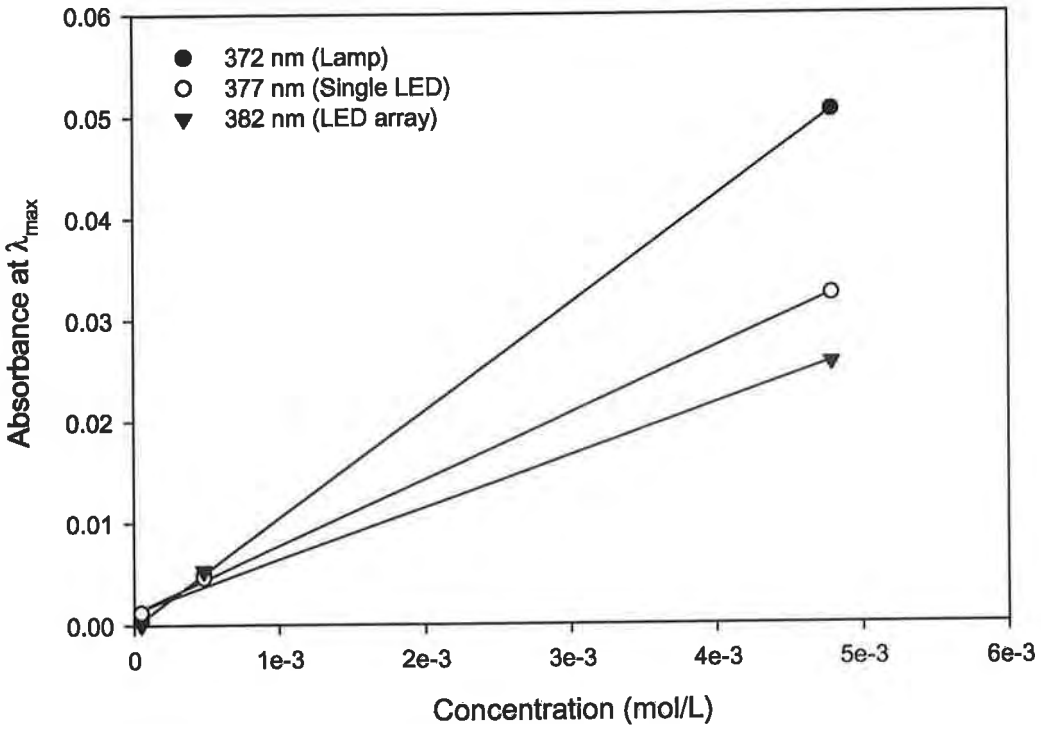

Figure 5.2 (b): Absorbance -v- concentration for Darocur 1173.

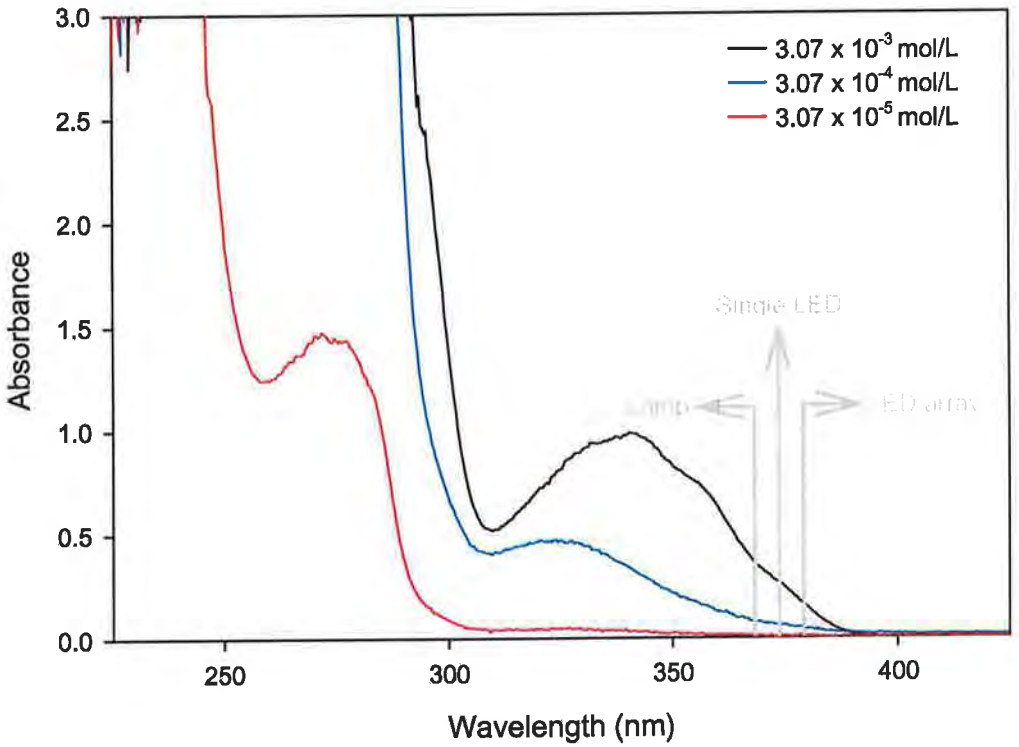

Figure 5.3 (a): UV/Vis absorption spectra of Irgacure 651.

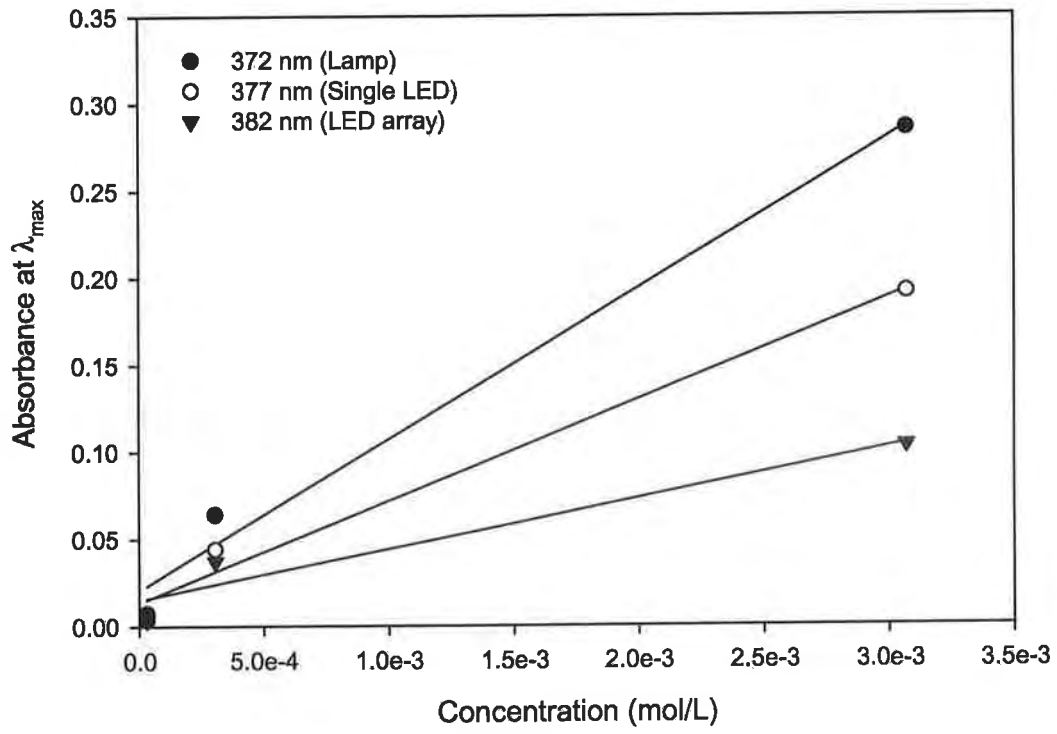

Figure 5.3 (b): Absorbance -v- concentration for Irgacure 651.

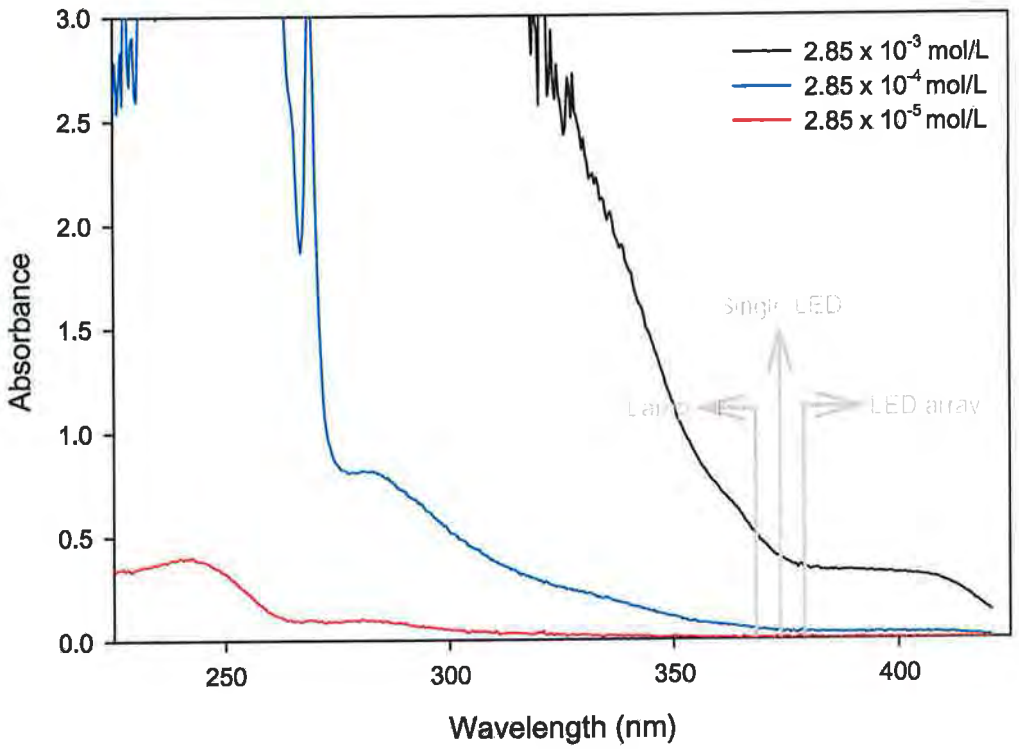

Figure 5.4 (a): UV/Vis absorption spectra of Irgacure 1800.

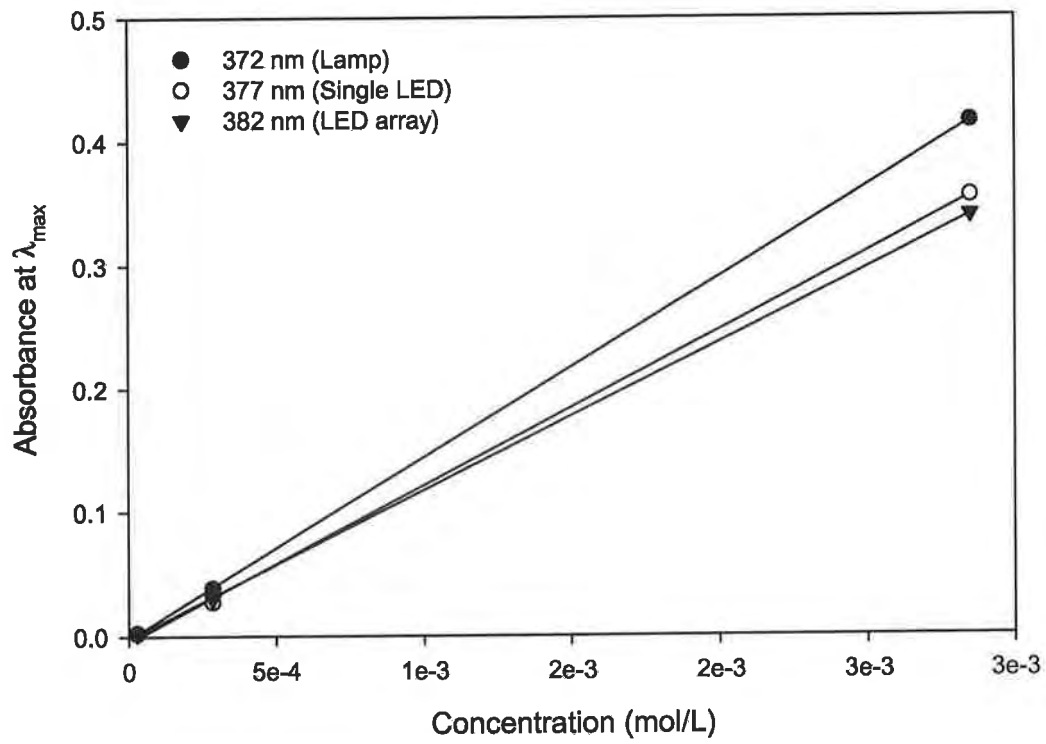

Figure 5.4 (b): Absorbance -v- concentration for Irgacure 1800.

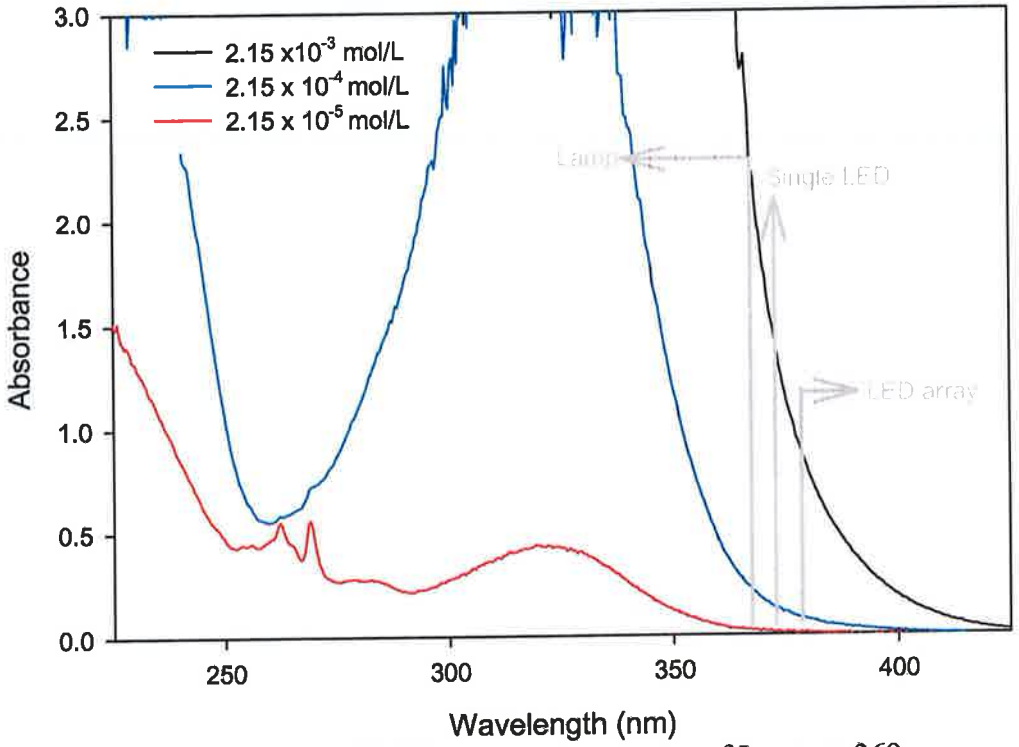

Figure 5.5 (a): UV/Vis absorption spectra of Irgacure 369.

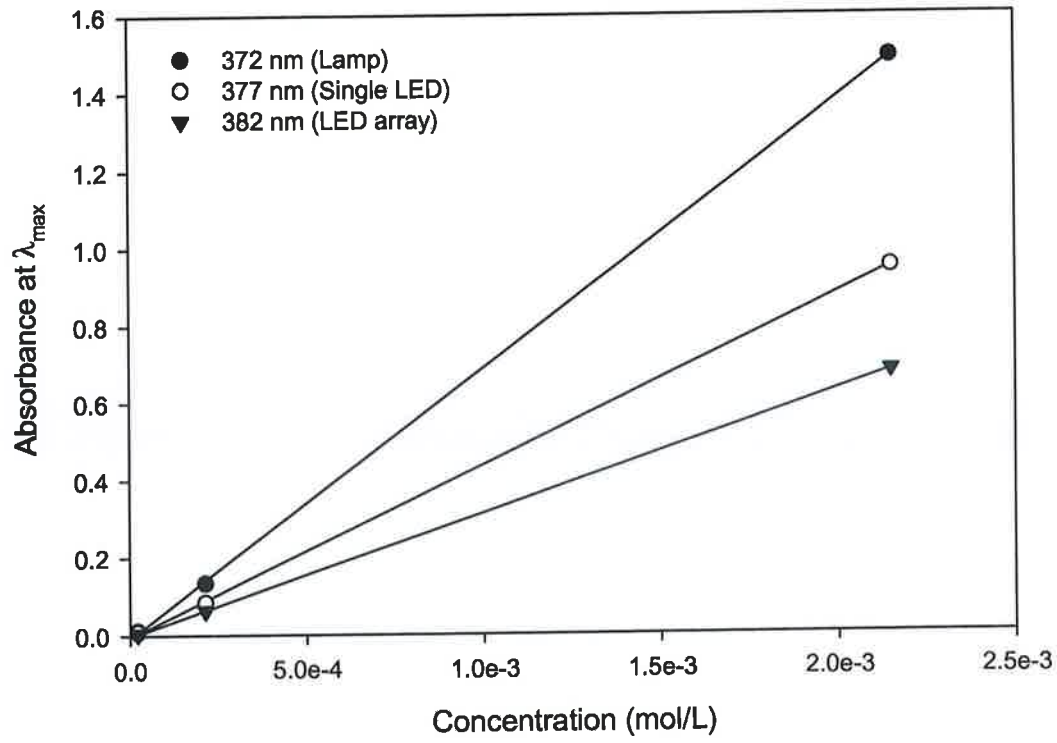

Figure 5.5 (b): Absorbance -v- concentration for Irgacure 369.

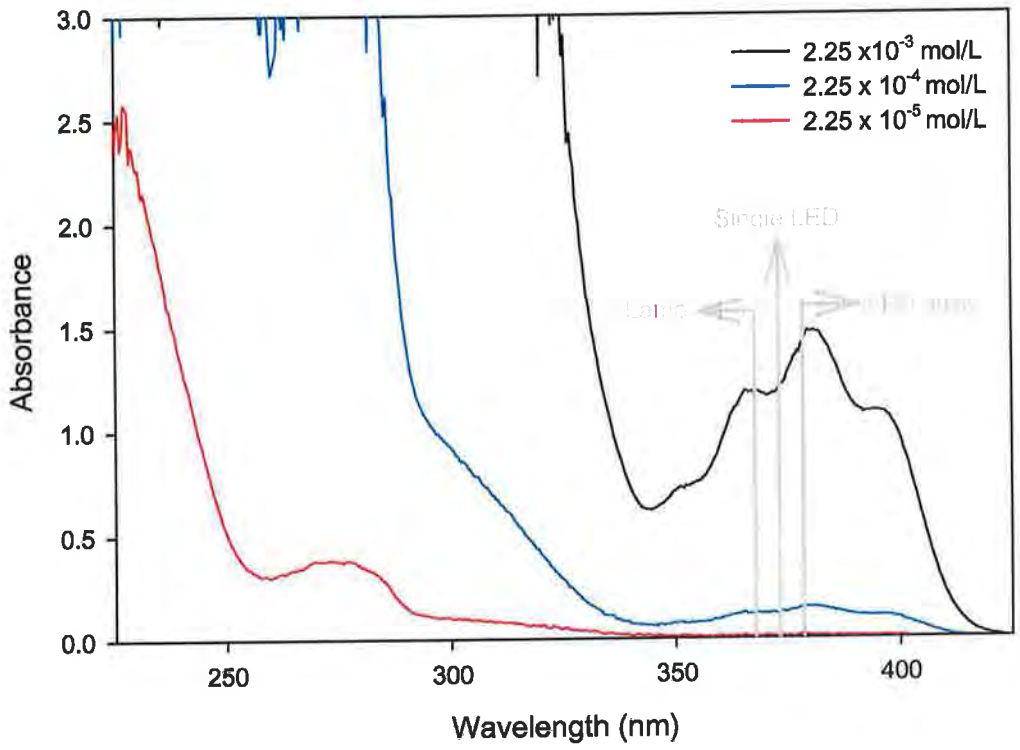

Figure 5.6 (a): UV/Vis absorption spectra of Darocur TPO.

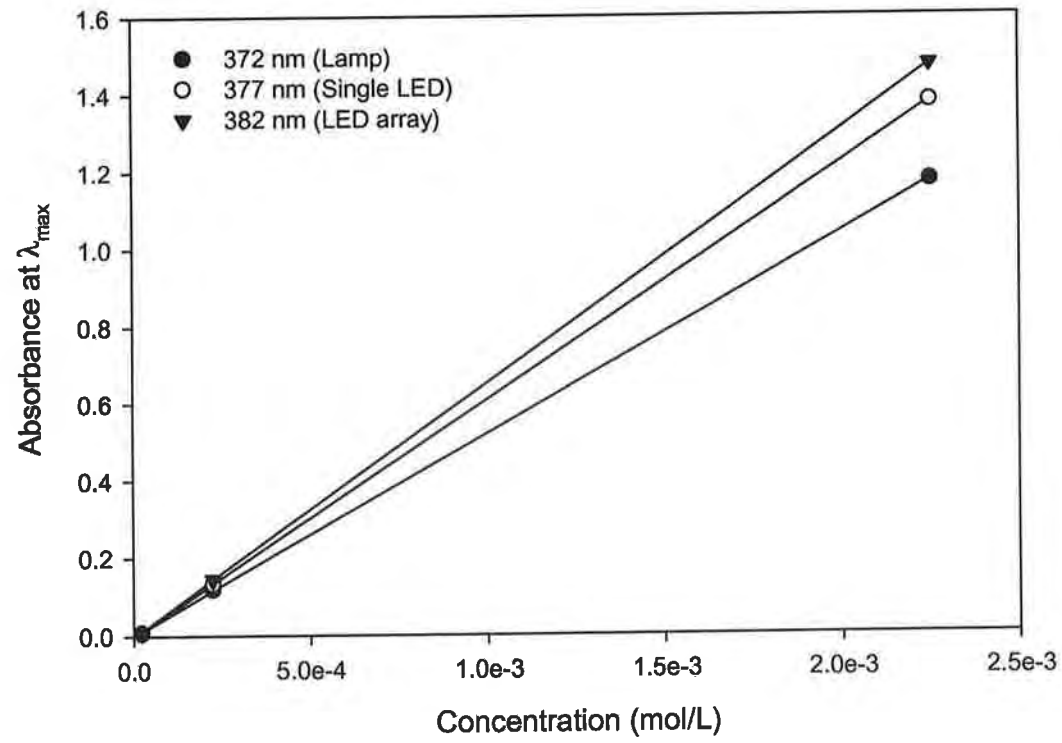

Figure 5.6 (b): Absorbance -v- concentration for Darocur TPO.

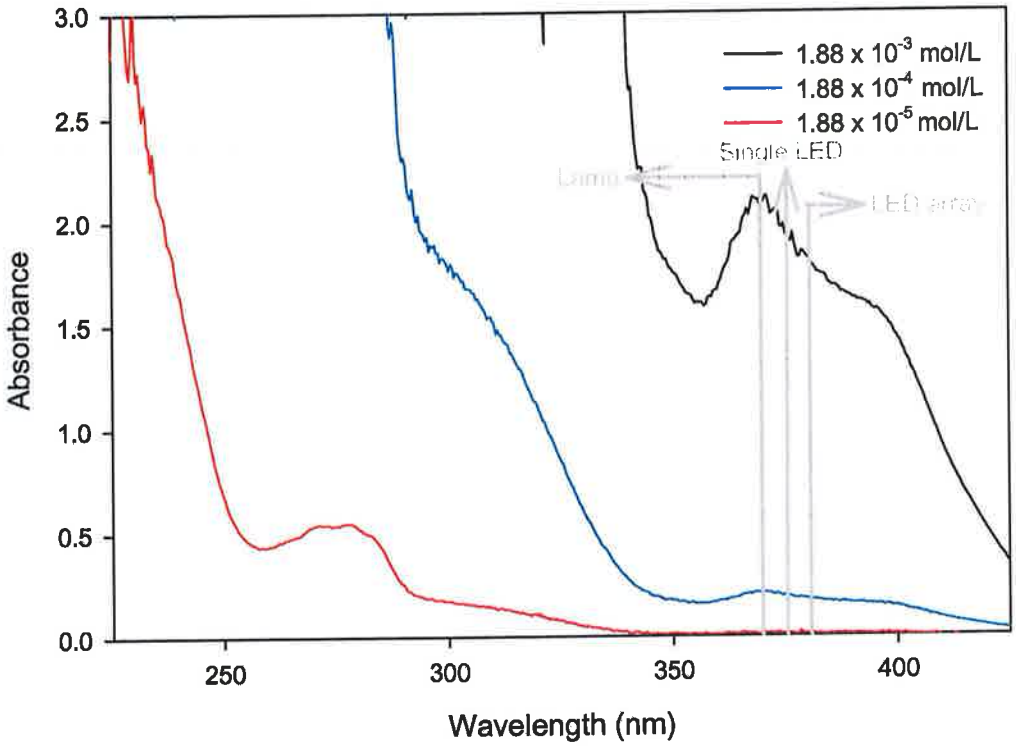

Figure 5.7 (a): UV/Vis absorption spectra of Irgacure 819.

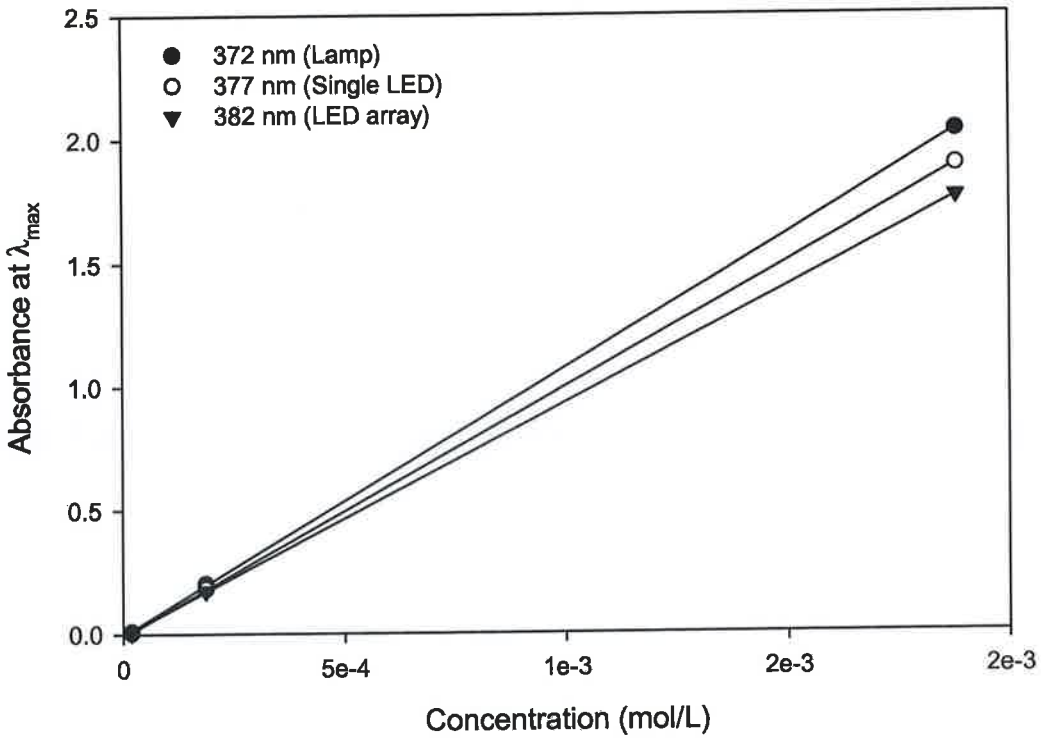

Figure 5.7 (b): Absorbance -v- concentration for Irgacure 819.

Table 5.1: Absorbance values for Darocur 1173 at the maximum emission wavelength of each light source.

Concentration (mol/L)	372 nm (Lamp)	377 nm (Single LED)	382 nm (LED array)
4.79×10^{-3}	0.0505 ±0.001	0.0324 ±0.001	0.0256 ±0.001
4.79×10^{-4}	0.0049 ±0.001	0.0046 ±0.001	0.0053 ±0.001
4.79×10^{-5}	0.0004 ±0.001	0.0012 ±0.001	0.0001 ±0.001

Table 5.2: Absorbance values for Irgacure 651 at the maximum emission wavelength of each light source.

Concentration (mol/L)	372 nm (Lamp)	377 nm (Single LED)	382 nm (LED array)
3.07×10^{-3}	0.2852 ±0.001	0.1912 ±0.001	0.1031 ±0.001
3.07×10^{-4}	0.0640 ±0.001	0.0441 ±0.001	0.0370 ±0.001
3.07×10^{-5}	0.0075 ±0.001	0.0036 ±0.001	0.0039 ±0.001

Table 5.3: Absorbance values for Irgacure 1800 at the maximum emission wavelength of each light source.

Concentration (mol/L)	372 nm (Lamp)	377 nm (Single LED)	382 nm (LED array)
2.85×10^{-3}	0.4152 ±0.001	0.3548 ±0.001	0.3394 ±0.001
2.85×10^{-4}	0.0385 ±0.001	0.0273 ±0.001	0.0298 ±0.001
2.85×10^{-5}	0.0027 ±0.001	0.0023 ±0.001	0.0024 ±0.001

Table 5.4: Absorbance values for Irgacure 369 at the maximum emission wavelength of each light source.

Concentration (mol/L)	372 nm (Lamp)	377 nm (Single LED)	382 nm (LED array)
2.15×10^{-3}	1.4898 ±0.001	0.9481 ±0.001	0.6775 ±0.001
2.15×10^{-4}	0.1335 ±0.001	0.0849 ±0.001	0.0634 ±0.001
2.15×10^{-5}	0.0125 ±0.001	0.0084 ±0.001	0.0042 ±0.001

Table 5.5: Absorbance values for Darocur TPO at the maximum emission wavelength of each light source.

Concentration (mol/L)	372 nm (Lamp)	377 nm (Single LED)	382 nm (LED array)
2.25×10^{-3}	1.1714 ±0.001	1.3758 ±0.001	1.4701 ±0.001
2.25×10^{-4}	0.1192 ±0.001	0.1330 ±0.001	0.1444 ±0.001
2.25×10^{-5}	0.0069 ±0.001	0.0088 ±0.001	0.0097 ±0.001

Table 5.6: Absorbance values for Irgacure 819 at the maximum emission wavelength of each light source.

Concentration (mol/L)	372 nm (Lamp)	377 nm (Single LED)	382 nm (LED array)
1.88×10^{-3}	2.0278 ±0.001	1.8872 ±0.001	1.7602 ±0.001
1.88×10^{-4}	0.2016 ±0.001	0.1822 ±0.001	0.1737 ±0.001
1.88×10^{-5}	0.0103 ±0.001	0.0047 ±0.001	0.0065 ±0.001

The molar absorptivity (ε_λ) for each photoinitiator at the maximum emission wavelength for each light source was calculated from figures 5.2 (b) - 5.7 (b) using the Beer-Lambert law, the values are presented in table 5.7.

Table 5.7: Molar absorptivity (ε_λ) for each photoinitiator at the maximum emission wavelength.

	ε_λ at 372 nm $L.mol^{-1}.cm^{-1}$ (lamp)	**ε_λ at 377 nm $L.mol^{-1}.cm^{-1}$ (single LED)**	**ε_λ at 382 nm $L.mol^{-1}.cm^{-1}$ (LED array)**
Irgacure 819	1082 ±0.5	1010 ±0.5	940 ±0.5
Irgacure 369	697 ±0.5	443 ±0.5	317 ±0.5
Darocur TPO	521 ±0.5	614 ±0.5	655 ±0.5
Irgacure 1800	146 ±0.5	126 ±0.5	120 ±0.5
Irgacure 651	87 ±0.5	58 ±0.5	29 ±0.5
Darocur 1173	11 ±0.5	7 ±0.5	5 ±0.5

Molar absorptivity (ε_λ) is an important value to take into account when choosing a photoinitiator for use in photopolymerisation processes as it gives an indication how much light of a particular wavelength the photoinitiator will absorb [1, 2]. From table 5.7 it is seen that Irgacure 819 has the highest ε_λ at the maximum emission wavelength for each of the light sources, indicating that this photoinitiator has the highest probability of absorbing the output radiation from each light source. For the fluorescent lamp the next highest absorbing photoinitiator is Irgacure 369, while for the single LED and the LED array the second highest absorbing initiator is Darocur TPO. Based purely on the ε_λ,

Darocur 1173 should produce the least amount of cure as it is the least absorbing photoinitiator for the lamp and the two LEDs.

However the absorbance values in tables 5.1-5.6 and the ε_λ values in table 5.7 are based on the absorption at λ_{max} for each light source. It assumes that the light sources are ideally monochromatic and that the photoinitiator will only absorb at λ_{max}, were as in fact these sources have a $\Delta\lambda$ of approximately 50 nm with the lamp also emitting in the visible region. Therefore the photoinitiators will absorb at other wavelengths that are in their absorption spectrum. It has been reported by Allen [3] that although certain photoinitiators exhibit equal or similar ε_λ values, suggesting a similar curing behaviour, the photochemistry of each compound may profoundly affect the generation of free radicals. Another factor not taken into account with these values is the quantum yield (Φ) which, as described previously in chapter 1, is the number of initiating species produced per photon absorbed [12]. It is reasonable to assume that Φ will vary for different photoinitiators.

Another point that should be noted is that the UV absorption and molar absorptivity values achieved in these set ups may be slightly different from the actual amount of absorption that will occur when the initiators are mixed with HEMA as the host material, acetonitrile in this case, is different [13]. G.J. Sun et al. [5] found that the maximum wavelength absorption shifted between 4-15 nm when the host solvent was changed. Molar absorptivity may also vary with concentration [13]. However these calculated ε_λ values do correspond well to the published ε_λ values [13, 14] for these photoinitiators considering the published

values were calculated with the photoinitiators dissolved in methanol and different concentrations.

5.2.4 Discussion

This part of the study was concerned with measuring the UV/vis absorption characteristics of the six photoinitiators to be used in the photopolymerisation of a HEMA monomer. As FTIR spectroscopy would be used to obtain the curing profile of each monomer/photoinitiator sample it was important to measure the absorption characteristics of NaCl plates.

From the UV/vis studies it was found that the NaCl plates absorb very little radiation over the output range of the three light sources, therefore they will allow transmission of the UV radiation onto the monomer sample and will not unduly interfere with the photopolymerisation process. The presence of the photoinitiator in the monomer sample increases the absorption in the wavelength region of interest; this is because the photoinitiator is photosensitive and is capable of absorbing radiation a required wavelength.

The next part of the research involved conducting a Beer-Lambert law study of the six different photoinitiators that were available. There were a number of reasons for this. The first was to ensure that each photoinitiator absorbed over the wavelength regions emitted by each source. Next was to see the effect increasing the concentration had on the amount of absorbance. Finally this study allowed for the calculation of ε_λ which gave an indication of how much radiation of a particular wavelength each photoinitiator absorbed. From this information the photoinitiator that had the highest absorbance at the λ_{max} of each source and which photoinitiator had the highest probability of absorption at that wavelength

was identified. Assuming that the photoinitiator with the highest ε_λ would produce the most free radicals theoretically then the photoinitiator that would potentially yield the highest percentage cure could be identified. If this was the case the monomer sample containing Irgacure 819 should produce the highest degree of cure as it has the highest absorbance values and the highest ε_λ values at the λ_{max} of each light source. While the monomer sample containing Darocur 1173 should yield the lowest cure as it had the lowest absorbance and ε_λ values at the λ_{max} of each light source. However experimentally this may not occur as the absorbance values and the ε_λ values discussed previously are based on at the λ_{max} of each light source and do not take into account the effect the other wavelengths will have on the production of free radicals. Also it does not take into account the quantum yield of each photoinitiator. This point will be discussed further in the photopolymerisation study (section 5.3).

5.3 In-situ spectroscopy study of the photopolymerisation process

The objective of this study was to measure the extent of monomer to polymer conversion that occurred when the monomer was exposed to the three different light sources. In a manufacturing set up the monomer is continuously exposed to UV radiation until complete photopolymerisation has occurred. Therefore it was decided to use spectroscopy to monitor the curing process in-situ so that a continuous profile of the curing process could be obtained. This procedure involved placing the light sources directly into the system used to measure the degree of cure. The degree of conversion (DC) has been studied by several groups using a number of different methods, including; differential

scanning calorimetry [10, 15], Raman spectroscopy [16, 17], nuclear magnetic resonance spectroscopy [18] and Fourier transform infrared (FTIR) spectroscopy [16, 19, 20]. This study utilised two of these techniques namely FTIR and Raman spectroscopy.

5.3.1 Fourier transform infrared (FTIR) spectroscopy

Initially FTIR spectroscopy was used to prove the concept that a UV-LED could initiate a photopolymerisation process. This section discusses how FTIR spectroscopy was used to measure and examine the UV-photoinitiated curing profile of a HEMA sample. This process was first attempted at the start of the research when only the single LED was available. It was then repeated with the LED array when that came on the market. The problem with this set up was that the layout of the spectrometer was such that the fluorescent lamp was too big to fit into the bench were the sample was to be irradiated. Therefore it was not possible to obtain the curing profile of the fluorescent lamp in this set up.

An infrared spectrum of the blank NaCl plates was first recorded as background, after which a small drop of the monomer sample containing the photoinitiator Darocur TPO (2.25×10^{-3} mol/L concentration) was placed into the sample holder which consisted of the two NaCl plates. An infrared spectrum of the uncured monomer was then recorded. As this was just an initial study to prove the concept only one photoinitiator was used. In FTIR spectroscopy the beam passes perpendicular through the sample therefore each LED was placed to the side of the plates to avoid interference with the FTIR beam. After ensuring correct alignment of the LED the sample was irradiated for a total of twenty minutes with an FTIR spectrum being recorded at every one minute interval.

Before the monomer sample was used it was flushed with oxygen free nitrogen to remove any oxygen that could hinder photopolymerisation. Figure 5.8 shows a typical FTIR spectrum of the HEMA monomer before and after UV exposure for a given time. The reduction in intensity of the reference peak (1174 cm^{-1}) is due to the phase change of the sample as the liquid monomer becomes a solid polymer. This effect is taken into account when calculating the percentage photopolymerisation [21].

The degree of cure (DC) or percentage cure was calculated using equation 4.2.

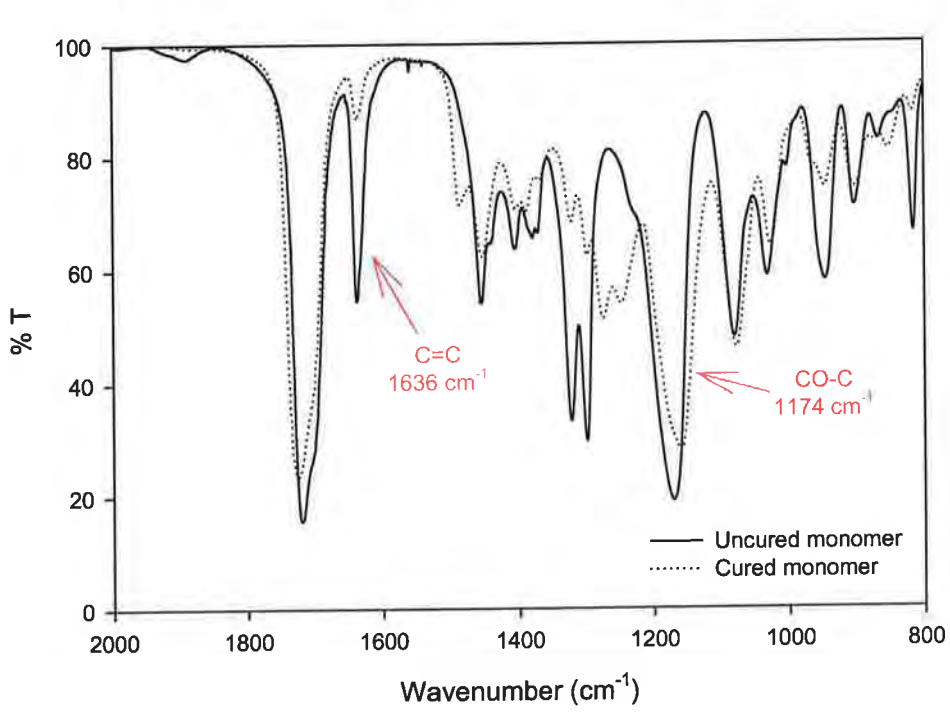

Figure 5.8: Typical FTIR spectra of the HEMA monomer before and after UV exposure for a given time.

Figure 5.9 displays the curing profile achieved with the single LED and the LED array. Both curing profiles exhibit low initial cures in the first 2 minutes of exposure. As expected due to its higher intensity the LED array yielded a higher final percentage cure (61 %) compared to the 46 % achieved with the single LED. However it was hoped that a higher final percentage cure would be achieved with the LED array. It can be concluded that the main reason for the fact it didn't is due to the positioning of the LED. In this set up the LED array was placed to the side of the NaCl plates meaning the radiation from the LED had to pass through the unpolished side of the plate reducing the amount of radiation reaching the monomer. To overcome this problem Raman spectroscopy was used, the Raman set up allowed for the LED to be placed directly under the monomer allowing for in-situ monitoring of the cure without the loss of any radiation. This method is discussed in the next section. Although a low percentage cure was achieved in the FTIR set up it proved the concept that LEDs could be used to photopolymerise the polymer HEMA.

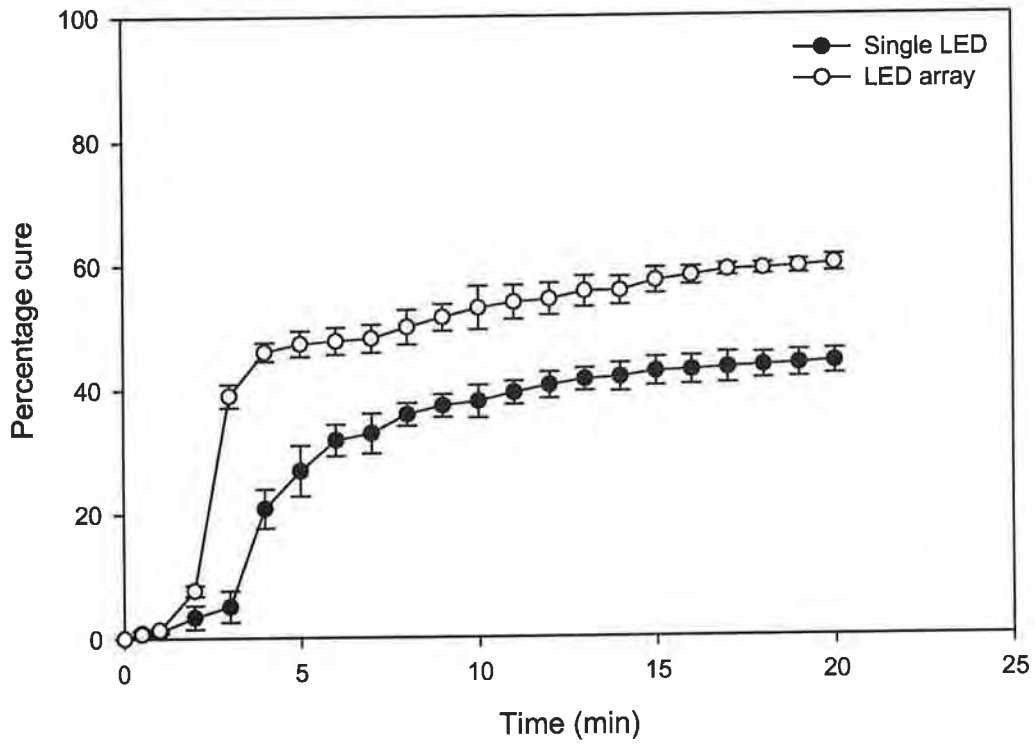

Figure 5.9: In-situ curing profile achieved with the single LED and LED array.

5.3.2 Raman Spectroscopy

The advantage of Raman spectroscopy over FTIR spectroscopy is that the monomer sample could be cured and monitored in-situ as the layout of the Raman spectrometer is such that the LED could be placed directly under the sample. The curing profile of the monomer samples containing each photoinitiator were obtained with Raman spectroscopy.

As the percentage cure achieved with the single LED in the previous FTIR in-situ set up was low it was decided not used to use it here. Once again the same problem encountered with the fluorescent lamp was experienced here; the layout of this spectrometer was such that it was impossible to place the lamp

under the monomer sample. Therefore the in-situ curing profile of the fluorescent lamp could not be obtained.

To ensure that the exposure area of the monomer sample was the same size as the output area of the LED (i.e. 10 mm) part of the LED array was masked off so that the spectrometer would only 'see' the area of the sample being illuminated. This ensured that any non-illuminated uncured monomer would not interfere with the final values for percentage cure. Here quartz slides which are UV transparent were used in place of NaCl plates. A small drop of one of the monomer samples was placed onto the quartz slide and a glass cover slip put over it to prevent oxygen infusion which would inhibit photopolymerisation [22], an initial uncured spectrum was recorded. The sample was then exposed to UV radiation from the LED, which was situated directly below the sample, for thirty seconds and another spectrum recorded. This procedure was repeated a number of times until the C=C peak at 1636 cm^{-1} had sufficiently disappeared signalling polymerisation. Figure 5.10 shows typical Raman spectra of the HEMA monomer before and after UV exposure for a given time.

Each of the monomer samples were cured in this way and the percentage cure calculated using equation 4.3.

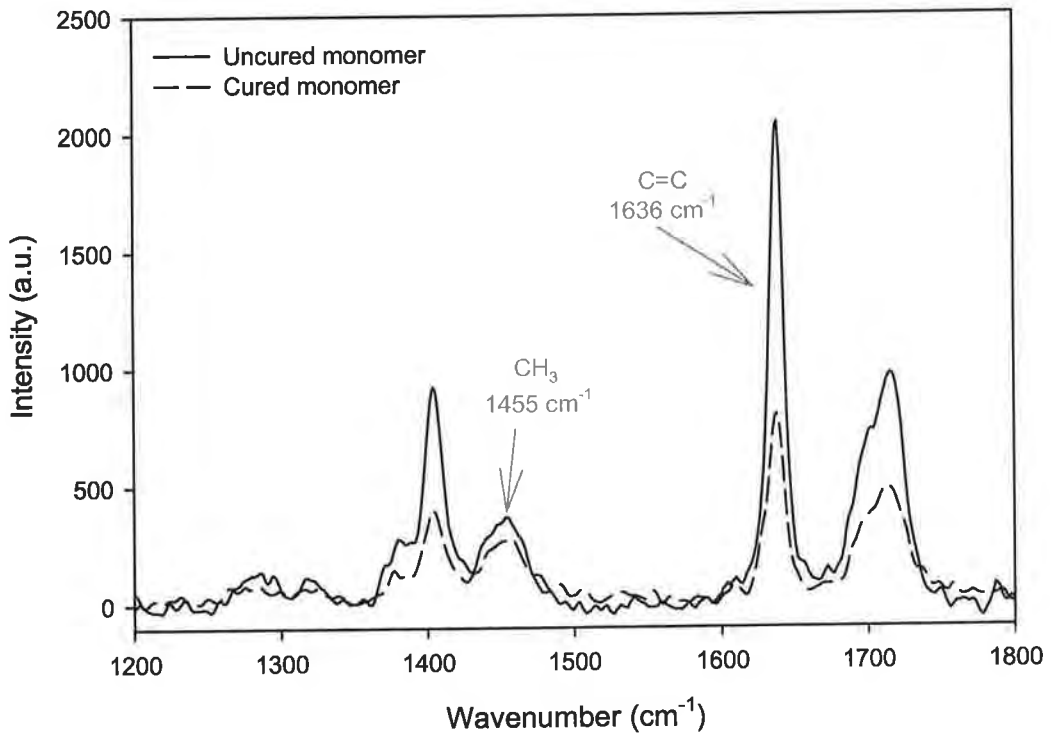

Figure 5.10: Typical Raman spectra of the HEMA monomer before and after UV exposure.

This preliminary study was intended to prove the concept that UV-LEDs can be used to cure HEMA using a variety of photoinitiators. Raman spectroscopy was used to in-situ monitor the photopolymerisation process. Figure 5.11 shows an overlay of the percentage cure using the LED array against time for each photoinitiator monitored in-situ by Raman spectroscopy. This figure is for illustration purposes only and shows that (a) UV-LEDs can cause photopolymerisation and (b) that Raman spectroscopy can be used to in-situ monitor the photopolymerisation process.

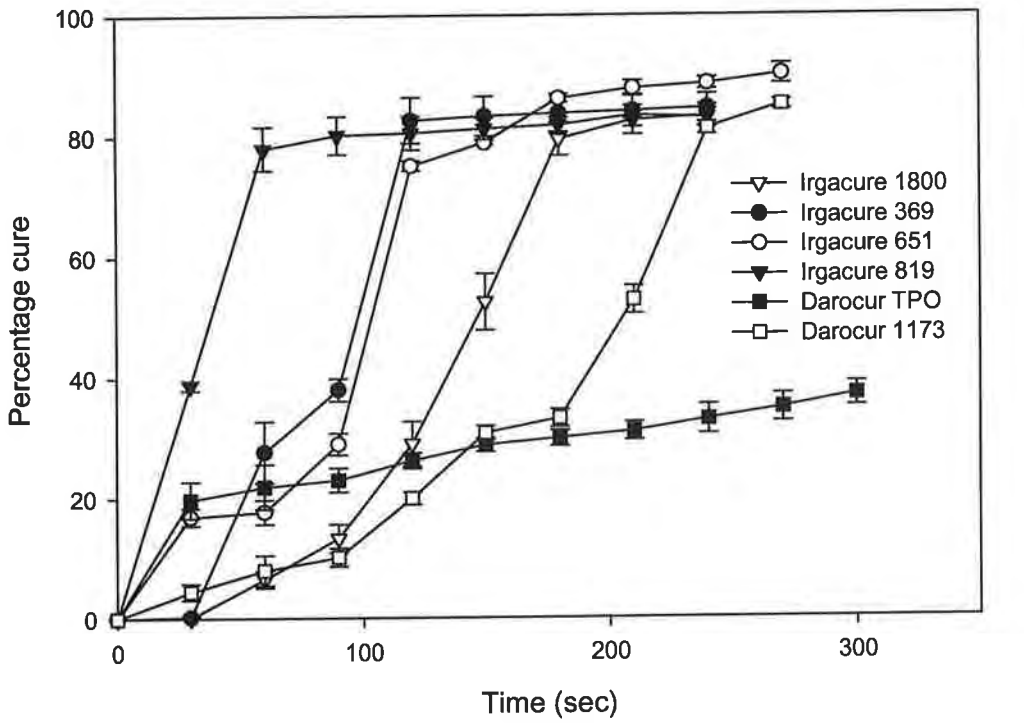

Figure 5.11: Percentage cure achieved for in-situ photopolymerisation using the LED array.

5.3.3 Discussion

Both FTIR and Raman spectroscopy were used to prove the concept that the UV-LEDs could be used to initiate photopolymerisation. The percentage cure achieved in FTIR spectroscopy experimental set up was low. It could be concluded that this was due to the positioning of the LEDs in the FTIR spectrometer. This problem was overcome with Raman spectroscopy, were the layout of this spectrometer was such that the LED could be placed directly below the monomer sample. This allowed for continuous monitoring of the photopolymerisation process during UV radiation exposure by the LED array.

It was not possible to cure in-situ with the fluorescent lamp using these spectrometers as the size of the lamp and ballast prevented it from being placed in the spectrometer. Therefore although the concept that UV-LEDs could initiate a photopolymerisation reaction had been proven this set up did not allow for an intercomparison between the amount of cure achieved with the LEDs and the traditionally used fluorescent lamp. Therefore it was decided to use a different set up which would involve the monomer sample being cured external to the spectrometer. Although this new set up would not give a constant curing profile it would allow an intercomparison of the degree of conversion achieved between each source which is one of the main aims of this research.

The problem encountered in this section further emphasised a major advantage that LEDs have over conventional fluorescent lamps, the size and shape of the LEDs makes them ideal for using in environments were bulky lamps can not be easily fitted.

5.4 Investigation into the degree of cure achieved with each light source

As FTIR spectroscopy is the one technique that has been used extensively in research to measure the degree of conversion [16, 19, 20, 23] it was decided to use this technique for the rest of this study. There were two sections to this study, the first part allowed for a comparison between the UV-LED and the UV lamp as a UV source for photopolymerisation. The second part was concerned with the identification of the best photoinitiator to use with each source, i.e. at the same concentration which photoinitiator yielded the highest percentage cure for the fluorescent lamp and the LEDs. For both sections the monomer samples were exposed to the maximum intensity achievable by each light source.

5.4.1 Comparison of the single LED to other UV sources

To date mercury fluorescent or halogen lamps have been the main source of UV radiation in photopolymerisation processes [21, 24, 25]. With the development of solid state lighting (SSL) numerous studies [26-31] have proposed replacing these lamps with blue LEDs in the manufacturing of biomaterials, such studies have been mainly interested in the polymerisation of oral biomaterials where traditional light curing units (LCUs) were based on halogen technology. One such study [32] has shown that the new blue LED LCUs produced a degree and depth of cure significantly greater than that obtained using halogen lamps. The first part of this study was to ensure that the UV-LEDs could initiate photopolymerisation in the monomer sample to the same degree as the traditionally used fluorescent lamps, after which an intercomparison between each source could be made. After an initial spectrum of the uncured monomer was

recorded each monomer sample was exposed to one light source for two minutes and another spectrum was obtained, this procedure was repeated periodically until the C=C vibrational band at 1636 cm^{-1} had decreased significantly indicating photopolymerisation had occurred. Before the monomer sample was used it was flushed with oxygen free nitrogen to remove any oxygen that could hinder photopolymerisation [22, 33, 34]. Once again the degree of cure (DC) or percentage cure was calculated using equation 4.2.

Figure 5.12 shows the curing profile achieved for each light source using Irgacure 1800 as the photoinitiator. The sample was exposed to UV radiation until the spectra showed minimal or no changes in the peak height at 1636 cm^{-1} or until the peak height became too small to be distinguished from noise. Therefore it could no longer be used in the calculation of percentage cure. The initial percentage cure achieved with the fluorescent lamp and the LED array is very similar and at two minutes the percentage cure reached is almost identical. The single LED displays a slower curing profile, compared to the other two light sources during the first 10 minutes of exposure. However after 18 minutes it gave a final cure of 72% which is comparable to that achieved with the LED array (79%). The lamp reaches a final cure of 83% after 12 minutes of exposure. This is because the intensity of the single LED is lower compared to that of the LED array and the fluorescent lamp.

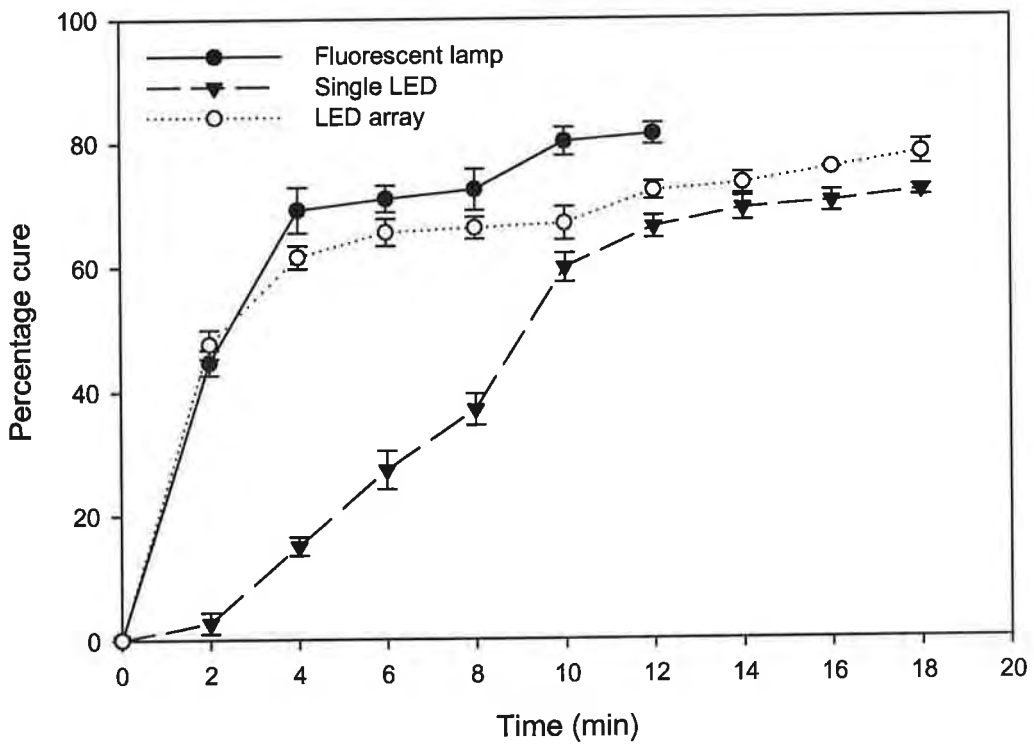

Figure 5.12: Curing profile achieved with each light source using Irgacure 1800.

Further photopolymerisation studies showed that the single LED was not always a reliable source for curing the monomer/photoinitiator sample, as upon calculation the monomer sometimes appeared to give a negative percentage cure even though the plates were stuck together signalling photopolymerisation. On studying the spectra it was found that the negative values for percentage cure occurred because the C=C peak decreased and then increased over time which lead to the calculated cure rate increasing and decreasing overtime. This did not occur with the fluorescent lamp or the LED array. Upon separation of the NaCl plates some liquid monomer residue was found among the polymerised polymer. One possible reason for this may be that the size of the sample curing area for the single LED was smaller than the sample area for the lamp and LED array, so more

liquid monomer is masked off from the UV radiation. Therefore after polymerisation it is possible that the unpolymerised monomer in the masked area flowed into the polymerised region, resulting as an increase in the peak intensity of the C=C peak in the spectrum, this would in turn distort the percentage cure calculations. Due to this and the fact it was more likely that the LED array should be used in commercial photopolymerisation processes due to its higher output intensity it was decided to discontinue using the single LED in this research.

5.4.2 Comparison of UV-LED array and the UV lamp as a UV source for photopolymerisation

Figures 5.13-5.18 give the curing profiles achieved with the six photoinitiators while tables 5.8-5.13 give the values for ε_λ along with the percentage cures achieved with each photoinitiator after 2 and 20 minutes of exposure.

The curing profiles achieved using Darocur 1173 as the photoinitiator are displayed in figure 5.13. From this figure it can be seen that the monomer exhibits a slow initial cure, however after a period of time the percentage cure increases. Although the ε_λ at each λ_{max} for this photoinitiator is the lowest calculated the final percentage is not low in comparison. This initiator exhibited the highest final percentage cure when exposed to the fluorescent lamp (76 %); a final percentage cure of 65 % was achieved with the LED array.

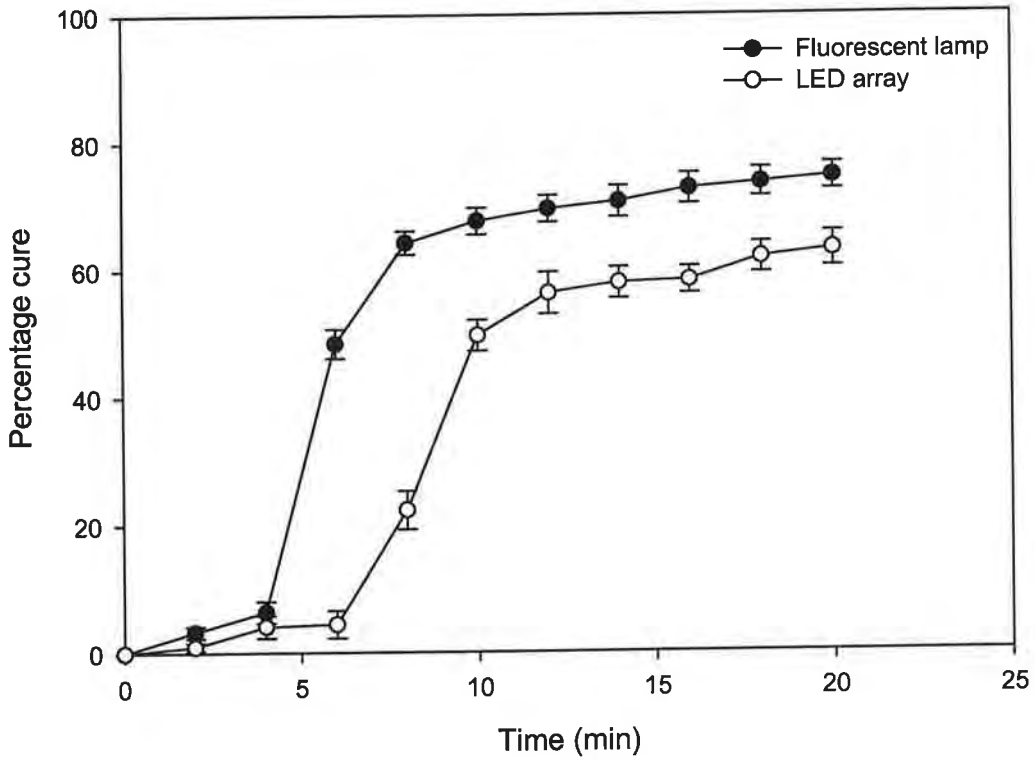

Figure 5.13: Curing profile achieved with each light source using Darocur 1173.

Table 5.8: Comparison between the molar absorptivity (ε_λ) at λ_{max} and the percentage cure achieved with each light source after 2 and 20 minutes of exposure using Darocur 1173.

	ε_λ at each λ_{max} L.mol^{-1}.cm^{-1}	**Percentage cure after 2 minutes**	**Percentage cure after 20 minutes**
Fluorescent Lamp	11	4%	76%
LED array	5	1%	65%

The percentage cures achieved with Irgacure 651 are displayed in figure 5.14. Although the ε_λ at the λ_{max} of the fluorescent lamp is nearly three times

bigger than the ε_λ at the λ_{max} of the LED array the final percentage cures achieved are very equivalent with 78% and 74% conversion for the fluorescent lamp and the LED array respectively. The curing profiles exhibited for each light source are also similar in that they both produce a low initial cure that increases rapidly between two and four minutes before levelling out at six minutes.

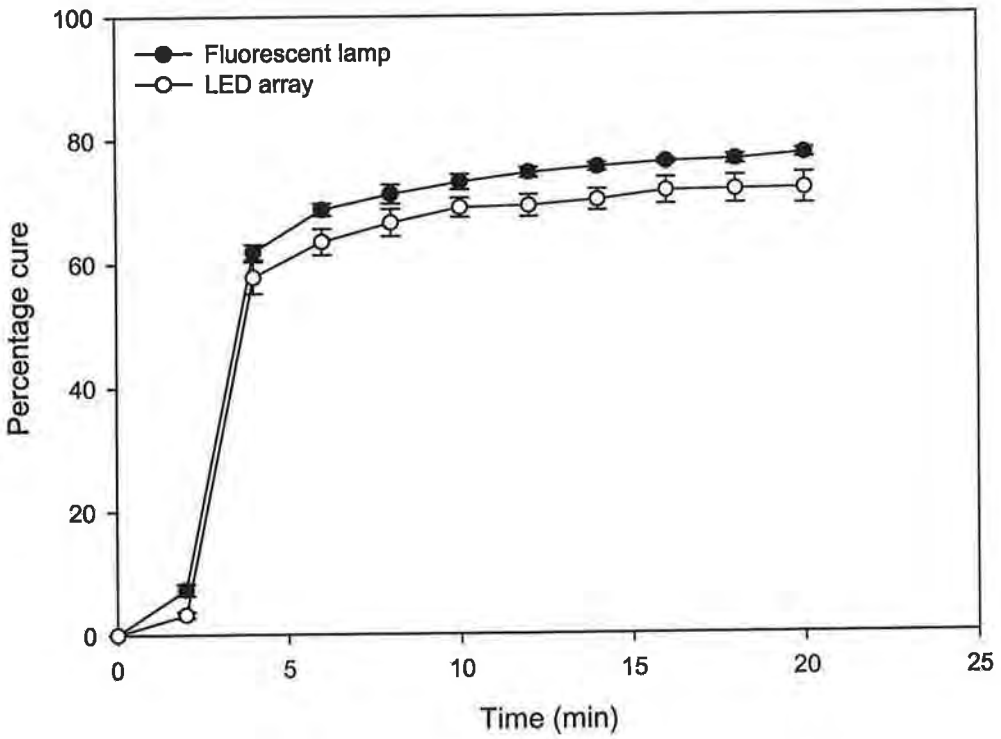

Figure 5.14: Curing profile achieved with each light source using Irgacure 651.

Table 5.9: Comparison between the molar absorptivity (ε_λ) at λ_{max} and the percentage cure achieved with each light source after 2 and 20 minutes of exposure using Irgacure 651.

	ε_λ at each λ_{max} L.mol^{-1}.cm^{-1}	**Percentage cure after 2 minutes**	**Percentage cure after 20 minutes**
Fluorescent Lamp	87	8%	78%
LED array	29	4%	74%

Figure 5.15 displays the curing profiles achieved when the Irgacure 369 photoinitiator is used. While there is a difference of over 20% between the two percentage cures achieved, there is also a difference in the ε_λ at the λ_{max} of each light source, with the lamp displaying a ε_λ that is over twice that for the LED array. Although there is a difference in the final cure rates their curing profiles are similar in that after five minutes the percentage cure increases substantially before they plateau out to some extent.

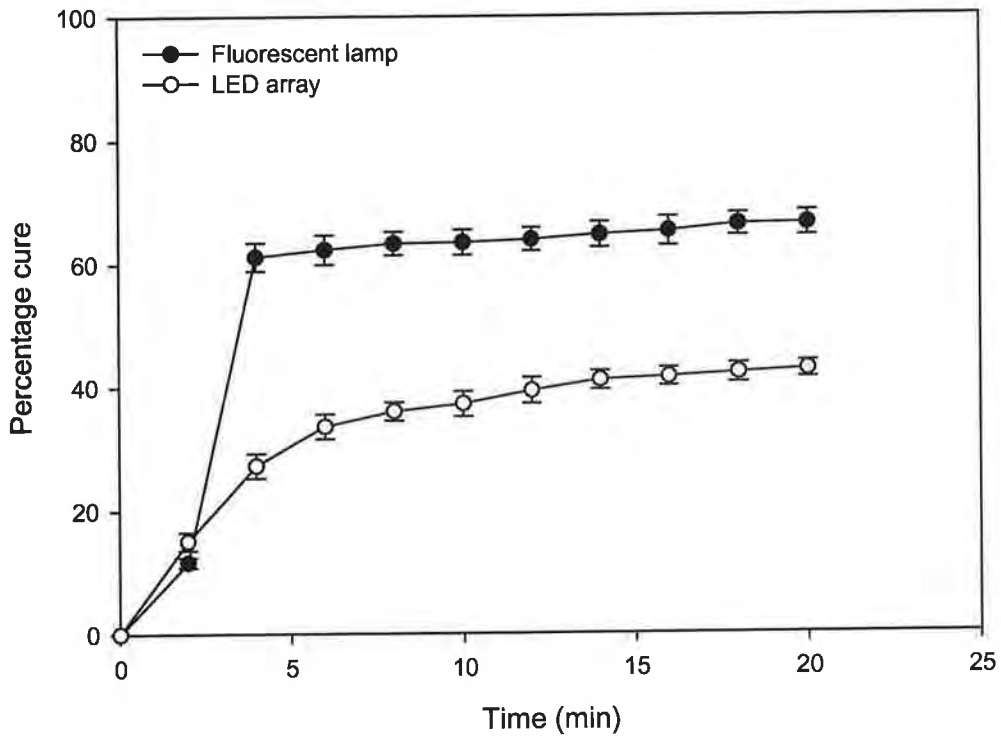

Figure 5.15: Curing profile achieved with each light source using Irgacure 369.

Table 5.10: Comparison between the molar absorptivity (ε_λ) at λ_{max} and the percentage cure achieved with each light source after 2 and 20 minutes of exposure using Irgacure 369.

	ε_λ at each λ_{max} $L.mol^{-1}.cm^{-1}$	Percentage cure after 2 minutes	Percentage cure after 20 minutes
Fluorescent Lamp	697	12%	68%
LED array	317	16%	44%

The curing profiles achieved using Darocur TPO as the photoinitiator are shown in figure 5.16. The curing profiles and percentage cure achieved with the

lamp and the LED array are similar (difference of less than 10%) even though there is a difference in the ε_λ at the λ_{max} of each light source.

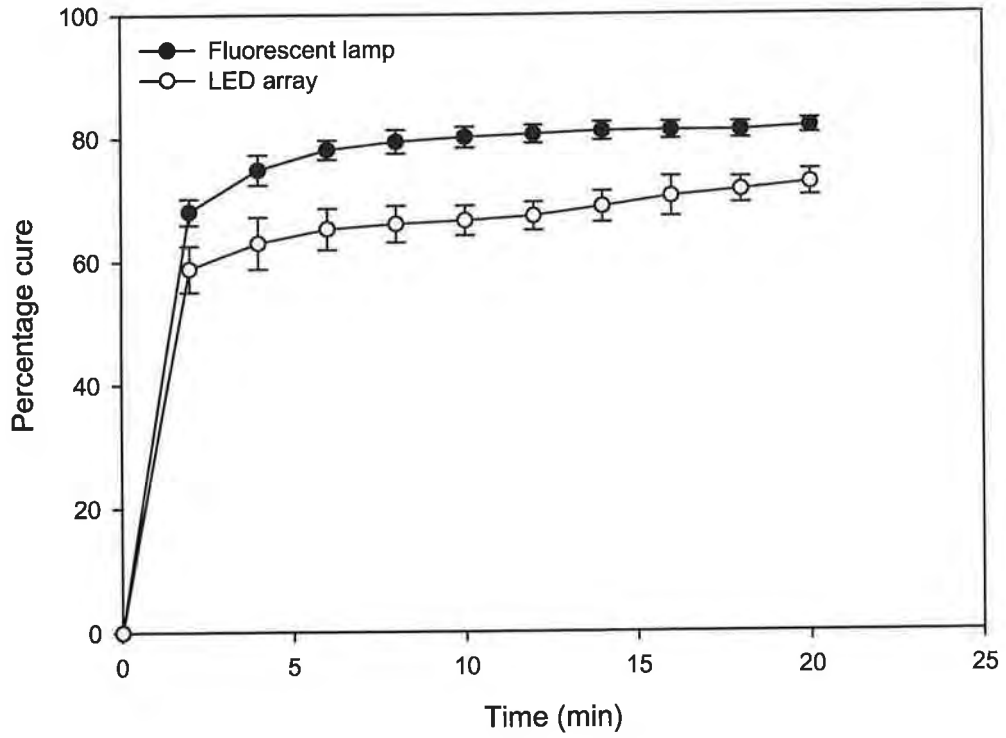

Figure 5.16: Curing profile achieved with each light source using Darocur TPO.

Table 5.11: Comparison between the Molar Absorptivity (ε_λ) at λ_{max} and the percentage cure achieved with each light source after 2 and 20 minutes of exposure using Darocur TPO.

	ε_λ at each λ_{max} $L.mol^{-1}.cm^{-1}$	2 minutes (% cure)	20 minutes (% cure)
Fluorescent Lamp	521	70%	83%
LED array	655	61%	74%

Figure 5.17 displays the curing profiles achieved using Irgacure 819. Here there is a large difference in the percentage cure achieved using each light source even though there is not a huge difference in the ε_λ at the λ_{max} of each source. However, their temporal profiles are similar in that they both plateau after 2 minutes of exposure.

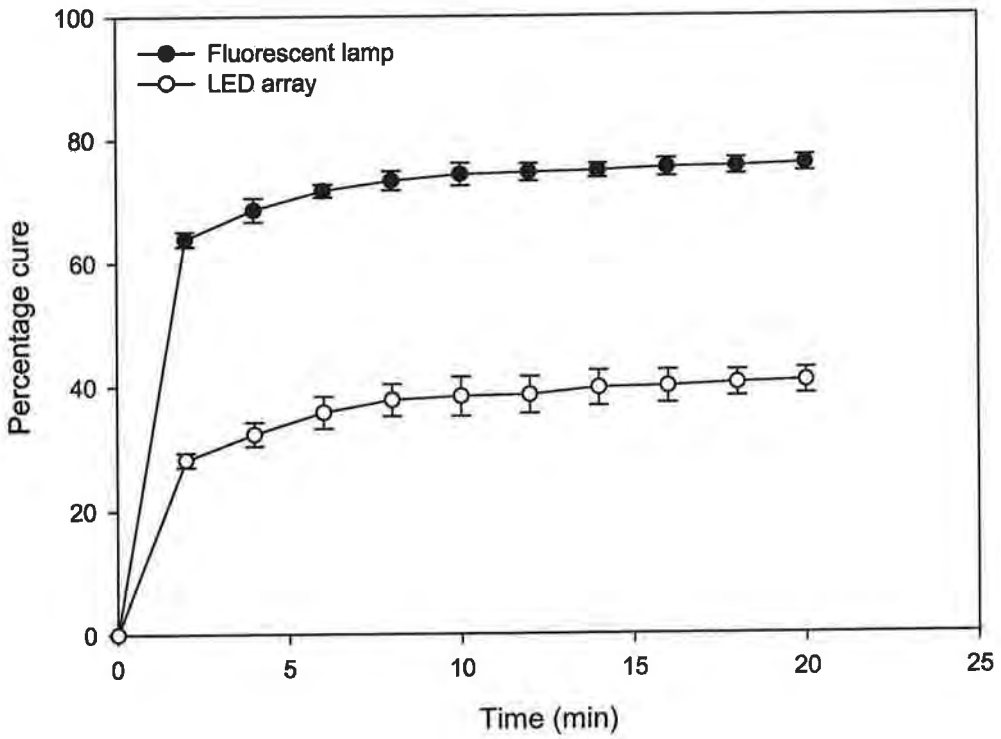

Figure 5.17: Curing profile achieved with each light source using Irgacure 819.

Table 5.12: Comparison between the Molar Absorptivity (ε_λ) at λ_{max} and the percentage cure achieved with each light source after 2 and 20 minutes of exposure using Irgacure 819.

	ε_λ at each λ_{max} $L.mol^{-1}.cm^{-1}$	2 minutes (% cure)	20 minutes (% cure)
Fluorescent Lamp	1082	65%	77%
LED array	940	29%	42%

Figure 5.18 displays the curing profile of Irgacure 1800; once again there is a large difference in the percentage cure achieved with the two light sources even though the ε_λ at the λ_{max} for each are not hugely dissimilar. Like Irgacure 369 this photoinitiator exhibits a higher initial percentage cure when exposed to the LED array. However following on from this the percentage cure of the sample exposed to the fluorescent lamp increases greatly to give a final percentage cure at 20 minutes of 81%.

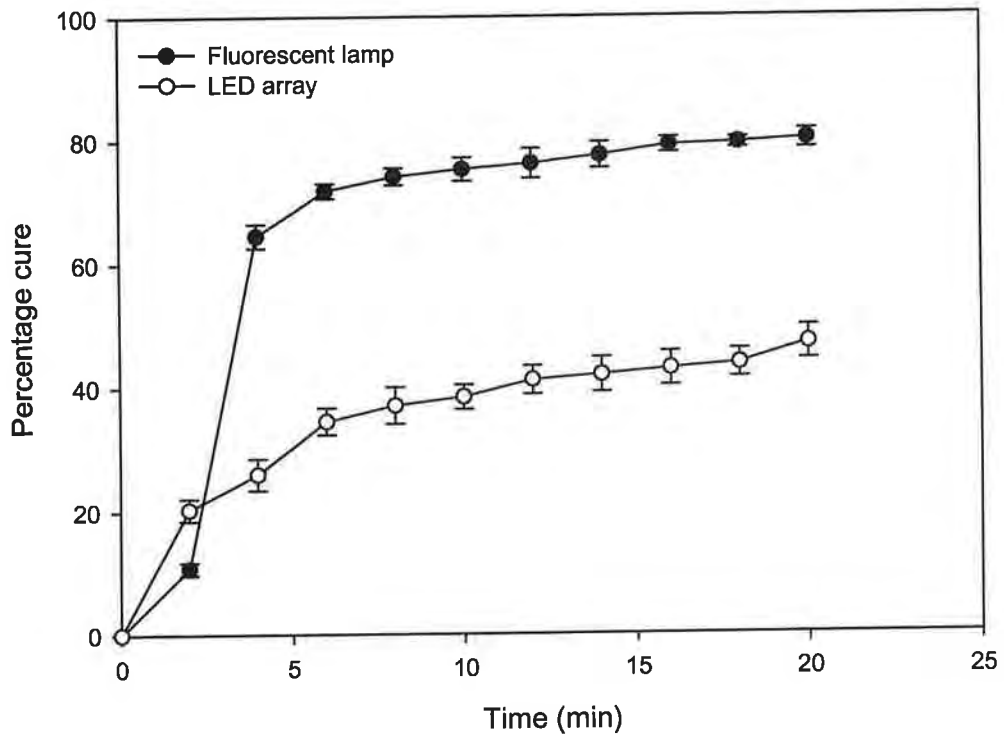

Figure 5.18: Curing profile achieved with each light source using Irgacure 1800.

Table 5.13: Comparison between the Molar Absorptivity (ε_λ) at λ_{max} and the percentage cure achieved with each light source after 2 and 20 minutes of exposure using Irgacure 1800.

	ε_λ at each λ_{max} $L.mol^{-1}.cm^{-1}$	2 minutes (% cure)	20 minutes (% cure)
Fluorescent Lamp	146	11%	81%
LED array	120	22%	49%

5.4.3 Discussion

This study was concerned with comparing the percentage cure achieved with each light for a certain photoinitiator. As such each monomer sample was exposed to the fluorescent lamp and the LED array for a set period of time and the percentage cure achieved for each then calculated and compared. Tables 5.8 to 5.13 give the ε_λ for each photoinitiator at the maximum emission wavelength of each source and the percentage cure achieved at 2 and 20 minutes of exposure. From these tables it can be seen that although Darocur 1173 had the lowest ε_λ, indicating that this photoinitiator had the lowest possibility of absorbing the output radiation from the sources, the final percentage cure after 20 minutes is not the lowest achieved.

Another surprising result came when Irgacure 819 was used as the photoinitiator. This photoinitiator had the highest ε_λ values at the λ_{max} of each source (1082 $L.mol^{-1}.cm^{-1}$ for the lamp, 940 $L.mol^{-1}.cm^{-1}$ for the LED array) yet it did not produce the highest percentage cures after 20 minutes of exposure. In fact this photoinitiator yielded the lowest percentage cure that was achieved with the LED array.

Although Irgacure 651 had comparably low ε_λ for each source the final percentage cures achieved were high, even though the initial cure was low. Darocur TPO was the only photoinitiator to display both high initial and final cures for both sources.

This study has proven that (1) UV-LEDs can be used to produce a degree of cure comparable to that achieved with fluorescent lamps and (2) when choosing a photoinitiator to be used in photopolymerisation processes you can not solely

rely on the ε_λ at the λ_{max} of the source being used. The reason for this is that even though a photoinitiator had a high ε_λ at the λ_{max} of a particular source it did not necessarily give the highest final cure and likewise a high final cure could be achieved for photoinitiators that had low values of ε_λ. Therefore other factors such as quantum yield should be considered when choosing a photoinitiator to be used in photopolymerisation. This study also proved that even though photoinitiators exhibit equal or similar ε_λ values the photochemistry of each may profoundly affect the generation of free radicals, as was reported by Allen [3].

5.5 Effect of photoinitiator type on degree of conversion

5.5.1 Introduction

The previous FTIR study was concerned with proving the concept that UV-LEDs could photopolymerise a HEMA sample to the same degree as the currently used fluorescent lamps. That study also allowed for an intercomparison between the degrees of cure achieved with each source for a certain photoinitiator. This part of the thesis was concerned with identifying the photoinitiator that yields the highest percentage cure for each UV source. A concentration of 6×10^{-3} mol/L was chosen for each monomer sample, this allowed each monomer sample to have the same concentration of photoinitiator so a direct comparison between the degrees of cure could be made. FTIR spectroscopy was once again used to measure the curing process that occurred with each monomer after which the degree of conversion was calculated.

5.5.2 Photopolymerisation studies

The same NaCl plate set up as used previously was once again utilised. An initial spectrum of the uncured monomer was recorded after which each of the six monomer/photoinitiator samples were individually exposed to one of the light sources for two minutes and another spectrum recorded. This was repeated periodically for a total of twenty minutes. Once again the light sources were placed as close to the sample as possible to ensure maximum intensity, as would be the case in a manufacturing process.

5.5.2.1 Fluorescent Lamp

Figure 5.19 shows an overlay of the curing profiles achieved for each photoinitiator using the fluorescent lamp. The maximum photopolymerisation achieved was 83% occurring with the Darocur TPO sample. The rest of the monomer samples gave final percentage cures of between 76% and 81%, except for Irgacure 369 which gave the lowest percentage cure of 68%. Darocur TPO and Irgacure 819 gave high initial percentage cures after two minutes, 70% and 65% respectively, while the other four photoinitiators exhibited low initial cures after two minutes of exposure. The curing profiles achieved for all six initiators with this light source are all similar in that after about four minutes of exposure to the UV radiation they plateau. Although Darocur 1173 displayed the slowest initial cure it did not yield the lowest final percentage cure.

Table 5.14 gives the ε_λ for each photoinitiator at the maximum emission wavelength of the fluorescent lamp and the percentage cure achieved at 2 and 20 minute intervals of exposure. The highest initial and final percentage cures

occurred with the sample containing Darocur TPO which had a ε_λ value of 521 $L.mol^{-1}.cm^{-1}$, making it the third most possible absorbing photoinitiator. The sample containing Irgacure 369 which had the second highest ε_λ value (697 $L.mol^{-1}.cm^{-1}$) yielded the lowest final percentage cure (68%). Although the two photoinitiators that had the lowest ε_λ (Irgacure 651 and Darocur 1173) did display the lowest initial cures after two minutes they did not produce the lowest final percentage cures. In fact the three least absorbing photoinitiators all displayed relatively high final degrees of conversion, proving that other factors apart from the ε_λ affects the amount of cure achieved.

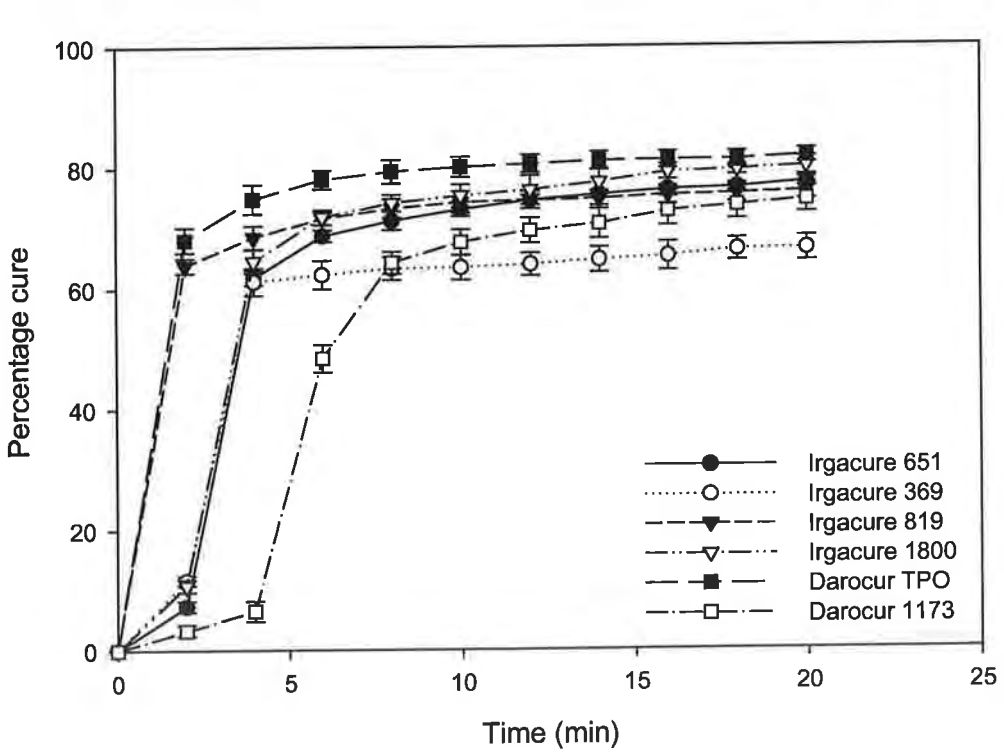

Figure 5.18: Percentage cure -v- time for fluorescent lamp and each photoinitiator.

Table 5.14: Comparison between the molar absorptivity (ε_λ) at λ_{max} of the fluorescent lamp and the percentage cure achieved.

Photoinitiator	ε_λ at 372 nm $L.mol^{-1}.cm^{-1}$ (lamp)	Percentage cure after 2 minutes	Percentage cure after 20 minutes
Irgacure 819	1083	65%	77%
Irgacure 369	697	12%	68%
Darocur TPO	521	70%	83%
Irgacure 1800	146	11%	81%
Irgacure 651	87	8%	78%
Darocur 1173	11	4%	76%

5.5.2.2 LED Array

Figure 5.20 shows an overlay of the percentage cure achieved for each photoinitiator using the LED array. The monomer samples containing both Darocur TPO and Irgacure 651 gave the highest percentage cures (~74%) with Darocur TPO once again giving the highest initial percentage cure. Irgacure 1800 (49%), Irgacure 369 (44%) and Irgacure 819 (42%) all gave low final percentage cures and produced similar curing profiles. Darocur 1173 produced a different curing profile than that achieved with the other photoinitiators for this light source in that it displayed a very slow initial cure over the first six minutes.

Table 5.15 gives the ε_λ for each photoinitiator at the maximum emission wavelength of the LED array and the percentage cure achieved at 2 and 20 minute intervals of exposure. Irgacure 819, which had the highest ε_λ value (940 $L.mol^{-1}.cm^{-1}$), indicating it should be the most absorbing photoinitiator at the λ_{max} of the LED array, yielded the lowest final percentage cure; although it did produce the second highest initial cure. The two monomer samples that produced the

highest final cures (74%) were Darocur TPO and Irgacure 651 which had the second highest and lowest ε_λ values respectively. This indicates once again that ε_λ values can not be solely used when deciding what photoinitiator to use for photopolymerisation processes.

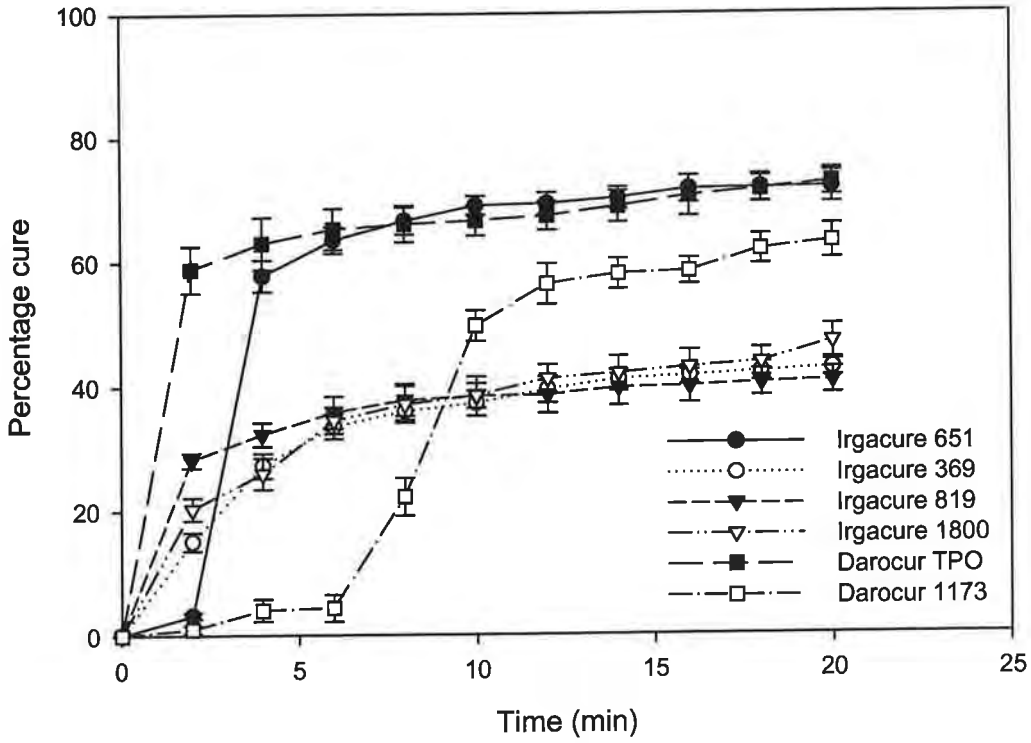

Figure 5.19: Percentage cure -v- time for LED array and each photoinitiator.

Table 5.15: Comparison between the molar absorptivity (ε_λ) at λ_{max} of the LED array and the percentage cure achieved.

Photoinitiator	**ε_λ at 382 nm $L.mol^{-1}.cm^{-1}$ (LED array)**	**Percentage cure after 2 minutes**	**Percentage cure after 20 minutes**
Irgacure 819	940	29%	42%
Darocur TPO	655	61%	74%
Irgacure 369	317	16%	44%
Irgacure 1800	120	22%	49%
Irgacure 651	29	4%	74%
Darocur 1173	5	1%	65%

Figure 5.20 shows the two best photoinitiators for the fluorescent lamp and the LED array. From this figure it can be clearly seen that after the initial four minutes of exposure the curing profiles are all similar and there is only a difference of less than 10 % between the lowest LED array final cure and the highest fluorescent lamp final cure. The sample containing Darocur TPO yields a high initial percentage cure for each light source while the other two photoinitiators exhibit low initial degrees of conversion. Therefore a photoinitiator can be chosen depending on the type of cure required, i.e. if a quick cure time is required Darocur TPO would be recommended while if a low initial cure is required one of the other photoinitiators should be chosen depending what light source is being used.

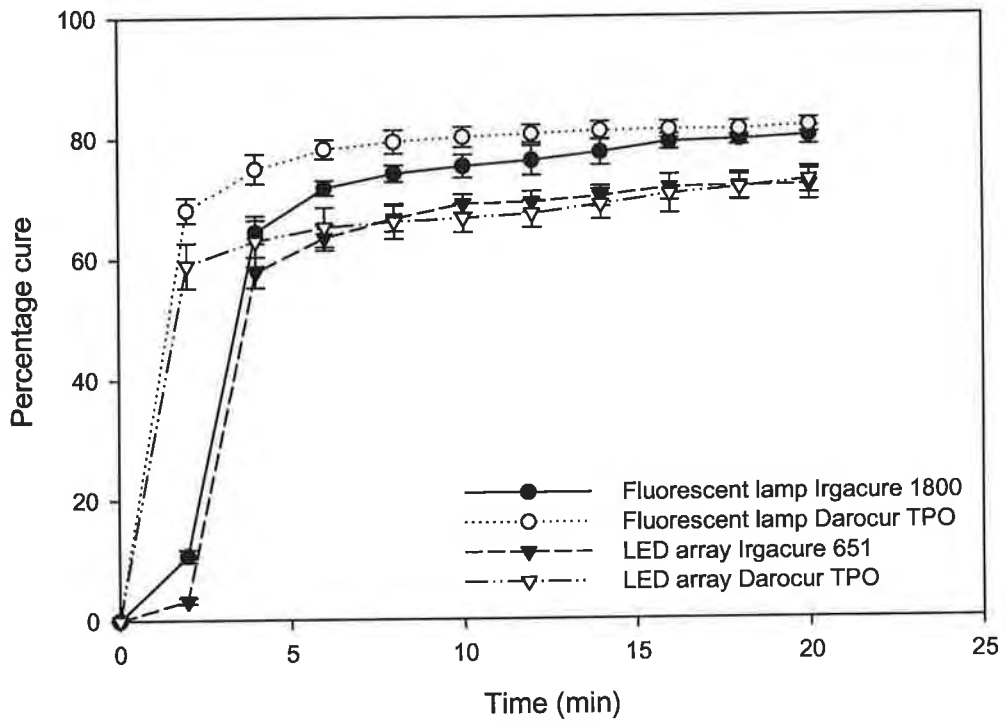

Figure 5.20: Curing profiles using the two best photoinitiators for the fluorescent lamp and the LED array.

5.5.3 Discussion

From the UV/vis studies Irgacure 819 had the highest ε_λ values for each light source. Therefore in principle the monomer sample containing this photoinitiator should produce the highest percentage cure. For this photoinitiator the lamp should produce a higher cure than the LED array as this photoinitiator has a higher ε_λ value at λ_{max} of the lamp (1082 $L.mol^{-1}.cm^{-1}$), compared to 940 $L.mol^{-1}.cm^{-1}$ for the LED array. However although a higher percentage cure was achieved with the lamp, in the curing studies this photoinitiator did not yield the highest final percentage cure for either light source. In fact for the LED array this photoinitiator exhibited the lowest percentage cure for all six photoinitiator

samples. While Darocur 1173 is the least absorbing photoinitiator at the λ_{max} of each source it did produce a relatively high final cure, although in each case the initial cure was the lowest seen; therefore proving that something other than ε_λ affects the amount of free radicals produced.

After twenty minutes of exposure the monomer sample that yielded the highest final cure for each source was the one containing Darocur TPO, this sample also produced the highest initial cure after two minutes of exposure. The curing profiles achieved with the fluorescent lamp are all similar with the final percentage cures varying from 83% to 68%, or 83 % to 76% if Irgacure 369 is excluded. On the other hand the final percentage cures achieved with the LED array vary greatly from 74% to 42%. There are a number of possible reasons why there is a difference in the final percentage cures achieved using each photoinitiator and light source. The main reason for these differences is likely to be the difference in intensity of the UV radiation. These intensities were chosen because they were the maximum intensity of the sources and one of the aims of this work was to obtain the maximum percentage cure from each light source. By lowering the intensity of the lamp to that of the LED array would be to bias the study in favour of the LED array. Other reasons for the difference in percentage cures are that although the absorption spectrum of the photoinitiators in question envelope the emission spectra of the light sources the exact optimum wavelength that the initiator reacts to is not currently known. Also the efficiency of the photoinitiator may be wavelength dependent meaning that more free radicals will be created at a certain wavelength and therefore the monomer will undergo a higher DC. In addition to this, although photoinitiators have similar ε_λ values their

photochemistry may be different which can have a profound affect on the generation of free radicals. Therefore, although it has been proven that UV-LEDs can cure a HEMA monomer to almost the same degree as a fluorescent lamp, great care should be taken in choosing which photoinitiator to use.

5.6 Conclusion

While in some cases the LED exposed samples showed a lower level of photopolymerisation to that of the fluorescent lamp, similar temporal profiles are observed (figure 5.16). From the FTIR and Raman data it is not possible to determine if the calculated degree of conversion is caused by the production of short molecules (oligomers) or longer chain molecules (polymers). Consequently it is not known if both light sources yield similar size polymer chains in the final product which may affect the values achieved for percentage cure. This uncertainty that arises in the obtained pHEMA polymer can in the future be investigated by performing a chemical analysis on the polymers [25]. This may also affect the thermomechanical properties of pHEMA, which will be discussed in chapter 6.

It was proven that although a photoinitiator may have a high ε_λ value it does not necessarily guarantee that the monomer sample containing this photoinitiator will give the highest degree of conversion; likewise photoinitiators with low ε_λ values do not necessarily give low degrees of conversion. There are a number of possible reasons why there is a difference in the final percentage cures achieved. The main reason is likely to be the difference in intensity of the sources. Other reasons may be that although the photoinitiator has a high ε_λ values

at the λ_{max} of a light source this λ_{max} may not be the exact optimum wavelength that the initiator reacts to, also the efficiency of each photoinitiator at a certain wavelength may be different. Another reason for a higher cure being achieved with the lamp in some cases may be that the effect of heating is greater with the lamp. The increased heating will cause the temperature of the monomer to rise which in turn increases the molecular mobility and therefore the reactivity of the sample, resulting in a higher degree of cure [10, 25]. For potential polymer based product manufacturers it is the comparable final percentage cure that is important when considering LEDs as a replacement to conventional fluorescent lamps.

This study has proven the concept that UV-LEDs can initiate a photochemical process in a HEMA monomer and produce a degree of cure similar to that achieved with fluorescent lamps. LEDs have numerous advantages over the traditionally used fluorescent lamps, one of these is that they can be made to emit exactly at the required wavelength while having a narrow colour spectrum, whereas lamps such as Hg fluorescent lamps are fixed by their nature. This would allow for optimum photopolymerisation conditions where the emission output of the LED would exactly overlap the absorption spectrum of the photoinitiator. Therefore with further progress in LED technology an LED may be manufactured with emission characteristics that match the photoinitiators specifications perfectly, optimising the overall level of LED photopolymerisation. Due to the inherent advantages that LEDs have over fluorescent lamps and the fact that they produce a comparable photopolymerisation to that achieved with the lamps, it appears that UV-LEDs have the potential to replace these lamps in photopolymerisation processes. As UV-LED technology improves and becomes

more readily available, LED photopolymerisation is a viable possibility in replacing fluorescent lamps in the manufacturing process of biomaterials such as contact lenses.

5.7 References

[1] M.G. Neumann, W.G. Miranda Jr., C.C. Schmitt, F.A. Ruggeberg, I.C. Corrêa. "Molar extinction coefficients and the photon absorption efficiency of dental photoinitiators and light curing units". J. Dent. 2005; vol 33: pp.525.

[2] R.J. Anderson, D.J. Bendell, P.W. Groundwater. "Organic spectroscopic analysis". Cambridge: The Royal Society of Chemistry, 2004.

[3] N.S. Allen. "Photoinitiators for UV and visible curing of coatings: mechanisms and properties". J. Photochem. Photobiol., A 1996; vol 100: pp.101.

[4] C. Decker, K. Zahouily, D. Decker, T. Nguyen, T. Viet. "Performance analysis of acylphosphine oxides in photoinitiated polymerization". Polymer 2001; vol 42: pp.7551.

[5] G.J. Sun, K.H. Chae. "Properties of 2,3-butanedione and 1-phenyl-1,2-propanedione as new photosensitizers for visible light cured dental resin composites". Polymer 2000; vol. 41: pp. 6205.

[6] N.S. Allen. "Photopolymerisation chemistry". J. Photochem. Photobiol., A 2003; vol 159: pp.102.

[7] T. Corrales, F. Catalina, C. Peinado, N.S. Allen. "Free radical macrophotoinitiators: an overview on recent advances". J. Photochem. Photobiol., A 2003; vol 159: pp.103.

[8] C. Decker. "Light-induced polymerisation of photoinitiator-free vinyl ether/maleimide systems". Macromolecular Chemistry and Physics 1999; vol 200: pp.1005.

[9] J.P. Fisher, D. Dean, P.S. Engel, A.G. Mikos. "Photoinitiated polymerization of biomaterials". Annual Review of Materials Research 2001; vol 31: pp.171.

[10] C. Decker. "The use of UV irradiation in polymerization". Polym. Int. 1998; vol 45: pp.133.

[11] C. Decker. "Light-induced crosslinking polymerization". Polym. Int. 2002; vol 51: pp.1141.

[12] G. Odian. "Principles of Polymerization. 3rd Ed." New York: John Wiley & Sons Inc, 1991.

[13] T.P. Klun, L.D. Hibbard, K.M. Spurgeon, R.S. Culler. "Coatable compositions abrasive articles made therefrom, and methods of making and using same", U.S Patent 5667541. United States, 1997.

[14] A. Botella, J. Dupuy, A.A. Roche, H. Sautereau, V. Verney. "Photo-rheometry/NIR spectrometry: An in situ technique for monitoring conversion and viscoelastic properties during photopolymerization". Macromolecular Rapid Communications 2004; vol.25: pp.1155.

[15] W. Teshima, Y. Nomura, A. Ikeda, T. Kawahara, M. Okazaki, Y. Nahara. "Thermal degradation of photo-polymerized BisGMA/TEGDMA-based dental resins". Polym. Degrad. Stab. 2004; vol.84: pp.167.

[16] S. Kammer, K. Albinsky, B. Sandner, S. Wartewig. "Polymerization of hydroxyalkyl methacrylates characterized by combination of FT-Raman and step-scan FT-i.r. photoacoustic spectroscopy". Polymer 1999; vol 40: pp.1131.

[17] R. Di Maggio, F. Rossi, L. Fambri, A. Fontana. "Raman and Brillouin scattering measurements on hybrid inorganic-organic materials obtained from

tetraethoxysilane and methacrylic monomers". J. Non-Cryst. Solids 2004; vol. 345&346: pp.591.

[18] S.J. Martin. "Curing of complex monomer systems: A spectroscopic and thermal analysis", Doctural thesis. Department of Physics. Dublin: Trinity College, 2000.

[19] B. Hacioğlu, K.A. Berchtold, L.G. Lovell, J. Nie, C.N. Bowman. "Polymerization kinetics of HEMA/DEGDMA: using changes in initiation and chain transfer rates to explore the effects of chain-length-dependent termination". Biomaterials 2002; vol 23: pp.4057.

[20] J.L. Ferracane, E.H. Greener. "Fourier Transform Infrared Analysis of Degree of Polymerization in Unfilled Resins-Methods Comparison". J. Dent. Res. 1984; vol. 63:pp.1093.

[21] T.H. Yoon, Y.K. Lee, B.S. Lim, C.W. Kim. "Degree of polymerization of resin composites by different light sources". J. Oral Rehabil. 2002; vol 29: pp.1165.

[22] P.X. Ma, J.H. Elisseeff. "Scaffolding in tissue engineering". Florida: CRC Press, 2005.

[23] R. H. Halvorson, R. L. Erickson, C. L. Davidson. "The effect of filler and silane content on conversion of resin-based composite". Dent. Mater. 2003; vol 19: pp.327.

[24] B. Monroe, M. Weed, C. Gregory. "Borate coinitiators for photopolymerizable compositions". In: WO/1992/013900 WIPON, 1992.

[25] S.L. McDermott, J.E. Walsh, R.G. Howard. "A comparison of the emission characteristics of UV-LEDs and fluorescent lamps for polymerisation applications". Optics and Laser Technology 2008; vol. 40: pp.487.

[26] R.W. Mills, A. Uhl, K.D. Jandt. "Optical power outputs, spectra and dental composite depths of cure, obtained with blue light emitting diode (LED) and halogen light curing units (LCUs)". Br. Dent. J. 2002; vol 192: pp.459.

[27] A. Uhl, R.W. Mills, K.D Jandt. "Polymerization and light-induced heat of dental composites cured with LED and halogen technology". Biomaterials 2003; vol 24: pp.1809.

[28] R.W. Mills, A. Uhl, G.B. Blackwell, K.D. Jandt. "High power light emitting diode (LED) arrays versus halogen light polymerization of oral biomaterials: Barcol hardness, compressive strength and radiometric properties". Biomaterials 2002; vol 23: pp.2955.

[29] R.W. Mills, K.D. Jandt, S.H. Ashworth. "Dental composite depth of cure with halogen and blue light emitting diode technology". Br. Dent. J. 1999; vol 186: pp.388.

[30] F. Stahl, S.H. Ashworth, K.D. Jandt, R.W. Mills. "Light-emitting diode (LED) polymerisation of dental composites: flexural properties and polymerisation potential". Biomaterials 2000; vol 21: pp.1379.

[31] A. Uhl, R.W. Mills, K.D Jandt. "Photoinitiator dependent composite depth of cure and Knoop hardness with halogen and LED light curing units". Biomaterials 2003; vol 24: pp.1787.

[32] K. Fujibayashi, K. Ishimaru, N. Takahashi, A. Kohno. "Newly developed curing unit using blue light-emitting diodes". Dent. Jpn. (Tokyo). 1998; vol 34: pp. 49.

[33] M. Fernández-García, M.F. Torrado, G. Martínez, M. Sánchez-Chaves, E.L. Madruga. "Free radical copolymerization of 2-hydroxyethyl methacrylate with butyl methacrylate: determination of monomer reactivity ratios and glass transition temperatures". Polymer 2000;vol. 41: pp.8001.

[34] C. Iojoiu, M.J.M. Abadie, V. Harabagiu, M. Pinteala, B.C. Simionescu. "Synthesis and photocrosslinking of benzyl acrylate substituted polydimethylsiloxanes". Eur. Polym. J. 2000; vol 36: pp.2115.

Chapter 6 The effect of pulsed UV radiation on the thermomechanical properties of pHEMA

6.1 Introduction

As was seen previously with the development of the LED array, LED technology continued to develop throughout the duration of this research. However one of the most exciting advancements in LED technology for this research seen the development of the UV LED Cure-All Linear 100™ by UV Process Supply Inc. [1] (Chicago, USA). These LEDs are newly developed high intensity UV curing systems that according to the manufacturers can supply continuous, uniform UV light of unlimited duration for curing applications. Previous results (chapter 2-5) had proven the concept that UV-LEDs could be used as a replacement for fluorescent lamps in a photopolymerisation process. The next step was to see if the mechanical properties of the final polymer could be altered by exposing the monomer (containing mixed photoinitiators) to pulsed LEDs emitting in different regions of the electromagnetic spectrum. These large LED arrays allowed for this to be investigated as their instant on/off feature meant that they could be pulsed. This allowed the monomer sample with mixed photoinitiators to be exposed to alternating illumination (from different LED sources) quickly and simultaneously. This technique would not be possible with conventional lamps as they exhibited a warm up period and therefore could not be pulsed.

Dynamic mechanical analysis (DMA) is a technique used to study and characterise the mechanical properties of a material. Due to its sensitivity it is

used to detect transitions in polymers that cannot be detected by other techniques such as Differential Scanning Calorimetry (DSC).

This chapter gives a detailed account of how these new large LED arrays were characterised and then used to photopolymerise a test monomer. After which the mechanical properties of the pHEMA polymer were measured and compared to see if the properties could be altered by exposing the monomer to different output wavelengths being pulsed at different rates.

6.2 Characterisation of new large LED arrays

Like the single LED and the LED array previously used in this research before these large LED arrays could be used be in a photopolymerisation set up their emission characteristics needed to be measured. Two of these large LED arrays were purchased, one emitting in the UV region of the spectrum (375 nm) (figure 6.1) and the other in the visible blue region (450 nm) (figure 6.2). This was to allow for the monomer sample to be exposed to two different wavelength regions during photopolymerisation. These LEDs have a number of the desirable features outlined in table 1.1, chapter 1 that make them potentially ideal light sources for photopolymerisation processes. These features according to the manufacturers are instant on/off, tens of thousands of hours of lamp life and that they emit no heat. One of the main advantages of these new powerful LEDs is their scalability and geometry which means they can be banked together and simply integrated into the currently used photopolymerisation units while allowing for uniform UV light over the exact required area [2].

These LED devices are assembled on a rectangle chip-on-board (see figures 6.1 and 6.2) which is coated with a special white coating to maximise light

extraction and which according to the manufacturers does not degrade due to environmental extremes. They are powered by a universal wall adapter and have a typical radiant flux of 1050 mW at maximum rated forward current as quoted by the manufacturers.

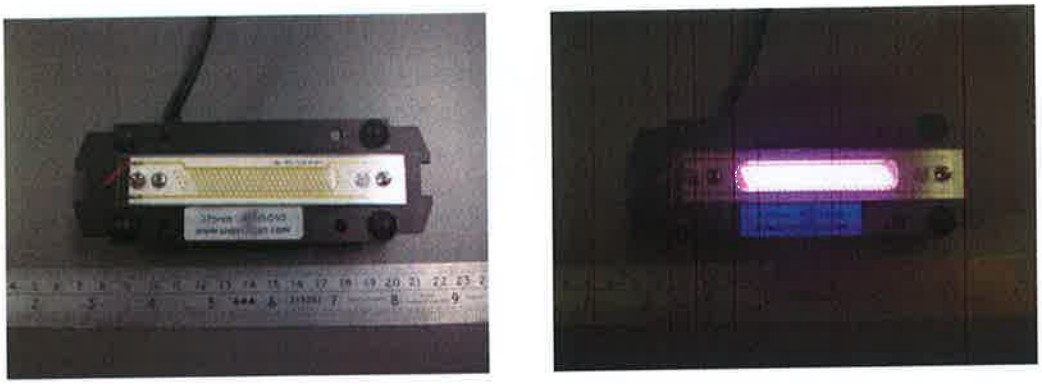

Figure 6.1: Photo of the 375 nm large LED array.

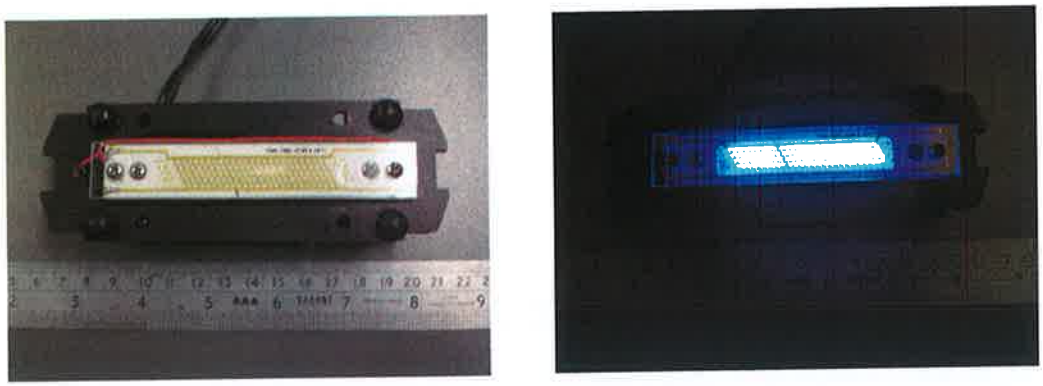

Figure 6.2: Photo of the 450 nm large LED array.

6.2.1 Warm up time and long term stability

As already stated warm up time is an important factor to be considered in manufacturing processes using photopolymerisation as it is the time after switch on for the device to achieve sufficient stability. It is important that the light source is emitting at a certain output intensity during photopolymerisation to ensure the

monomer is exposed to the correct amount of radiation. The Solar Light PMA2100 radiometer was once again used to measure the amount of radiation being emitted from each light source. The advantage to this radiometer is that there are a number of different sensors available that can be attached to the radiometer depending on the type of radiation being emitted. The PMA2107 UVA/B detector used previously was once again used to measure the amount of UV radiation being emitted from the 375 nm large LED array, while the PMA2121 blue light safety detector attachment was used to measure the blue light being emitted by the 450 nm large LED array. Although the PMA2121 blue light safety detector can be used to measure radiation below 400 nm its spectral response drops off significantly below this. Therefore it is generally used to measure radiation between 400 nm to 520 nm. The spectral response of this detector is shown in figure 6.3. Like the PMA2107 it incorporates a diffuser whose Lambertian angular response makes it suitable for measuring diffuse and/or direct radiation from extended light sources [3].

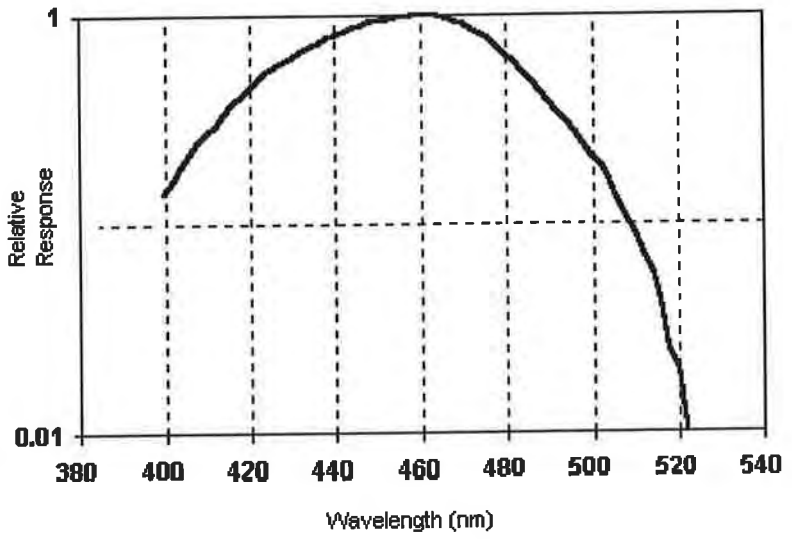

Figure 6.3: Spectral response curve of the PMA2121 blue light safety detector [4].

For each light source the corresponding detectors were held directly against the LED. The large LED arrays warm up time was measured by recording the output intensity every minute over a 30 minute period, after which the output intensity was recorded at one hour intervals to give an indication of their long term stability. Figures 6.4 and 6.5 show the stability and warm up time of the 375 nm and 450 nm large LED array respectively. From these graphs it can be seen that both LEDs exhibit an instant on/off feature as stated by the manufacturers or at least a warm up time undetectable in the time frame and produce constant output intensities over the eight hour monitored period. It should be noted that the 375 nm large LED array emits a considerably higher amount of UV radiation compared to that emitted by the single LED and LED array used in the previous photopolymerisation studies.

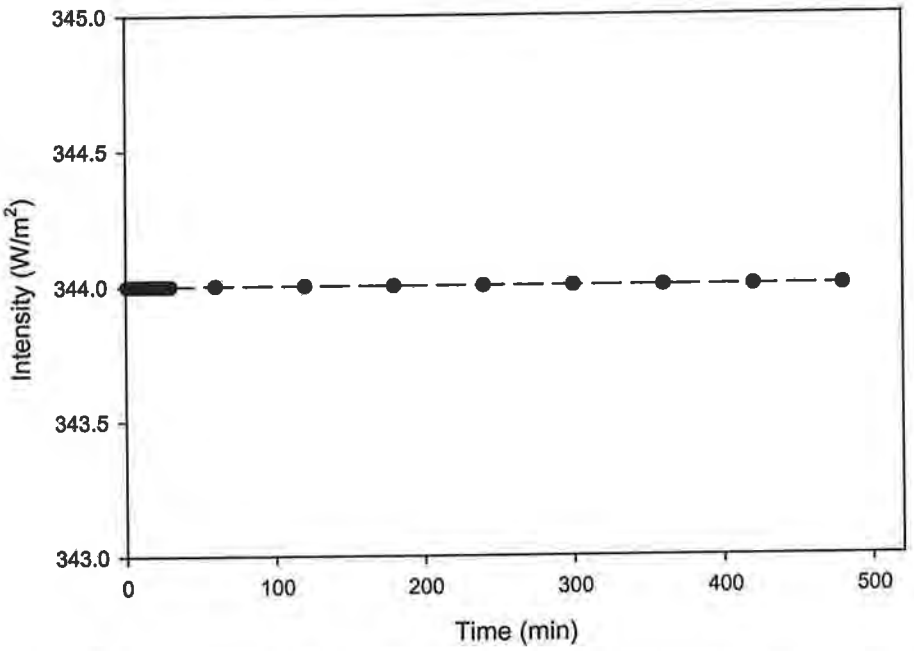

Figure 6.4: Warm up time and long term stability of the 375 nm large LED array as measured using the PMA2107 UVA/B detector.

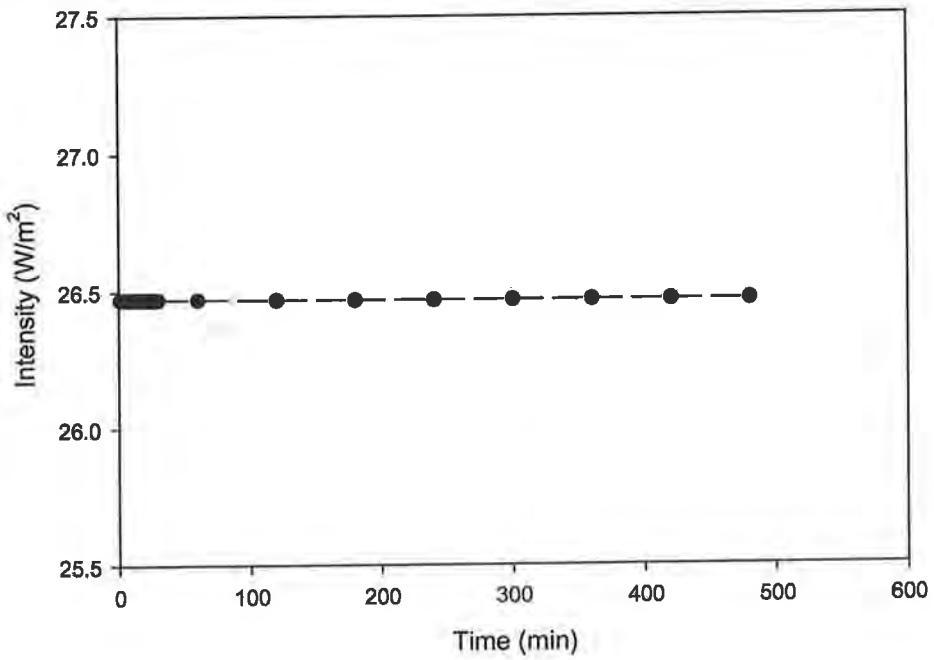

Figure 6.5: Warm up time and long term stability of the 450 nm large LED array as measured using the PMA2121 blue light safety detector.

6.2.2 Spectral output and peak wavelength

It was important to measure the spectral output and peak wavelength of each LED array so that corresponding photoinitiators that matched their output wavelength could be chosen. As the Ocean Optics IRRAD2000 spectrometer (Dunedin, Florida) operates over a broad spectral range (350 nm to 950 nm) it could be used to measure the spectral output and peak wavelength of each large LED array. This spectrometer was calibrated using a DH2000 calibrated deuterium-halogen light source as detailed in chapter 2, section 2.3.4. Each light source was coupled to the spectrometer using an optical fibre with a cosine-corrector irradiance probe attached. The spectral output of each large LED array was then recorded using the Ocean Optics software, OOIBase32 and normalised to one. Figure 6.6 shows the normalised spectral output of each large LED array, from this figure it was found that the 375 nm LED array and the 450 nm LED array had peak wavelengths of 380 nm and 445 nm respectively.

It can be seen from this figure that the output spectra of each LED array are well resolved, making them ideal to be used in this study where the monomer is to be photopolymerised with LEDs that have output wavelengths in different regions of the EM spectrum.

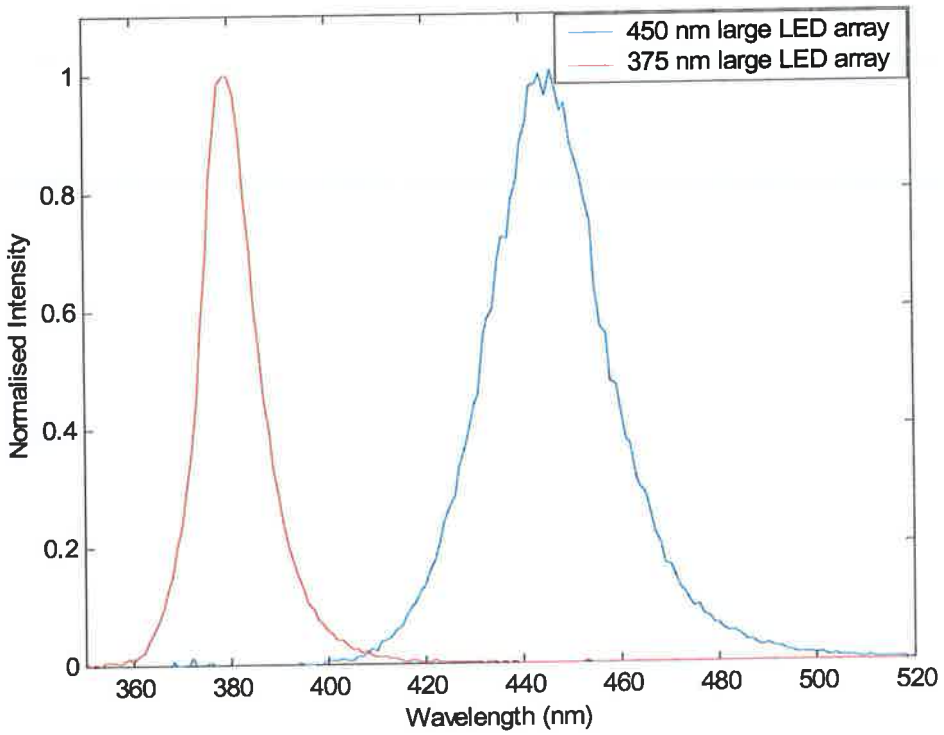

Figure 6.6: Spectral outputs of the 375 nm and 450 nm large LED arrays normalised to one.

6.2.3 Output Intensity

The output intensity of each large LED array was measured using the Ocean Optics set up previously discussed in section 6.2.2. The output spectrum of each LED array was recorded at a distance of 50 mm away from the optical fibre (figure 6.7). A distance of 50 mm was chosen as it allowed for a reasonably intense spectrum to be obtained for each light source without the detector being saturated. On examining the 375 nm LED array, it has a 380 nm peak intensity of approximately 4.1 W/m^2 at this distance, while its output peak is relatively narrow with a full-width at half-maximum (FWHM i.e. 50% bandwidth) of 13 nm. The 450 nm LED array on the other hand has a lower peak intensity of approximately

1.3 W/m^2 at 445 nm but has a higher FWHM of 20 nm, showing that the output of this LED array is over a wider spectral range. When the intensity is integrated under the FWHM for both light sources the output intensities were found to be 27 W/m^2 and 13 W/m^2 for the 375 nm and 450 nm LED arrays respectively, showing the 375 nm LED array to be approximately twice as intense as the 450 nm LED array.

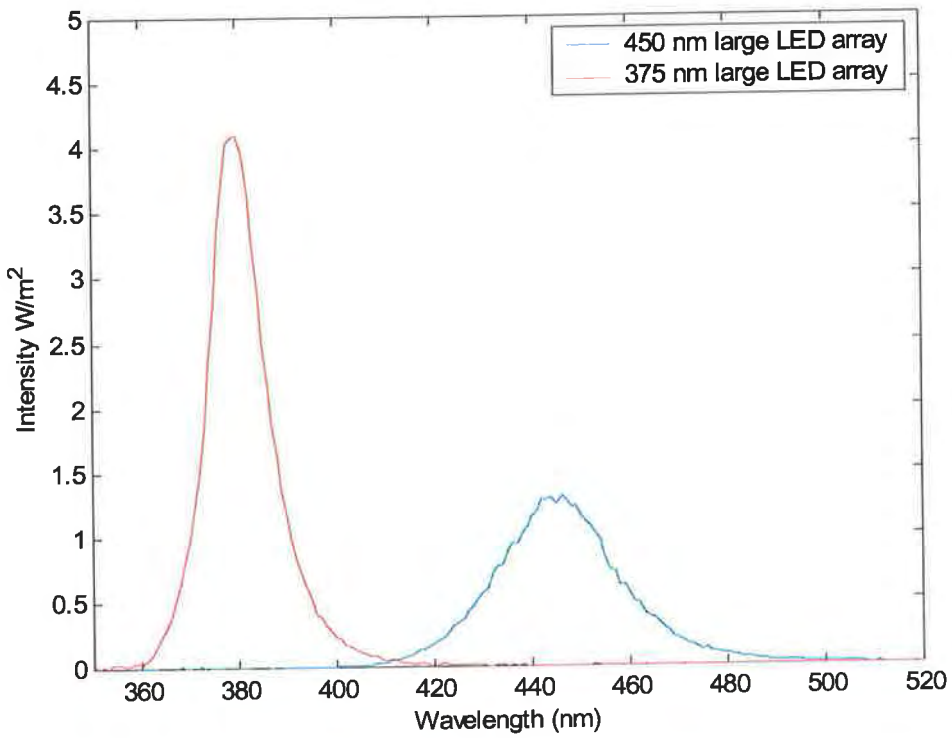

Figure 6.7: Spectral output of each LED array recorded at a distance of 50 mm.

As a comparison the intensity was also recorded using the Solar Light radiometer at a distance of 50 mm, this allowed for an approximate quantification of the total UV radiation output. To measure the output intensity of the 375 nm large LED array the Solar Light PMA2107 UVA/B detector was attached to the radiometer; this detector gave an intensity reading of 30.0 ±0.5 W/m^2. The

PMA2121 blue light safety detector recorded an intensity reading of 23.0 ±0.5 W/m^2 for the 450 nm large LED array. However the spectral response of each detector should be taken into account was measuring these intensity values. The spectral response curve of the PMA2121 blue light safety detector is shown in figure 6.3 while the spectral response of the PMA2107 UVA/B detector is shown previously in figure 2.7.

From these graphs it can be seen that the relative response of both detectors is not equal to 1 at the peak output wavelength of each source. The relative response of the PMA2107 UVA/B detector drops to approximately 0.6 at 375 nm. Therefore to obtain the correct intensity reading for the 375 nm large LED array using this detector the obtained 30 W/m^2 intensity value has to be divided by 0.6. This gave a corrected intensity value of about 50 W/m^2 for this large LED array.

The PMA2121 blue light safety detector response curve does not drop off by as big of a factor and has a relative response of 0.95 at 450 nm. Therefore the corrected intensity value for the 450 nm large LED array does not change a lot from the recorded value. When corrected for the relative response the true intensity reading for this LED is 24 W/m^2, compared to the recorded value of 23 W/m^2. Therefore using this quantified method it was found that the 375 nm large LED array is approximately twice as intense as the 450 nm large LED array, this ratio is in agreement with the previous Ocean Optics spectrometer findings.

Although the intensity values obtained using the two techniques are different it was found that the intensity ratios of the two sources are the same for both techniques with the 375 nm LED array output being approximately twice that

of the 450 nm LED array. Therefore although there is an inherent error involved when comparing the output using different techniques the results obtained for each do in fact correlate relatively well. This inherent error arises from how the different detection systems (i.e. Solar Light detectors and the Ocean Optics IRRAD2000 spectrometer) gathers radiation in different ways from the sources and their corresponding light fields [5].

6.2.4 Intensity at different distances

The two different radiation detection systems used previously (i.e. Solar Light radiometer and the Ocean Optics spectrometer) were used to measure the output intensity of these LEDs at different distances. The advantage of the Solar Light radiometer over the Ocean Optics spectrometer was that a quantification of the total radiation output could be directly determined; however unlike the Ocean Optics spectrometer a visual output of the wavelength spectra could not be ascertained.

For the distance measurements using the Solar Light radiometer the LED arrays were moved away from the detector at intervals of 10 mm and the intensity recorded at each distance. The PMA2107 UVA/B was used to measure the intensity of the 375 nm LED array (figure 6.8) while the PMA2121 blue light safety detectors were used to measure the radiation output of the 450 nm LED array (figure 6.9). The intensity readings in both figures have not yet been corrected for the relative response of the detector used.

From these figures it can be seen that intensity of the 375 nm LED array drops off quite quickly whereas the 450 nm LED array appears to saturate the PMA2121 blue light safety detector at distances less than 60 mm.

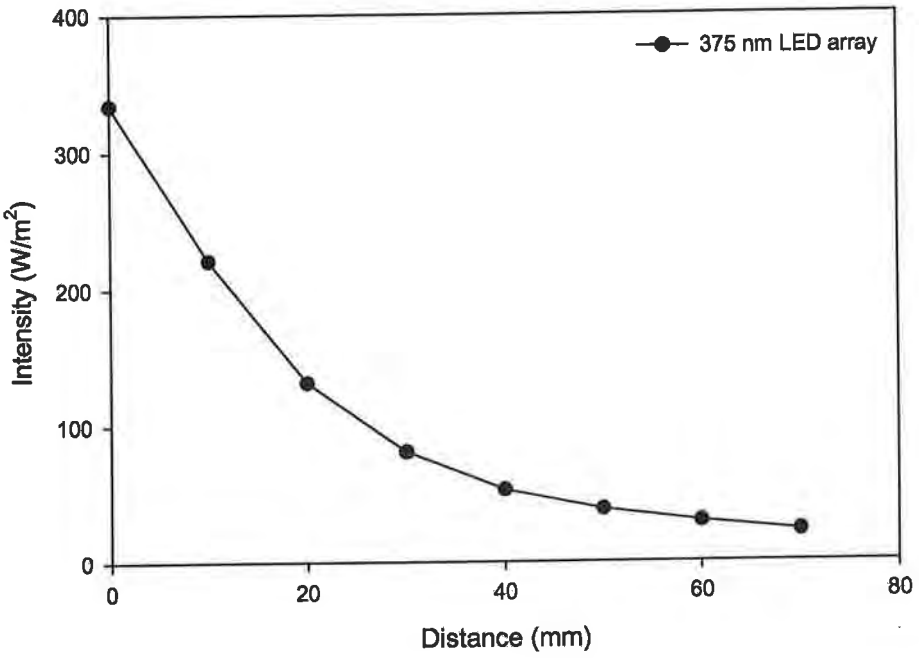

Figure 6.8: Intensity readings for the 375 LED arrays recorded at 10 mm distances using the PMA2107 UVA/B detector.

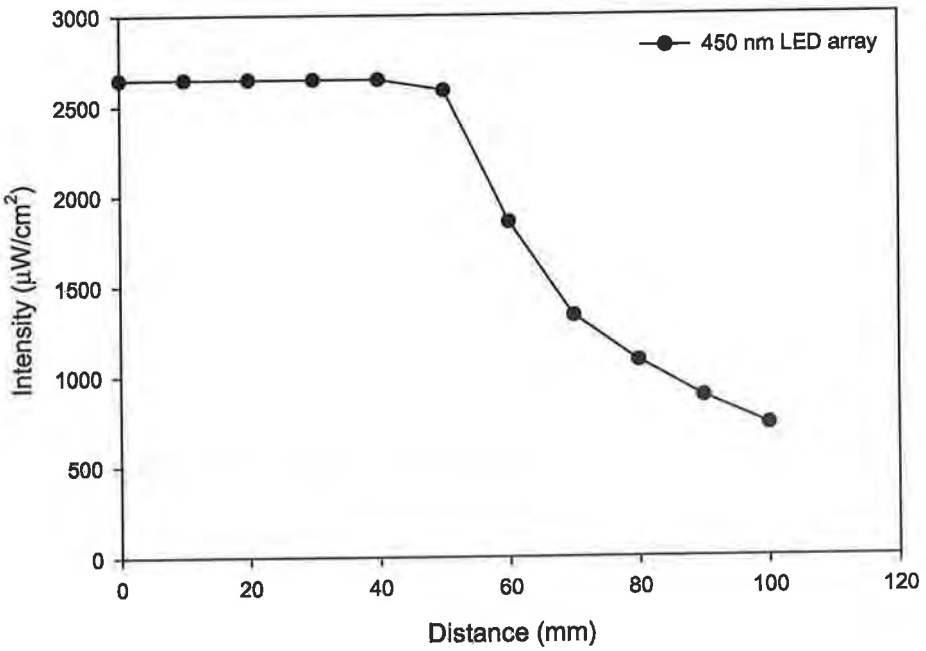

Figure 6.9: Intensity readings for the 450 nm LED array recorded at 10 mm intervals using the PMA2121 blue light safety detector.

The Ocean Optics IRRAD2000 spectrometer was then used to obtain the spectral output of each light source. Each light source was coupled to the spectrometer using an optical fibre with the cosine-corrector attached. A spectrum of each LED was recorded at distances of 45 mm, 50 mm, 60 mm, 70 mm and 80 mm away from the front end optics of the fibre. As the spectral output intensity of the 450 nm LED array was lower compared to the 375 nm LED array the spectral output of this LED at distances of 15 mm, 20 mm, 30 mm and 40 mm were also recorded. The spectral outputs of the 375 nm large LED array at these distances were not recorded as this LED saturated the detector at distances closer than 45 mm. The spectral output intensities as recorded by this spectrometer are displayed in figure 6.10. The spectra recorded at distances less than 45 mm are not displayed in this figure but will be used in the next calculation.

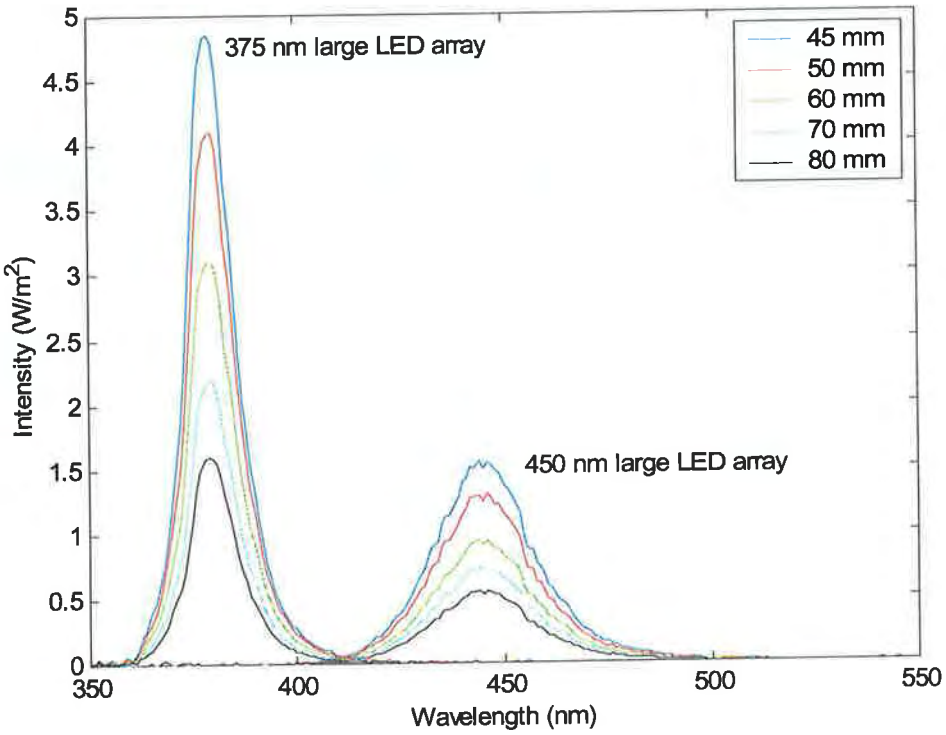

Figure 6.10: Spectral output for each LED array as recorded using Ocean Optics spectrometer.

In the previous photopolymerisation studies (chapter 5) the monomer samples were exposed and cured by the light sources at their maximum output intensities, which would probably be the case in a manufacturing set up. However for this photopolymerisation study to avoid having another variable in the experiment it was decided to have the monomer sample exposed to the same intensity from each LED array. The previous spectral output measurements were used to identify what distances to place each LED so that the monomer samples would be exposed to the same of amount of radiation from each source. For this the output intensities measured using the Ocean Optics spectrometer for each LED was plotted against the corresponding distance (figure 6.11). From this figure it

was found that if the 450 nm large LED array and the 375 nm large LED array were placed at distances of 25 mm and 50 mm respectively away from the monomer, the monomer would be exposed to the same intensity of 4.1 W/m^2 from each LED. Therefore for all future photopolymerisation studies the LEDs were placed at these distances.

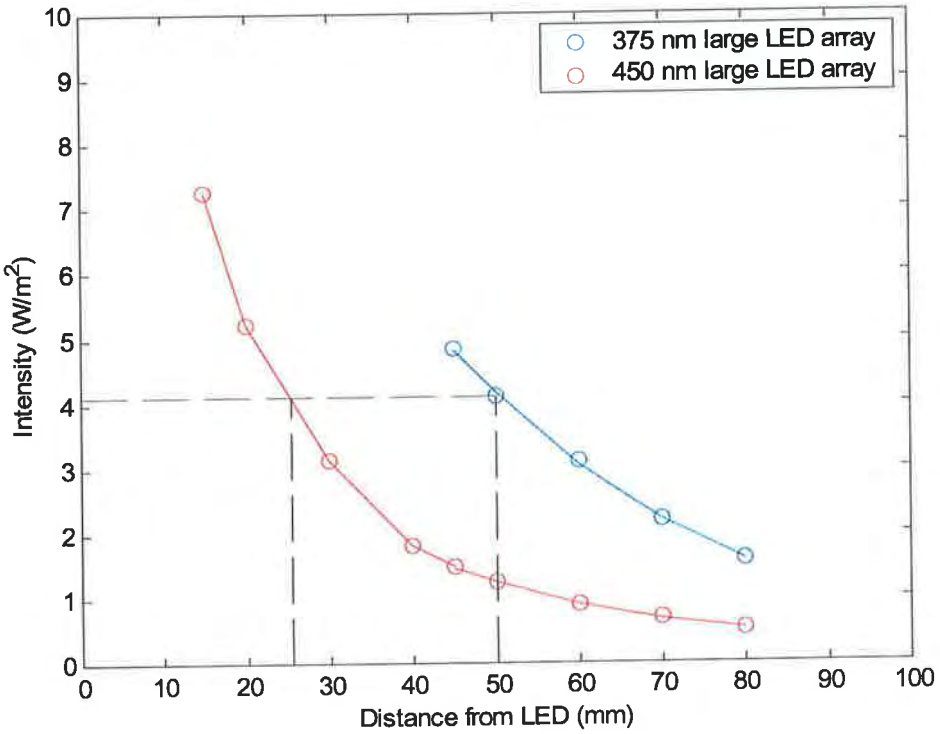

Figure 6.11: Intensity against distance for each LED array.

6.2.5 Discussion

When compared to table 2.1 both of these LED arrays exhibit a number of the desirable features for an ideal photopolymerisation light source. They have an instantaneous stable output after switch on and reach their maximum intensity output immediately remaining constant over time. Due to time constraints a lifetime study could not be conducted on these LEDs however according to the

manufacturers they have a lifetime of over 50,000 hours [1]. This long lifetime could reduce downtime for manufacturers as the light sources would have to be replaced less regularly. Their output spectra is also in the regions used for photopolymerisation and since they both emit at different regions of the EM spectrum they can be used in this study to potentially initiate two different photoinitiators in a HEMA sample allowing the effect of alternating radiation on photopolymerisation to be examined. The fact that these LEDs can be pulsed is another advantage that they have over the currently used fluorescent lamps, as the conventional emission sources can not be pulsed at a quick rate due to the stability time required.

For this photopolymerisation study it was decided to have the monomer samples exposed to the same intensity from each LED. The investigation studies into the characterisation of these LED arrays found that the 375 nm LED was approximately twice as intense as the 450 nm LED array and using the Ocean Optics readings it was found that to have the same intensity the 375 nm large LED array should be placed 50 mm away while the 450 nm large LED array should be placed at a distance of 25 mm. This large UV LED array emits a much higher amount of radiation and is more powerful than the previously used LEDs; this should result in a decrease in cure times as the rate of photopolymerisation increases with light intensity.

6.3 Initiation mechanisms of different photoinitiators

This section of the research was concerned with the potential of altering the percentage cure and mechanical properties of a polymer by using different wavelengths to initiate photopolymerisation. The first aim of the study was to

identify what photoinitiators could be used with each light source. From the previous UV/vis studies it was found that Darocur TPO had a high absorbance value at 375 nm. This photoinitiator was also recommended to use with the 375 nm large LED array by UV Process Supply Inc. (Chicago, USA) [1] and Ciba Speciality Chemicals Inc. (Basel, Switzerland) [6] who supplied the photoinitiators. Camphorquinone (CQ) has been identified as the most popular photoinitiator used in visible-light curing systems as it has an maximum absorbance peak at approximately 470 nm therefore it can be used in conjunction with the 450 nm large LED array [7, 8].

6.3.1 Photopolymerisation using CQ/amine and sample description

Preliminary curing studies in this work (not shown here) indicated that although CQ will induce photopolymerisation it is at a very low rate. Further research into the use of CQ as a photoinitiator found that is has a low polymerisation efficiency and as such it is generally used in conjunction with a coinitiator such as an amine in order to accelerate photopolymerisation [7, 9-13]. The CQ/amine photoinitiator system generates free radicals in a different way to other photoinitiators (e.g. Darocur TPO). CQ absorbs visible light in the blue region due to the $n \rightarrow \pi^*$ transition of the dicarbonyl group (Eq. 6.1). The excited $n \rightarrow \pi^*$ abstracts a hydrogen atom from the tertiary amine of the hydrogen donor (DH) which results in the production of a primary radical (amine radical) (Eq. 6.2) [9, 14]. It is this radical that then attacks the carbon double bonds of the monomer.

$$CQ \xrightarrow{h\nu} CQ^* \text{ (excited CQ)} \qquad \text{Eq. 6.1}$$

$$CQ^* + DH \rightarrow CQ\text{-}H + D\bullet \text{ (amine radical)} \qquad \text{Eq. 6.2}$$

Some amines decrease the rate of polymerisation while some of them increase the rate, the amine 4,4'-Bis-(dimethylamino)benzophenone (Sigma-Aldrich) [15] has a high relative acceleration value for photopolymerisation and has previously been used in conjunction with CQ [10]. The chemical structure of this amine and CQ are shown in figure 6.12. The monomer sample contained CQ and Darocur TPO at the same concentration of 6 x 10^{-4} mol/L, while the amine was used at a concentration 1 x 10^{-4} mol/L as used in previous studies [7, 9, 10].

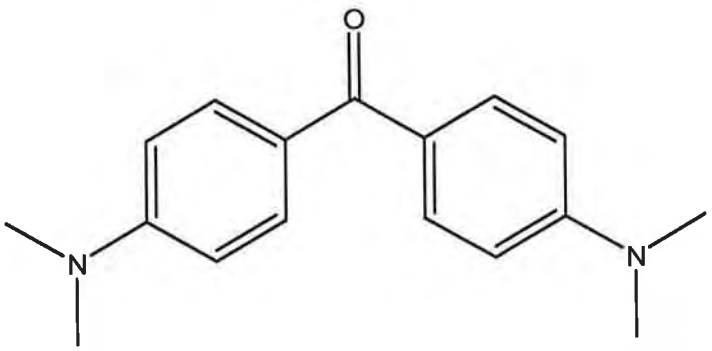

Amine 4,4'-Bis(dimethylamino)benzophenone MW = 268.35 $gmol^{-1}$

Camphorquinone 1,7,7 trimethyl-bicyclo[2,2,1]heptan-2,3-dione MW = 166.22 $gmol^{-1}$

Figure 6.12: Chemical structure of the amine and CQ.

6.4 UV/Vis absorption characteristics of photoinitiators

6.4.1 Introduction

UV/vis spectroscopy was used to obtain the absorbance spectra of the two photoinitiators and the amine used at different concentrations. The peak absorbance wavelength for each photoinitiator was determined as was the molar absorptivity (ε_λ), which is the probability of radiation at a certain wavelength being absorbed by the photoinitiators [16].

6.4.2 Molar Absorptivity (ε_λ) of the photoinitiators

To allow for the calculation of ε_λ a Beer-Lambert law study was conducted on Darocur TPO and CQ. The ε_λ would give an indication how much radiation at 375 nm and 450 nm (peak λ_{max} of each LED array) each photoinitiator would absorb. An absorbance study of the amine was also conducted to see if and where it absorbed. Each photoinitiator and amine was dissolved in acetonitrile and solutions of known concentrations were prepared. For Darocur TPO the concentrations used were 4.27×10^{-3} mol/L, 4.27×10^{-4} mol/L, 4.27×10^{-5} mol/L and 4.27×10^{-6} mol/L, for CQ concentrations of 47.24×10^{-3} mol/L, 23.62×10^{-3} mol/L, 4.72×10^{-4} mol/L and 4.72×10^{-5} mol/L were prepared. The absorbance spectra of the amine in acetonitrile at concentrations of 10^{-4}, 10^{-5}, 10^{-6} mol/L were also recorded. It was not possible to use the same concentrations for each photoinitiator, as some concentrations were too high such that the UV/Vis spectrometer recorded absorbance values of 3.

The same optically matched quartz cuvettes (10 mm) used in the previous Beer-Lambert law study (chapter 4, section 4.3) were once again used here. One

cuvette containing pure acetonitrile was placed in the reference holder while the other, containing the initiator in acetonitrile was placed in the sample cell holder. The absorbance spectrum of each photoinitiator was recorded over a range from 200 nm–800 nm, using an integration time of 0.48 sec and a 1.00 nm slit. The absorption spectra of Darocur TPO and CQ at different concentrations are shown in figures 6.13 and 6.14 respectively. Figure 6.13 shows a high absorbance at 375 nm for Darocur TPO, with no absorbance at 450 nm. Although the peak absorbance of CQ is at approximately 470 nm, which correlates well to published data [7, 16, 17] it also exhibits high absorbance at the λ_{max} of the 450 nm large LED array, making it ideal to use with this LED. A small over lap of this photoinitiators spectrum with the λ_{max} of the 375 nm large LED array can be seen in the tail end of the absorbance spectra (figure 6.14). Figure 6.15 shows the absorption spectra of the amine at different concentrations. From this graph it can be seen that the amine absorbs at both 375 nm and 450 nm. Therefore it may affect the percentage photopolymerisation.

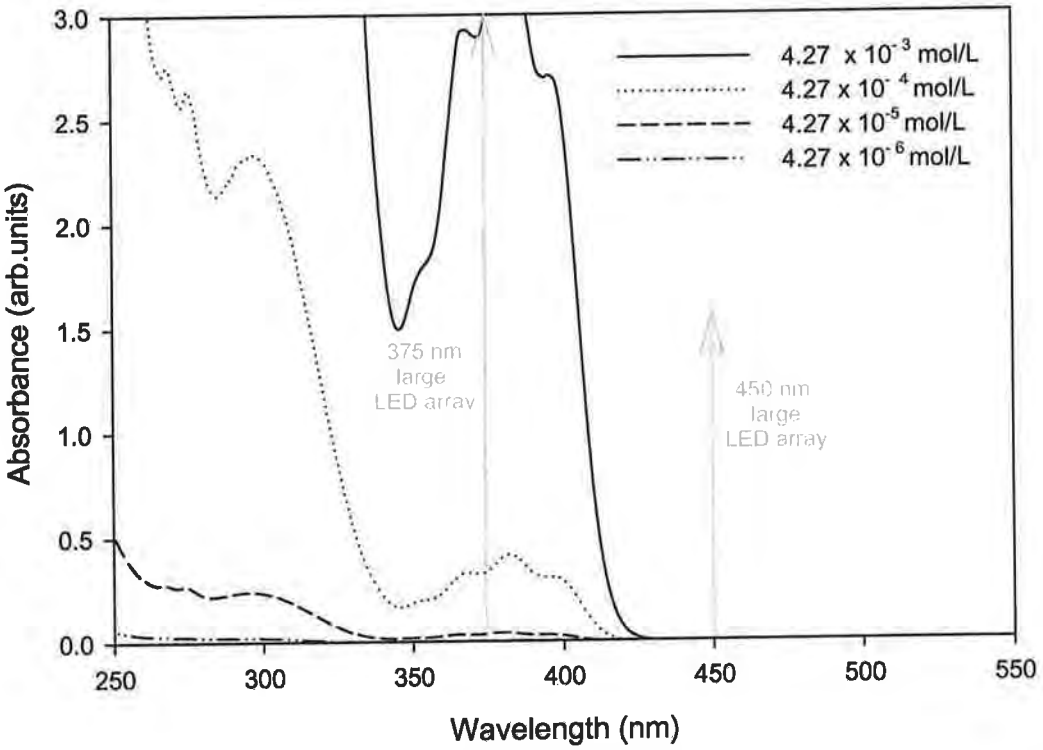

Figure 6.13: UV/Vis absorption spectra of Darocur TPO.

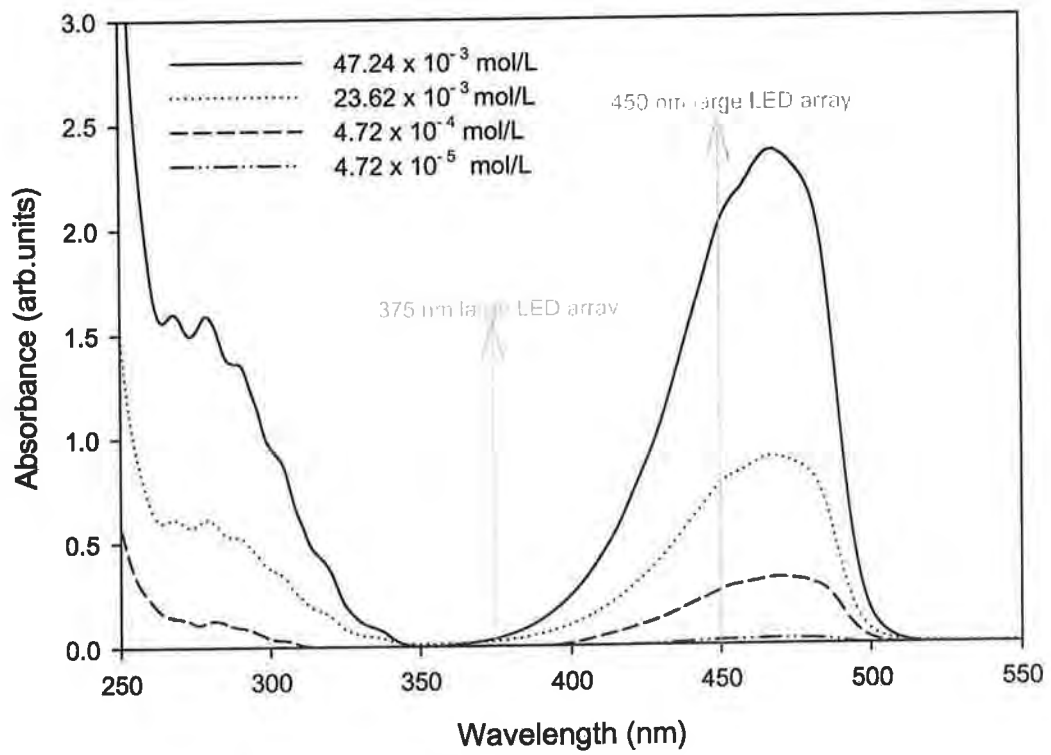

Figure 6.14: UV/Vis absorption spectra of Camphorquinone (CQ).

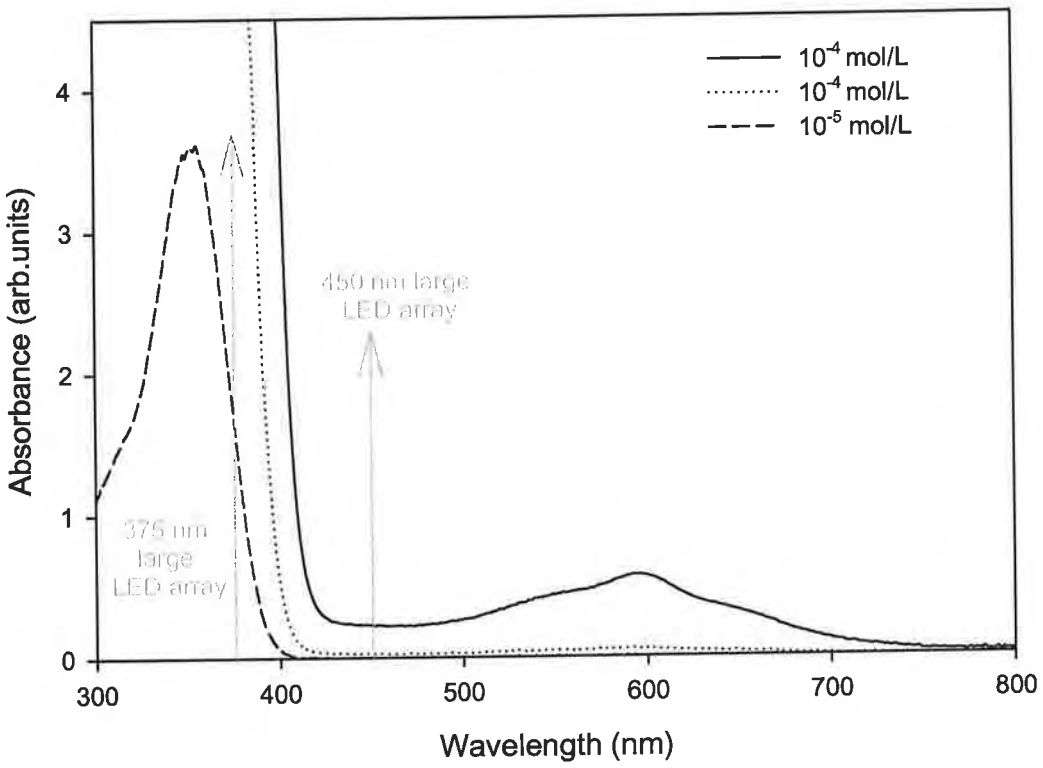

Figure 6.15: UV/Vis absorption spectra of the amine.

The aim of this study was to select two different photoinitiators that could be activated by two different wavelengths. The UV/vis study shows that Darocur TPO will only absorb radiation from the 375 nm LED large array and not radiation from the 450 nm large array, while the 450 nm LED large array should only initiate CQ and not Darocur TPO. The amine absorbs at both 375 nm and 450 nm. Figure 6.16 shows the absorbance of Darocur TPO at the λ_{max} of the 375 nm and 450 nm large LED arrays for different concentrations, this photoinitiator absorbs very little radiation at 450 nm meaning it will only absorb radiation from the 375 nm LED large array and should not undergo photoinitiation by the 450 nm LED large array.

Figure 6.17 shows the absorbance of CQ at peak wavelengths of 375 nm and 450 nm for different concentrations. Although CQ absorbs some radiation at 375 nm it is very small compared to the amount of absorbance that occurs at the λ_{max} of the 450 nm large LED array. Therefore this photoinitiator will absorb more radiation from this LED and it is this LED that should have a bigger effect on initiation. Table 6.1 gives the ε_λ values for each photoinitiator at the maximum emission wavelength for each LED as calculated using the Beer-Lambert law. Large values of ε_λ indicate a high probability of absorption at a certain wavelength [16], from the values in table 6.1 it is clear that each photoinitiator has a high probability of absorbing radiation from their corresponding LEDs. Darocur TPO has a ε_λ value of 700 $L.mol^{-1}.cm^{-1}$and 0 $L.mol^{-1}.cm^{-1}$ at 375 nm and 450 nm respectively, this is compared to a published value of 562 $L.mol^{-1}.cm^{-1}$ at 376 nm in methanol [18]. It was not possible to obtain a published value for the ε_λ of this photoinitiator at 450 nm; it can be assumed the reason for this is that it is not normally used with light source emitting in the visible region due to its low absorption in this area. CQ was found to have a ε_λ value of 40 $L.mol^{-1}.cm^{-1}$ at 450 nm. This corresponds well to published data where CQ has reported to have a ε_λ of 40 $L.mol^{-1}.cm^{-1}$ at 468 nm in acetonitrile [9] and 28 ± 2 $L.mol^{-1}.cm^{-1}$ at 470 nm in methyl methacrylate [16]. At 375 nm CQ was found to have a ε_λ of 1 $L.mol^{-1}.cm^{-1}$, like Darocur TPO and presumable for the fact the CQ is generally only used with light sources emitting in the visible region it was not possible to find a ε_λ value for CQ at 375 nm.

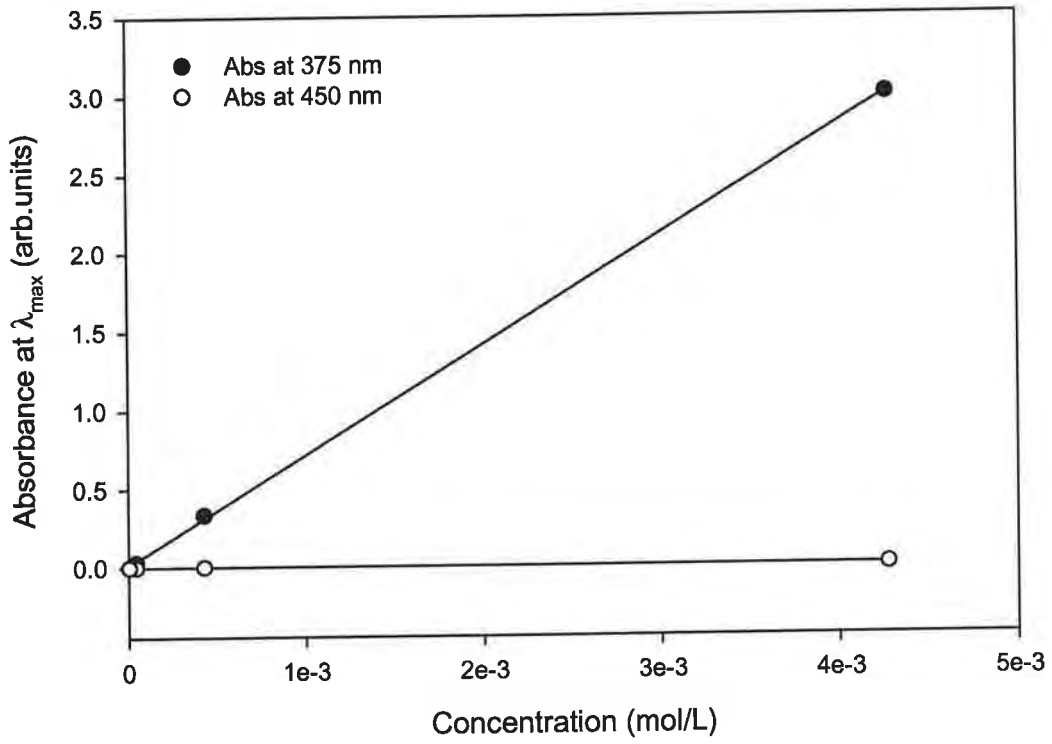

Figure 6.16: Absorbance -v- concentration for Darocur TPO at 375 nm and 450 nm.

Table 6.1: Molar absorptivity (ε_λ) for each photoinitiator at the maximum emission wavelength for each LED.

	ε_λ at 375 nm **L.mol^{-1}.cm^{-1}**	**ε_λ at 450 nm** **L.mol^{-1}.cm^{-1}**
Darocur TPO	700	0
CQ	1	40

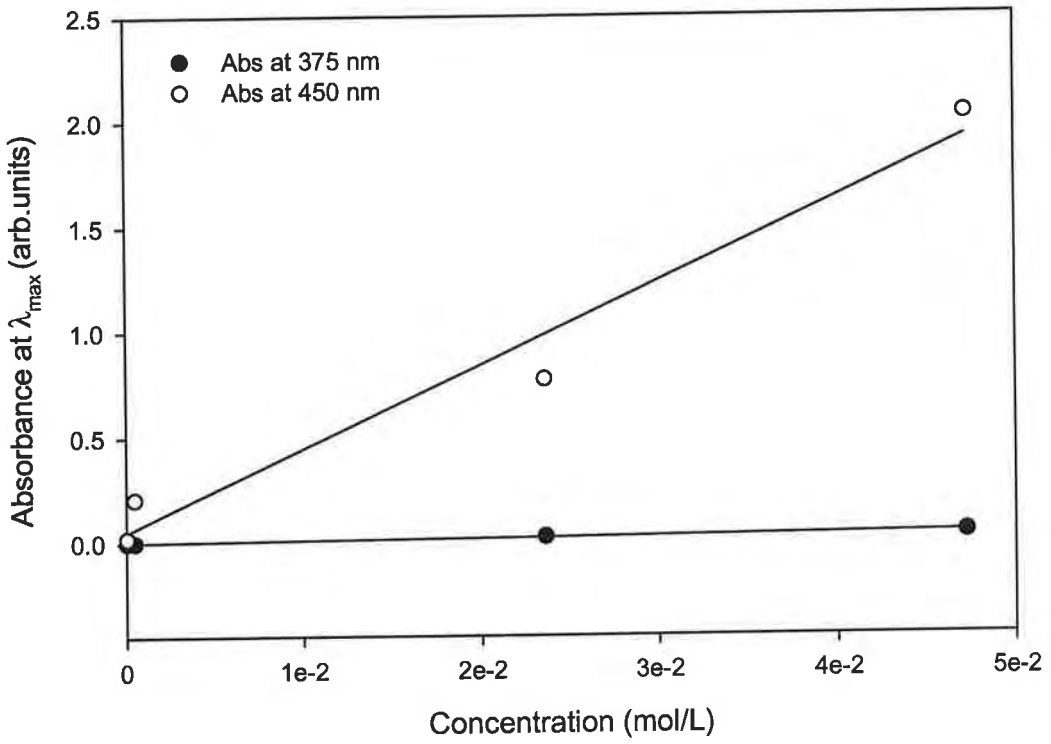

Figure 6.17: Absorbance -v- concentration for CQ at 375 nm and 450 nm.

6.4.3 Discussion

The spectral output of the 375 nm large LED array falls within the absorptive region of Darocur TPO. Furthermore there is an overlap of the emission spectra of the 450 nm large LED array with CQ making these photoinitiators ideal to be used in the photopolymerisation of the HEMA monomer. Both photoinitiators exhibit high ε_λ values at the λ_{max} of their corresponding LED arrays indicating that Darocur TPO should be initiated by the 375 nm large LED array only; with CQ being initiated by the 450 nm large LED array. Due to the small amount of absorption that occurs with CQ at 375 nm this photoinitiator may be initiated to a small degree by the 375 nm large LED array.

As mentioned previously the amine also absorbs in the wavelength region of the two large LED arrays and may have an affect on the amount of cure achieved.

6.5 Spectroscopic study of the photopolymerisation of HEMA with new photoinitiators/amine and the large LED arrays

6.5.1 Introduction

In the previous curing studies (chapter 5) the monomer samples were exposed to only one light source during photopolymerisation. This section of the study is concerned with the effect of alternating radiation on the percentage cure of the monomer samples. For this the HEMA/photoinitiator samples were exposed to the two large LED arrays which were pulsed at 10 s and 20 s intervals for a period of 360 s. The percentage cure that occurred with HEMA and the two different photoinitiator systems was once again monitored using FTIR spectroscopy. The UV/vis studies indicated that Darocur TPO should be initiated by the 375 nm large LED array only; with CQ exhibiting a potential strong initiation by the 450 nm large LED array, this photoinitiator may also undergo some initiation by the 375 nm LED as a small part of its absorbance spectrum overlaps with the λ_{max} of this LED. To see if this was the case, monomer samples were exposed to each LED array separately and the percentage cure measured. The monomer samples consisted of HEMA, TPO (6×10^{-4} mol/L), CQ (6×10^{-4} mol/L) and an amine coinitiator at a concentrations of 1×10^{-4} mol/L as used by Jakubiak et al [9, 10]. This amine acted as an accelerator in the photopolymerisation process.

6.5.2 FTIR study of the percentage cure achieved with new large LED arrays

For this study the sample holder consisted of two NaCl plates separated by a Teflon® spacer 0.1 mm thick. A background spectrum of the NaCl plates was recorded with the Nicolet Nexus FTIR spectrometer over a range of 4000 cm^{-1}–500 cm^{-1} (4 scans, resolution of 16 cm^{-1}), after which a small drop of monomer sample was placed between the two plates and a spectrum of this uncured monomer recorded. The sample was then removed from the spectrometer and exposed to radiation from one of the large LED arrays (either 375 nm or 450 nm) for 10 s and another spectrum was recorded immediately. This procedure was repeated for a total of 360 s. To ensure the monomer was exposed to the same intensity (4.1 W/m^2) the 375 nm large LED array was placed 50 mm away from the sample, while the 450 nm large LED array was placed at a distance of 25 mm. By comparing the percentage cure that occurred in each case here a direct comparison of the curing potential of each LED array could be made. Figure 6.18 shows typical FTIR spectra recorded during exposure to the radiation, the disappearance of the C=C peak at 1636 cm^{-1}, signalling photopolymerisation, can be clearly seen. The degree of cure was once again calculated by measuring the peak intensity of the C=C at 1636 cm^{-1} to the reference peak at 1174 cm^{-1}.

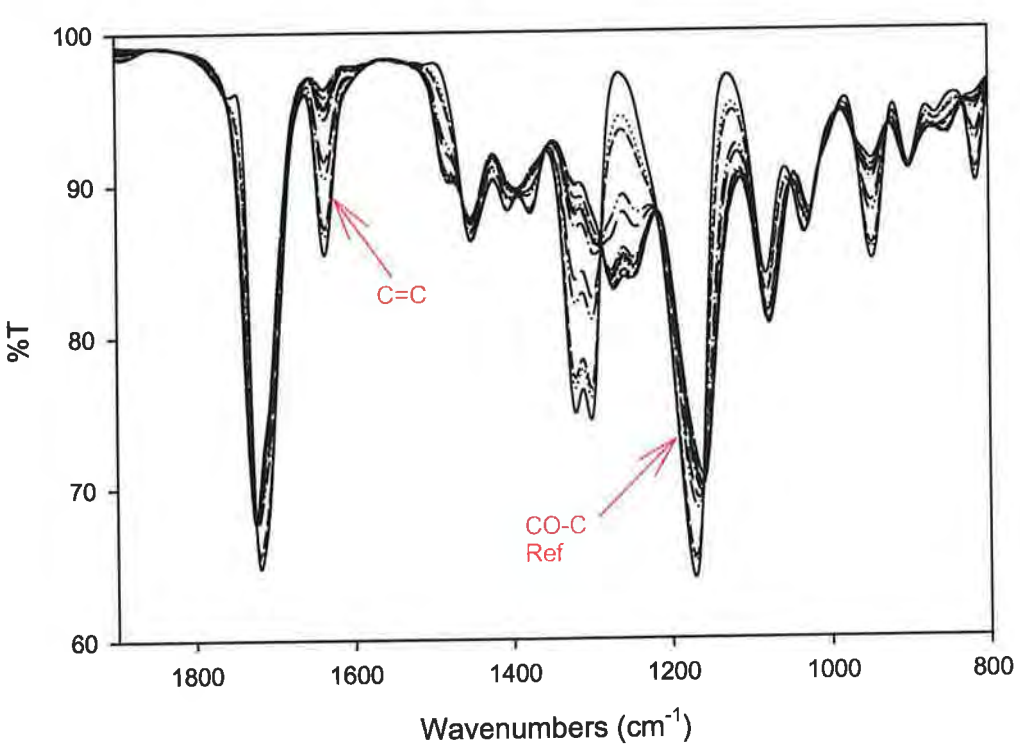

Figure 6.18: Typical FTIR spectra recorded during photopolymerisation.

Figures 6.19 and 6.20 show the percentage cure achieved when the monomer sample was exposed to each large LED array separately. It can be seen from these graphs that a lower percentage cure is achieved using only the 450 nm LED array (51%) compared to the 73% conversion achieved with only the 375 nm LED array. The amount of conversion achieved with the 375 nm LED array accelerated quickly after 20 s while the curing profile of the sample exposed to the 450 nm LED array exhibits a longer initiation time (100 s). It appears as if there is something inhibiting the initiation process and when this inhibiting species is used up (after 100 s) then the curing process accelerates or alternatively the production of free radicals is slow. This difference in final percentage cure may be due to the difference in ε_λ for each photoinitiator. Large values of ε_λ indicate a high

probability of absorption at a certain wavelength which lead to a large production of initiating species which results in an improvement in the overall degree of conversion [16]. The 375 nm large LED array was used to initiate TPO which had a ε_λ value of 700 $L.mol^{-1}.cm^{-1}$ at λ_{max} for this source, whereas CQ had a ε_λ value of only 40 $L.mol^{-1}.cm^{-1}$ at the λ_{max} for the 450 nm large LED array. Therefore there was a large difference in the probability of each photoinitiator absorbing their corresponding radiation, which would result in a reduction of free radicals produced even with the amine coinitiator present. It could be thought that a way to over come this problem would be to add more CQ initiator to the monomer sample. However adding more photoinitiator into a system does not necessarily result in an increase in photopolymerisation. Also as CQ is a solid yellow compound adding large amounts of it will lead to undesirable yellowing in the final polymer, this places practical limits on the concentration of CQ which in turn limits the degree of photopolymerisation attained [11, 14, 19]. Another reason for the lower percentage cure may be due to lower efficiency; when using visible lasers to initiate photopolymerisation Decker [20] reported that photoinitiators that absorb in this region are less efficient than UV photoinitiators due to the lower energy of visible photons.

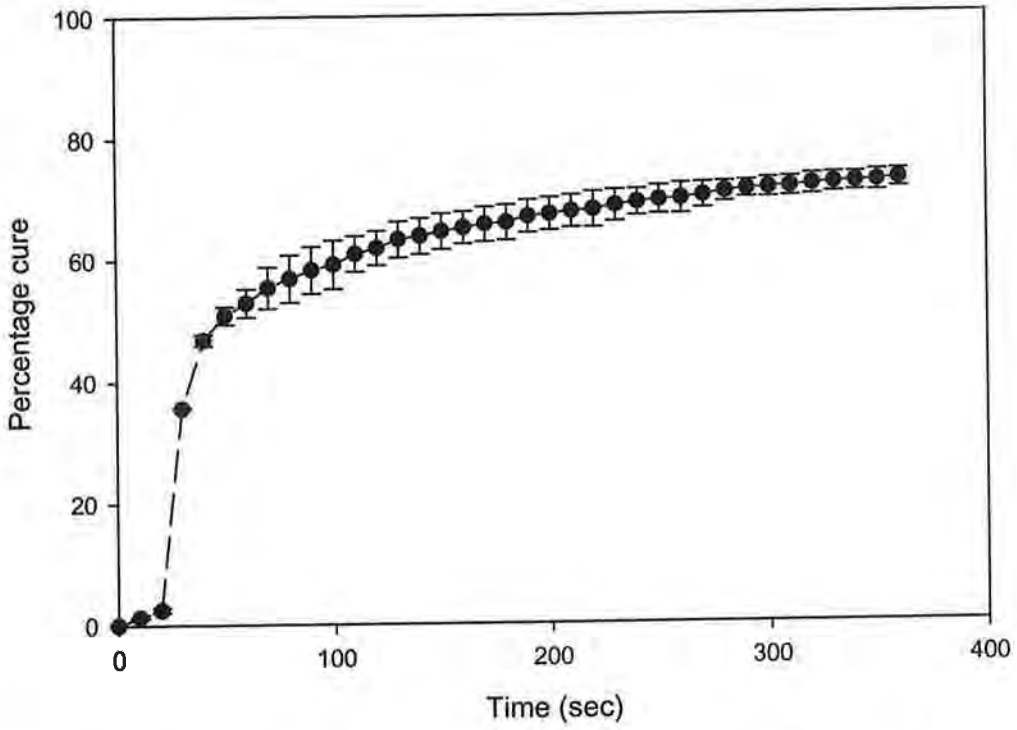

Figure 6.19: Curing profile achieved using 375 nm large LED array only (sample 1.1).

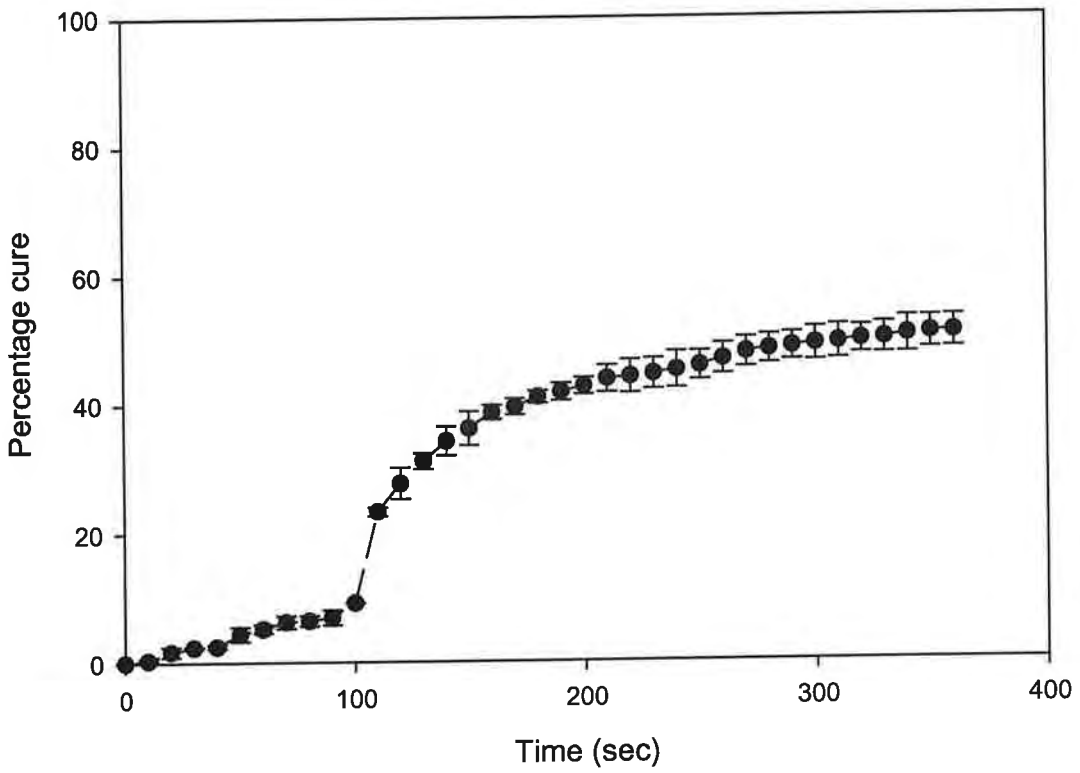

Figure 6.20: Curing profile achieved using 450 nm large LED array only (sample 1.2).

It was hoped that the photopolymerisation rates could be controlled by varying the amount of UV and blue radiation the monomer was exposed to. By controlling the photopolymerisation rate the mechanical properties of the final polymer may be controlled. This is discussed later in section 6.6. In order to investigate this matter the LEDs were pulsed at certain rates during photopolymerisation of the monomer. The ability to pulse and select different maximum peak wavelengths are properties which make LEDs very attractive for this study. It was decided to pulse the LEDs every ten and twenty seconds. A monomer sample was first exposed to the 375 nm large LED array for 10 s, then the 450 nm large LED array for 10 s (sample 1.3). The pulsing between the

different wavelengths lasted for 360 s. Another monomer sample was then irradiated by the two LEDs being pulsed again at 10 s but exposed to the 450 nm large LED array first followed by the 375 nm array (sample 1.4). These two processes were then repeated using pulse rates of 20 s for a total of 360 s (samples 1.5–1.6). In each case before the monomer sample was used it was flushed with oxygen free nitrogen to remove any oxygen that could hinder photopolymerisation [21, 22].

The curing profiles achieved using the pulsed LEDs are displayed in figures 6.21-6.24. When pulsed at 10 s the HEMA sample that was exposed to the 450 nm large LED array first exhibited a significantly higher final cure of 78% (figure 6.22) compared to 50% conversion that was seen when the sample was exposed to the 375 nm large LED array first (figure 6.21). The curing profile of the HEMA polymer formed when exposed to the 375 nm LED array first showed a gradual increase in percentage cure whereas the curing profile of sample 1.4 showed a steeper increase in the degree of conversion. This suggests that sample 1.3 (figure 6.21) has not achieved autoacceleration (the steep rise in percentage cure with time) [23] while figure 6.22 (sample 1.4) shows autoacceleration. However for the 20 s pulsing this was reversed with sample 1.5 (375 nm LED array first) exhibiting a steeper increase in cure (autoacceleration) than sample 1.6 (450 nm LED array first). Sample 1.5 also underwent a higher degree of conversion (76%) percentage cure compared to the 54% achieved with sample 1.6. Therefore it can be concluded that the pulse rate and the order of wavelength exposure can greatly affect the rate of cure and thus the final percentage cure.

From the results achieved here there appears to be some sort of competing process in which maybe one affects the lifetime of the photoinitiator species in the system. It appears that by pulsing at different times not only is the amount of radicals produced altered but their molecular mobility becomes restricted, which will have an effect on the percentage cure achieved. For example when the sample is initiated with only 375 nm radiation (figure 6.19) it can be seen that it takes 20 s for autoacceleration to occur. When the sample is cured first with the 375 nm LED array for 10 s then the 450 nm LED array for 10 s (figure 6.17) it appears as if Darocur TPO has not had the time it needs to autoaccelerate (at least 20 s). This is confirmed in figure 6.23 when the sample was first cured with the 375 nm radiation for 20 s. Here it appears that there is enough time and enough radicals produced to result in autoacceleration of the cure process. However the process appears to be more complicated than this as when the 450 nm is used as the initial light source (figures 6.22 and 6.24) the opposite curing profiles are produced. A short initial pulse (10 s) of 450 nm radiation seems to produce a photospecies which aids the autoacceleration process when the 375 nm radical is applied after 10 s. This photospecies may be short lived as a longer exposure time (20 s) with the 450 nm radiation at the start does not aid the autoacceleration process of the cure (figure 6.20). The absorption of the amine at both 375 nm and 450 nm might somehow have a part in this effect. Alternatively the exposure of the 450 nm radiation to the sample could produce a photospecies which is terminating the polymer chain production resulting in short chain polymers.

These different curing modes may therefore be used to control the degree of conversion and change the mechanical properties of the formed polymer which

will be investigated in the next section. The percentage cures achieved along with the irradiation process and sample numbers are given in table 6.2.

Table 6.2: Percentage cure achieved with each different irradiation process.

Sample Number	Irradiation Process	Percentage Cure
1.1	375 nm large LED continuous	73%
1.2	450 nm large LED continuous	52%
1.3	Pulse 10 s: 375 nm first 450 nm second	50%
1.4.	Pulse 10 s: 450 nm first 375 nm second	78%
1.5	Pulse 20 s: 375 nm first 450 nm second	76%
1.6	Pulse 20 s: 450 nm first 375 nm second	54%

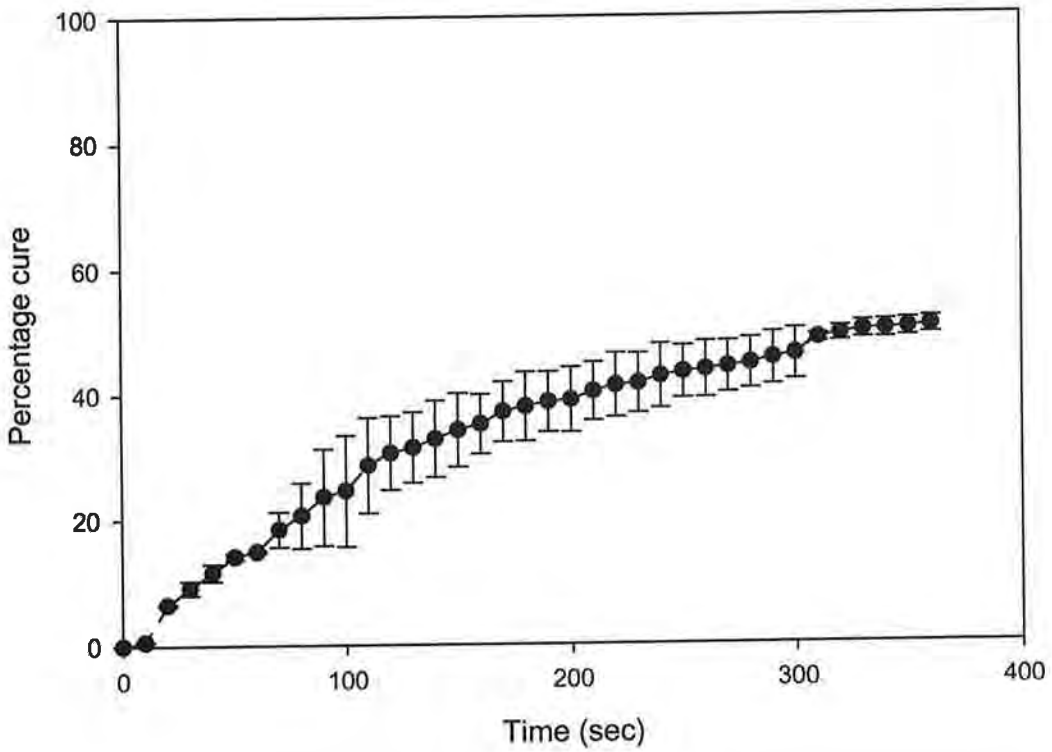

Figure 6.21: Curing profile achieved using 10s pulsed LEDs exposing monomer to 375 nm LED array first, then to 450 nm LED array (sample 1.3).

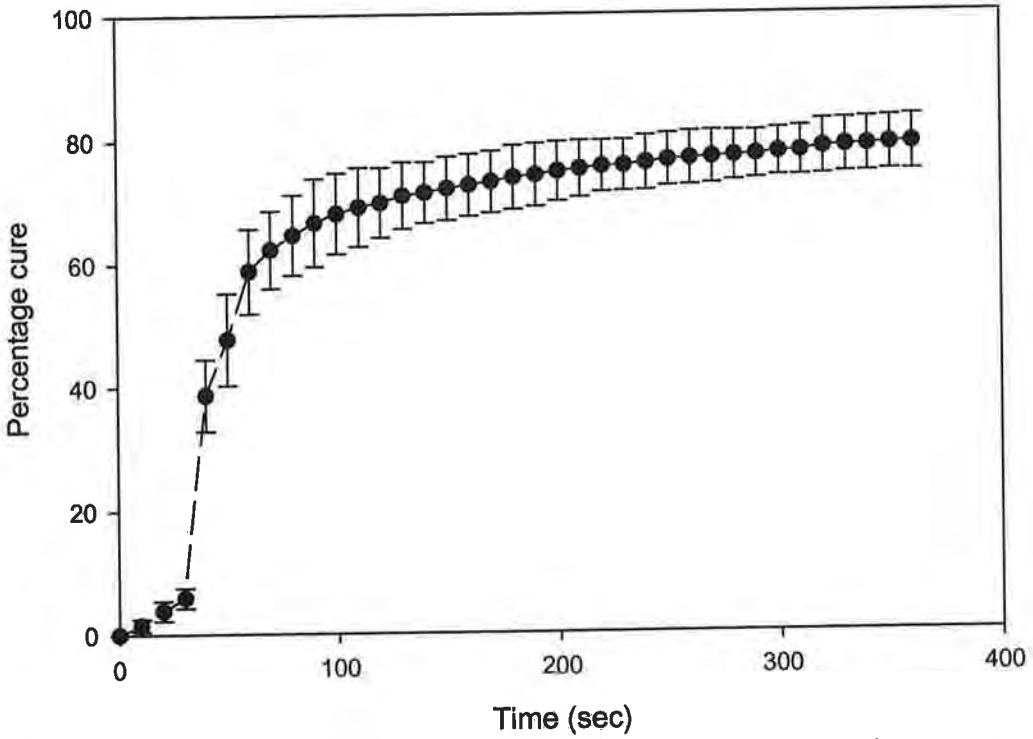

Figure 6.22: Curing profile achieved using 10s pulsed LEDs exposing monomer to 450 nm LED array first, then to 375 nm LED array (sample 1.4).

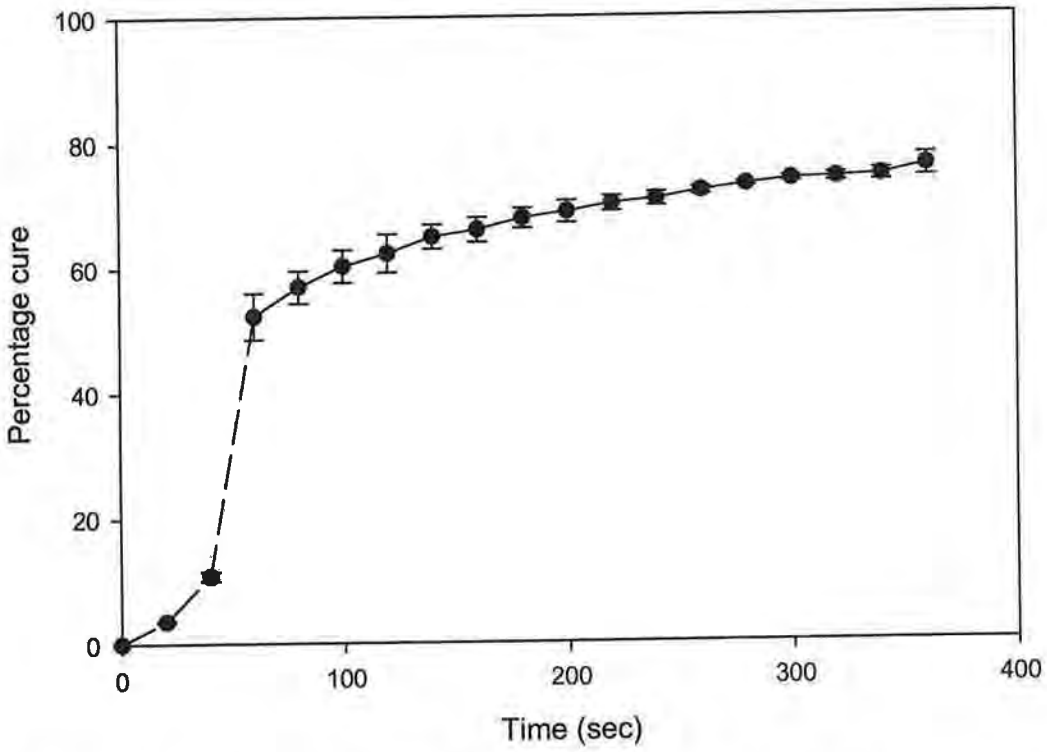

Figure 6.23: Curing profile achieved using 20s pulsed LEDs exposing monomer to 375 nm LED array first, then to 450 nm LED array (sample 1.5).

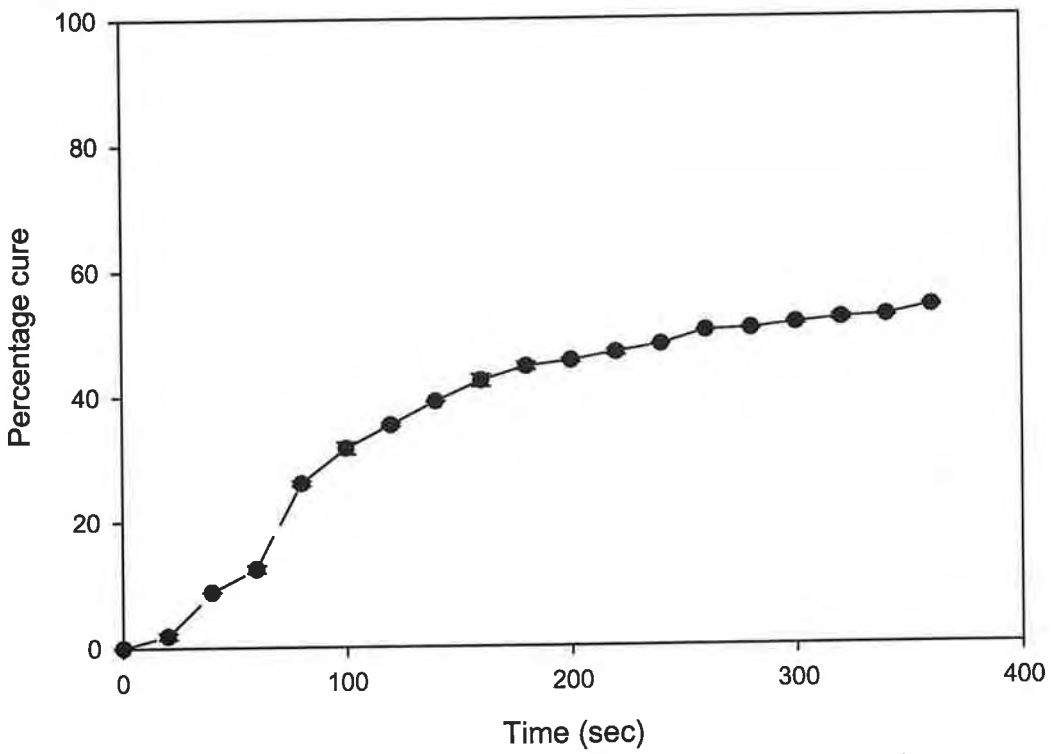

Figure 6.24: Curing profile achieved using 20s pulsed LEDs exposing monomer to 450 nm LED array first, then to 375 nm LED array (sample 1.6).

6.5.3 Discussion

FTIR spectroscopy was once again utilised to successfully monitor the curing profiles achieved with the new large LED arrays. When no pulsing was used the monomer exposed to the 375 nm LED only yielded a significantly higher percentage cure than that achieved when the 450 nm LED was used, indicating that the UV radiation at 375 nm is more efficient at producing free radicals than visible light this may be due to the higher ε_λ value at the λ_{max} of the 375 nm LED array. This study showed that the curing profiles of the monomer samples can be affected by using alternating radiation during photopolymerisation. The curing profiles were not only affected by the wavelength of radiation used but also by the duration of the pulsing. By varying the type of wavelength and pulse rate a slow

or fast cure could be obtained, this rate of initiation then affected the final amount of conversion. Therefore the order of wavelength and pulse time can be chosen depending on the type of curing profile required.

From these results there appears to be competing processes in which the initiation of one photoinitiator affects the lifetime of the other photoinitiator species in the system. As discussed in section 6.3.1 both photoinitiators use different mechanisms to produce free radicals. As the initiating radicals are only formed at the polymer/monomer interface [24] it is the understanding that the flow of radicals produced by the irradiation with one source may be blocked when the sample is irradiated with the other light source. In other words the flow of the free radicals is limited by the production of the other free radicals which may result in molecular mobility restrictions or the irradiation by the second source is causing a termination in the free radical production of the first source.

As these different curing modes affect the degree of conversion they may also affect the mechanical properties of the formed polymer which will be investigated in the next section.

6.6 Dynamic Mechanical Thermal Analysis

6.6.1 Introduction

The FTIR studies showed that pulsing affected the curing profiles of the monomer sample. Dynamic Mechanical Thermal Analysis (DMA) was next used to see if pulsing affects the thermal-mechanical properties of the final polymer. DMA is concerned with measuring the mechanical and viscoelastic properties of a sample as a function of temperature and/or frequency. It is typically used to

measure the glass transition (T_g) temperature and other transitions in a polymer. DMA can recognise small transition regions that are beyond the resolution of DSC. This type of technique requires the sample to be subjected to an oscillating stress (σ) which produces a corresponding deformation or strain (ε). For the great bulk of commercial polymers mechanical properties are of fundamental interest as polymers must exhibit a specified range of mechanical properties suitable for their application. DMA is a very important tool to measure mechanical properties of polymers and applications that involve hydrogels such as contact lenses, as DMA mimics the cyclic loads of differing magnitudes involved in wear [25].

6.6.2 Instrumentation

As already stated in DMA an oscillating stress is applied to the sample, this oscillating stress usually follows a sinusoidal waveform and will produce a corresponding oscillating strain. The measured strain will lag behind the applied stress by a phase difference (δ) (figure 6.25) unless the material is perfectly elastic. The ratio between the peak stress and strain gives a value for the complex modulus (E*), which consists of an in-phase component (storage modulus, E') and a 90° out-of-phase loss modulus (E") (figure 6.26 and Eq. 6.3). The storage modulus E' quantifies the materials ability to store energy (elastic behaviour), while the loss modulus E" measures the materials ability to dissipate energy by flow (viscous behaviour) [26, 27]. The ratio between these two modules gives the mechanical damping factor (tan δ) which is a measure of how well the material can disperse energy (Eq. 6.4).

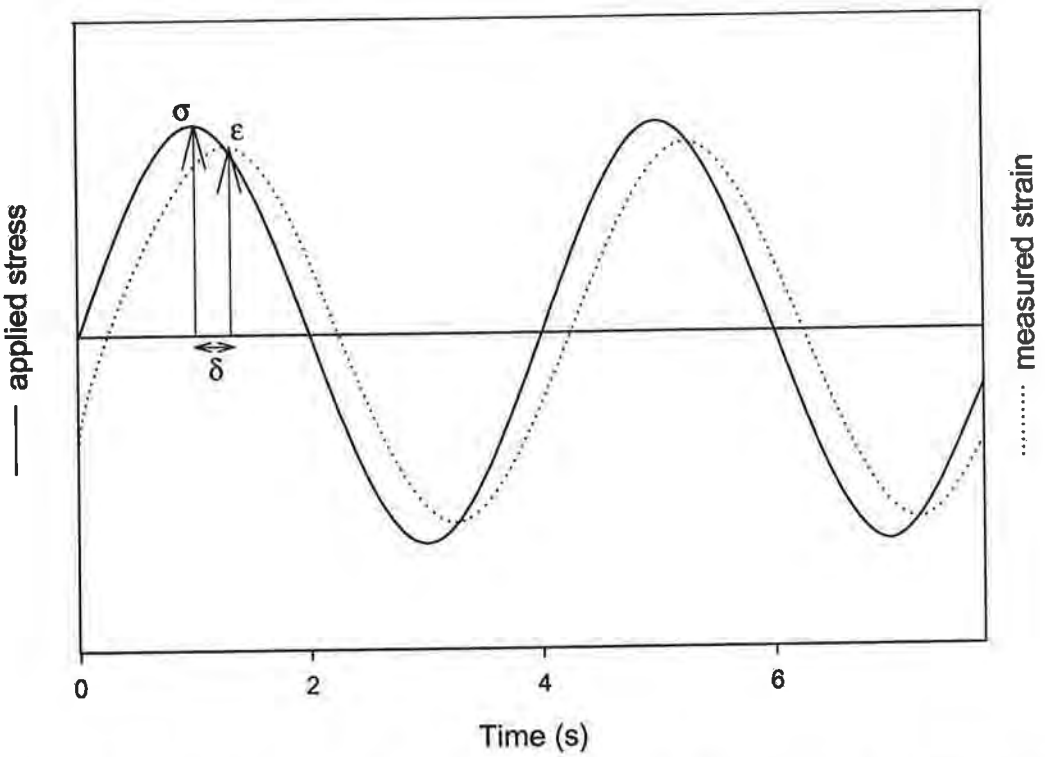

Figure 6.25: Relationship between applied stress and measured strain during DMA testing.

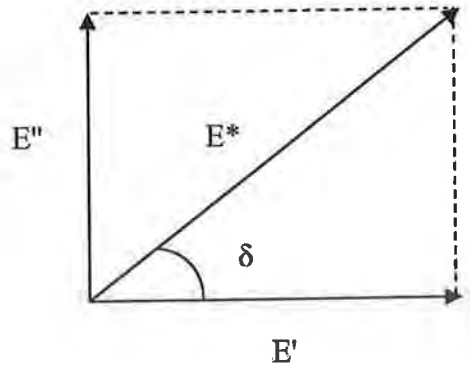

Figure 6.26: Illustration of the relationship between the complex modulus E* and its components.

$$E^* = E' + iE'' \qquad \text{Eq. 6.3}$$

$$\tan\delta = \frac{E''}{E'} \qquad \text{Eq. 6.4}$$

DMA allows samples to be analysed in a variety of deformation modes including bending, shear, compression and tension. The operation of a DMA instrument is relatively straight forward. The sample is mounted into the instrument using a certain clamp depending on the type of deformation to be performed. A stress is applied with a defined frequency to the sample through a motor as the sample deforms the amount of displacement is measured by a sensor. The strain is then calculated from this displacement. During a DMA analysis the temperature can be varied allowing the modulus to be recorded as a function of temperature. The magnitude of the applied stress and the resultant strain are used to calculate the stiffness of the material under stress. Tan δ is then determined using the phase lag between the stress and strain. A typical DMA response curve shows the storage modulus, loss modulus and tan δ over a certain temperature range. From this graph transitions that are unique to the sample such as T_g can be determined [28-30].

6.6.3 Sample Preparation

A new monomer sample containing the same concentration of Darocur TPO/CQ/Amine as used in the previous FTIR studies was used here. The mechanical properties of six polymers formed by pulsing the LEDs were investigated, i.e. polymer formed when monomer exposed to the 375 nm large LED array only, the 450 nm large LED array only and the polymers formed with

the pulsed LEDs (10 and 20 s) which were then alternated. The dimensions of the samples for DMA analysis needed to be approximately 30 mm long, 5 mm wide and 1 mm thick. Therefore a different curing set up needed to be used. Spacers with dimensions 60 mm x 40 mm x 1 mm were secured onto a Teflon® sheet and the monomer injected into the well area. The monomer was then covered with a glass slide and sealed. The first monomer sample (sample 2.1) was exposed to the 375 nm large LED array only for a total of 900 seconds to ensure complete photopolymerisation. This irradiation time was longer than previously used for the FTIR studies as the sample in this case was much thicker and therefore required a longer exposure time. After irradiation the sample which was now attached to the glass slide was placed in boiling water for a period 2-3 hours until the polymer could be easily peeled away from the slide. The polymer was then cut into rectangular sized DMA samples measuring 30 mm x 5 mm x 1 mm. The hydrated polymer was then placed between two sheets of Teflon® with a weight on top and allowed to dry for 72 hours. After the 72 hours the polymer was allowed to further dry in the atmosphere for 24 hours. The polymer form of HEMA (pHEMA) is rigid when dry but when saturated with water it becomes soft, it was important for DMA analysis that the formed polymers be fully dry as (1) wet samples break easily under stress in the DMA and (2) the water content in hydrogels has an effect on the storage modulus and T_g as it acts as a plasticizer reducing T_g [25, 26, 31, 32].

This process was then repeated for a second sample (sample 2.2) using the 450 nm large LED array only. After which another sample (sample 2.3) was exposed to the 10 s pulsed arrays irradiating first with the 375 nm large LED array

for 10 s followed by the 450 nm large LED array for 10 s and vice versa (sample 2.4). This was then repeated using the arrays pulsed at 20 s (samples 2.5 and 2.6). In all case to ensure the monomer was exposed to the same intensity (4.1 W/m^2) the 375 nm and 450 nm large LED arrays were placed at respective distances of 50 mm and 25 mm away from the sample. To remove any oxygen from the monomer that may inhibit polymerisation the monomer was flushed with oxygen free nitrogen before photopolymerisation. Table 6.3 gives a list of the allocated sample numbers and the different pulse rates used.

Table 6.3: Irradiation process and sample number

Sample Number	Irradiation Process
2.1	375 nm large LED continuous
2.2	450 nm large LED continuous
2.3	Pulse 10 s: 375 nm first 450 nm second
2.4.	Pulse 10 s: 450 nm first 375 nm second
2.5	Pulse 20 s: 375 nm first 450 nm second
2.6	Pulse 20 s: 450 nm first 375 nm second

6.6.4 Method

DMA was conducted on the Perkin Elmer Diamond DMA instrument in tension mode. The temperature range of each analysis was from -50 to 250 °C at a frequency of 1 Hz and amplitude of 5 μm. A preloaded force of 0.010 N was used to maintain sample tension. Typically the samples are compared by exposing them to a frequency of 1 Hz, while data of all frequencies are used to calculate

activation energies (i.e. the energy required to cause a transition). As this study is only concerned with inter-comparing the samples and not identifying the activation enthalpy the samples were only exposed to a frequency of 1 Hz over a range of temperatures [33]. A frequency of 1 Hz was also chosen as the β transition (discussed later) is only observed at this frequency [31]. For each sample the storage modulus (E'), the loss modulus (E'') and the mechanical damping factor (tan δ) were obtained from which transitions such as the glass transition temperature (T_g) can be measured (a typical DMA graph is shown in figure 6.27).

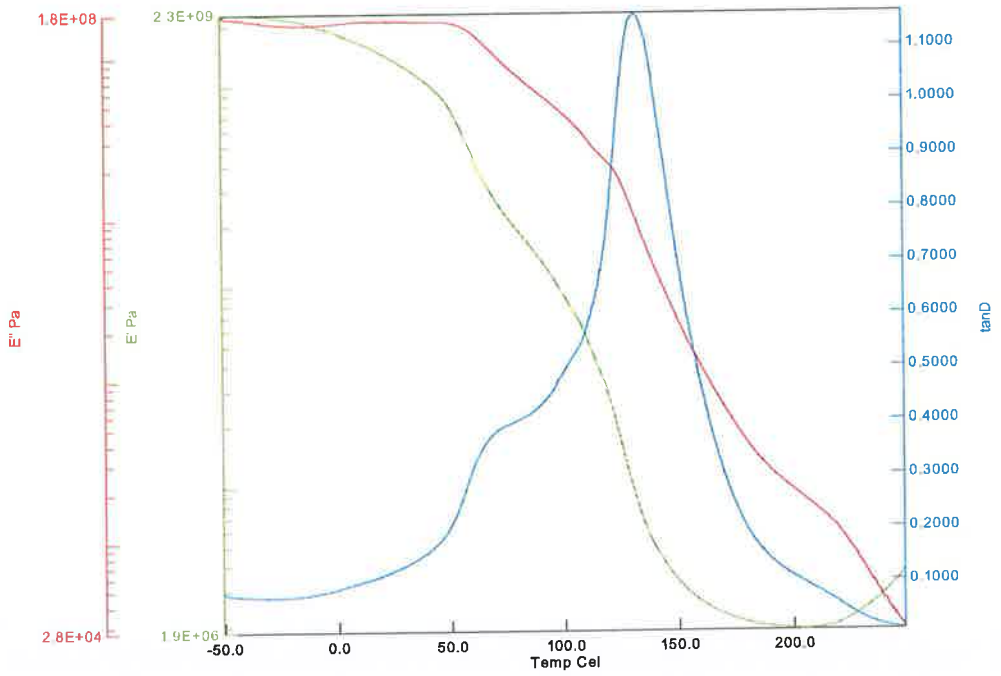

Figure 6.27: Typical DMA graph of pHEMA.

6.6.5 Results

In previous mechanical studies of pHEMA conducted by Gates et al [34] and Mohomed et al [31] it was found that dry pHEMA exhibits two sub-T_g relaxations which are associated with the polymers properties in the glassy state. These relaxations are known as the γ and β relaxations [35] and are secondary transitions that involve conformational changes that do not require main chain movement [36]. In pHEMA the γ relaxation is associated with the rotation of the hydroxyethyl group, while the β relaxation is attributed to the rotation of the ester side group. Mohomed et al [31] reported that the γ transition occurs between a temperature range of -135 to -116 °C for frequencies between 1-100 Hz, while Gates et al [34] observed the β transition at 28 °C. The γ transition is absent from the data presented here as the dynamic mechanical properties of the polymers were not obtained for temperatures below -50 °C.

In DMA work the glass transition is often called the α transition and varies widely for different amorphous polymers. This transition marks the onset of large scale displacement of the main chain and represents the glassy-to-rubbery transition temperature [35, 37]. Typically T_g is defined as the temperature at which the maximum occurs in tan δ or E" [38]. In this study the tan δ curves will be used to measure T_g. The glass transition is a transition that only occurs in amorphous polymers or in an amorphous region of a partly crystalline polymer. An amorphous polymer is one whose chains are not arranged in ordered crystals but are strewn around even though they are in a solid state. At low temperatures amorphous polymers are glassy, hard and brittle as only vibrational motions are possible. As the temperature increases they go through the glass-rubber transition

[39]. At T_g the amorphous polymer or the amorphous portions of a polymer soften due to the onset of long-range molecular motion and above T_g the polymer exhibits a rubbery region in which there is a loss of rigidity due to enhanced polymeric chain mobility [38]. The exact temperature at which the polymer chains become free to rotate and exhibit a change in mobility depends on the structure of the polymer. The more flexible the backbone of the polymer is then the easier the polymer will move and therefore the lower the T_g. The glass transition temperature is an important factor as it influences the polymer properties and its potential applications [22].

6.6.5.1 Storage Modulus

Although a typical DMA curve gives data for both the storage and loss modulus, it is the storage modulus that is of most interest as it gives information about the elastic behaviour of the polymer. The FTIR studies showed that the controlled pulsing of the two LED arrays does affect the rate of photopolymerisation and the final percentage cure of the polymer. The DMA study was conducted to investigate whether the controlled pulsing of the LEDs would also affect the mechanical properties of the polymer. The storage modulus (E') for the polymers produced when continuously exposed to the 375 nm large LED array only and pulsed first with the 375 nm large array then with the 450 nm large LED array at different pulse rates, are shown in figure 6.28. It can be seen from this graph that there is a significant difference in the initial storage modulus (approx. 5×10^9 Pa) for the polymer formed when a 20 s pulse rate was used (sample 2.5), compared to the other two polymers which have E' values of 2.2×10^9 Pa and 2.6×10^9 Pa for samples 2.1 and 2.3 respectively. This indicates that

the polymer formed with a pulse rate of 20 s will be more resistant to stretching in the glassy state than the other two polymers. This greater resistance to tensile force may be due to the presence of longer polymer chains formed during photopolymerisation which means greater entanglement of the chains. As the temperature increases the storage modulus decreases. This is not unexpected as increasing temperature in effect speeds up disentanglement which means the molecules in the polymer can move around more easily resulting in a decrease in rigidity, indicating the polymer transforms from its glassy to rubbery state. At approximately 28-30 °C the E' of samples 2.1 and 2.3 are equal indicating that at this temperature both polymers will exhibit that same degree of rigidity, after this temperature sample 2.1 has a higher E' value than sample 2.3.

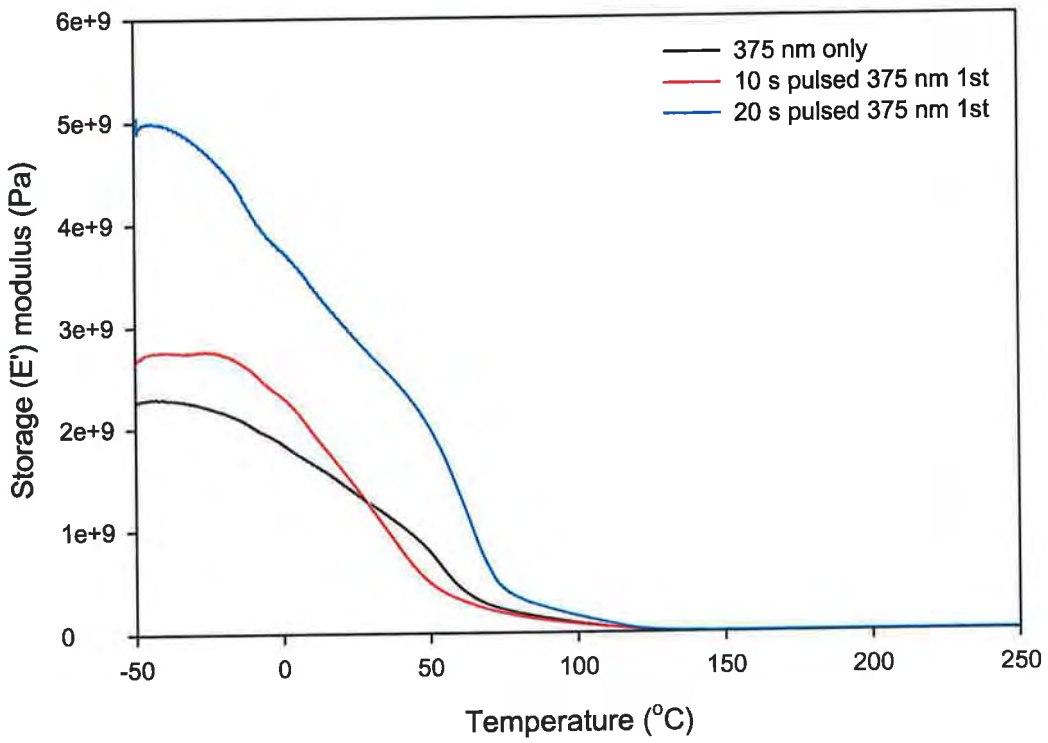

Figure 6.28: Storage Modulus achieved for the three polymers exposed to (1) the 375 nm large LED array only (2) exposed to 375 nm large LED array first for 10 s pulsed, then to the 450 nm array (3) exposed to 375 nm large LED array first for 20 s pulsed, then to the 450 nm array.

Figure 6.29 shows the storage modulus for the polymers formed when the monomer was exposed to the 450 nm large LED array only and when the monomer was exposed first to the 450 nm pulsing LED and the 375 nm LED second at different pulse rates. Unlike the curves in figure 6.24 the initial storage modulus of these polymers are all very similar (approx between 4.0 – 4.2 x 10^9 Pa). The three curves also drop off in the same degree with no crossover in modulus as was seen in samples 2.1 and 2.3. Once again the polymer formed with the 20 s pulsed has the highest storage modulus. Although there doesn't seem to

be a trend in the E' values of the six polymers it appears that increasing the pulse rate increases the storage modulus as in each case the 20 s pulse rate has the highest value followed by the 10 s with the polymers exposed to one type of radiation exhibiting the lowest E'. This indicates that the duration of the pulses (10 s or 20 s) has an affect on the final mechanical properties of the polymers.

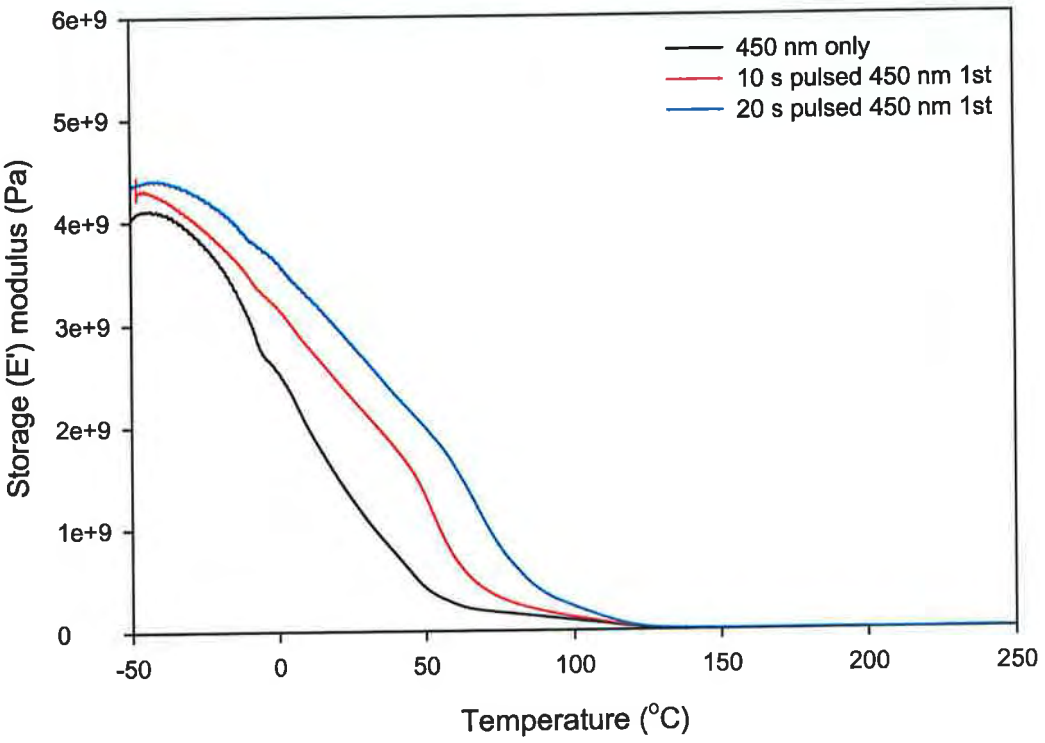

Figure 6.29: Storage Modulus achieved for the three polymers exposed to (1) the 450 nm large LED array only (2) exposed to 450 nm large LED array first for 10 s pulsed, then to the 375 nm LED (3) exposed to 450 nm large LED array first for 20 s pulsed then to the 375 nm LED.

Figures 6.30 and 6.31 shows the affect radiation wavelength (375 nm or 450 nm) has on the storage modulus of the final polymer. The pulse rate was kept constant at either 10 s or 20 s. The effect of altering the wavelength at a 10 s pulse

rate is shown in figure 6.30, while the 20 s pulse rate results are shown in figure 6.31.

With a 10 s pulse rate (figure 6.30) the polymer formed when exposed to the 450 nm LED array has the highest storage modulus (4.25 x 10^9 Pa), meaning it is more resistant to tensile force than the polymer formed when exposed to the 375 nm LED array first. This higher storage modulus corresponds to a fast curing profile (figure 6.22) in the FTIR studies. As a higher storage modulus implies the molecules in the polymer are more resistant to flow, due to increased entanglement it can be assumed that long chain polymers are formed during fast cure. The storage modulus of the polymer formed when exposed to the 375 nm LED array is low with a value of 2.6 x 10^9 Pa meaning its polymer chains can move around more easily. This lower storage modulus corresponds to a slow cure rate (figure 6.21); as a lower E' means the polymer chains can flow more easily due to less entanglement short chain polymers must be formed during a slow cure. Normally a slow cure rate would result in large sized polymer molecules [23]. However in this case it is proposed that this slow cure profile (figure 6.21) is due to the premature termination of the polymer chain, as autoacceleration of the polymerisation process is not reached. This results in short chain polymers which lead to a low E' value (figure 6.30). Although FTIR studies do not give an indication of the chain length future studies involving Gel Permeation Chromatography (GPC) can be undertaken to measure chain length.

The storage modulus of this polymer is flat in the temperature range of -50 to -17°C implying that in this region the resistance of this polymer to tensile force is not greatly affected by temperature.

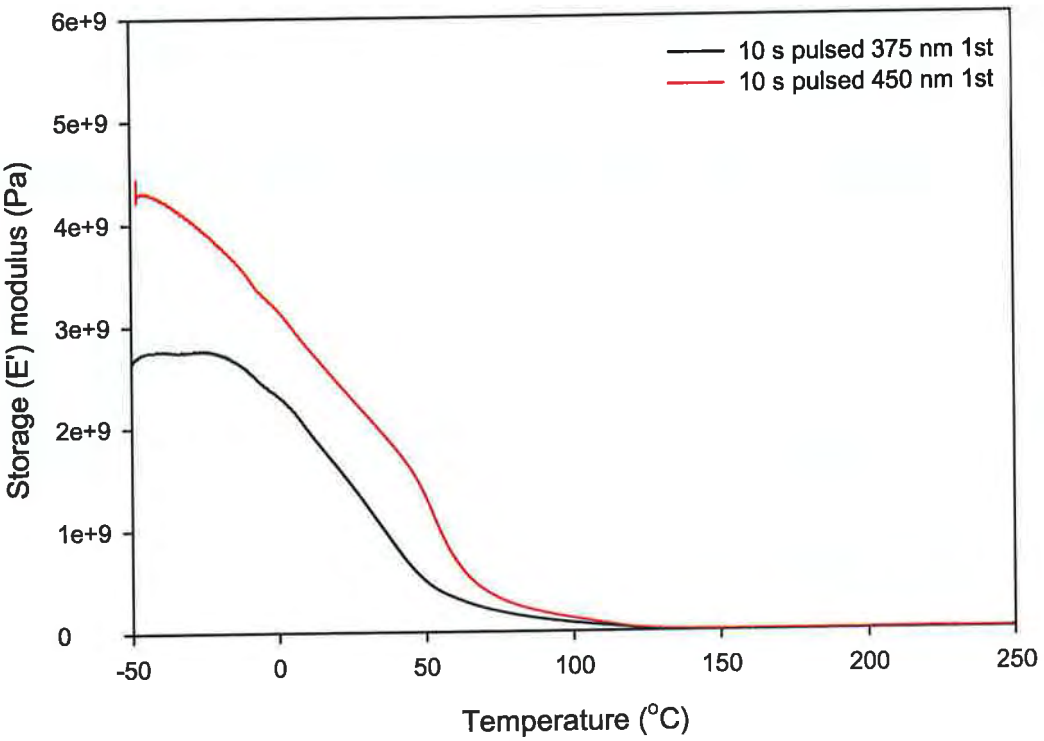

Figure 6.30: Effect of changing wavelength at 10 s pulsing.

The effect of wavelength at a 20 s pulse rate is shown in figure 6.31, the storage modulus of both polymers are quite similar with sample 2.5 (375 nm first) having a E' of 4.90 x 10^9 Pa compared to 4.32 x 10^9 Pa for sample 2.6 (450 nm first). Once again the higher storage modulus corresponds to longer chain length. This implies that pulsing with the 375 nm LED array for 20 s first leads to slightly longer chain length (higher E') than pulsing with the 450 nm first. This agrees with the quicker (figure 6.23) and slower (figure 6.24) cure profiles seen in the FTIR studies. Between approximately 10-50 °C the storage modulus of both polymers is almost exact and falls off to the same degree while just after 50 °C their E' is the same. After 50 °C sample 2.6 is more resistant to tensile force than sample 2.5 this is seen in the higher E' value.

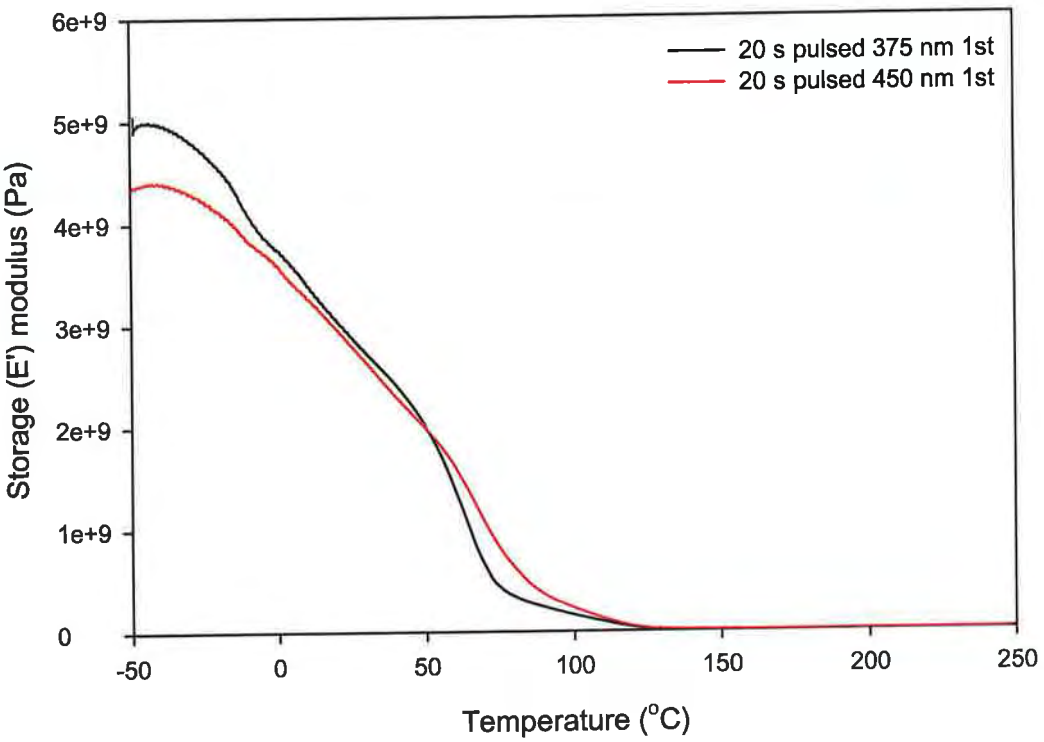

Figure 6.31: Effect of changing wavelength at 20 s pulsing.

Table 6.4 gives the initial storage modulus and cure information achieved in the previous studies for the four polymers. The two highest degrees of cure correspond to high initial storage modulus. However the polymers used in DMA may have different percentage cures than those indicated as the boiling of the samples during preparation will further polymerise the samples past the percentage cures indicated by FTIR. Therefore it is the rate of photopolymerisation, either slow or fast (whether or not autoacceleration has occurred) and its effect on chain length and hence E' that is of importance here. It is proposed here that the slow cure is a result of premature termination. In this study the terms slow and fast are relative terms and are just used as a guide. Although samples 2.4 and 2.6 have different cure rates, (fast and slow respectively), their initial storage moduli are

similar. Both of these polymers were formed by exposing the monomers to the 450 nm LED array first. Therefore although their cure rate is different the type of chain length formed must be similar i.e. long polymer chains are formed. This shows that the curing mechanism using the two sources and two photoinitiators is not a simple process and that further work needs to be carried out to fully understand the process. However this study does show that by varying the wavelength and the pulse duration the mechanical properties (E') of the polymer can be affected.

Table 6.4: Comparison between percentage cure, cure rate and storage modulus.

Sample ID	DMA Sample Number	Initial Storage Modulus (Pa)	FTIR Sample Number	Percentage Cure (indicated by FTIR)	Cure Information (relative)
10 s pulsed 375 nm/450 nm	2.3	2.62×10^9	1.3	50%	Slow/no autoacceleration
10 s pulsed 450 nm/375 nm	2.4	4.25×10^9	1.4	78%	Fast/ autoacceleration
20 s pulsed 375 nm/450 nm	2.5	4.90×10^9	1.5	76%	Fast/ autoacceleration
20 s pulsed 450 nm/375 nm	2.6	4.32×10^9	1.6	54%	Slow/no autoacceleration

E' is a measure of stiffness (rigidity) of the material and varies from polymer to polymer, higher E' values imply higher rigidity. Table 6.5 gives the storage modulus values of commonly used commercial polymers. In figures 6.28–6.31 it was shown that E' decreases as temperature increases which is not unexpected because as temperature increases the molecules have more energy to move around and therefore the polymer becomes less rigid and more elastic. It has been reported [27, 40] that some polymers exhibit an area of flat modulus over a certain temperature range however only one of the pHEMA polymers (sample 2.3, between -50 to -17°C) exhibit such a trend. The lack of such flat regions indicates that the stiffness of the pHEMA is greatly affected by temperature.

Table 6.5: Typical storage modulus values at break of some commonly used commercial polymers [41].

Polymer	**Modulus (x 10^9 Pa)**
Polyethylene (low density)	0.17-0.28
Polyethylene (high density)	1.07-1.09
Polypropylene	1.17-1.72
Poly(vinyl chloride)	2.41-4.14
Polystyrene	2.28-3.28
Poly(methyl methacrylate)	2.24-3.24
Polytetra-fluoroethylene	0.40-0.55

It should be noted that E' drops significantly as the pHEMA samples pass through the glass transition (~ 130 °C) where it leaves the glassy phase and enters

the rubbery phase The storage modulus as a function of temperature for each polymer formed is shown in figure 6.32. This figure shows that the measured value of E' shows a steep fall as temperature increases until the modulus for all polymers is approximately the same at temperatures exceeding 100 °C, implying that chain movement no longer changes above this temperature. Table 6.6 gives the storage modulus for each polymer at room temperature (T_r), which was taken to be 22 °C, this temperature is also indicated in figure 6.28. J. Gracida et al [42] reported a maximum E' of 1300 MPa (1.3 x 10^9 Pa) at 1Hz for pure pHEMA at room temperature. While this is similar to the values obtained for the polymers that were cured using only one LED array it is considerable less than the values achieved for the polymers formed using the pulsed LEDs. Therefore not only does pulsing during photopolymerisation affect the mechanical properties of the final polymer it may potentially be used to increase the polymer's resistance to applied forces allowing the polymer to be used in new areas where higher mechanical properties are required.

Table 6.6: Storage modulus at room temperature for each polymer.

Sample Number	Sample ID	Storage modulus at 22 °C (Pa)
2.1	375 nm LED only	1.4×10^9
2.2	450 nm LED only	1.4×10^9
2.3	10 s pulsed 375 nm/450 nm	1.6×10^9
2.4	10 s pulsed 450 nm/ 375 nm	2.4×10^9
2.5	20 s pulsed 375 nm/450 nm	3.0×10^9
2.6	20 s pulsed 450 nm/ 375 nm	2.9×10^9

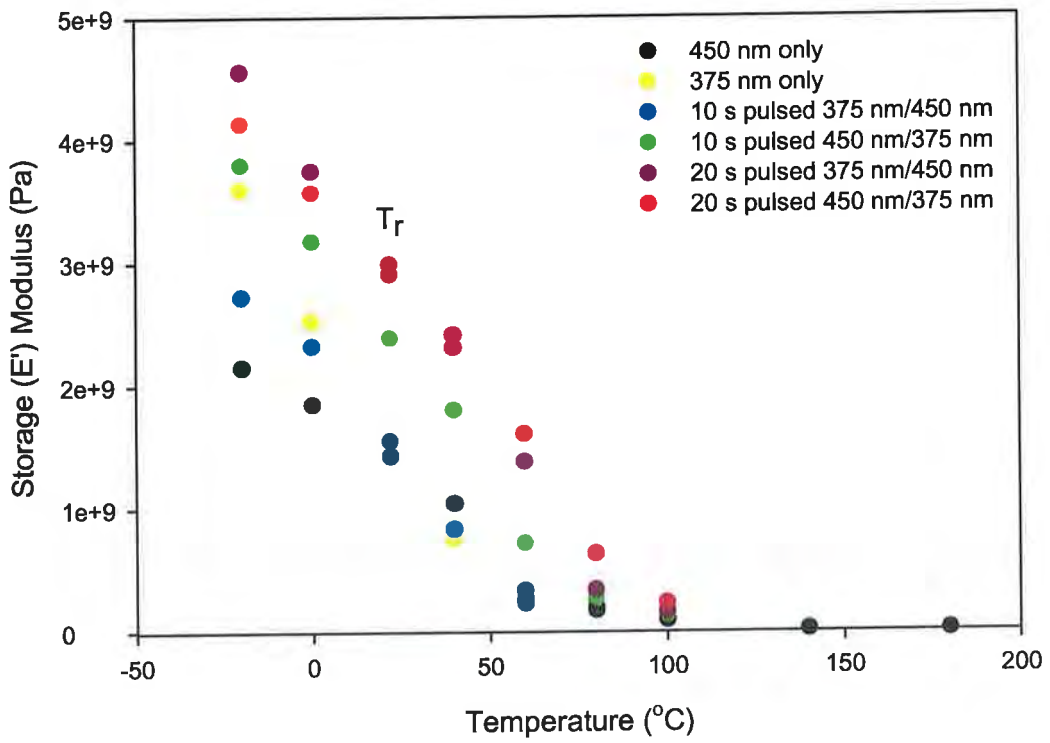

Figure 6.32: Storage modulus of each polymer as a function of temperature with room temperature (T_r) indicated.

6.6.5.2 Tan δ curves and measurement of the glass transition temperature

Another way of looking at the mechanical properties of polymers is to measure their mechanical damping factor (tan δ) values as a function of temperature. The tan δ of a polymer is a measure of how well a material can disperse energy and is a ratio of the storage and loss modulus. As tan δ is a measure of the ratio of the energy dissipated (E") to the energy stored (E') in the material, more energy is stored in the material with lower values of tan δ [27]. As a polymer passes through its glass transition temperature (T_g) its tan δ goes through a maximum [43], typically it is these tan δ curves that are used to measure the glass transition temperature. For DMA work the glass transition is often called the α transition and is the primary relaxation transition in a polymer. It is at this transition that the polymer converts from a glass-like state, in which there is restricted motion of the polymeric chains, to a rubber-like state in which there is a loss in rigidity due to increased chain mobility [38]. The temperature limits of utility of a polymer are governed by T_g therefore it is an important property to measure.

The high temperature α transition (glass transition) of each pHEMA can be clearly seen in the tan δ curves, figure 6.33. It can be observed that the glass transition position for all polymers is approximately the same with T_g values of between 130-133 °C. This corresponds well to the pHEMA T_g value of 133 °C determined by L.V. Karabanova et al [44]. Lower T_g values for pHEMA have been reported in other literature [22, 34, 45] where pHEMA has been quoted as having T_g values of between 358 - 378.8 K (≈ 85 -105 °C). Salmerón Sánchez et al [37] reported the highest T_g value of 140 °C for pure pHEMA. Although the T_g

values for the six polymers are similar the amplitude of their tan δ values differs. As the height of the tan δ peak decreases the bands become narrower. S. Li et al [46] have reported that a reduction in peak intensity of tan δ is consistent with the restriction of polymer chain mobility. This study is in agreement with this finding as higher tan δ values corresponds to higher E' values (at T_g) thus implying greater restriction on polymeric chain motion (table 6.7). The 10 s 450 nm/375 nm pulsed sample had the highest tan δ value of 1.34 at its T_g value, whereas the 10 s 375 nm/450 nm pulsed sample displayed the lowest value (1.13). In fact the two highest tan δ values occurred when the monomer was exposed to the 450 nm large LED array first.

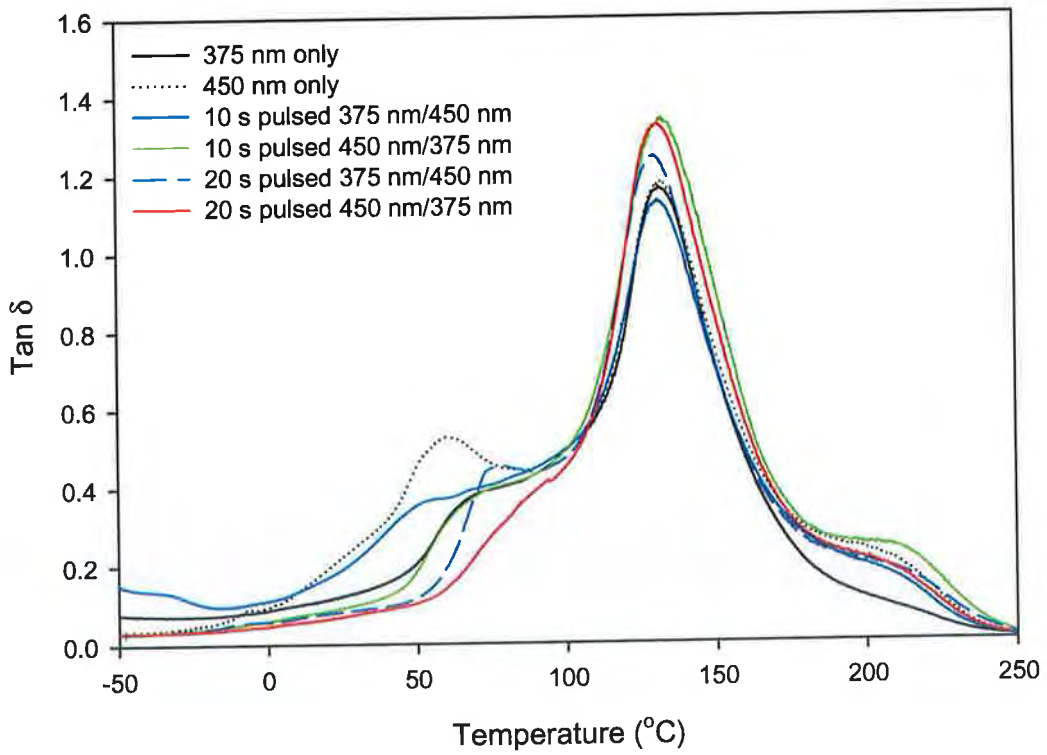

Figure 6.33: DMA measurements of mechanical damping factor (tan δ) versus temperature for the six polymers.

Table 6.7: Comparison of T_g, Tan δ and E' values for each pHEMA polymer.

Sample Number	Sample ID	T_g (°C)	Tan δ (at T_g)	E' (Pa) (at T_g)
2.1	375 nm LED only	131.5	1.16	0.88×10^7
2.2	450 nm LED only	132.0	1.18	0.94×10^7
2.3	10 s pulsed 375 nm/450 nm	131.2	1.13	1.02×10^7
2.4	10 s pulsed 450 nm/ 375 nm	132.6	1.34	1.23×10^7
2.5	20 s pulsed 375 nm/450 nm	130.1	1.24	1.19×10^7
2.6	20 s pulsed 450 nm/ 375 nm	131.1	1.33	1.30×10^7

6.6.5.3 Sub-glass transition relaxations

At temperatures below T_g secondary relaxations may be seen, these transitions are denoted as β, γ etc. designated in alphabetical order as a function of decreasing temperature [35, 38]. Unlike the T_g transition that is associated with a large scale increase in mobility these transitions do not require main chain movement. In pHEMA the β transition is attributed to the rotation of the ester side group while the γ relaxation is associated with the rotations of the hydroxyethyl group [31, 34]. Gates et al observed the β relaxation at 28 °C, with Mohomed et al observing the γ relaxation at -135 °C both of these transition temperatures were recorded at a DMA frequency of 1 Hz. Although in some E'-temperature graphs there is a recognisable change in slope at the secondary transitions, the tan δ plots are usually used to identify the temperature of such transitions [36].

As shown in figure 6.33 the polymers exhibit a shoulder in the low temperature side of the main α relaxation which can be attributed to its secondary β transition [37]. The γ transition is absent from the data presented here as the dynamic mechanical properties of the polymers were not obtained for temperatures below -50 °C. It can be seen from these graphs that the β transition temperature (T_β) is more affected by the irradiation process than the T_g, with the T_β shifted by about 25 °C. As the β transition is associated with the rotation of the ester side group the pulsing of the LEDs affects this rotation implying a difference in how the polymer is arranged. A higher T_β implies that the polymer is more densely packed resulting in more restricted rotation. Although it is difficult to determine the exact T_β (due to the overlap α peak) the order at which the T_β occurs is the same as the order of the E' in figure 6.28 in that lower T_β correspond to lower E' values. The polymers formed with 20 s pulsing have the highest T_β values while these polymers also exhibited the highest E' values. The lowest T_β values are observed with the polymers formed from the 450 nm LED only and the 10 s pulsed 375 nm LED first.

When comparing polymers 2.1 (375 nm only) and 2.2 (450 nm only), which are the two extremes of irradiation, the β transition is at a higher temperature (~ 68 °C) for sample 2.1 compared to a T_β of ~60°C for sample 2.2, with the β peak of sample 2.1 being less prominent. This implies that the use of UV radiation shifts the β transition to a higher temperature. This can be further seen when comparing samples 2.2, 2.4 and 2.6, which are in order of increasing exposure to UV radiation. As the samples are exposed to more UV radiation the T_β increases while the peak of T_β becomes less notable. When comparing samples

2.1 to sample 2.3 (which had less UV exposure as it was also exposed to 450 nm) the β transition is shifted to a lower temperature for sample 2.3, this is not unexpected as this sample was exposed to less UV radiation. However sample 2.5 does not follow this trend as its β transition is at a higher temperature again. Indicating again that photopolymerisation with two pulsed LEDs and two photoinitiators leads to a complex curing mechanism.

From the change in the T_β it can be concluded that how the polymer is cured will have an effect on the mechanical properties of the polymer albeit a subtle effect as T_g does not change drastically. As the β transition is due to the rotation of the ester group the curing process effects this side chain making it harder to rotate which is why they require more energy (seen as a higher temperature in the DMA graph) to move, this may be due to a different packing arrangement which causes less free volume. All the β transition temperatures observed in this study are higher than the T_β of 28 °C reported by Gates et al [34].

6.6.6 Discussion

DMA was used to successfully prove that the dynamic mechanical properties of a final polymer can be affected by pulsing. The main factors affected were the storage modulus and the position of the β transition, while the glass transition was not drastically affected. It was found that pulsing at a 20 s rate produced polymers with a higher E' value indicating greater resistance to tensile force. It appears that increasing the pulse rate increases the polymer rigidity and resistance to stretching as in each case the 20 s pulse rate had the highest value followed by the 10 s with the polymers exposed to one type of radiation exhibiting the lowest E'. Only one of the polymers formed (sample 2.3) exhibited an area of

flat modulus over a certain temperature range. The lack of such a flat region indicated that the stiffness of the polymers formed was greatly affected by temperature. The E' values of pHEMA achieved using the pulsed LEDs were significantly higher than the storage modulus for pHEMA reported by J. Gracida [42]. This implied that not only does pulsing during photopolymerisation affect the mechanical properties of the final polymer it can be used to increase the polymers resistance to applied forces allowing a final polymer to be the synthesised with desired mechanical properties.

The shape and position of the sub-glass β transition was greatly affected by the type of wavelength and the pulse rate used. It appears that as the samples were exposed to more UV radiation the T_β increased while the peak of T_β became less notable. A higher T_β implies that the polymer is more densely packed resulting in more restricted rotation of the ester group this may be due to a different packing arrangement being formed which resulted in less free volume. All the β transition temperatures observed in this study were higher than the T_β reported by Gates et al [34]. Although a change in the T_β and its shape is not as dramatic as a shift in T_g it does show that controlled pulsing has an affect on the polymers final properties which should be further studied.

6.7 Conclusion

Like the previous LEDs used in this study the new large LED arrays exhibited a number of desirable features for an 'ideal' photopolymerisation source. Although pulsing would have been possible with the previous LEDs, due to the size the large LED arrays were used to investigate the effect of alternating illumination on the curing process.

FTIR spectroscopy was used to successfully prove that the degree of conversion and cure rate of the monomer samples can be affected by using pulsed radiation at different wavelengths during photopolymerisation. The curing profiles potentially were not only affected by the irradiation wavelength but also by the duration of the pulsing. By varying the type of wavelength and pulse rate used either a slow or fast cure could be obtained, this rate of initiation then affected the final amount of conversion. Therefore depending on the type of curing profile required a certain order of wavelength and pulse time can be chosen.

DMA was then used to investigate what effect different pulse rates had on the mechanical properties of a final polymer. The properties investigated were the storage modulus, the glass transition temperature and the position of the sub-T_g relaxations. It was found that increasing pulse rate leads to a higher storage modulus therefore by exposing the monomer to longer pulse times during synthesis a polymer with higher rigidity can be formed which can consequently determine the polymers usage. The glass transition temperatures of each polymer formed were very similar signifying the irradiation process did not have a great effect on the temperature at which the polymers transformed from a glass-like state to a rubber-like state. However DMA did prove that the irradiation process had a significant affect on the rotation of the ester side group which resulted in the β transition varying over a 25 °C range. Although this change is not as dramatic to the polymer properties as a change in T_g would be, it does prove that the mechanical properties of a final polymer can be affected by pulsing.

From this study it can be concluded that the mechanical properties of pHEMA are affected and can be altered by the type of light source used as well as

the exposure times. The properties of these polymers can potentially be varied to suit a particular application and property requirement (i.e. hardness, elasticity). This type of photopolymerisation system is completely novel to this research and it is the ability to pulse and select different maximum peak wavelengths that make LEDs very attractive for this study as it is not possible to pulse conventional emission sources such as Hg fluorescent lamps.

6.8 References

[1] http://www.uvprocess.com/product.asp?code=UV+LED+++C. accessed 15 November 2006.

[2] A. Uhl, B.W. Sigusch, K.D Jandt. "Second generation LEDs for the polymerization of oral biomaterials". Dent. Mater. 2004; vol 20: pp.80.

[3] http://www.solar.com/pma2107.htm accessed 08 March 2007.

[4] http://www.solar.com/pma2121.htm accessed 08 March 2007.

[5] S.L. McDermott, J.E. Walsh, R.G. Howard. "A comparison of the emission characteristics of UV-LEDs and fluorescent lamps for polymerisation applications". Optics and Laser Technology 2008; vol. 40: pp.487.

[6] http://www.ciba.com/ accessed 20 November 2006.

[7] W. Teshima, Y. Nomura, N. Tanaka, H. Urabe, M. Okazaki, Y. Nahara. "ESR study of camphorquinone/amine photoinitiator systems using blue light-emitting diodes". Biomaterials 2003; vol 24: pp. 2097.

[8] U. Lohbauer, C. Rahiotis, N. Krämer, A. Petschelt, G. Eliades. "The effect of different light-curing units on fatigue behavior and degree of conversion of a resin composite". Dent. Mater. 2005; vol 21: pp.608.

[9] J. Jakubiak, X. Allonas, J.P. Fouassier, A. Sionkowska, E. Andrezejewska, L.Å. Linden, J.F. Rabek. "Camphorquinone-amines photoinitiating systems for the initiation of free radical polymerization". Polymer 2003; vol 44: pp.5219.

[10] J. Jakubiak, A. Wrzyszczyński, L.Å. Linden J, .F. Rabek. "The role of amines in the camphorquinone photoinitiated polymerization of multifunctional monomer". J. Macromol. Sci., Chem. 2007; vol 44: pp.239.

[11] Y.J. Park, K.H. Chae, H.R. Rawls. "Development of a new photoinitiation system for dental light-cure composite resins". Dent. Mater. 1999; vol 15: pp.120.

[12] E. Andrzejewska, L-Å Lindén, J.F. Rabek. "The role of oxygen in camphorquinone-initiated photopolymerization". Macromolecular Chemistry and Physics 1998; vol 199: pp.441.

[13] G.J. Sun, K.H. Chae. "Properties of 2,3-butanedione and 1-phenyl-1,2-propanedione as new photosensitizers for visible light cured dental resin composites". Polymer 2000; vol. 41: pp. 6205.

[14] D.C. Watts. "Reaction kinetics and mechanics in photo-polymerised networks". Dent. Mater. 2005; vol. 21: pp.27.

[15] http://www.sigmaaldrich.com/catalog/search/ProductDetail/ALDRICH/147834 accessed 16 April 2007.

[16] M.G. Neumann, W.G. Miranda Jr., C.C. Schmitt, F.A. Ruggeberg, I.C. Corrêa. "Molar extinction coefficients and the photon absorption efficiency of dental photoinitiators and light curing units". J. Dent. 2005; vol 33: pp.525.

[17] J.C. Ontiveros, R.D. Paravina. "Light-emitting diode polymerization: A review of performance, part 1". Acta Stomatologica Naissi 2006; vol 22: pp.601.

[18] T.P. Klun, L.D. Hibbard, K.M. Spurgeon, R.S. Culler. "Coatable compositions abrasive articles made therefrom, and methods of making and using same", U.S Patent 5667541. United States, 1997.

[19] M.G. Neumann, C.C. Schmitt, G.C. Ferreira, I.C. Corrêa. "The initiating radical yields and the efficiency of polymerization for various dental

photoinitiators excited by different light curing units". Dent. Mater. 2006; vol 22: pp.576.

[20] C. Decker. "Light-induced crosslinking polymerization". Polym. Int. 2002; vol 51: pp.1141.

[21] C. Iojoiu, M.J.M. Abadie, V. Harabagiu, M. Pinteala, B.C. Simionescu. "Synthesis and photocrosslinking of benzyl acrylate substituted polydimethylsiloxanes". Eur. Polym. J. 2000; vol 36: pp.2115.

[22] M. Fernández-García, M.F. Torrado, G. Martínez, M. Sánchez-Chaves, E.L. Madruga. "Free radical copolymerization of 2-hydroxyethyl methacrylate with butyl methacrylate: determination of monomer reactivity ratios and glass transition temperatures". Polymer 2000;vol. 41: pp.8001.

[23] G. Odian. "Principles of Polymerization. 3rd Ed." New York: John Wiley & Sons Inc, 1991.

[24] C. Decker. "The use of UV irradiation in polymerization". Polym. Int. 1998; vol 45: pp.133.

[25] J.V. Cauich-Rodriguez, S. Deb, Smith R. "Effect of cross-linking agents on the dynamic mechanical properties of hydrogel blends of poly(acrylic acid)-poly(vinyl alcohol-vinyl acetate)". Biomaterials 1996; vol. 17: pp.2259.

[26] L Ambrosio, R De Santis, L Nicolais. "Composite hydrogels for implants". Proc. Inst. Mech. Eng. [H]. 1998; vol. 212: pp.93.

[27] J.M. Yang, H.M. Li, M.C. Yang, C.H. Shih. "Characterization of acrylic bone cement using dynamic mechanical analysis". J. Biomed. Mater. Res. 1999; vol. 48: pp.52.

[28] Triton Technology "Introduction of dynamic mechanical analysis". www.triton-technology.co.uk/pdf/TTInf_DMA.pdf.

[29] Perkin Elmer. "Diamond Dynamic Mechanical Analyzer".

[30] K.P. Menard. "Dynamic Mechanical Analysis: A practical introduction". Florida: CRC Press, 1999.

[31] K. Mohomed, T.G. Gerasimov, F. Moussy, J.P. Harmon. "A broad spectrum analysis of the dielectric properties of poly(2-hydroxyethyl methacrylate)". Polymer 2005; vol 46: pp.3847.

[32] J.W. Gooch. "Encyclopaedic dictionary of polymers vol. 1 A-M": Springer, 2007.

[33] L. Woo, M.T.K. Ling, S.P. Westphal. "Dynamic mechanical analysis (DMA) and low temperature impact properties of metallocene polyethylenes". Thermochim. Acta 1996; vol. 272: pp.171.

[34] G. Gates, J.P. Harmon, J. Ors, P. Benz. "Intra and intermolecular relaxations 2,3-dihydroxypropyl methacrylate and 2-hydroxyethyl methacrylate hydrogels". Polymer 2003; vol. 44: pp.207.

[35] Royal Society of Chemistry. "Principles of thermal analysis and calorimetry". UK: RSC, 2002.

[36] D. Campbell, R.A. Pethrick, White JR. "Polymer characterization. Physical techniques. 2nd Ed." Gloucestershire: Stanley Thornes Ltd, 2000.

[37] M. Salmerón Sánchez, R. Brígido Diego, S.A.M. Iannazzo, J.L. Gómez Ribelles, M. Monleón Pradas. "The structure of poly(ethyl acrylate-co-hydroxyethyl methacrylate) copolymer networks by segmental dynamics studies based on structure relaxation experiments". Polymer 2004; vol. 45: pp.2349.

[38] D.S. Jones. "Dynamic mechanical analysis of polymeric systems of pharmaceutical and biomedical significance". Int. J. Pharm. 1999; vol.179: pp.167.

[39] L.H. Sperling. "Introduction to physical polymer science. 4th Ed." New Jersey: John Wiley & Sons, 2006.

[40] C.C. Chu, J.A. von Fraunhofer, H.P. Greisler. "Wound closure biomaterials and devices". Florida: CRC Press, 1997.

[41] M.P. Stevens. "Polymer chemistry: an introduction. 3rd Ed." New York: Oxford University Press, 1999.

[42] J. Gracida, F. Perez-Guevara, J. Cardoso-MartÍnez. "Thermal and dynamic mechanical properties of binary blends of bacterial copolyester poly(hydroxybutyrate-co-hydroxyvalerate) (PHBHV) with poly(2-hydroxyethylmethacrylate) (PHEMA)". J. Mater. Sci. 2005; vol. 40: pp.2565.

[43] E.L. Charsley, S.B. Warrington. "Thermal analysis - techniques and applications". Cambridge: The Royal Society of Chemistry, 1992.

[44] L.V. Karabanova, G. Boiteux, O. Gain, G. Seytre, L.M. Sergeeva, E.D. Lutsyk. "Miscibility and thermal and dynamic mechanical behaviour of semi-interpenetrating polymer networks based on polyurethane and poly(hydroxyethyl methacrylate)". Polym. Int. 2004; vol.53: pp.2051.

[45] J. Brandup, E.H. Immergut, E. Grulke. Polymer handbook 4th Ed. New York: John Wiley, 1998.

[46] S. Li, A. Shah, A.J. Hsieh, R. Haghighat, S.S. Praveen, I. Mukherjee, E. Wei, Z. Zhang, Y. Wei. "Characterization of poly(2-hydroxyethyl methacrylate-silica) hybrid materials with different silica contents". Polymer 2007; vol.48: pp.3982.

Chapter 7 Conclusions and future work

7.1 Main aims and key findings

The aim of this study was to investigate the potential of UV-LEDs in replacing traditionally used fluorescent lamps in the manufacturing of biomaterials, namely contact lenses. Throughout history lighting technology has constantly strived to develop an 'ideal' light for use in different applications, including domestic and industrial uses, and photopolymerisation applications are no exception. Therefore with the recent development of SSL, which eliminates many of the physical and commercial drawbacks associated with traditional lamps, it was foreseen that these new UV-LEDs could be a viable possibility for use in photopolymerisation processes.

Before the UV-LEDs could be used in a photopolymerisation process their emission characteristics needed to be measured and compared to those of the traditionally used fluorescent lamps. To allow for this comparison a number of different experimental techniques were used to investigate each light sources respective outputs which included wavelength, intensity, warm up time and stability. One of the main problems encountered when characterising the different light sources was how to relate the light output from a fluorescent tube to that of an LED so that a reasonable logical inter-comparison could be made. To overcome this problem the lamp was completely masked off except for an area equal to the diameter of the LED, making the output nature of the sources reasonable similar so that certain specification comparisons could be made. Throughout this study UV-LED technology continued to develop and as such a

number of different LEDs were used in this research. It can be seen from the results obtained that as this technology evolved the specifications of the LEDs available improved with not only the output intensity increasing but also the lifetime of the LEDs. Overall from these studies it was found that the UV-LEDs used in this study were comparable to the lamps in terms of intensity, maximum peak wavelength and spectral output and as such exhibited the potential to replace fluorescent lamps in photopolymerisation processes.

As these UV-LEDs had not been used in the photopolymerisation of HEMA initial proof of concept needed to be proven. For this a number of test monomer samples, each containing a different photoinitiator, were prepared. UV/vis spectroscopy was first used to measure the absorption properties of each initiator therefore allowing the molar absorptivity to be calculated. Both Raman and FTIR spectroscopy were then used to record the photopolymerisation process by monitoring the disappearance of the characteristic spectral peaks. These three spectroscopic techniques were of great importance as they gave information on the curing profiles of the HEMA samples and allowed for an intercomparison between the expected and determined cure profiles achieved.

Although in come cases the LED exposed samples exhibited a lower level of photopolymerisation to that of the fluorescent lamp similar temporal profiles were observed. Therefore these initial studies did prove the concept that UV-LEDs could initiate a photochemical process in a HEMA monomer and depending on the photoinitiator used could produce a degree of cure similar to that achieved with fluorescent lamps. This study did produce one surprising result in that although a photoinitiator may have a high ε_λ value it does not necessarily guarantee that the

monomer sample containing that photoinitiator will give the highest degree of conversion and likewise photoinitiators with low ε_λ values will not necessarily produce low degrees of conversion. Therefore other factors such as quantum yield and efficiency should also be considered when choosing a photoinitiator for photopolymerisation processes. This finding requires additional research and is discussed further in section 7.2. The success of these initial findings which proved that UV-LEDs could cure a test monomer allowed for the study to be taken further by investigating what affect pulsed radiation would have on the curing process and the thermomechanical properties of the polymer.

The fact the LEDs have the ability to be pulsed while allowing for the selection of different maximum peak wavelengths made LEDs very desirable for this study, as it allowed the development of a photopolymerisation system that is completely novel to this research. This sort of photopolymerisation system would not be possible with fluorescent lamps as due to their design they cannot be pulsed at quick rates. For this study two LED arrays were used one emitting at 375 nm and the other at 450 nm, as one of these LEDs emitted in the visible region a different photoinitiator to those previously examined had to be used. As the photoinitiator most commonly used with visible emitting light sources had a low polymerisation efficiency when used on its own it had to be used in conjunction with a coinitiator, namely an amine. This photoinitiator/amine system generates free radicals in a different way to the previous photoinitiators and from the results achieved it appears that there is a competing process between the two systems of radical production, which is affected by the type and order of radiation used to cure the sample. By varying the type of wavelength and pulse rate a slow or fast

cure could be obtained, this rate of initiation then affected the final amount of conversion. This process is complex as not only is the amount of radicals produced affected by different pulse times but it also appears that their molecular mobility can be restricted, consequentially affecting percentage cure. From this study it can be concluded that in some cases the switching on of another wavelength can affect the autoacceleration process of one of the photoinitiators resulting in a halt in radical production. However this is further complicated as by using a different initial light source a photospecies which can actually aid the autoacceleration process can be produced.

The final section of this thesis used DMA to investigate how the different curing modes which affected the percentage cure, could be used to alter the mechanical properties of the formed polymer. The mechanical properties investigated were the storage modulus, sub-glass transition relaxations and the glass transition temperature. Upon investigating the values obtained for the storage modulus it was found that increasing the pulse rate lead to higher storage modulus values. The storage moduli measured in this study were also higher than those values previously published for pure pHEMA, showing that pulsed radiation may be used to increase the final polymers resistance to applied forces. The position of the sub-glass β transition was also affected by pulsing, shifting by about 25 °C, while the glass transition was not as drastically affected. Once again higher β transitions than those previously published were found with the polymer formed using a 20 s pulse rate having the highest transition temperature. As the β transition is associated with the rotation of the ester group and a higher T_β associated with a more densely packed polymer it appears that the polymers being

formed with the different pulse rates have different packing arrangements which results in less free volume. Although a change in T_β is not as dramatic as a change in T_g would be it does show the controlled pulsing has an effect on the polymers final properties. Overall from this DMA study it can be concluded that the final mechanical properties of a polymer can be affected by exposing the monomer to pulsed radiation during synthesis which therefore has the potential to allow the production of a polymer with desired mechanical properties for a certain application (i.e. increased hardness or elasticity).

Due to the inherent advantages that LEDs have over fluorescent lamps and the fact that they produce a comparable photopolymerisation as that achieved with the lamp it appears that UV-LEDs have the potential to replace these lamps in photopolymerisation processes. As LED technology improves and becomes more readily available (reducing cost), LED photopolymerisation is a viable possibility in replacing fluorescent lamps in the manufacturing process of biomaterials such as contact lenses.

7.2 Future work

Overall the original objective to prove that UV-LEDs could initiate a photopolymerisation process has been satisfied. However for a complete understanding of the UV-LED induced photopolymerisation process some of the findings require further investigation. One such study of interest would be to quantify free radical production, particularly in the initiation stage. This would be particularly beneficial when pulsed radiation is used as there appears to be a competing process between the two different photoinitiator mechanisms. Analysis of the flow of free radicals would allow for the determination into how and if the

production of one type of free radical is limited by the production of the other free radicals resulting in molecular mobility restrictions or early termination.

One of the most unexpected findings in this research was that although a photoinitiator may have a high ε_λ value it did not necessarily guarantee that the monomer sample containing this photoinitiator would give the highest degree of conversion; likewise photoinitiators with low ε_λ values did not necessarily give low degrees of conversion. However as these ε_λ values were only based on the λ_{max} for each light and did not take into account the absorption of other wavelengths by the photoinitiator it may be more beneficial to measure the quantum yield and use these values as an indicating factor to the best photoinitiator.

In some cases LED exposed samples showed a lower level of photopolymerisation to that achieved with the fluorescent lamp. From the FTIR and Raman data it was not possible to determine if the calculated degree of conversion is caused by the production of short molecules (oligomers) or longer chain molecules (polymers). Consequently it is not known if both light sources yield similar size polymer chains in the final product which may affect the values achieved for percentage cure. GPC could be used to measure the chain length of each polymer formed.

As the DMA study was only concerned with inter-comparing the mechanical properties of the formed polymer the samples were only exposed to one frequency (1 Hz), a further study could utilise a range of frequencies allowing for the activation energy to be calculated.

The curing methodology used in this study is not only limited to the manufacturing of contact lenses, where the narrow emission of the UV-LEDs would be particularly beneficial in the manufacturing of UV blocking lenses, but also has the potential to be used in a number of industries where manufacturers wish to maintain the advantageous properties of UV light curing while allowing for lower power consumption, minimal heat production, minimum maintenance and longer lifetime reducing manufacturers' costs.

Publications and Presentations

1. S.L. McDermott, J.E. Walsh, R.G. Howard. "A comparison of the emission characteristics of UV-LEDs and fluorescent lamps for polymerisation applications". Optics & Laser Technology. 2008, 40:487-493.
2. S.L. McDermott, J.E. Walsh, R.G. Howard. "A novel application of UV-LEDs in the contact lens manufacturing process". Proc. SPIE, 2005, 5826:119-130.
3. S.L. McDermott, J.E. Walsh, R.G. Howard. "A novel application of UV-LEDs in the contact lens manufacturing process". IOP Spring Weekend, Kildare, April 2005.
4. S.L. McDermott, J.E. Walsh, R.G. Howard. "A novel application of UV-LEDs in the contact lens manufacturing process". SPIE conference, RDS Dublin, April 2005.
5. S.L. McDermott, J.E. Walsh, R.G. Howard. "Spectroscopic analysis of the photopolymerisation of biomaterials". IOP Spring Weekend, Westport, April 2003.